Universitat Autònoma de Barcelona

EVALUATION OF THE THERAPEUTIC POTENTIAL OF ABTL0812 IN NEUROBLASTOMA

Laia París Coderch

PhD thesis

EVALUATION OF THE THERAPEUTIC POTENTIAL OF ABTL0812 IN NEUROBLASTOMA

PhD thesis presented by

Laia París Coderch

To obtain the degree of

PhD in Biochemistry, Molecular Biology and Biomedicine

Tutor: Dr. Ibane Abasolo Olaortua

Directors:

Dr. Miguel F. Segura Ginard

Dr. Aroa Soriano Fernández

Student: Laia París Coderch

Doctorat en Bioquímica, Biologia Molecular i Biomedicina
Departament de Bioquímica i Biologia Molecular
Universitat Autònoma de Barcelona

2019

ABSTRACT

Abstract

Neuroblastoma (NB) is the most prevalent extracranial solid tumor of the infancy and the third most common childhood cancer. High-risk neuroblastomas (HR-NB) are very aggressive and develop resistance to current therapies. Hence, HR-NB remain a major obstacle for pediatric oncologists since there are no alternative curative options available.

ABTL0812 is a novel first-in-class antitumor drug that is currently under phase Ib/IIa clinical trials in adult patients with advanced solid tumors, showing excellent tolerability results. Previous studies described that ABTL0812 mechanism of action is based on the disruption of the AKT/mTOR pathway. Given that (1) constitutively enhanced PI3K/AKT/mTOR signaling correlates with poor prognosis and chemoresistance in HR-NB, and that (2) the PI3K/AKT/mTOR axis integrates relevant targets for HR-NB, we sought to address whether ABTL0812 could be potentially used for the treatment of HR-NB patients.

For the purpose of the study, the therapeutic potential of ABTL0812 was analyzed in a set of clinical representative NB cell lines *in vitro*. All cell lines showed a similar sensitivity to ABTL0812 regardless of their genetic profile. Remarkably, ABTL0812 did not cause DNA-damage or genotoxicity, thus indicating that fewer side effects would be expected. Moreover, oral administration of ABTL0812 in HR-NB xenografts impaired tumor growth and confirmed a good tolerability profile. Furthermore, our findings reveal that ABTL0812 induced NB cell death via long-term activation of the endoplasmatic reticulum stress and the unfolded protein response. Interestingly, ABTL0812 also induced transcriptional repression and destabilization of MYCN, a major oncoprotein in NB. Finally, ABTL0812 showed a good combination profile with other chemotherapeutic drugs, and a synergistic effect when combined with the differentiating agent 13-*cis*-retinoic acid.

In conclusion, our results support that ABTL812 mechanism of action may represent an alternative approach to provide safer and more effective anti-cancer therapeutic strategies in pediatric tumors.

Resumen

El neuroblastoma (NB) es el tumor sólido extracraneal más común en la infancia y el tercer cáncer más común en niños. Los NB de alto riesgo (HR-NB) se caracterizan por ser muy agresivos y desarrollar resistencias a terapia. Por ello, el HR-NB sigue siendo un obstáculo para los oncólogos pediatras, ya que no existen opciones terapéuticas efectivas.

El ABTL0812 es un fármaco antitumoral *first-in-class* que actualmente está bajo ensayos clínicos de fase Ib/IIa para pacientes adultos con tumores sólidos avanzados. Dichos ensayos están dando muestras de una excelente tolerabilidad por parte del ABTL0812. Estudios previos han descrito que el mecanismo de acción del ABTL0812 está basado en la interrupción de la vía de señalización de AKT/mTOR. Dado que (1) esta vía está constitutivamente activada en los HR-NB y correlaciona con mal pronóstico y quimioresistencia, y que (2) el eje PI3K/AKT/mTOR integra dianas terapéuticas relevantes para el HR-NB, nos propusimos averiguar si el ABTL0812 podría usarse para el tratamiento de los pacientes con HR-NB.

Para esto, se analizó el potencial terapéutico del ABTL0812 *in vitro* en un panel de líneas celulares clínicamente representativas de NB. Todas las líneas exhibieron una sensibilidad similar, independientemente de su perfil genético. Notablemente, el ABTL0812 produjo sus efectos citotóxicos sin ser genotóxico o causar daños en el DNA, por lo que sería esperable una menor aparición de efectos secundarios. Asimismo, la administración oral de ABTL0812 en xenografts de HR-NB inhibió el crecimiento tumoral y demostró una alta tolerabilidad. Además, nuestros resultados desvelaron que el ABTL0812 inducía la muerte celular del NB a través de la activación a largo plazo del estrés de retículo endoplasmático i la respuesta a proteínas desplegadas. Remarcablemente, el ABTL0812 también indujo la represión de la transcripción y desestabilización de MYCN, una oncoproteína de gran relevancia para el NB. Finalmente, el ABTL0812 exhibió un buen perfil de combinación con otros fármacos quimioterapéuticos y un efecto sinérgico en combinación con el agente de diferenciación 13-*cis*-ácido retinoico.

En conclusión, nuestros resultados sugieren que el mecanismo de acción del ABTL0812 podría representar una vía de aproximación alternativa para proporcionar terapias más seguras y efectivas a los pacientes con tumores pediátricos.

INDEX

INDEX

ABBREVIATIONS

Abbreviations

(v/v)	Volume/volume
^{31}I-mIBG	131I- metaiodobenzylguanidine
13-cRA	13-cis-retinoic acid
ABTL	ABTL0812
ACD	Autophagic cell death
AHSCT	Autologous hematopoietic stem cell transplantation
ALK	Anaplastic lymphoma kinase
ALT	Alanine transaminase
AMP	Adenosine monophosphate
AMPK	AMP-activated protein kinase
ARID1A/1B	AT-rich interactive domain 1A and 1B
AST	Aspartate aminotransferase
ATCC	American Type Culture Collection
ATF4	Activating transcription factor 4
ATF6	Activating transcription factor 6
ATG	Autophagy related protein
ATP	Adenosine triphosphate
ATRX	α-thalassemia/mental retardation syndrome X-linked
AU	Arbitrary units
AURKA	Aurora kinase A
BAD	Bcl2-associated agonist of cell death
BAK	Bcl-2 homologous antagonist/killer
Bcl-2	B-cell lymphoma 2
Bcl-x_L	B-cell lymphoma-extra large
BID	BH3-interacting domain death agonist
BMP	Bone morphogenetic protein
BSA	Bovine serum albumin
C3	Caspase-3
Ca^{2+}	Calcium
CaMKII	Calcium/calmodulin-dependent protein kinase type II alpha chain
CASP8	Caspase-8

CBC	Complete blood count
CDDP	Cisplatin
cDNA	Complementary DNA
CHMP	Committee for Medicinal Products for Human Use
CHOP	C/EBP homologous protein
CK-NAC	Creatin kinase enzymatic activity
CNA	Copy number alteration
CNV	Copy number variant
COG	Children's Oncology Group
Ct	Control
CT	Computed tomography
DDR	DNA damage response
DI	DNA index
DMSO	Dymethil sulfoxide
DNA	Deoxyribunucleic acid
DRAM	Damage-regulated autophagy modulator
EFS	Event free survival
eIF2α	Eukaryotic initiation translation factor 2α
EMA	European Medicines Agency
ER	Endoplasmatic reticulum
ERAD	ER-assisted degradation
ERSE	ER stress response element
FBS	Fetal bovine serum
FBW7	F-box/WD repeat-containing protein 7
FDA	Food and Drug Administration
FGF	Fibroblast growth factor
GAPDH	Glyceraldehyde-3-phosphate dehydrogenase
GD2	Disialoganglioside
GM-CSF	Granulocyte-macrophage colony-stimulating factor
GNB	Ganglioneuroblastoma
GRP78	Glucose-regulated protein 78
GSK3β	Glycogen synthase kinase 3β
GWAS	Genome-wide association studies

H2AX	Histone H2AX
HCQ	Hydroxychloroquine
HR-NB	High-risk neuroblastoma
HSP90	Heat shock protein 90
IC_{50}	Half maximal inhibitory concentration
IDRF	Image-defined risk factor
IL-2	Interleukin-2
IMDM	Iscove's Modified Dulbecco's Medium
INPC	International Neuroblastoma Pathology Classification
INRG	International Neuroblastoma Risk Group
INGRSS	International Neuroblastoma Risk Group Staging System
INSS	International Neuroblastoma Staging System
Ip	Intraperitoneal
IRE1	Inositol-requiring enzyme-1α
ITS	Insulin-transferrin-selenium supplement
JNK1	c-Jun N-terminal kinase 1
L27	60s ribosomal protein L27
LDH	Lactate dehidrogenase
LC3-I	Cytosolic-associated protein light chain 3
MAX	Myc-associated factor X
MAT	Myeloablative therapy
Mcl-1	Myeloid cell leukemia 1
MDR	Multidrug-resistance
MEM	Minimum Essential Medium
mTOR	Mammalian target of Rapamycin
MRD	Minimal residual disease
mRNA	Messenger RNA
miRNA	Micro RNA
MRD	Minimal residual disease
MRI	Magnetic resonance imaging
MSKCC	Memorial Sloan Kettering Cancer Center
MYCN	V-Myc avian myelocytomatosis viral oncogene neuroblastoma derived homolog
NANT	New Approaches to Neuroblastoma Therapy

NB	Neuroblastoma
NC	Neural crest
NDDS	New Drug Development Strategy
NTRK1	Neurotrophic tyrosine kinase receptor type 1
ODD	Orphan Drug Designation
OMS	Opsoclonus myoclonus syndrome
OS	Overall survival
PA	Pepstatin A
PARP-1	Poly (ADP-ribose) polymerase-1
PBS	Phosphate buffered saline
PDX	Patient-derived xenograft
PERK	Protein kinase RNA-like endoplasmatic reticulum kinase
PET	Positron emission tomography
PHECC	Public Health England Culture Collections
PHOX2B	Paired like homeobox 2b
PI	Propidium iodide
PI3K	Phosphatidylinositol-4,5-bisphosphate 3-kinase
PMAIP1	Phorbol-12-myristate-13-acetate-induced protein 1
PRAS40	Proline-rich AKT substrat
PUMA	p53 up-regulated modulator of apoptosis
PVDF	Polyvinylidine diflouride
qRT-PCR	Quantitative reverse transcription polymerase chain reaction
QVD-OPh	Quinolyl-valyl-O-methylaspartyl-[2,6-difluorophenoxy]-methyl ketone
RA	Retinoic acid
RARE	Retinoic acid response element
RARR	Retinoic acid response region
RET	Rearranged during transfection
RIDD	Regulated IRE1-dependent decay
RNA	Ribonucleic acid
RT	Reverse transcription
S9	9000 supernatant fraction
SA	Sympathoadrenal
SCA	Segmental chromosomal aberration

SEM	Standard error of the mean
SEER	Surveillance, Epidemiology and End Results program
SIOPEN	Society of Pediatric Oncology Europe Neuroblastoma
siRNA	Small interfering RNA
SNP	Single nucleotide polymorphism
TBI	Total body irradiation
TBS-T	Tris-buffered saline with Tween-20
TRB-3	Tribbles homolog 3 protein
TERT	Telomerase reverse transcriptase gene
TRIB3	Tribbles homolog 3 gene
TrkB	BDNF/NT-3 growth factors receptor
TSC2	Tuberous **s**clerosis **c**omplex **2**
ULK	Unc-51 like autophagy activating kinase
UPR	Unfolded protein response
UPS	Ubiquitin-proteasome system
USP7	Ubiquitin-specific protease 7
XBP1	X-box binding protein 1
VPS34	Vacuolar protein sorting
WB	Western blot

INTRODUCTION

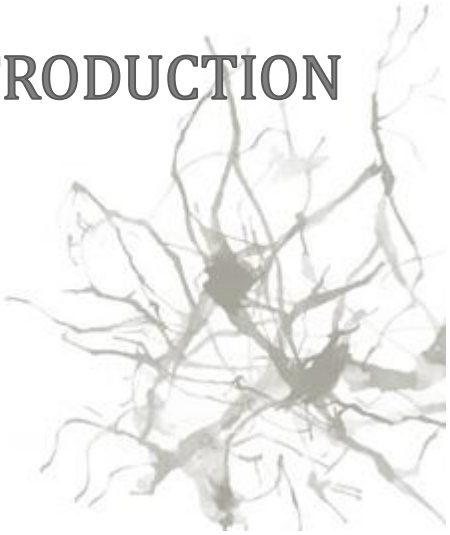

1. Introduction

1.1 Neuroblastoma

From 1975, advances in childhood cancers treatments and supportive care have substantially improved the overall 5-year survival rate to approximately 80%. For many pediatric cancers, such progress has been made redressing treatment modalities introduced decades ago with corrections made to improve disease-free survival while minimizing treatment-related morbidity. However, such increase in average survival holds on steady advances for some cancers, primarily leukemias and lymphomas, whereas improvements for a number of solid tumors have halted in a plateau over the past decades, which remain at very low rates of survival. Thus, unfortunately, cancer continues being the second leading cause of death (following accidents) in children aged five to fourteen years in the developed countries. Moreover, surviving patients still may remain at risk of recurrence or progression of their primary cancer and at an increased risk of developing subsequent long-term and late effects derived from aggressive therapies, such as other malignancies, chronic diseases, and functional impairments. Considering this scenario, better understanding of treatment-related toxicities is needed to guide the design of more effective and safer treatments. Furthermore, it would also be essential to delve into cellular pathways promoting cell growth and survival in childhood cancer, increase the number of pediatric clinical trials and ease cooperation among national and international childhood cancer research groups to achieve sustained progress in childhood cancer management [1,2].

The most common childhood cancers include leukemias and lymphomas, central nervous system tumors (CNS), neuroblastomas (NB), renal and bone tumors, soft tissue and epithelial sarcomas and gonadal germ cell tumors (Figure 1). Among them, the most diagnosed cancers in children are lymphoid leukemia, neuroblastoma and non-Hodgkin lymphoma [2].

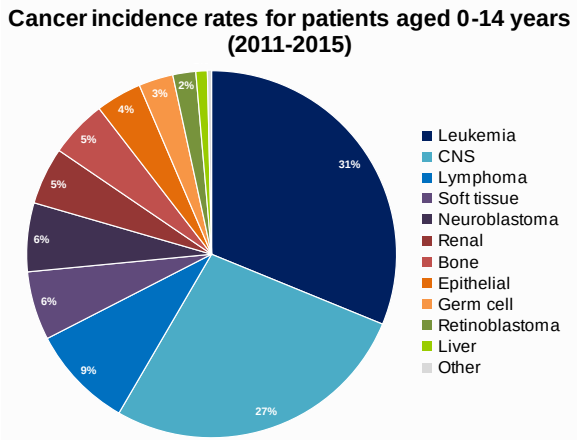

Figure 1. Childhood cancer incidence rates (2011-2015). Age-adjusted and age-specific (0-14 years) SEER cancer incidence rates from 2011 to 2015 (US population).

NB is the third most common childhood cancer and the most prevalent extracranial solid tumor of the infancy, representing 8-10% of all diagnosed childhood cancers in USA and Europe, and represents ~15% of all cancer-related deaths in the pediatric population. Despite being the most common malignancy diagnosed during the first year of life, NB is considered an ultra-orphan condition, with less than one thousand new cases per year in North America. Nearly 500 new cases are reported annually, and its incidence in North America and Europe is 10.5 cases per million in children under fifteen years of age. With a median age at diagnosis of approximately nineteen months, most patients are diagnosed between birth and five years of age. Ninety percent of the cases are diagnosed before the age of five, the 30% of which are diagnosed by the first year of age. Less than 10% of the patients are diagnosed older than ten years of age. Although NB occurs rarely in adolescents and young adults, outcomes are much poorer in this age group [3–6]. The incidence of NB is slightly higher among boys than girls (1,2:1) and it occurs more frequently in white populations (9,7 cases per million) than black populations (6,8 cases per million), although individuals with African and Native-American heritage have a higher prevalence of malignant phenotype and worse event-free survival than individuals from European pedigree [7–9].

NB has a broad pattern of clinical presentation, behavior and outcome. Prognosis ranges from spontaneous and complete regression to aggressive, drug-resistant, metastatic, refractory tumors that make NB run for the highest morbidity and mortality rates among childhood cancers. In general, outcomes in patients with NB have improved over the last thirty years with 5-year survival rates rising from 52% to 74%. However, this progress is mainly attributable to increased cure rates among patients with the more benign form of the disease. While low-risk NB 5-year survival rates reach up to 92% of patients, the rates among children with high-risk NB (HR-NB) remain below 50%, and less than 10% in those patients that relapse, despite dramatic escalations in the intensity of therapy provided [4,5,7,10,11]. This clinical course heterogeneity is characterized by many factors such as age at diagnosis, stage of disease, and distinct biologic features of the tumor that predict survival outcomes. In the following sections, the current understanding of NB biology, clinical presentation, diagnosis and risk stratification, based treatments, novel therapies and challenges of this disease will be exposed.

1.1.1 Neuroblastoma origins

NB is an embryonic neuroendocrine tumor. Embrionary tumors arise during intrauterine or early postnatal ages from an immature organ or tissue. In the case of NB, it is thought to be originated *in utero* from the primitive neuroectodermal cells of the developing sympathetic nervous system, probably from sympathoadrenal (SA) progenitor cells that later on differentiate to sympathetic ganglion cells or adrenal chromaffin cells.
It is widely accepted that embryonic tumors initiate during a time frame of the tissue maturation process when rapid cell expansion is quickly followed by an orderly transition to a terminally differentiated state. At that point, the corresponding progenitor cells from normal embryogenesis are tough to suffer a first hit that allows them to continuously over-proliferate. Around/after birth, a second hit may confer these cells a mechanism for surviving in the early postnatal environment, transforming them in pre-cancerous cells. Finally, a third hit entailing genomic instability will sentence them to become cancer cells (Figure 2). Thus, in the NB context, understanding the development of neural crest-derived SA system can help comprehend and indentify pathways involved in tumor initiation in neuroblasts.

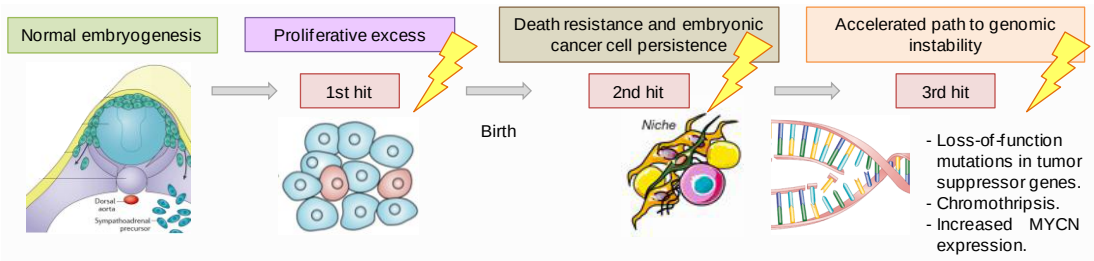

Figure 2. Model of embryonal tumorogenesis. The embryonal-to-cancer cell transtition takes place in early childhood. Malignant transformation of embryonal cells need three hits to develop: (1) prenatal proliferative excess in the tissue of origin, (2) acquisition of mechanisms to survive in the post-embryogenic and post-natal environment and (3) an accelerated pathway towards genomic instability.

The neural crest (NC) is a transient embryonic cell population that arises between the third and fifth week of pregnancy during gastrulation and neural tube formation (Figure 3A). During development, NC cells migrate extensively from the neural tube via epithelial-to-mesenchymal transition and differentiate into diverse tissues, including much of the craniofacial skeleton, sympathetic and peripheral nervous system, adrenal chromaffin cells and melanocytes. Development, maintenance, and differentiation of this multipotent cell population are highly complex processes that rely on spatially and temporally regulated extrinsic signals. Mutations or imbalances during any of these processes may generate tumor initiating neuroblasts [3,10].

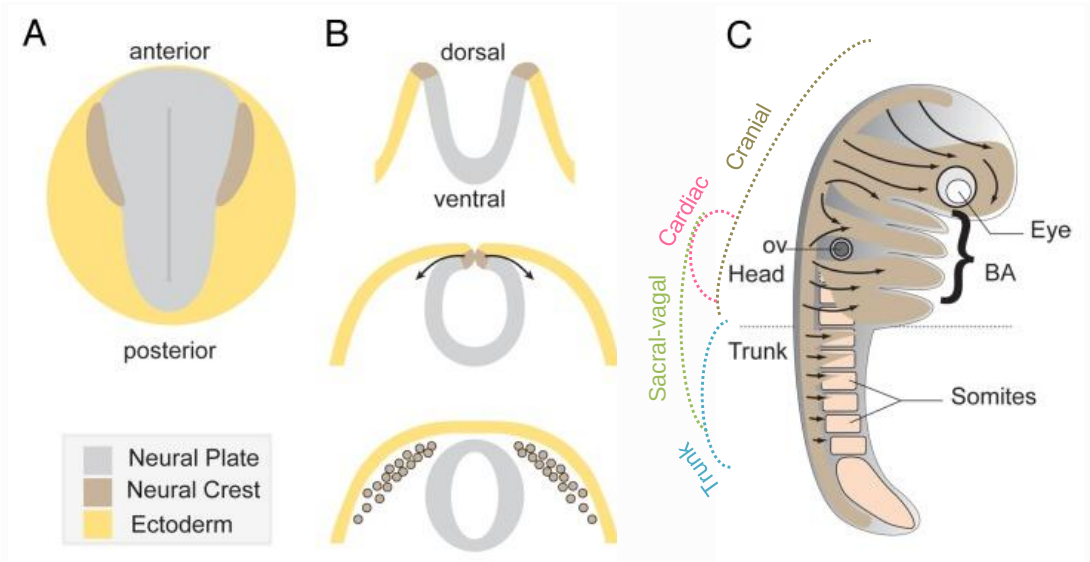

Figure 3. Neural crest formation, delamination and migration. (A) Dorsal view of a vertebrate embryo at early gastrulation stage (3rd pregnancy week). (B) Neural tube formation, neural crest delamination and migration. (C) Principal NC cells migratory routes through the embryo. Figure adapted from [12].

Primitive neural tube cells induction for NC specification is mediated by interconnected BMP, WNT, FGF and Notch/Delta signaling pathways. Following the expression of NC priming genes, another set of transcription factors is activated to maintain this NC in a pluripotent state. It deserves to be mentioned that the main factors involved in progenitor pluripotency maintenance are c-Myc and related MYCN. Of note, *MYCN* amplified NB are typically high-grade, aggressive cancers, consisting of primarily undifferentiated or poorly differentiated neuroblasts. Hence, as will be further discussed, *MYCN* amplification is one of the most relevant markers of poor prognosis in NB [13].

A third wave of transcription factors coordinate NC delamination (also referred as epithelial-mesenchymal-transition) and migration. Sox9, Sox10, FoxD3, Snail2 and Twist1 are transcription factors involved in this stage. Delamination enables NC cells to migrate from the developing neural tube to many primitive anatomical structures for further speciation and differentiation (Figure 3B). Migratory NC cells can be broadly subdivided into four functional types: cranial, cardiac, sacral-vagal and trunk (Figure 3C). Trunk NC cells are restricted to become SA precursors. They aggregate at the dorsal aorta to develop into cells of the peripheral nervous system, including sympathetic ganglia and the adrenal gland, the main sites in which NB arises. PHOX2B transcription factor and BMP are key elements to prime NC cells to SA differentiation and acquire neuronal characteristics [3,7,8]. Transient high expression of MYCN at this point is crucial to regulate NC migration and expansion; then, after directing cells dispersion, MYCN protein levels gradually decrease in differentiating sympathetic neurons [10,14]. The data suggests that NB initiation may occur at an embryonic period during NC migration or SA speciation due to continued MYCN expression. *PHOX2B* is another gene whose

mutations and loci loss (4p13) are considered first hits in NB pathogenesis [6,15] (Figure 4).

The second hit is tough to happen during final stage of sympathoadrenal maturation, when substantial cell death occurs to get rid of excessive cells generated during embryogenesis. Local nerve growth factor (NGF) deprivation characterizes this remodeling period of the nervous system. Embryonic cells which have already undergone abnormal genetic changes would be able to persist and proliferate through cell death signals in this prenatal and postnatal environment. Death resistance gain coupled to aberrant continued MYCN expression represents a potential pathological step towards cancer that will be consolidated with the acquisition of additional alterations leading to postnatal malignant cells transformation [14].

These facts are consistent with the hypothesis, based on differentiation markers expression patterns, that the earliest cell of origin for NB seems to be a trunk NC cell which has not received or responded to factors that determine sympathetic ganglion or chromaffin cell fate and neither responds to trophic factors withdrawal [14]. Nevertheless, delamination, migration and differentiation of NC cells and final shaping of the SA nervous system are regulated by a complex series of epigenetic and transcriptional programs, so the totality or precise molecular hits that give rise to NB are still unknown.

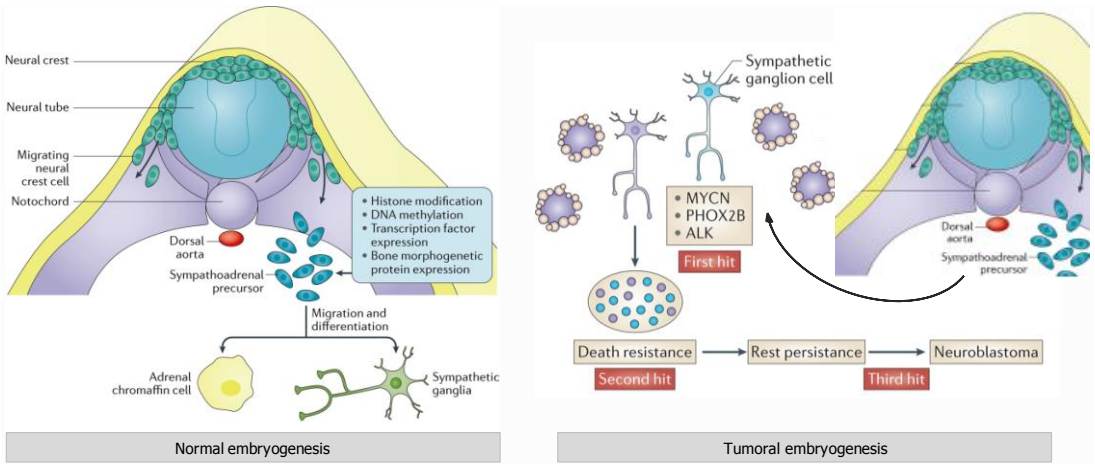

Figure 4. Neural crest development and NB pathogenesis. During development, neuroblast progenitors migrate from the NC around the neural tube to a region immediately close to the dorsal aorta. At this site, they become SA precursors and undergo speciation into mature neurons of the sympathetic ganglia or chromaffin cells of the adrenal medulla. Delamination, migration and differentiation are tightly regulated by epigenetic events and expression of MYCN, BMPs and Phox2b among other transcription factors. Alterations in this process like sustained expression of the proto-oncogen MYCN or mutations on PHOX2B and ALK may bring on the first hit to transform SA progenitors into neuroblastoma cancer cells. Figure adapted from [8,14].

1.1.2 Neuroblastoma predisposition

There have not been identified any strong or consistent environmental or genetic risk factors associated with NB. Nevertheless, although most cases of NB are sporadic, familiar NB represents 1-2% of cases; these rare cases provide insight into NB genetic etiology. Two autosomal dominant genes with incomplete penetrance have been associated to hereditary cases of NB: *PHOX2B* and *ALK*. Loss-of-function mutations in *PHOX2B* have been detected in patients with Hirchsprung disease and other neurochristopathies, which co-segregate with syndromic NB. PHOX2B mutant proteins appear to be oncogenic in a dominant negative manner and prevent appropriate NC maturation. Germline gain-of-function mutations in *ALK* were identified in 2008 as the main predisposing factor for familiar NB (Figure 5). However, the "second hit" mutation (following Knudson's "two-hit" model) has not yet been identified. Additional germline mutations likely to predispose to NB can be either inherited or arise *de novo*, but no accepted algorithm is available to determine who should be screened for germline mutations or how to counsel families in which a child has a clear predisposition allele for NB. The lack of mutations found in tumors at diagnosis and recurrent patterns of whole chromosome or large segmental DNA copy number alterations suggest that NB predisposition is genetically heterogeneous, and initiation of tumorigenensis could need multiple alterations [6–8,16,17].

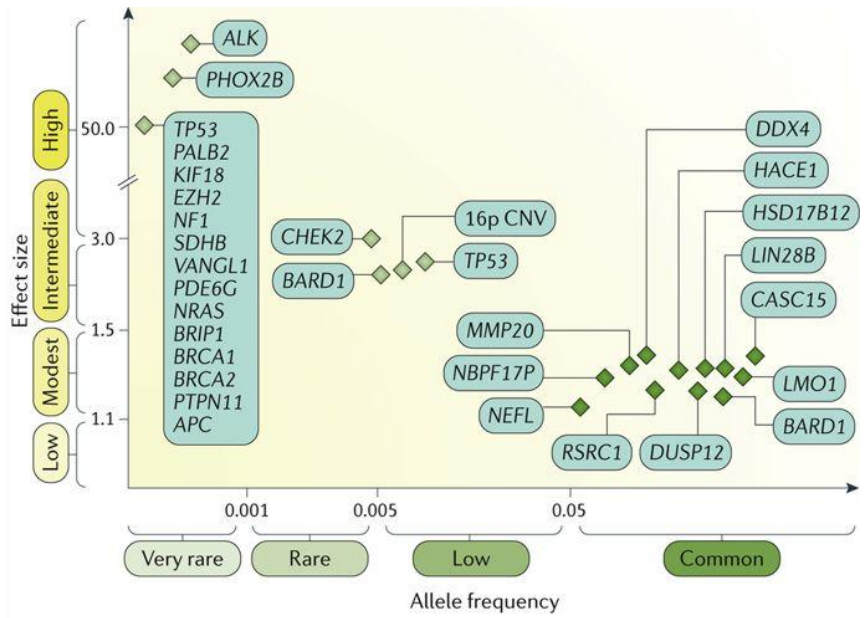

Figure 5. Genetic predisposition to NB. *ALK* and *PHOX2B* mutations cause familial NB with high penetrance. *ALK* and *PHOX2B* mutant alleles are very rare in the population and are inherited in an autosomal dominant Mendelian manner. Other genes with rare damaging mutations in the germline that can predispose to NB have been identified (*TP53*, *NRAS*, *BRAC2,* etc.), but the clinical relevance of many of these mutations remain to be determined. Several common polymorphisms (*BARD1*, *LMO1*, etc.) that individually have a relative small effect on tumor initiation can cooperate to lead to sporadic NB tumorigenesis. Figure adapted from [8].

Genome-wide-association studies (GWAS) have revealed germline genetic variants that may predispose to sporadic NB and be associated with tumor phenotype. GWAS-defined DNA variants suggest that the interplay between multiple common genomic variations, which taken individually have a relatively modest effect on susceptibility, may influence the initiation of tumorigenesis during neurodevelopment. Twelve highly significant and validated single-nucleotide-polymorphisms (SNPs) associated with NB susceptibility have been identified to date (Table 1 and Figure 5). Particularly, *LIN28B* has been found to have a crucial role in neurogenesis controlling cell growth and maintenance of an undifferentiated phenotype of neuroblasts. Polymorphic alleles within *LIN28B* that confer protein overexpression correlate with increased MYCN levels and with the development of HR-NB [18,19].

In addition, these studies have also shown that a relatively common copy-number variation at 1q21.1, alterations in the locus 16p12-13, and constitutional chromosome rearrangements or germline deletions on 1p36 and 11q14-23 locus are associated with familial NB [4,6–8,11,20–23]. Several of these DNA variations have been found to influence gene and protein expression and have potent oncogenic or tumor-suppressive functions in tumorigenesis and disease progression. Therefore, further studies are focusing on the translational potential of cancer susceptibility genes.

Table 1. SNPs related to NB susceptibility

Gene	Location	Risk group
DUSP12	1q23	Low
HSD17B12	11p11.2	
DDX4	5q11.2	
IL31RA	5q11.2	
FLJ22536	6p22	High
FLJ44180	6p22	
CASC15	6p22	
CASC14	6p22	
BARD1	2q35	
LMO1	11p15.4	
HACE1	6q16.3	
LIN28B	6q16.3	

1.1.3 Neuroblastoma genetic alterations

Many sporadic NB genetic features have been identified to correlate with clinical outcome and have been used for patient risk stratification and treatment selection for more than twenty years. The available data suggests that NB genetic aberration patterns fall into two broad categories: (1) tumors with whole chromosome gains, lack of structural changes, and hyperdiploid karyotype; and (2) tumors with segmental chromosomal aberrations (SCAs) and diploid DNA content. While the formers are associated with favorable prognosis, the latter tend to be associated with worse outcomes. SCAs include partial losses and gains of chromosomal regions predicted to encode tumor suppressors and oncogenes, respectively. Some of these cytogenetic changes are implicated in the pathogenesis and aggressiveness of NB tumors (i.e. *MYCN* amplification) and have proven to be useful in predicting clinical behavior [4,5,11,24].

1.1.3.1 Segmental chromosomal copy number alterations

Almost all high-risk neuroblastomas show recurrent segmental chromosomal aberrations. SCAs can arise from unbalanced chromosome translocations or gains and losses of smaller fragments due to defects in DNA maintenance or repair pathways. The most frequent SCAs detected in NB are segmental losses at 1p, 3p, 4p, 11q and 14q; and 1q, 2p, and 17q gains. The high frequency of SCAs coupled with the lack of recurrent mutations in protein-coding genes led to the hypothesis that chromosome deleted regions may contain tumor suppressor genes while the gained regions may harbor oncogenes. Although SCAs in 3p, 4p, 14q and 2p are relatively common, the most found in high-risk/stage 4 NB that behave as significant prognostic factors are 17q, 1p and 11q [22,24,25]. Trisomy of 17q occurs in over 50% of NBs representing the most frequent SCA in NB. Gain of 17q correlates with adverse clinical outcome, older age, *MYCN* amplification, diploidy and commonly occurs with 1p deletion [26,27]. Deletion of 1p occurs in 23-35% of NBs and is highly associated with *MYCN* amplification, HR-NB clinical features and poor prognosis [28]. For its part, loss of 11q is detected in up to 30-40% of NBs. Though they also correlate with poor prognosis, tumors with 11q deletion generally lack 1p deletions and *MYCN* amplification. Thus, it has been suggested they may represent a distinct tumor category in the subset of patients with advanced-stage disease without *MYCN* amplification [29,30].

Recent studies demonstrate that the prognostic impact of segmental alterations is more significant than the individual chromosome losses or gains. Comprehensive cytogenetic prospective studies should further determine whether the presence of SCAs provide valuable prognostic information to identify additional subsets of NB patients with aggressive disease, particularly within the *MYCN* non-amplified tumors. Therefore, detection of SCAs may become essential in the assessment of NB patients potentially replacing tests that detect single-gene losses or gains [24,31].

1.1.3.2 Tumor cell ploidy

DNA index (DI), DNA content or ploidy is the amount of DNA within the nucleus of tumor cells. Changes of total DNA content presumably result from mitotic dysfunction. DNA content has been used for risk assignment and is an important indicator of treatment success. NBs with a higher DNA content (DI>1), i.e. hyperdiploid or near-triploid tumors, carry whole chromosome copy number changes and are associated with lower tumor stage, better response to therapy and an overall more favorable prognosis than diploid tumors (DI=1). Diploidy and/or tetraploidy are more common in advanced-stage tumors and correlate with SCAs, *MYCN* amplification, poor outcome and refractory disease. Nevertheless, the prognostic value of ploidy on the outcome of NB is more accurate in infants less than twelve months of age and patients with disseminated disease. This is probably because older patients tend to have structural chromosome rearrangements other than hyperploidy [32–34].

1.1.3.3 *MYCN* amplification

The *MYCN* oncogene (*V-Myc avian myelocytomatosis viral oncogene neuroblastoma derived homolog,* so-called because of its identification in NB cells) is located at the distal short arm of chromosome 2 (2p24.1). *MYCN* amplification (>10 copies per cell) was identified in the early 80's as a prognostic factor and is present in approximately the 20-30% of NB tumors [35]. Although the exact mechanism by which amplification occurs is unknown, it usually results in fifty to four-hundred gene copies per cell, leading to the production of abnormally high levels of *MYCN* mRNA and protein [13,36]. The incidence of *MYCN* amplification in high-risk tumors is about 50% [4,10]. Many studies have demonstrated its strong correlation with rapid disease progression, poorly differentiated tumors, invasive-metastatic behavior, resistance to treatment and significantly worse outcome, independently of age and disease-stage at diagnosis. Thus, it remains one of the strongest poor prognosis indicators in NB and is used as a biomarker for risk stratification [6,11,13,37,38].
In addition to NBs, *MYCN*-amplification is observed in other tumors of the nervous system like medulloblastomas, retinoblastomas, astrocytomas, meningiomas and glioblastoma multiforme. Furthermore, it has been also described in the following non-neuronal tumors: castration-resistant neuroendocrine prostate cancers, T-cell lymphomas, leukemias, rhabdomyosarcomas, Wilms tumors, breast tumors, small-cell lung cancers, and pancreatic tumors (reviewed in [39].

MYCN is a member of the *MYC* proto-oncogenes family together with *MYC* (encoding C-MYC) and *MYCL* (encoding L-MYC). All three tumor-associated *MYC* genes have a characteristic structure composed of highly conserved functional domains interspersed with areas of diminished conservation. These subtle differences encode for discrete, independent, domains of the individual MYC polypeptides, although overall MYC proteins share similar functional roles [40–42]. MYCN is a master regulator of transcription specifically expressed in neuronal precursor cells during normal embryonic development

(until two-three months of age). Before this age, elevated levels of MYCN orchestrate cell proliferation and expansion of the developing nervous system; when embryogenesis is finished, MYCN levels diminish and allow cells to enter in a resting G0 phase and differentiate [10,43]. Clinical and experimental observations have shown that *MYCN* misexpression in migrating neural crest cells is an initiating event of NBs. Studies in transgenic mice exhibited that overexpression of MYCN is sufficient to drive neuroblast transformation and development of NB [44]. This is due because *MYCN* amplification turns *MYCN* into a proto-oncogene able to activate genes that affect cancer hallmarks such as sustained growth and proliferation, vasculogenesis, metastasis, genomic instability, ribosome biogenesis, metabolism, apoptosis; and repress genes that drive differentiation and cell adhesion. Therefore, even though MYCN's short half-life, the elevated MYCN steady-state levels in *MYCN*-amplified cells (over one-hundred times higher than normal cells) forces cells to be permanently entering G1 phase, unable to step out into G0 [42,45,46].

MYCN encodes for a 60kDa nuclear transcription factor consisting of an N-terminal transcription activator domain and a C-terminal DNA binding/protein interaction domain. MYCN is activated by phosphorylation and can both promote and repress the expression of its target genes. Phosphorylation is also important for the regulation of MYCN protein stability [40,47,48]. The DNA-binding capacity of MYCN is mediated through a basic helix-loop-helix (b-HLH) and a leucine-zipper motif (LZ) comprised in the C-terminal domain. The b-HLH-LZ domain allows MYCN to interact and form heterodimers with the b-HLH-LZ protein MAX in the nucleus. The resulting MYCN/MAX complex binds to DNA with high affinity and specificity to CACA/GTG sequences (also termed E-box sequences) found in the promoters of its target genes [42,49,50]. It is believed that E-boxes are present in ~25% of known promoters, which explains the great impact of MYCN overexpression in the whole cell transcriptome. Although the presence of an E-box enhances MYCN chromatin binding, recent publications demonstrate that E-boxes are not sufficient to explain occupancy of promoters by MYCN/MAX complexes. Most likely, along with direct DNA interaction, interplay with resident chromatin proteins and other players of the transcription machinery, plus recruitment of nuclear transcription cofactors to its N-terminal, seems to be essential to target MYCN/MAX to its chromatin binding sites and assist transcription of specific genes. MYCN transcriptional repression activities are supported by the recruitment of co-repressors, such as EZH2, Sp1 and MIZ1. Interaction between MYCN and the EZH2 methyltransferase subunit of the polycomb repressor complex 2 suggests that MYCN could be mediating genetic inhibition through methylation of target promoters [51]. Concurrently, interaction with Sp1 and MIZ1 at promoters is thought to silence gene expression via recruitment of the histone deacetylase HDAC1 [52] (Figure 6). Adding further complexity to this system, there are evidence that MYCN influence extends beyond its role as a classic transcription factor for individual genes. MYCN also regulates miRNAs and long noncoding RNA expression, mRNA translation and global transcription through re-organization of euchromatin by regulation of histone acetylation/methylation or displacement of nucleosomes [41,47,53–55]. As a whole, MYC proteins activate and repress transcription of approximately the 10-15% of the entire

genome. This major regulation is held on the theory that MYC proteins act on a large number of genes transcribed by all three RNA polymerases, yet only studies directly situating MYCN at RNA polymerase II promoters have been published. Genes targeted by MYCN involve diverse cellular functions in malignancy: cell proliferation, differentiation, DNA repair, apoptosis, metabolism, angiogenesis, nucleotide biosynthesis, ribosomal assembly and cell adhesion and migration [45,56–60].

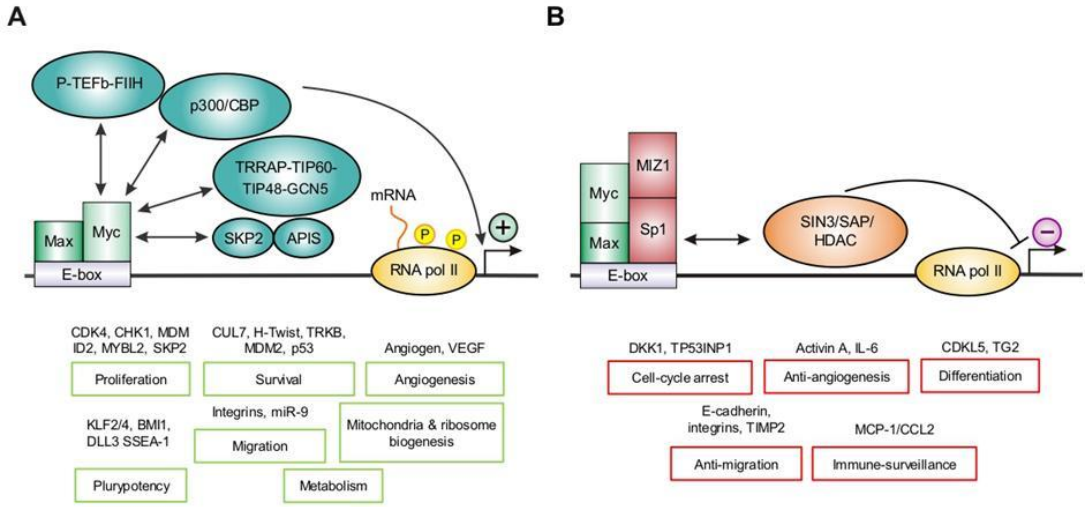

Figure 6. Cellular processes controlled by MYCN transcriptional activity. (A) Transcription activation by MYCN/MAX dimer binding to an E-box sequence. Recruitment of histone acetyl transferases (P300/CBP and TRRAP-TIP60/TIP48/GCN5 complexes) leads to an open chromatin state; while MYCN-promoted phosphorylation of the C-terminal domain of RNA polymerase II (through P-TEFb and TFIIH) stimulates transcriptional elongation. (B) MYCN/MAX-mediated repression. Binding to co-repressors MIZ1 and Sp1, recruitment of histone deacetylases (HDAC) through the adaptor protein SIN3, and recruitment of DNA methylase 3a (Dnmt3a; not shown), represses the chromatin and inhibits transcription of target genes. Figure adapted from [42].

1.1.3.4 *ALK* mutations or amplification

The anaplastic lymphoma kinase *(ALK)* (chromosome 2p23) encodes for *a* 200kDa cell-surface tyrosine kinase receptor involved in nervous system development. Pathogenic *ALK* gain of function mutations have been found in familial and sporadic NB tumors (~50% and ~10% of cases, respectively). *ALK* abnormalities include copy number gain (2-3%) and missense activating mutations (8-14%). *ALK* mutations in sporadic NB tumors are observed in tumors from all clinical risk groups and are associated with poor outcome in 5–15% of cases. High ALK protein levels also correlates with poor outcomes independent of mutation status [61–64]. *ALK* mutations are mainly concentrated in three residues from the kinase domain: R1275, F1174 and F1245, which can be substituted by different aminoacids (Figure 7). The common ALK^{F1174L} mutation has been found to be able to drive NB in mice models, hence, *ALK* is considered an oncogenic driver of NB [65,66]. Furthermore, *ALK* amplification usually correlates with *MYCN* amplification, supposedly

because both are closely located in chromosome 2p. Specially, F1174L mutation is highly associated with *MYCN*-amplification. It is also estimated that *ALK* takes part in MYCN overexpression by enhancing *MYCN* transcription and stabilization. Thus, patients harboring both alterations have worse event-free survival expectations than patients with none [67–69]. For all of this, ALK is considered a predictive biomarker and therapeutic target for a selected group of NB patients. However, early-phase clinical trials using targeted therapy against ALK in NB have been disappointing and further investigations require patients stratification based on ALK alterations [67,70,71].

Besides NB, aberrant ALK protein activity has been described in other tumors such as anaplastic large-cell lymphoma, diffuse large B-cell lymphomas, inflammatory myofibroblastic tumors, non-small-cell lung cancer, squamous cell carcinoma, melanoma, glioblastoma multiforme, retinoblastoma, rhabdomyosarcomas, Ewing sarcoma, some subtypes of breast cancer, malignant fibrous histiocytoma and leiomyosarcoma (for a review see [72–74].

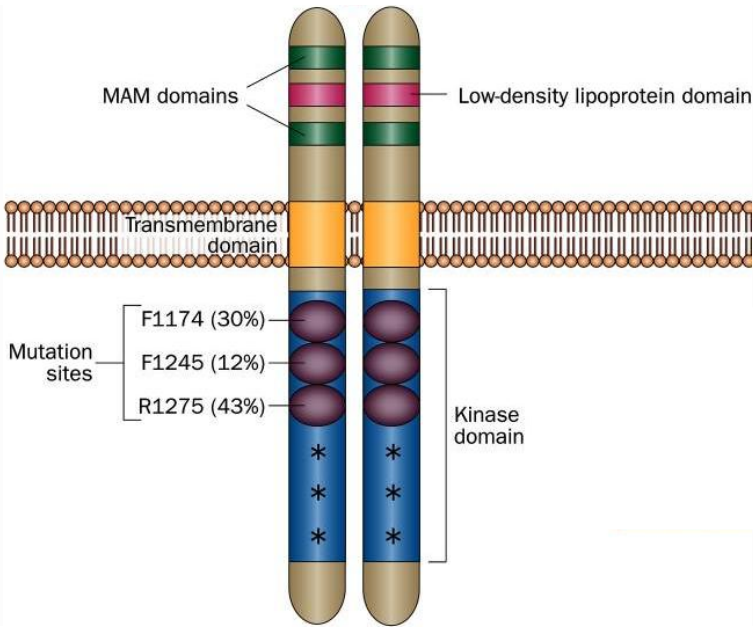

Figure 7. Schematic representation of ALK protein structure and mutations found in NB. ALK is composed by an extracellular domain that contains two MAM domains and a low-density lipoprotein domain, a transmembrane domain and an intracellular kinase domain. Mutations in the residues R1275, F1174 and F1245 are three most common ALK mutations in NB (frequency provided in brackets). Other low frequency mutations (>20) are noted with an asterisk. Figure adapted from [71]

1.1.3.5 Other somatic genetic alterations

Over the past few years, some extra recurrently mutated genes have been identified in NBs, although the general frequencies of mutations are low or restricted to a few

subpopulations of patients. GWAS, whole exome, and whole genome sequencing studies uncovered mutations in *ATRX*, *TERT*, *ARID1A/1B*, *LIN28B*, *NTRK1*, *PTPN11*, *MYCN*, *TP53, PTPRD* and *NRAS* [18,21,75–80]. Below, some of the most remarkable candidates are summarized.

α-Thalassemia/mental retardation syndrome X-linked gene (*ATRX*) encodes a RNA helicase protein involved in chromatin remodeling, nucleosome assembly and telomere maintenance. Otherwise, it is also thought to have a role in epigenetic regulation [81]. *ATRX* loss-of-function mutations are detected in approximately 10% of NB cases, but this percentage increases up to 44% in the subset of children older than 12 years with metastatic disease. Loss of *ATRX* expression correlates with chronic progressive chemo-resistant disease, late recurrences and poor outcome. However, *ATRX* mutations are usually mutually exclusive from *MYCN* amplification [4,76,82].

Other genes involved in chromatin remodeling that are thought to have a role in NB pathogenesis are the polycomb complex genes AT-rich interactive domain 1A and 1B (*ARID1A/1B*). Deletions and point mutations of *ARID1A* and *ARID1B* have been detected in approximately 11% of NB tumors and are associated with early resistance to therapy and low survival rates [78].

Recurrent genetic rearrangements in a region proximal to the promoter of telomerase reverse transcriptase gene (*TERT*) were recently described in approximately 20-25% of HR-NBs. Studies have shown that these mutations place *TERT* side to strong transcription enhancers confiscating its activity to increase expression of *TERT* [75,83]. Intriguingly, MCYN positively regulates *TERT* transcription but *TERT* mutations are usually not present in tumors with *MYCN* amplification. Thus, it is hypothesized that all HR-NBs require a way to activate *TERT* either by MYCN signaling or mutation of the proximal promoter region [8,76,82].

Finally, another gene that has been found mutated in NB is *NTRK1*, which encodes the tyrosin kinase receptor A (TRKA) [79,84]. The TRK receptors regulate growth and differentiation of the nervous system and are thought to have a role in NB pathogenesis. High expression of TRKA is normally found in low risk NBs and has been reported to indicate favorable prognosis [85–87], perhaps because it may mediate apoptosis or differentiation in this tumors. In addition, MYCN appears to down-regulate TRKA by deacetylation and/or methylation of *NTRK1* promoter to induce a repressed chromatin state [52,88,89]. On the other hand, high expression of TRKB (encoded by *NTRK2*) is found in unfavorable tumors, particularly those with *MYCN* amplification, and might provide a constitutive active autocrine survival pathway in HR-NB. It is assumed that the pathways induced by TRKB are implicated in resistance to chemotherapy and up-regulation of *MYCN* transcription [85,86,90].

1.1.4 Neuroblastoma clinical presentation and diagnosis

NB is a neuroendocrine tumor originated from the cells of the developing sympathetic nervous system. About 50% of NBs arise in the adrenal medulla while the rest originates along the paraspinal ganglia or other sympathetic ganglia, anywhere from the neck to the pelvis.

Most patients are asymptomatic with tumors that are incidentally diagnosed on routinely physical examinations. However, some patients do present clinical signs and symptoms tightly dependent on the site of the primary tumor, extent of metastatic disease and associated paraneoplastic syndromes. Approximately, half of patients present localized or regional disease at diagnosis. Primary tumors can arise from anywhere in the sympathetic nervous system but the majority does in the adrenal medulla (~50%). Primary site location is associated with age and outcome, and tumors occurring at the adrenal medulla predict poorer survival than tumors in other regions [4,91]. Whereas localized disease is often an incidental finding, large abdominal tumors can cause hypertension, abdominal distension and pain due to compression of abdominal viscera. Pelvic tumors may cause constipation, bladder dysfunction and low extremity pain or weakness. Thoracic tumors are more common in infants and can cause dysphagia, dyspnea, or rarely, thoracic outlet syndrome. Tumors closer to the neck might damage the cervical ganglion causing Horner syndrome, symptoms of which include ptosis, miosis, enophthalmos and anhidrosis. Tumors arising in any of these locations can grow along spinal nerves towards the spinal cord and invade the neural foramina, what can lead to spinal cord compression and neurological deficits such as progressive paralysis [5,8].

Children with extensive metastatic disease tend to be quite unwell at presentation. Regional lymph node spread is detected in 35% of patients at the time of diagnosis, whereas distant metastatic disease is detected in approximately the 50% of cases [4,8]. Metastases are disseminated through lymphatic and hematologic routes, and the most common sites include bone marrow and cortical bone. Nevertheless, infants can present a different pattern of metastases characterized by blue subcutaneous skin nodules (associated with a favorable prognosis) and massive liver infiltration, which might develop with respiratory distress, coagulation disorders or renal impairment. Metastasis in other organs can appear with bone pain, fever, weight loss, symptoms of anemia or thrombocytopenia, and proptosis, periorbital ecchymosis and visual impairment in the case of periorbital metastasis [92–94].

In a very rare phenomenon, NB can originate associated paraneoplastic syndromes. When tumor cells secrete vasoactive intestinal peptide, “VIPomas”, this can lead to intractable watery diarrhea in some patients [95]. Paraneoplastic presentation with opsoclonus myoclonus syndrome (OMS) has also been reported in 2-3% of patients. OMS is a rare neurological disorder associated with favorable NB tumors characterized by opsoclonus (spontaneous, rapid, multidirectional eyes movements), myoclonus (involuntary muscle twitching) and cerebellar ataxia. OMS neurologic symptoms are most

likely attributable to an autoimmune process against anti-neuronal bodies that cross-react with cerebellar tissue [96].

NB diagnosis requires a combination of laboratory tests, radiographic imaging and histopathological assessment of the tumor tissue. Tumor stage, pathology and prognostic molecular features are determined at diagnosis. According to these characteristics plus age at diagnosis, patients will be stratified in different risk groups.

The median age at diagnosis of NB is between eighteen and twenty-two months. Approximately 40% of patients are diagnosed at infancy (<1 year of age) and 90% of patients under five years of age. Age at diagnosis is an important risk factor: patients aged under eighteen months are more likely to have spontaneous regressing disease or to only require surgical management; whereas children older than eighteen months tend to have metastatic, life-threatening tumors, usually refractory to treatment. As for adolescents and adults, they rarely develop NB (<5% of all cases) but the disease usually has poor overall outcome in this age group [3–6,8,97].

The medical tests used to confirm diagnosis of a clinical suspicion of NB divide into five further pillars: complete blood works, urine and serum laboratory tests, radiographic imaging and metastatic evaluation, pathology assessment and tumor genomic characterization. Initially, a complete blood count, prothrombin and partial thromboplastin time, and levels of uric acid, electrolytes, creatinine and liver function indicators, should be tested. Urine composition should also be analyzed. Nearly all NB patients have increased levels of catecholamines or its metabolites (dopamine, homovanillic acid and vanillylmandelic acid) in the urine. The amount and ratios of chatecolamine metabolites detected correlate with the differentiation grade of tumor cells and is associated with biologically unfavorable disease [98]. Additionally, detection of larger neuron-specific enolase, lactate dehydrogenase or ferritin in serum has been described as NB unfavorable prognostic markers, even though they are not disease-specific [99–101] (Table 2).

NB imaging by computed tomography scan (CT) or magnetic resonance imaging (MRI) is used to determine extent of primary disease and evaluate the spread of regional or distant metastatic deposits. Radiographic imaging is a useful tool to delimit surgical excision and specify tumor staging as it reveals the presence of image-defined risk factors (IDRFs) [102]. In case of metastatic disease, ^{123}iodine-metaiodobenzylguanidine (^{123}I-mIBG) positron emission tomography/computed tomography scan (PET/CT) ensures localization of metastatic disease in soft tissues, bone and bone marrow (Table 2). ^{123}I-mIBG uses radiolabelled mIBG, a norepinephrine analogue that selectively concentrates in sympathetic nervous tissue. However, in NB patients non-avid for ^{123}I-mIBG (~10%) it can be substituted for ^{18}F-fluorodeoxyglucose or ^{99}technetium bone scintigraphy. Nevertheless, complete staging and diagnosis of metastatic disease would require tissue biopsies and bone marrow aspirates for histological examination [103–106].

Table 2. Medical tests for neuroblastoma diagnosis

Laboratory tests
Complete blood test
Prothrombin time and partial thromboplastin time
Electrolyte, creatinine, uric acid and liver function levels
Urine dopamine, HVA and VMA levels and ratios
NSE, ferritin and lactate deshydrogenase levels
Tumor imaging
CT or MRI of primary site, chest, abdomen and pelvis
CT or MRI of the head and neck if clinically involved
^{123}I-mIBG scan
^{18}F-fluorodeoxyglucose scan for ^{123}I-mIBG non-avid tumors
Pathology tests
Tumor biopsy with IHC (differentiation grade, MKI, stromal content)
Bone marrow aspirate and/or metastatic tissue biopsy with IHC
Molecular tests
MYCN FISH
aCGH or other study for SCAs
DNA ploidy
Optional: genomic sequencing for relevant mutations

HVA, homovanilic acid; VMA, vanillylmandelic acid; NSE, neuron-specific enolase; IHC, immunohistochemistry; MKI, mitosis-karyorrexis index; FISH, fluorescent *in situ* hybridization; aCGH, array comparative genomic hybridization; SCA, segmental chromosomal aberration.

Tumor histological characterization and the grade of neuroblastic differentiation are essential for NB diagnosis (Table 2). They are two of the major criteria to classify tumors into favorable and unfavorable categories as they are compelling risk factors proven to predict outcome. Additionally, the presence of stromal Schwannian cells and the mitosis-karyorrexis index (MKI) are other important histological features taken under consideration. Based on the histological evaluation, the International Neuroblastoma Pathology Classification (INPC) differentiates peripheral neuroblastic tumors in four categories with different clinical behavior: neuroblastoma, ganglioneuroblastoma intermixed, ganglioneuroblastoma nodular and ganglioneuroma (Table 3). The neuroblastoma category is further divided into three subtypes (undifferentiated, poorly differentiated and differentiating) depending on the grade of neuroblastic differentiation. Most NBs are undifferentiated tumors composed of immature small round blue cells (neuroblasts) with hyperchromatic nuclei that positively stain for neuron specific enolase, tyrosine hydroxylase, synaptophysin, and NB84. On the other hand, ganglioneuroblastomas (GNB) show partial histological neural differentiation, while ganglioneuromas are the most differentiated tumors, consisting of mature neurons clusters surrounded by a dense Schwannian cells stroma [7,107].

Table 3. International NB Pathology Classification

Category and subtype	Stroma development	Prognostic	MKI	Age (years)
Neuroblastoma				
Undifferentiated	Schwannian-poor (0 or <50%)	Unfavourable	Any	Any
Poorly differentiated	Schwannian-poor (0 or <50%)	Unfavourable	>4%	Any
		Unfavourable	Any	>1,5
		Favourable	<4%	<1,5
Differentiating	Schwannian-poor (0 or <50%)	Unfavourable	Any	>5
		Unfavourable	>4%	<1,5
		Unfavourable	>2%	1,5 to 5
		Favourable	<4%	<1,5
		Favourable	<2%	1,5 to 5
GNB nodular	Schwannian-rich/dominant/poor	Unfavourable/favourable		
GNB intermixed	Schwannian-rich	Favourable		
Ganglioneuroma	Schwannian-dominant	Favourable		

GNB, ganglioneuroblastoma; MKI, mitosis-karyorrexis index.

Tumor molecular biology is also assessed at diagnosis because it provides additional information to allocate tumor risk classification. *MYCN* amplification, diploidy and 17p, 17q and/or 11q SCAs are associated with poor prognosis. *MYCN* amplification is frequently determined using fluorescent *in situ* hybridization (FISH), but, in spite of this technique, determination of a *MYCN* genetic expression signature or increased MYCN protein levels might also correlate with poor outcome in tumors without *MYCN* amplification. For its part, ploidy and 17p, 17q and/or 11q SCAs are respectively assessed by flow cytometry and array comparative genomic hybridization (aCGH). Incorporation of next generation sequencing techniques to NB diagnosis would facilitate simultaneous assessment of amplifications, deletions, SCAs and other relevant mutations (i.e. *ALK* and/or RAS pathway proteins) from a single small tumor biopsy sample, allowing patients to early benefit from precision therapy [8,36,76].

1.1.5 Neuroblastoma staging and risk stratification

The International Neuroblastoma Staging System (INSS) has been the most widely accepted standard criteria for NB staging used for the past three decades. The INSS was principally based on the feasibility of surgical resection and metastases [108]. In 2009, the International Neuroblastoma Risk Group (INRG) task force (formed by the major international pediatric cooperative groups) published their recommendations for a new staging and risk group stratification system, the INGRSS. The INGRSS was designed to homogenize NB pretreatment risk groups to facilitate the comparison between risk-based clinical trials conducted by different cooperative groups internationally, hence providing insight into the best treatment strategies. Unlike the previous INSS, the INRGSS stratifies patients according to pre-treatment tumor characteristics that have been found to influence outcome in patients, being NB INGR stage one of them. The INRG stage is determined by radiological imaging based on the extent of disease at the time of diagnosis and image-defined risk factors (IDRFs). IDRFs identify elements that represent a life-threatening condition for the patient and/or threats for surgical resection (Table 4). Thus, IDRFs are predictive of worse event-free and overall survival.

Table 4. Imagine-defined risk factors in neuroblastoma

All sites
Tumor size
Tumor fragility
Tumor extension within two body compartments
Intraspinal tumor extension
Infiltration of adjacent organs/structures
Neck
Encasement of carotid, vertebral artery and/or jugular vein
Encasement of brachial plexus roots
Compression of the trachea
Extension to base of skull
Thorax
Encasement of subclavian vessels
Encasement of aorta and/or major branches
Lower mediastinal tumor
Compression of trachea and/or principal bronchii
Abdomen
Encasement of celiac axis
Encasement of superior mesenteic artery, aorta or vena cava
Encasement of iliac or hypogastric vessels
Compromise of kindey or ureter
Pelvis tumor crossing the sciatic notch

There are four INRG stages: local stages L1 and L2; and metastatic stages M and MS. L1 tumors are locally restricted to one body compartment and do not meet criteria for any IDRFs. L2 are locorregional tumors with the presence of one or more IDRF. Patients classified as M have distant metastasis; and MS stage describes a subset of patients under eighteen months of age with metastatic disease restricted to the liver, skin and/or bone marrow.

Together with the INGR stage, the whole of the tumor characteristics considered by the INGRSS classification are: INGR stage, patient age, histologic category, grade of tumor differentiation, *MYCN* amplification status, segmental chromosomal aberration events and DNA ploidy. Depending on the presence or absence of these prognostic factors, patients are stratified into very-low-risk, low-risk, intermediate-risk or high-risk groups, what aids clinicians to assign the treatment plan (Table 5). Very-low-risk is defined as an EFS of >85%, low-risk EFS is 75-85%, intermediate-risk EFS is 50-75% and high-risk EFS is <50% [109–111].

Table 5. Modified international neuroblastoma risk groups

INGR stage	Age (months)	Histologic category	Grade of differntiation	*MYCN*	Genomic profile	Ploidy	Risk group
L1	Any	GNB nodular, NB	Any	-	Any	Any	Very-low
L1/L2	Any	GN, GNB intermixed	Any	-	Any	Any	Very-low
L2	<18	GNB nodular, NB	Any	-	Favourable	Any	Low
L2	≥18	GNB nodular, NB	Differentiating	-	Favourable	Any	Low
MS	<12	Any	Any	-	Favourable	Any	Low
L2	<18	GNB nodular, NB	Any	-	Unfavourable	Any	Intermediate
L2	≥18	GNB nodular, NB	Differentiating	-	Unfavourable	Any	Intermediate
L2	≥18	GNB nodular, NB	Poor or undifferentiated	-	Any	Any	Intermediate
M	<18	Any	Any	-	Any	Hyperdiploid	Intermediate
M	<12	Any	Any	-	Unfavourable and/or diploid		Intermediate
MS	12-18	Any	Any	-	Favourable	Any	Intermediate
MS	<12	Any	Any	-	Unfavourable	Any	Intermediate
L1	Any	GNB nodular, NB	Any	+	Any	Any	High
L2	≥18	GNB nodular, NB	Poor or undifferentiated	+	Any	Any	High
M	12-18	Any	Any	-	Unfavourable and/or diploid		High
M	<18	Any	Any	+	Any	Any	High
M	≥18	Any	Any	-	Any	Any	High
MS	12-18	Any	Any	-	Unfavourable	Any	High
MS	<18	Any	Any	+	Any	Any	High

Actualization of the INRG pre-treatment classification (first published in [111]) with emergent genomic data and current treatment approaches. INRG, International Neuroblastoma Risk Group; GN, ganglioneuroma; GNB, ganglioneuroblastoma; NB, neuroblastoma; +, amplified; -, non-amplified; Favorable corresponds to absence of SCAs; Unfavorable corresponds to presence of SCAs.

1.1.6 Neuroblastoma clinical management

Two major international cooperative groups have been historically leading the establishment and introduction of therapeutic strategies for the treatment of NB, the Children's Oncology Group (COG) in the USA and the International Society of Pediatric Oncology European Neuroblastoma (SIOPEN) in Europe. COG and SIOPEN treatment guidelines depend on the patients' specific risk category. Successful patient tailoring according to risk stratification has been improved in the last few years thanks to the better understanding of NB biology and pre-treatment prognostic risk. This deeper knowledge has resulted in the INGRSS classification. The INRGSS provides the optimal management strategy, trying to minimize or avoid treatment in low/intermediate-risk patients. Since the efficacy and safety of less interventionist regimens in NB with favorable biology has been demonstrated, there has been a move towards less aggressive chemotherapeutic and surgical therapy [112–115]. However, as risk group population increases, treatment intensifies and becomes more aggressive. The treatment of NB is multimodal and can include a wide range of therapies ranging from only observation to surgery, chemotherapy, myeloablative chemotherapy with autologous stem cell rescue (AHSCT), radiotherapy, differentiation therapy, immunotherapy or targeted therapies.

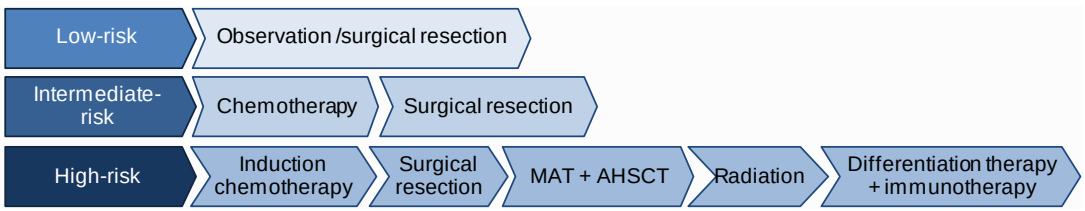

Figure 8. NB treatment overview by risk classification. Patients with asymptomatic very-low and low-risk disease are managed with surgical resection or observation alone, with tumors likely to spontaneously regress. Intermediate patients are treated with 2-8 cycles of chemotherapy, depending on response, as well as primary tumor surgical resection. High-risk patients are treated with intensive multimodal therapy, including chemotherapy, surgery, myeloablative therapy (MAT) with autologous hematopoietic stem cell transplantation (AHSCT), radiation to tumor bed, immunotherapy and differentiation maintenance therapy.

1.1.6.1 Very-low-risk and low-risk neuroblastoma

Very-low-risk and low-risk NB (Table 5) account for nearly 50% of all diagnosed NB. In this subset of patients, cooperative group trials from the COG and SIOPEN evaluating reductions in therapy demonstrated that a five-year OS greater than 90% could be achieved with minimal therapy [8,112,116].

For patients with very-low-risk or low-risk disease without clinical symptoms, surgery alone could be sufficient (Figure 8). Even if resection is not complete, residual disease is not considered a risk factor for relapse and patients can be safely observed without going through chemotherapy. Minimal chemotherapeutic intervention in low-risk patients is indicated only for symptomatic or progressive patients. Still, the number of chemotherapy

cycles should be limited to the resolution of clinical symptoms or until >50% tumor volume reduction is achieved [112,113,115,117,118].

In addition to this guidelines, infants <6 months of age who present small adrenal masses can remain under observation without any treatment. Unless the tumor grows or spreads, the only requirement would be serial monitoring with physical exams, ultrasound tumor imaging and analysis of VMA/HMA urine ratio. These very-low-risk tumors often regress spontaneously and patients have excellent survival outcomes. Together with the fact that any surgical problem at this age may cause serious side effects, non-medical intervention has been established as the standard. Furthermore, some authors argue that this protocol could be extended to older patients [115,119]. The observation protocol was reported in a COG pilot study by Nuchtern and colleagues (NCT00445718) [119]. It is worth mentioning that despite the general excellent prognosis of this patients, the standards set by the COG prospective trial recommend a move from observation to surgical resection if there is a 50% increase in tumor volume, a 50% increase in above catecholamines baseline levels, or if abnormal catecholamine ratios or levels do not return to baseline within a period of six-twelve weeks, respectively.

Nevertheless, the data collected supports continuous attempts to reduce surgery and chemotherapy exposure for most low-risk asymptomatic patients.

1.1.6.2 Intermediate-risk neuroblastoma

This cohort comprises INGR stage L2 tumors *MYCN* non-amplified but either undifferentiated or with unfavorable genomic features, and stage M tumors <18 months and MS tumors <12 months diploid DNA index or unfavorable histopathological features (Table 5). The scheduled treatment for intermediate-risk patients is moderated multi-agent chemotherapy plus surgical resection. Intermediate-risk chemotherapy consists of two to eight cycles of carboplatin, cyclophosphamide, doxorubicin and etoposide regimen depending on the response to treatment. The drug doses given to these patients are less intensive than those prescribed to high-risk patients. Total surgical resection of the residual primary tumor is indicated when possible, but complete resection is not essential (Figure 8). Survival following surgical resection and chemotherapy is higher than 90% for children [114,120,121]. However, treatment with chemotherapy alone for patients older than one year with unresectable disease and unfavorable features might not be enough. These tumors have an estimated overall 5-year survival of 70% and should be given a more intensive regimen including local radiotherapy [122,123].

Moreover, adaptation to a chemotherapeutic regimen reduced in length and intensity is being evaluated for specific subsets of intermediate-risk patients depending on response to therapy, genomic profile and histology. Thus far, two prospective COG trials (NCT00003093 and NCT00499616) have reported excellent OS rates when patients were treated for a shorter time and with lower doses compared to previously used regimens. Ongoing COG study for non high-risk disease NCT02176967 and SIOPEN LINES trial

NCT01728155 for low- and intermediate-risk NB are supposed to determine the impact of further decrease or even elimination of chemotherapy for intermediate-risk patients with favorable histology and genetic features.

1.1.6.3 High-risk neuroblastoma

Approximately, more than 80% of patients with HR-NB are children older than eighteen months of age with INRG stage M disease, and patients from twelve to eighteen months with stage M disease and unfavorable tumor biological features (*MYCN* amplification, unfavorable genomics and/or diploid). The remaining HR-NB patients are either older than twelve months with stage MS and unfavorable genomics or patients with *MYCN* amplification regardless of age or any other characteristic (Table 5) [111]. The 5-year overall survival probability for patients with HR-NB has improved over the last twenty years from less than 30% (patients diagnosed from 1990 to 1994) to the current 50% (patients diagnosed from 2005 to 2010) [124]. Continuous evolution of treatment regimens to more intense therapies are at the base of this progress. Nevertheless, long-term survival rates remain poor and further advances in treatment are imperative, specially focusing on sharpening chemotherapy regimens and complementing it with targeted therapies.

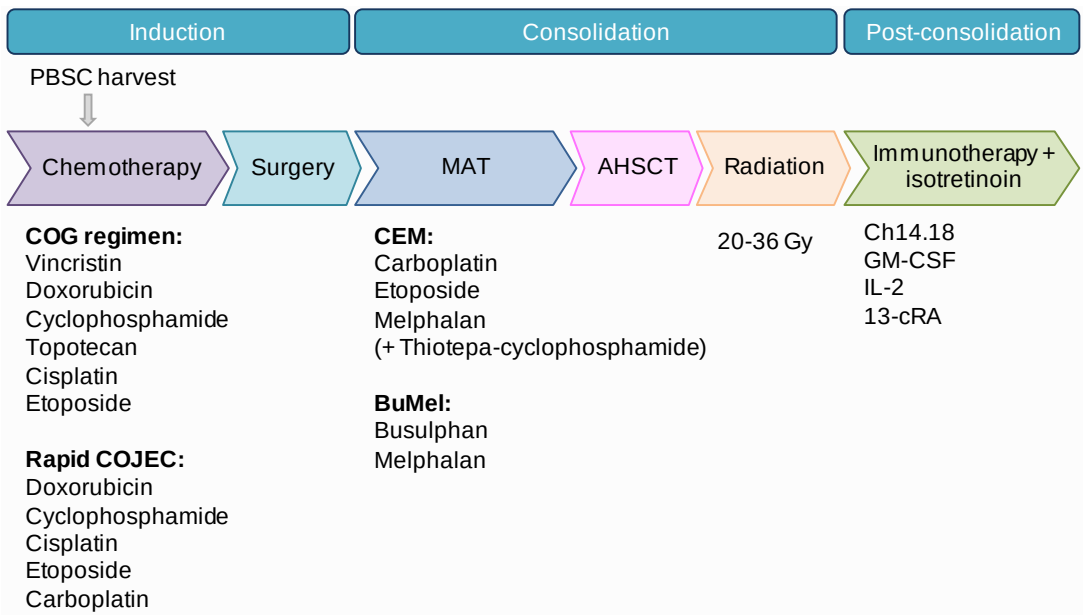

Figure 9. Overall treatment strategy for HR-NB. Current standard-of-care treatment approach for HR-NB consists of three treatment blocks. (1) Induction therapy includes combination chemotherapy, peripheral blood stem cells harvest (PBSC) and cytoreductive primary tumor resection after ≥3 cycles of chemotherapy. (2) In consolidation therapy, high-dose MAT with AHSCT are used to eliminate remaining disease, followed by radiotherapy to the primary tumor bed. (3) Post-consolidation therapy for minimal residual disease includes anti-GD_2 antibody, cytokines and isotretinoin.

Current treatment for HR-NB is multimodal and encompasses three sequential phases (Figure 9). Phase I consists of induction chemotherapy and local control. The aim of induction treatment is to improve surgical resectability by reducing tumor size in primary and metastatic sites using a combination chemotherapy regimen. Induction chemotherapy regimens change between centers, but in general the North American induction regimens (COG standards) consist of four cycles of combined administration of vincristine, doxorubicin, cyclophosphamide and, more recently, topotecan, alternated with 2 cycles of cisplatin and etoposide, accounting for a total of 6 chemotherapy cycles delivered every 21 days [125,126]. In Europe, the SIOPEN uses a time-intensive regimen termed "rapid COJEC" (SIOPEN HR-NBL-1) whereby cycles are delivered at 10 day intervals. Rapid COJEC comprises two courses of vincristine (O), carboplatin (J), etoposide (E); four courses of cisplatin (C) and vincristine; and two courses of vincristine, etoposide and cyclophosphamide (C) [127,128]. Nearly at the end of induction therapy, or at least after three chemotherapy cycles, delayed surgical resection of the primary tumor is scheduled to remove the residual cancer bulks [129,130]. Following surgical operation, any remaining induction chemotherapy cycles are completed. Response to induction therapy is an important prognostic indicator as patients achieving a complete or very good partial remission at the end of induction chemotherapy have significantly greater EFS than patients who have not so good results [131–135].

Phase II or consolidation therapy is meant to eliminate any residual disease following induction chemotherapy and surgical local control. It consists of high-dose myeloablative therapy (MAT) supported by autologous hematopoietic stem cell transplantation (AHSCT) near the end of induction chemotherapy, although several trials have shown it can be done after only two induction cycles [125,126]. Furthermore, for some years now, autologous stem cell rescue from peripheral blood is a reality.
The North American MAT standard of care consists on high-myeloablative doses of carboplatin, etoposide and melphalan (CEM). However, the COG's NCT00567567 clinical trial is studying the upgrade of MAT regimen using high-dose thiotepa-cyclophosphamide followed by CEM (supported by AHSCT after each myeloablative conditioning) [136–138]. On the other hand, the SIOPEN trial NCT01704716 settled busulfan and melphalan (BuMel) combination as the European standard of care for MAT over the traditional CEM regimen [139]. In any case, the addition of intense myeloablative chemotherapy followed by autologous stem cell rescue to HR-NB treatment has meant a significant improvement in EFS [140,141]. Following AHSCT recovery, consolidation therapy generally embraces local external radiation to primary tumor bed.

Finally, phase III or post-consolidation maintenance therapy is meant to eradicate minimal residual disease (MRD) to prevent relapse. Maintenance therapy consists of administration of isotretinoin (13-*cis*-retinoic acid, 13-cRA) in combination with the anti-ganglioside 2 (GD_2) antibody ch14.18 (dinutuximab, or the European biosimilar ch14.18/CHO) and cytokines such as GM-CSF (granulocyte-macrophage colony-stimulating factor) and IL-2 (interleukin-2) [7,8,124,142–145]. Isotretinoin is an oral non-cytotoxic differentiation treatment that has been shown to mediate tumor cell

differentiation and reduce proliferation of NB cells *in vitro*. On its behalf, GD_2 is a disialoganglioside expressed on neuroectodermal tumors, including NB, but limited to neurons and skin melanocytes in non-transformed cells. The addition of isotretinoin treatment and immunotherapy after intensive induction chemotherapy and MAT+AHSCT has demonstrated to significantly improve the 5-year EFS of HR-NB patients [134,146,147].

1.1.6.4 Relapsed neuroblastoma

Although the outcome for patients with HR-NB has improved over the last decades thanks to therapy improvements, survival remains poor, with less than 50% of children likely to achieve long-term cure [7,109]. The main factor of disease progression is related to conventional chemo- and radiotherapy mechanism of action. While chemo- and radiotherapy exert its anti-tumoral effect through induction of DNA damage to trigger the apoptotic program, the majority of childhood malignancies (including HR-NB) present dysfunctional cell cycle arrest and apoptosis regulation, what leads to treatment failure. Resistance to chemotherapeutics can be intrinsic (selective pressures permit a pre-existing minor population of resistant tumor cells to predominate over time) or acquired (cells become resistant after exposure to chemotherapy). The molecular mechanisms implicated in drug resistance range from stochastic mutation of drug targets during the course of treatment to various adaptive responses, such as increased expression of therapeutic targets, increased rates of drug efflux, alterations in drug metabolism, diversion through compensatory signaling pathways, constitutive activation of survival pathways and/or inactivation of programmed cell death pathways [148,149]. For example, relapsed NB tumors usually show mutations predicted to hyperactivate the RAS-MAPK signaling pathway that were not present in the primary tumors. Thus, apparently cell subclones with mutations associated with therapy-resistance expand over time, possibly under the selective pressure of chemotherapy [150]. Epigenetic changes, tumor microenvironment factors and/or presence of tumor cells “hidden” in sites of low-drug penetration (relapses often arise in the bone or bone marrow) have also been identified as important contributors to chemoresistance [151,152]. HR-NB cells have been shown to carry many alterations in apoptotic proteins, such as defective p53 [153], overexpression of *BCL2* [154,155] and *MCL1* [156,157], deletion or epigenetic methylation of *CASP8* [158,159], *BIN1* [160], *MYCN* overexpression [161,162], and others (Table 9).

The acquisition of drug resistance mechanisms often takes place during induction phase. If the resistant tumor cells are not eliminated at the end of myeloablative and maintenance therapy, there’s a high probability of disease progression or relapse months to years after treatment from residual cells refractory to further therapy [8,163–165]. Although there are manageable cases in which prolonged disease stabilization after tumor recurrence is possible, relapsed patients rarely live more than one or three years without disease progression or death [7,8].

The most effective current salvage treatments for relapsed HR-NB are combinations of

the chemotherapeutic drugs topotecan, irinotecan, temozolomide and cyclophosphamide; and the radioiodinated metaiodobenzylguanidine therapy (^{131}I-mIBG). Topotecan and irinotecan are camptothecin derivatives able to block DNA and RNA synthesis by inhibiting topoisomerase I activity. They have demonstrated activity as single agents in clinical studies and are commonly used in the relapse setting because of their efficacy and acceptable toxicity profile [166,167]. Phase II clinical trials that included topotecan showed efficacy in combination with vincristine and doxorubicin (TVD regimen) [168,169], cyclophosphamide [170,171], etoposide plus cyclophosphamide [172] and temozolomide [173]. From those, the TVD has been established as standard backbone chemotherapy regimen as it has been incorporated to the SIOPEN frontline trial for patients failing to achieve a complete response with induction chemotherapy (HR-NBL-1/E-SIOP treatment protocol). Furthermore, despite TVD, the combination topotecan plus temozolomide (TOTEM) is also commonly used as second-line treatment for patients with progressive NB. Temozolomide is an O^6-guanine alkylating agent that has determined efficacy and moderate tolerability profile in phase II studies [174]. The rationale to combine temozolomide and topotecan was based on the hypothesis that methylation of O^6-guanine by temozolomide would lead to topoisomerase I recruitment, increasing the probability of inducing camptothecin-mediated DNA damage [175,176]. The same logic was applied to clinical trials that combine irinotecan and temozolomide. Phase I/II studies demonstrated efficacy and low toxicity of irinotecan plus temozolomide in refractory/relapsed NB patients [177,178], what contributed to its regular use as second-line regimen mainly in North America.

On the other hand, ^{131}I-mIBG therapy, a norephrine analogue taken up by NB cells, is widely accepted as salvage treatment too. It has proven to be one of the most effective therapies for HR-NB with a high response rate of 30-40% in refractory and relapsed disease [179–182]. Since NB tumors are generally radiosensitive, current New Approaches to Neuroblastoma Therapy (NANT) clinical trials are focusing on the combination of ^{131}I-mIBG with radiosensitizers and additional anticancer agents in recurrent/relapsed patients (NCT02035137) [183]. Moreover, ^{131}I-mIBG radiation is also being tested in phase I trials during induction (NCT01175356, NCT03126916) or consolidation therapies (NCT00798148, NCT03061656) [184].

Targeted therapies for refractory/relapsed neuroblastoma

Nevertheless, despite current salvage therapies can grant partial or even complete response, chemotherapy-refractory and relapsed NB remains a major obstacle for pediatric oncologists and there are no alternative curative options available. The combination of a resistant disease, a decreased bone marrow reserve and an impaired function of critical organs, due to previous chemotherapy and radiotherapy, severely limits the implementation of further therapeutic regimens. The urgent need for alternative clinically effective options for the recurrence/relapse setting has led to the progress of an expanding variety of new agents and combinations of targeted therapies with chemotherapy (Table 6). Targeted therapies involve treatments aimed to interfere with molecular targets that have a unique expression within the tumor cells while are usually

absent in normal body cells; and have prospered during the past several years since progressive genomic sequencing technologies have provided the tools to discover new tumoral molecular aberrations and therapeutic targets.

Molecular guided therapies

Collaborative programs as the Therapeutically Applicable Research to Generate Effective Treatments (TARGET) are collecting large datasets on common genetic alterations in primary and relapsed NB with the aim to integrate them into an individualized clinical management in a future. To mention some achievements of these proposals, molecular guided therapies like the use of ALK inhibitors like crizotinib (NCT01606878, NCT02034981), ceritinib (NCT02780128), lorlatinib (NCT03107988) and entrectinib (NCT02650401) are being tested in patients with somatic activating ALK mutations or translocations. Crizotinib had previously reported to have good tolerability and antitumor activity in children harboring ALK translocations (NCT00939770) [185]. Other examples of molecularly guided therapies in clinical trials include the study of NTRKs inhibitors (NCT03155620), the MEK inhibitor trametinib, the p53-MDM2 inhibitor HDM201, the CDK4/6 inhibitor Ribociclib (NCT02780128 for the last three) and the TrkB inhibitor lestaurtinib (NCT00084422, [186]) (Table 6).

HDAC inhibitors

Histone deacetylase inhibitors (HDAC) and hypomethylating agents decitabine, vorinostat and depsipeptide, have also completed at least phase I clinical trials for refractory/relapsed HR-NB. While alternative strategies of combining decitabine should be explored to reach its therapeutic threshold [187], the phase I NANT trial NCT01208454 found that high doses of vorinostat on an interrupted schedule in combination with isotretinoin was tolerable and prolonged stable disease in MRD patients, what warrants further investigation [188]. Besides, a phase II is already underway to analyze clinical activity of vorinostat combined with ^{131}I-mIBG compared to ^{131}I-mIBG monotherapy and ^{131}I-mIBG/vincristine/irinotecan (NCT02035137) [183]; and broader combination studies using vorinostat are ongoing (NCT02559778) to identify HR-NB patient populations that may have improved responses. On the other hand, phase I COG trial NCT00053963 demonstrated that biologically-relevant doses of depsipeptide (Romidepsin) are well tolerated in children with refractory or recurrent solid tumors or leukemia, what will eventually led the way to a phase II [189]. Lastly, fenretinide is a synthetic retinoid analogue proven to cause apoptosis in multiple NB cell lines, even those resistant to other retinoids. Phase I trials of a novel formulation of fenretinide delivered in an oral powderized lipid complex (LXS) have shown improved bioavailability and promising results with administration of fenretinide/LXS alone (NANT's NCT00295919) [190] or in combination (NCT02163356) (Table 6).

PI3K/AKT/mTOR inhibitors

Rapalogs and AKT inhibitors are targeted therapies that deserve a particular mention. Signaling through mTOR pathway (PI3K/AKT/mTOR) is constitutively activated in NB and is crucial for tumor growth and survival. Supporting preclinical observations where treatments with mTOR inhibitors hinder NB xenografts growth [163,191,192], several clinical trials were designed to test the efficacy of PI3K/AKT/mTOR pathway inhibitors in refractory/relapsed NB (Table 6). Starting from the pathway' top, the safety and tolerability of the pan-PI3K inhibitor SF1126 have been put to test in a NANT's phase I clinical trial for children with relapsed NB (NCT02337309). Phase 1b expanded arm of the oral AKT inhibitor perifosine (NCT00776867), from the Memorial Sloan Kettering Cancer Cener (MSKCC), confirmed the safety and tolerability of therapeutic serum levels of perifosine and demonstrated promising prolonged disease stabilization in relapsed NB patients [193]. Ongoing phase II trials in refractory/relapsed NB include the combination of metronomic administration of sirolimus (also known as rapamycin, an mTOR inhibitor) and dasatinib (a tyrosin-kinase inhibitor) with irinotecan and temozolomide (NCT01467986, from Regensburg University); and sirolimus metronomic administration in combination with celecoxib, etoposide and cyclophosphamide (NCT02574728, from Emory University). Discouragingly, although rapamycin analogs and AKT inhibitors were expected to deliver promising therapeutic results, the majority of them failed in phase II trials. One of the reasons underlying rapalogs' limited scope for action is that oncogenic PI3K/AKT/mTOR activation usually stems from diverse redundant pathways, what hinders clinical efficacy of these inhibitors as monotherapies. Furthermore, mTOR inhibition can activate AKT due to negative feedback loops, leading to activation of compensatory pathways or rebounded activation of uninhibited isoforms [194,195]. All of these have been associated to shorter time to progression in clinical trials [145,196]. For example, a COG's phase I trial showed good tolerability of temsirolimus (sirolimus derivative) in combination with irinotecan and temozolomide in children with relapsed or refractory solid tumors (NCT01141244), so phase II was launched [197]. However, in phase II (NCT01767194) the combination did not meet protocol-defined criteria to be selected for further study, as only 1 out of 18 patients achieved partial response [198]. In a like manner, a follow-up phase II of temsirolimus in children with advanced NB (NCT00106353 by Pfizer) neither did reach primary criteria standards for efficacy [199].

Other target inhibitors

The Aurora A kinase inhibitor MLN8237 or alisertib (NCT01601535) [200] and the VEGF inhibitor Bevacizumab (NCT02308527) are two examples of targeted therapies under clinical trials in combination with systemic chemotherapy. Moreover, difluoromethylornithine (DFMO) is an inhibitor of the ornithine decarboxylase (rate-limiting enzyme in polyamine synthesis and downstream target of MYC) being studied as targeted therapy in combination with chemotherapy and immunotherapy (Table 6) (NCT03794349, NCT02139397, NCT02030964, NCT01059071) [201].

Other treatments currently in phase I or phase II studies include the use of Zometa and Nifurtimox (Table 6). Bone metastasis and progressive osteoclasts degradation are aggravating circumstances that substantially contribute to the morbidity and mortality of HR-NB. Because of it, the NANT has designed a clinical trial using a bisphosphonate (zoledronic acid, Zometa), which is administered in adult malignancies to prevent bone loss. One phase I clinical trial combining Zometa and metronomic cyclophosphamide (NCT00206388) has shown a tolerable toxicity profile and prolonged disease stability [202]. These data prompted a successive study by the NANT consortium adding the antiangiogenic agent Bevacizumab (NCT00885326). Nifurtimox is an anti-parasitic agent used to treat Chagas disease currently being assessed in phase II clinical trials for refractory/relapsed NB or medulloblastoma administered along with topotecan and cyclophosphamide (NCT00601003).

Immunotherapy

Multiple phase I or phase II studies combinations of monoclonal anti-GD_2 antibodies in combination with standard chemotherapy regimens (NCT01767194, NCT01183897, NCT01183884, NCT01183416) [198] or betaglucan adjuvant (NCT02743429) are ongoing. Remarkably, the prospective phase II trial NCT00072358 by the MSKCC already demonstrated significant efficacy of the mouse anti-GD_2 antibody 3F8 plus GM-CSF and 13-cRA in patients who were treated for relapsed NB [203]. Other immunotherapeutic strategies in development include immune checkpoint inhibitors [204], immune insulin-like growth factor inhibitors (IMC-A12) (NCT00831844), anti-GD_2 vaccines (NCT00911560, NCT00703222, NCT01192555), cytolytic $CD8^+$ T lymphocytes engineered to express chimeric antigen receptors directed against GD_2 (NCT00085930, NCT02761915, NCT02765243, NCT02919046, NCT03373097, NCT02173093) [205] and infusion of haploidentical NK cells alone (NCT02100891) or combined with anti-GD_2 antibody therapy (NCT01576692, NCT02573896, NCT02650648, NCT03209869, NCT03242603) [206] (Table 6).

Table 6. Open trials for refractory and relapsed NB

Title	Drug/agent	Mol. target	Therapeutic class	Enrollment	Phase	Sponsor	NCT id.
A phase 1 study of crizotinib (IND#105573) in combination with conventional chemotherapy for relapsed or refractory solid tumors or anaplastic large cell lymphoma	Crizotinib, topotecan, cyclophosphamide	ALK, c-Met	Molecularly guided therapy and systemic chemotherapy	65	I	COG	NCT01606878
AcSé CRIZOTINIB: secured access to crizotinib for patients with tumors harboring a genomic alteration on one of the biological targets of the drug	Crizotinib	ALK, c-Met	Molecularly guided therapy and systemic chemotherapy	246	II	UNICANCER	NCT02034981
Phase I study of lorlatinib (PF-06463922), an oral small molecule inhibitor of ALK/ROS1, for patients with ALK-driven relapsed or refractory neuroblastoma	Lorlatinib, topotecan, cyclophosphamide	ALK	Molecularly guided therapy and systemic chemotherapy	40	I	NANT	NCT03107988
Next generation personalized neuroblastoma therapy (NEPENTHE)	Ceritinib, trametinib, HDM201, Ribociclib	ALK, MEK1/2, HDM2, CDK4/6	Molecularly guided therapy	105	I	Children's Hospital of Philadelphia	NCT02780128

Title	Drug/agent	Mol. target	Therapeutic class	Enrollment	Phase	Sponsor	NCT id.
A phase I/Ib, open-label, dose-escalation and expansion study of entrectinib (RXDX-101) in children and adolescents with recurrent or refractory solid tumors and primary CNS tumors, with or without TRK, ROS 1, or ALK fusions	Entrectinib	TRKA/B/C, ALK, ROS1	Molecularly guided therapy	190	I	Hoffmann-La Roche	NCT02650401
NCI-COG pediatric MATCH (Molecular Analysis for Therapy Choice) screening protocol	Ensartinib, erdafitinib, larotrectinib, olaparib, palbociclib, LY3023414, selumetinib sulfate, tazemetostat, ulixertinib, vemurafenib	NTRKs, FGFRs, EZH2, SMARCB1, SMARCA4, TSC1, TSC2, mTOR, MAPK, ALK, ROS, BRAF V600, ATM, BRCA1, BRCA2, RAD51C, RAD51D, Rb	Molecularly guided therapy	1000	II	NCI	NCT03155620
Phase I/II study of MLN8237 in combination with irinotecan and temozolomide for patients with relapsed or refractory neuroblastoma	MLN8237, irinotecan, temozolomide	Aurora A kinase	Targeted therapy and systemic chemotherapy	44	I/II	NANT	NCT01601535
Activity study of bevacizumab with temozolomide ± irinotecan for neuroblastoma in children (BEACON)	Bevacizumab, temozolomide, irinotecan, topotecan	VEGF	Targeted therapy and systemic chemotherapy	160	II	University of Birmingham	NCT02308527
A phase II randomized study of irinotecan/temozolomide/dinutuximab with or without eflornithine (DFMO) in children with relapsed, refractory or progressive neuroblastoma	Irinotecan hydrochloride, temozolomide, dinutuximab, sargramostin, DFMO	ODC	Targeted therapy, systemic chemotherapy, immunotherapy	95	II	COG	NCT03794349
A phase I/II trial of DFMO in combination with bortezomib in patients with relapsed or refractory neuroblastoma	DFMO, bortezomib	ODC, proteosome	Targeted therapy	38	I/II	Spectrum Health Hospitals	NCT02139397
N2012-01: phase I study of DFMO and celecoxib with cyclophosphamide/topotecan for patients with relapsed or refractory neuroblastoma	DFMO, celecoxib, cyclophosphamide, topotecan	ODC	Targeted therapy, systemic chemotherapy, immunotherapy	30	I	NANT	NCT02030964
Randomized phase II Pick the Winner Study of ^{131}I-MIBG, ^{131}I-MIBG with vincristine and irinotecan, or ^{131} I-MIBG with vorinostat for resistant/relapsed neuroblastoma	^{131}I-MIBG, vincristine, irinotecan, vorinostat	HDAC, NET	Targeted therapy, systemic radiotherapy, systemic chemotherapy	105	II	NANT	NCT02035137
Phase I study of fenretinide (4-HPR, NSC#374551) Lym-X-Sorb (LXS) oral powder plus ketoconazole plus vincristine in patients with recurrent or resistant neuroblastoma	Fenretinide, ketoconazole, vincristine	N/A	Targeted therapy and systemic chemotherapy	42	I	South Plains Oncology Consortium	NCT02163356
Prospective, open label, randomized phase II trial to assess a multimodal molecular targeted therapy in children, adolescent and young adults with relapsed or refractory high-risk neuroblastoma	Dasatinib, rapamycin, irinotecan, temozolomide	mTOR	Targeted therapy and systemic chemotherapy	114	II	University of Regensburg	NCT01467986
AflacST1502: a phase II study of sirolimus in combination with metronomic chemotherapy in children with recurrent and/or refractory solid and CNS tumors	Sirolimus, celecoxib, etoposide, cyclophosphamide	mTOR	Targeted therapy and systemic chemotherapy	60	II	Emory University	NCT02574728
NCI-COG pediatric MATCH (Molecular Analysis For Therapy Choice)- phase 2 subprotocol of Ly3023414 in patients with solid tumors	LY3023414	mTOR	Targeted therapy	144	II	NCI	NCT03213678
A phase II trial of Nifurtimox for refractory/relapsed neuroblastoma or medulloblastoma	Nifurtimox, topotecan, cyclophosphamide	ROS	Systemic chemotherapy	100	II	Spectrum Health Hospitals	NCT00601003
3F8/GM-CSF immunotherapy plus 13-*cis*-retinoic acid for primary refractory neuroblastoma in bone marrow: a phase II study	3F8/GM-CSF, 13-cRA	G_{D2}	Immunotherapy	31	II	MSKCC	NCT01183897
Phase II study of monoclonal antibody ch14.18/CHO continuous infusion in patients with primary refractory or relapsed neuroblastoma	Ch14.18/CHO	G_{D2}	Immunotherapy	40	II	University Medicine Greifswald	NCT02743429
Phase I study of oral yeast β-glucan and intravenous anti-G_{D2} monoclonal antibody 3F8 among patients with metastatic neuroblastoma	3F8, β-glucan	G_{D2}	Immunotherapy	45	I	MSKCC	NCT00492167
Phase II study of anti-G_{D2} 3F8 antibody and GM-CSF for high-risk neuroblastoma	3F8/GM-CSF	G_{D2}	Immunotherapy	340	II	MSKCC	NCT00072358

Title	Drug/agent	Mol. target	Therapeutic class	Enrollment	Phase	Sponsor	NCT id.
Phase I/II trial of a bivalent vaccine with escalating Doses of the immunological adjuvant OPT-821, in combination with oral β-glucan for high-risk neuroblastoma	Adjuvant OPT-821 in a G_{D2L}/GD_{3L} vaccine linked to KLH, β-glucan	G_{D2}	Immunotherapy	260	I/II	MSKCC	NCT00911560
A phase I/II study of immunization with lymphotactin and interleukin 2 gene modified neuroblastoma tumor cells after high-dose chemotherapy and autologous stem cell rescue in patients with high-risk neuroblastoma	SKNLP, SJNB-JF-IL2, SJNB-JF-Lptn	N/A	Immunotherapy	7	I/II	Baylor College of Medicine	NCT00703222
A phase I/II study using allogeneic tumor cell vaccination with oral metronomic cytoxan in patients with high-risk neuroblastoma (ATOMIC)	SKNLP, SJNB-JF-IL2, SJNB-JF-LTN	N/A	Immunotherapy and systemic chemotherapy	11	I/II	Baylor College of Medicine	NCT01192555
Administration of peripheral blood T-cells and EBV specific CTLs transduced to express G_{D2} specific chimeric T cell receptors to patients with neuroblastoma	EBV specific G_{D2}-CTLs	G_{D2}	Immunotherapy	19	I	Baylor College of Medicine	NCT00085930
A Cancer Research UK phase I trial of anti-G_{D2} chimeric antigen receptor (CAR) transduced T-cells (1RG-CART) in patients with relapsed or refractory neuroblastoma	1RG-CART/m^2	G_{D2}	Immunotherapy	27	I	Cancer Research UK	NCT02761915
Anti-G_{D2} 4th generation chimeric antigen receptor-modified T Cells (4SCAR-G_{D2}) targeting refractory and/or recurrent neuroblastoma	Anti-G_{D2} CART	G_{D2}	Immunotherapy	30	II	Zhujiang Hospital	NCT02765243
Phase I/II study of anti-G_{D2} chimeric antigen receptor-expressing T cells in pediatric patients affected by high-risk and/or relapsed/refractory neuroblastoma	G_{D2}-CART01	G_{D2}	Immunotherapy	42	I/II	Bambino Gesù Hospital and Research Institute	NCT03373097
Treatment of neuroblastoma and G_{D2} positive tumors with activated T cells armed with OKT3 X humanized 3F8 bispecific antibodies (GD2Bi): a phase I/II study	IL-2, G_{D2}Bi-aATC, GM-CSF	G_{D2}	Immunotherapy	40	I/II	University of Virgina	NCT02173093
Phase 2 solid tumor immunotherapy trial using HLA-haploidentical transplant and donor natural killer cells: the STIR trial	Allogeneic HCT and donor NK cells infusion	N/A	Immunotherapy	20	II	Medical College of Wisconsin	NCT02100891
A phase I dose escalation study of autologous expanded natural killer (NK) cells for immunotherapy of relapsed/refractory neuroblastoma with dinutuximab +/- lenalidomide	Ch14.18, donor NK cells infusion, lenalidomide	G_{D2}	Immunotherapy	24	I	NANT	NCT02573896
Phase I study of the humanized anti-G_{D2} antibody Hu3F8 and allogeneic natural killer cells for high-risk neuroblastoma	Cyclophosphamide, donor NK cells infusion, HuF8, rIL-2	G_{D2}	Immunotherapy and systemic chemotherapy	36	I	MSKCC	NCT02650648
Treatment of relapsed or refractory neuroblastoma with ex-vivo expanded and activated haploidentical NK cells and Hu14.18-IL2	Donor NK cells infusion and HuF8	G_{D2}	Immunotherapy	6	I	University of Wisconsin	NCT03209869
Pilot study of anti-G_{D2} and expanded, activated natural killer cell infusion for neuroblastoma	Anti-G_{D2} antibody and donor NK cells infusion	G_{D2}	Immunotherapy	5	I/II	Singapore National University Hospital	NCT03242603

Mol. target, molecular target; NCT id., National Clinical Trial identifier number; ODC, ornithine decarboxylase; ROS, reactive oxygen species; NET, norepinephrine transporter; HDAC, histone deacetylase; COG, Children's Oncology Group; NANT, New Approaches to Neuroblastoma Therapy; MSKCC, Memorial Sloan Kettering Cancer Center.

1.1.6.5 Accelerating drug development for neuroblastoma

Despite all these new selected agents and targeted therapies under study, further advances in the understanding of HR-NB molecular biology are urgently needed in order to enhance the identification of tumor specific genetic alterations and biomarkers that may harbor therapeutic potential, as well as to define patients at greatest risk of treatment failure or recurrence. Thanks to the improvements in technology, it is expected that future

studies will move toward more refined risk classifications and treatments based on precision tailored therapies.

However, for the moment, in order to accelerate the development of new alternative drugs for patients with HR-NB and promote their introduction into clinical trials, the Innovative Therapies for Children with Cancer (ITCC), the European Network for Cancer Research in Children and Adolescents (ENCCA) and the International Society of Pediatric Oncology Europe Neuroblastoma Group (SIOPEN) established in conjunction the New Drug Development Strategy (NDDS) project in 2012. The aim of the NDDS is to accelerate the development of new targeted-drugs for patients with NB and promote their introduction into clinical trials. In agreement with the NDDS, the selection of therapeutic targets for drug development must be subjected to tumor biology, tumor-specificity and must have been validated to be essential for tumor progression. Based on pre-clinical efficacy data, potential combinations and availability of biomarkers, the prioritized targets for NB were: ALK, MEK, CDK4/6, MDM2, MYCN, BIRC5 and CHK1 [207]. Drugs targeting MYCN were ranked as high priority as its expression has been found to be selectively confined on the tumor tissue in several pediatric solid tumors with poor outcome [38,39,208,209]. However, the majority of the compounds being developed to target MYCN are still in preclinical studies or in adult cancer clinical trials. Only one CHK1 inhibitor, one methylating agent and some drugs that hamper MYCN stability are being tested in pediatric cancer clinical trials. Isotretinoin is the only being used in therapy [39,210].

1.2 Lipid analogs as alternative cancer therapies

It is almost imperative to find additional options for cancer therapy based on selective agents that target specific characteristics and/or deregulated pathways in cancer cells. These agents are considered to have better tolerability and fewer side effects than non-specific chemotherapeutic drugs. According to this strategy, one therapeutic alternative is the use of lipid analogues. Lipid analogues are small synthetic derivatives from natural lipids characterized for having low toxicity profile in animal models but high citotoxicity in a broad spectrum of human tumor cell lines *in vitro*. Lipid-derived drugs are designed to modify membrane lipid structures of cells and/or internal organelles to induce alterations in the propagation of disease-specific signaling cascades and/or hamper phospholipid homeostasis [211]. Therefore, unlike conventional chemotherapy/radiation, they do not interact directly with DNA hence should be regarded as a safer option.
The development of lipid analogues for its clinical use against cancer is at an early but promising stage. However, relatively few have made it through phase I/II studies because of the incidence of side effects. For example, selective inhibitors of prostaglandin synthase COX-2 have shown antitumor efficacy *in vitro* and *in vivo* in several cancer models [212–214], but its association with increased cardiovascular risk in long-term clinical trials has discouraged from doing further research [215–217]. Similarly, besides its extensively reviewed anticancer activity, clinical development of synthetic alkylphospholipids (ALPs) was limited at first due to systemic toxicities found during clinical trials. Nevertheless, continuous structural ALPs modifications have succeeded in producing compounds with fewer toxic side effects that still maintain its cytotoxic activity against a variety of cancer cell lines. This achievement enabled the revival of this strategy and warrants further ALPs clinical investigation [218–221]. For instance, the AKT inhibitor perifosine is under clinical trials for recurrent pediatric solid tumors (including NB) as single-agent (NCT00776867) and in combination with temsirolimus (NCT01049841) [222].

Monounsaturated and polyunsaturated fatty acid analogues are other lipid-derivatives that have demonstrated antitumoral activity. It has been reviewed that addition of free fatty acids into membranes or alteration of phospholipids composition changes many biophysical parameters of the membranes, produces membrane microdomain alterations, destabilizes the lamellar phase and influences cell signaling through modulation of the G-proteins, adenylyl cyclase, Ras-MEK-ERK and protein kinase C intracellular pathways [211]. Thus, fatty acids lipid therapy has been proposed to pharmaceutically reform the activity of disease-specific protein/lipid signal cascades. Besides, hydroxylation of fatty acids hinders fatty acid metabolism and enlarges its therapeutic time window inside the cell, a characteristic largely used for their molecular design [223].

1.2.1 ABTL0812, a first-in-class anti-cancer polyunsaturated fatty acid derivative

ABTL0812 is a novel and first-in-class antitumor drug encompassed in the chemically modified fatty acids category. ABTL0812 is the sodium salt formulation derivative from 2-hydroxy-linoleic acid, an essential polyunsaturated ω6 fatty acid made up of eighteen carbons (chemical name: sodium 2-hydroxylinoleate). Previous pre-clinical studies have demonstrated that ABTL0812 is able to induce cell death in a broad panel of cancer cell lines without affecting viability of non-tumoral cells. Moreover, ABTL0812 also proved to reduce tumor growth both, administered alone or in combination with chemotherapy in human lung, endometrial, pancreatic, glioblastoma, cholangiocarcinoma and breast tumor xenografts with an excellent safety profile in comparison to other targeted anticancer therapies [224,225,unpublished data]. Moreover, toxicology studies in animals have shown that ABTL0812 is well tolerated and does not increase toxicity when administered in combination with chemotherapy. Based on this promising pre-clinical data, ABTL0812 moved to clinical stage and in 2016 a phase I/Ib first in human as single-agent in adults with advanced solid tumors (NCT02201823) was successfully completed demonstrating its safety and tolerability. No dose-limiting toxicities were detected, maximum tolerated dose was not achieved and no clear dose-related trends in the incidence of adverse events were detected, illustrating the high safety and tolerability of ABTL0812. In addition, several long-term disease stabilizations were achieved indicating potential signs of efficacy. Three patients with colorectal cancer had stable disease for fourteen (two patients) and nineteen weeks (one patient), one patient with endometrial cancer was stable for fifty-nine weeks and one patient with cholangiocarcinoma was stable for seventy-eight weeks [226,227]. These promising results allowed further clinical development of ABTL0812 and led to an ongoing phase Ib/IIa clinical trials in adult patients with advanced solid tumors. It is being tested as first-line therapy combined with paclitaxel and carboplatin for patients with advanced endometrial cancer and squamous non-small cell lung cancer (NCT03366480). To date, the phase Ib part has been successfully completed, demonstrating that ABTL0812 does not increase the toxicities of chemotherapy [228]. The phase II part started in May 2018 and is currently ongoing. In addition, a phase I/II study will start in September 2019 using ABTL0812 as first line therapy in combination with gemcitabine and nab-paclitaxel (Abraxane) in patients with advanced metastatic pancreatic cancer.

ABTL0812 mechanism of action has been described [224]. ABTL0812 binds to PPAR receptors subsequently inducing the up-regulation of the pseudokinase TRB-3, which can interact with AKT and prevent its phosphorylation by upstream kinases. Thus, AKT phosphorylation levels were measured in platelets as a pharmacodynamic biomarker in the phase I trial NCT02201823, detecting a dose-dependent inhibition that reached a maximum of 90% of AKT inhibition in the cohort 5 (ABTL0812 at 1300mg three times a day) compared to cohort 1 (500mg once a day). This observation confirms the mechanism of action of ABTL0812 in patients. Given the fact that enhanced PI3K/AKT/mTOR signaling pathway is crucial for NB tumor growth, survival, metabolism, angiogenesis, chemoresistance and correlates with poor prognosis; we hypothesized whether disruption

of the PI3K/AKT/mTOR axis via ABTL0812 could be clinically effective for the treatment of HR-NB patients [229–233]. Moreover, the PI3K/AKT/mTOR axis integrates all the NDDS prioritized targets for HR-NB and directly regulates active MYCN stabilization [234,235].

Besides, as well as the expected impact on tumor cell growth, Erazo and colleagues also noticed that ABTL0812' blockage of AKT activation by upstream kinases PDK1 and mTORC2 inhibited the activation of the mTORC1 complex and brought with it the induction of autophagic cell death (Figure 10).

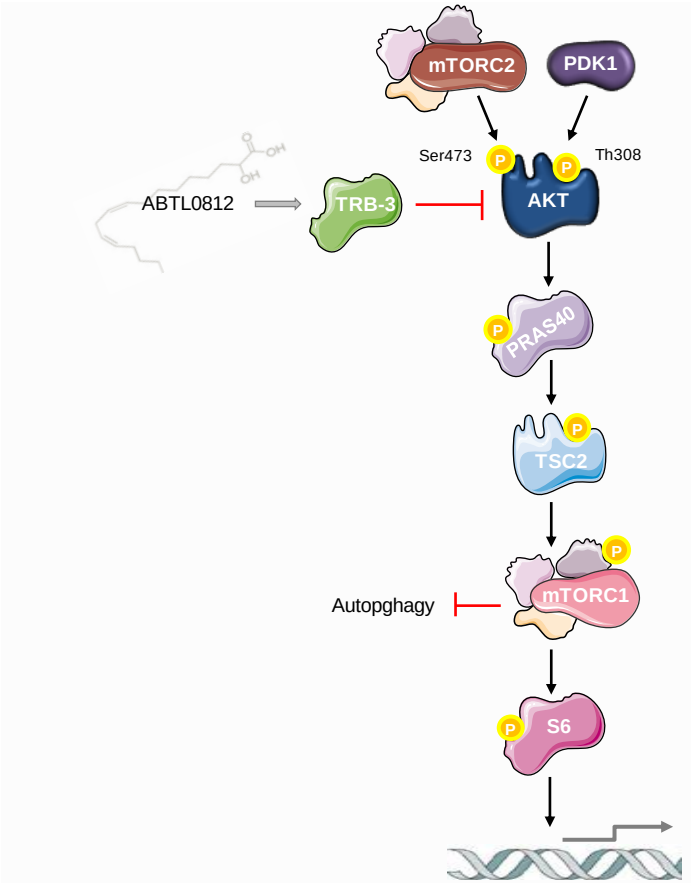

Figure 10. ABTL0812 mechanism of action. Schematic representation of ABTL0812 mechanism of action described by Tatiana Erazo *et al*. ABTL0812 would induce the pseudokinase TRB-3, which prevents AKT activation by upstream kinases, resulting in an inactive form of AKT. Because AKTmodulates the activation of mTORC1 by phosphorylating and inactivating the mTORC1 protein repressors TSC2 and PRAS40, ABTL0812-mediated inhibition of AKT results in reduced phosphorylation of PRAS40 and TSC2, impairing mTORC1 activity and inducing autophagy.

1.3 Autophagy

Autophagy is a homeostatic and evolutionary conserved process that degrades cellular organelles, proteins, lipids, carbohydrates and nucleic acids and maintains cellular biosynthesis during nutrient deprivation or metabolic stress. By digesting the unnecessary or dysfunctional cellular components, autophagy helps to prevent the accumulation of toxic cellular wastes and to outlast periods of nutrient deprivation by recycling the degraded content. However, several studies have set fort autophagy implication in a broader list of biological processes such as development, aging, microorganisms' clearance, tumor suppression, metabolism, immunity, inflammation, cell death and differentiation and a number of pathologies [236].

Autophagy is considered to be a dynamic process that comprises three sequential steps: (1) formation of double membrane vesicles known as autophagosomes, (2) the fusion of autophagosomes with lysosomes and (3) degradation of autolysosomes [237]. Stress, nutrient deprivation, growth factor depletion, increases in the AMP/ATP ratio and hypoxia are the most typical stimulus to trigger autophagy through mTOR inhibition. The mTOR transduction pathway is a master regulator of cell homeostasis that integrates growth factor, amino acids, glucose and energy status signals [238].

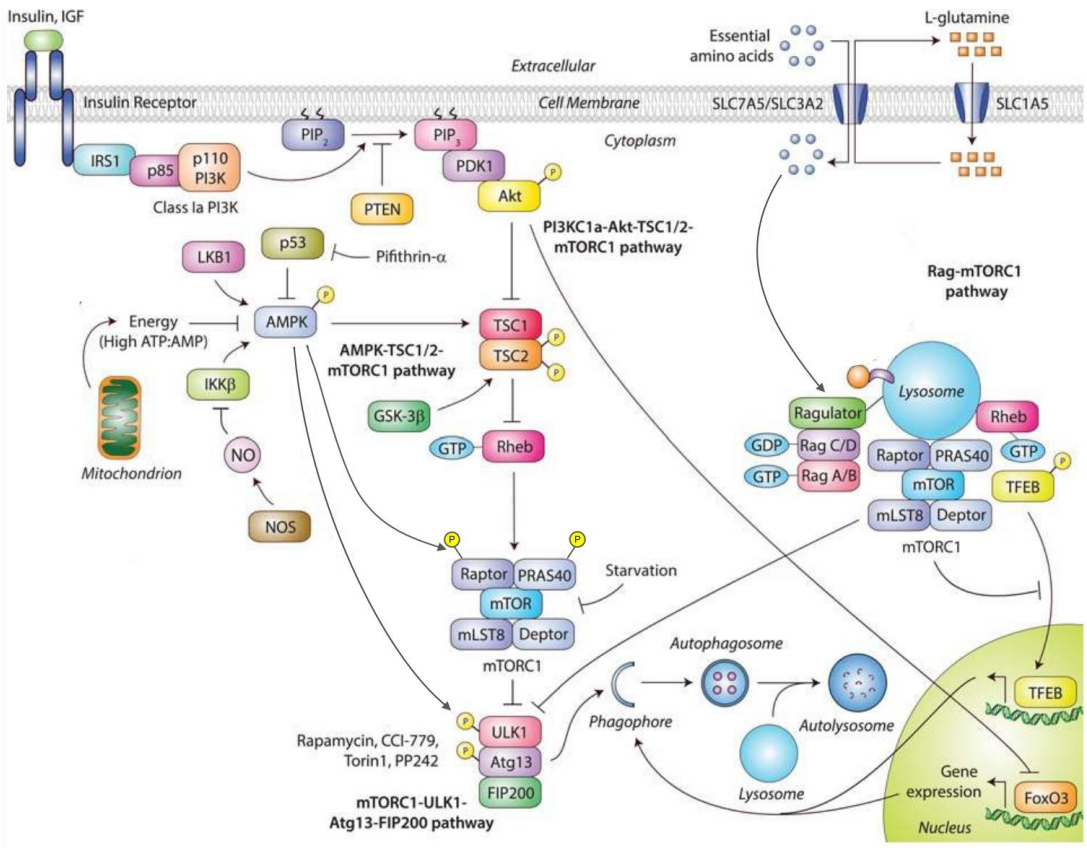

Figure 11. Regulation of autophagy via mTOR signaling. Diverse signals like amino acids, growth factors, energy status and stressors activate mTORC1, which negatively regulates autophagy. (1) Insulin and growth factors act through the PI3K/AKT/TSC/mTORC1 pathway by binding to their cell-surface leading to inhibition of TSC1/2, thereby allowing Rheb to activate mTORC1 and inhibit autophagy. In addition, activated AKT inhibits FoxO3-mediated transcription of autophagy genes. (2) Influx of amino acids activates the Rag/mTORC1 pathway recruiting mTORC1 on the lysosomal surface where Rheb causes its activation, leading to suppression of autophagy. Lysosome-localized activated mTORC1 also sequesters TFEB to prevent its nuclear translocation and transcription of autophagy and lysosomal genes. (3) Energy status and stress signals act through the AMPK/TSC/mTORC1 pathway to modulate autophagy. High ATP/AMP ratio, NO or cytoplasmic p53 inhibits AMPK, thereby preventing TSC1/2 activation that causes Rheb to activate mTORC1 and inhibit autophagy. Active AMPK also triggers autophagy through Raptor inhibition and direct ULK1 phosphorylation. The ULK1–ATG13–FIP200 complex regulates autophagosome synthesis downstream of mTORC1. Figure adapted from [239].

In physiological conditions, amino acids stimulate the Rag-GTPase proteins, which shift mTORC1 into the same compartment where is its direct activator Rheb [240,241]. Otherwise, insulin induces mTORC1 through parallel pathways. Insulin triggers the PI3K/AKT pathway leading to phosphorylation of the AKT substrates PRAS40 and TSC2. Phosphorylation of these targets negatively regulates their activity, allowing mTORC1 dissociation from PRAS40 and bond to Rheb-GTP thanks to TSC2 inhibition [242,243]. Therefore, amino acid or glucose depletion abrogate mTOR signaling and contribute to autophagy initiation. On the other hand, expression of AMPK during energy shortage leads to TSC2 phosphorylation on distinct serines from those targeted by other kinases (such as p-AKT), stimulating TSC2 inhibition of mTOR [244]. Moreover, AMPK also phosphorylates and inactivates the mTOR partner Raptor, and engages autophagy through directly phosphorylation of ULK1 [245–247] (Figure 11).

Once the cell has sensed there is an imbalance in cellular homeostasis, mTORC1 dephosphorylation causes dissociation and activation of the ULK1 kinase complex (ULK1, FIP200, ATG13 and ATG101), which controls initiation of autophagy in mammals. Following ULK1 activation, an expanding cup-shaped structure originates from the endoplasmatic reticulum (ER) membrane, giving rise to the formation of autophagosome precursors, or phagophores. The process encompassing phagophore lengthening and maturation is called nucleation. Nucleation is regulated by other ATG proteins (autophagy related proteins) encompassed in the PI3K class III complex (PI3KC3), recruited by the ULK1 complex to the phagophore formation sites on the ER. The PI3KC3 complex is composed by Beclin 1, VPS34, VPS15 and ATG14L, which mark the sites where the double-membranes will fuse. After nucleation, expansion and growth of the phagophores is controlled by ATG9 lipid supply from the Golgi and other organelles, and the ubiquitin-like conjugation system ATG12-ATG5-ATG16, which dissociate when the phagophore develops into an autophagosome. The ubiquitin-like system promotes the recruitment and conversion of cytosolic-associated protein light chain 3 (LC3-I) to the membrane-bound, lipidated form LC3-II (LC3-I conjugated to phosphatidylethanolamine, PE). LC3 lipidation is critical for proper autophagic vesicle formation and expansion. Moreover, LC3-II recruits autophagy-related adaptor/receptor proteins such as sequestosome 1 (SQSTM1/p62), which is able to recognize and tag substrate proteins, protein aggregates, and damaged

organelles, and allows cargo recruitment into the autophagosomes. The late events in autophagy involve the final maturation and fusion of autophagosomes with lysosomes to form an autolysosome. While ATG proteins are retrieved from the autophagosome membrane after maturation, LC3-II remains on mature autophagosomes until after fusion with lysosomes. Hence, LC3-I/LC3-II conversion is the most common marker used to monitor autophagy from induction to autophagosome breakdown. The autophagic circuit is completed when the autolysosome digestive machinery degrades the luminal content of the vesicles and the remaining components are recycled back to the cytosol [248–250] (Figure 12).

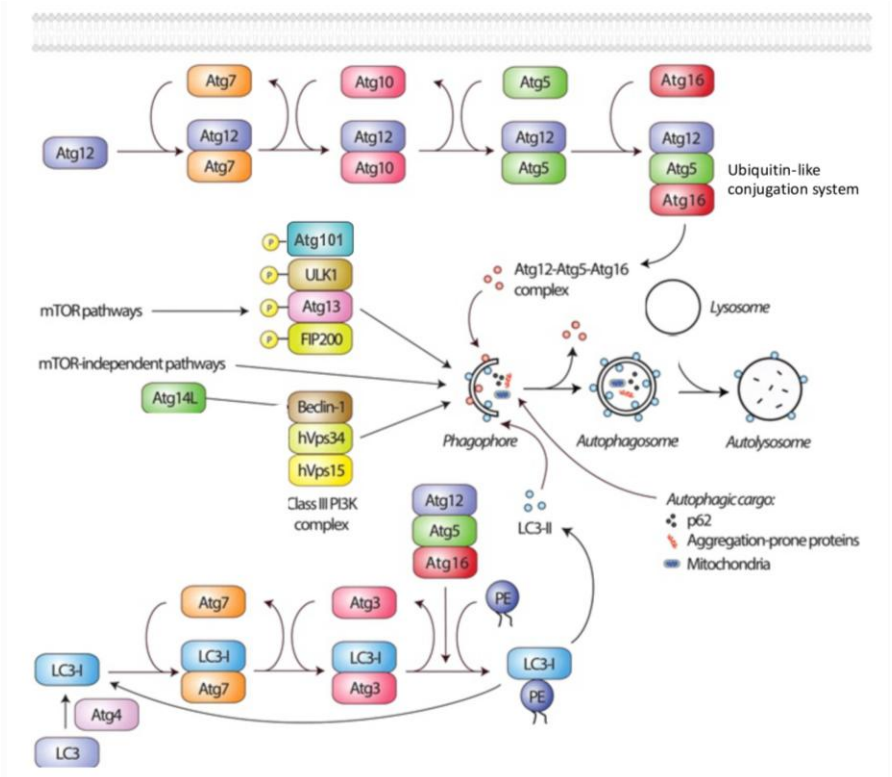

Figure 12. Autophagosome formation and the autophagic cycle. Autophagy initiates with the progressive segregation of cytoplasmic material by double-membrane structures commonly known as phagophores or isolation membranes. The ULK1-ATG13-ATG101-FIP200 complex regulates autophagosome synthesis downstream of the mTOR signaling pathways. The PI3KC3 complex, comprising VPS34, Beclin-1, ATG14L and VPS15, regulates the nucleation phase of the autophagosome synthesis. Phagophores nucleate from the ER, Golgi apparatus, plasna membrane, mitochondria and recycling endosomes. Expansion and elongation of the phagophores are controlled by the ubiquitin-like conjugation system ATG5-ATG12-ATG16. The ubiquitin-like conjugation system is also involved in the LC3-PE conjugation (LC3-II). Autophagic cargo consisting of non-specific or specific substrates such as p62, aggregation-prone proteins or mitochondria, is degraded in the autolysosomes and recycled. Figure adapted from [239].

1.3.1 The mTOR-independent ER stress-related autophagy

Intracellular Ca^{2+} signaling controls a plethora of cellular processes, including gene transcription, metabolism, regulation of the cell's energy status and cell death; thereby impacting on cell function and survival. The major intracellular Ca^{2+}-storage organelle is the ER. In homeostatic conditions, basal and constitutive Ca^{2+} release from the ER to the mitochondria sustains mitochondrial bioenergetics through NADH production and ATP synthesis, and regulates essential processes for the cell growth such as the synthesis of tricarboxylic acid intermediates, nucleotides, lipids and proteins [251,252]. Therefore, imbalances in the Ca^{2+} flux compromises the ATP production and generates metabolic stress, which induces the pro-survival autophagic flux as an energy saving mechanism [253,254]. As the ATP production decreases, the AMP-activated protein kinase (AMPK) is activated. AMPK is a fast highly conserved sensor of the AMP/ATP ratio levels that switches on catabolic pathways when the cellular energy status is disturbed. Stimulation of AMPK actively phosphorylates TSC2 and Raptor, what is followed by mTOR inactivation and consequently ULK1 dissociation [255–257]. Moreover, AMPK can trigger autophagy not only through inactivation of mTOR but also by direct phosphorylation of ULK1 and Beclin 1 [245,246,258]. In addition, feedback signaling from AMPK further inhibits mTOR, resulting in increased activated ULK1 levels [259].

The most sensitive organelle to disturbances on the cell's physiological conditions is the ER. The term "ER stress" reflects a situation where proper ER functioning is impaired, what can be caused by a variety of physiological and/or pathological insults, such as disturbances in the Ca^{2+} levels, glucose deprivation, infections, toxins, hypoxia, oxidative stress, hypoglycemia, aberrant protein expression, aging and an excessive increase in protein synthesis [259]. As an adequate ER Ca^{2+}-filling is essential for protein folding and post-translational modifications performed on the ER, Ca^{2+} stores depletion induces ER stress and triggers various Ca^{2+}-regulated autophagy pathways. As it has been exposed, abnormal Ca^{2+} release from the ER stimulates the activity of AMPK, initiating the AMPK/TSC2/mTOR autophagy cascade [260–262]. Moreover, besides triggering autophagy via AMPK signaling, the ER can activate autophagy through diverse Ca^{2+}-independent mechanisms under stress conditions. Eukaryotic cells sense and cope with ER stress inducing the unfolded protein response (UPR) signaling pathways. The UPR is composed of three branches, each one triggered by a highly conserved sensor-protein located on the membrane of the ER: (1) the inositol-requiring enzyme-1α (IRE1), (2) the protein kinase RNA-like endoplasmatic reticulum kinase (PERK) and (3) the activating transcription factor 6 (ATF6) [259,263–266]. These three canonical sensors can regulate autophagy through different pathways during ER stress (Figure 13). The IRE1 target c-Jun N-terminal kinase 1 (JNK1, also termed MAPK8) triggers autophagy by direct phosphorylation of the Bcl-2 proteins Bcl-2 and Bcl-x_L. In normal conditions, the Bcl-2 proteins inhibit autophagy by sequestering Beclin 1, as while Beclin 1 is bound to Bcl-2 it is unable to activate the PI3K complex. Therefore, phosphorylation of Bcl-2 proteins by JNK1 disrupts their interaction with Beclin 1 and allows proceeding of the autophagic pathway [262,267,268]. In addition, Beclin 1 is transcriptionally up-regulated by JNK1 and

spliced XBP1, a transcriptional regulator downstream IRE1 [269]. On the other hand, several studies have highlighted the role of the PERK in autophagy induction during ER stress [262,270,271]. Activation of the PERK/eIF2α/ATF4/CHOP axis results in downstream expression of TRB-3 (tribbles homolog 3), a protein that positively regulates autophagy via inhibition of the AKT/mTOR pathway [266,272]. Furthermore, the PERK/eIF2α/ATF4 pathway up-regulates transcription of ATG12 and ULK1 [273,274]. Finally, despite being ATF6 the least characterized UPR branch in the context of autophagy, it has been well established that ATF6 signaling triggers autophagy through up-regulation of the death-associated protein kinase-1 (DAPK1), which phosphorylates and activates Beclin 1, thus promoting autophagy [275,276].

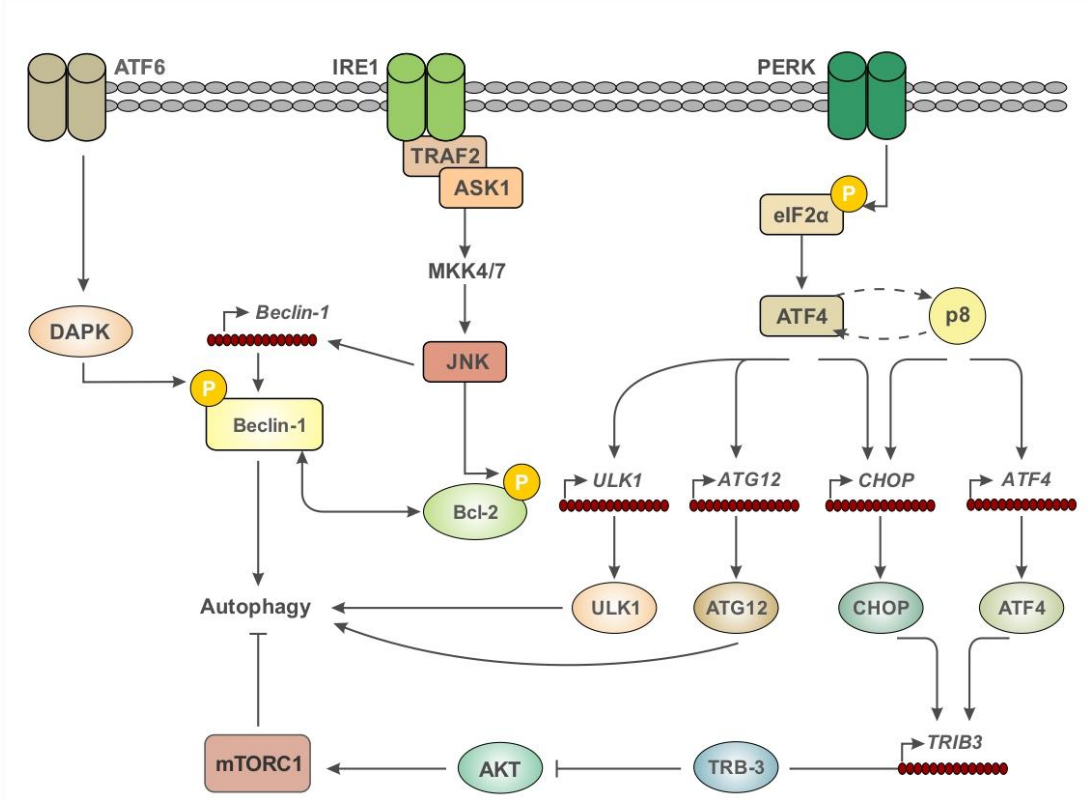

Figure 13. Mechanisms connecting ER stress and autophagy. The three UPR branches regulate different signal pathways that lead to autophagy activation. ATF6 up-regulates DAPK1, which phosphorylates Beclin 1 promoting its dissociation from Bcl-2, which also promotes its dissociation from Beclin 1. PERK signaling can lead to autophagy through ATF4-dependent increased expression of ULK1 and ATG12. Alternatively, ATF4 promotes the up-regulation of the pseudo-kinase TRB-3, which causes the inhibition of the AKT/mTORC1 axis to stimulate autophagy. Figure adapted from [262].

.

1.3.2 Autophagy in cancer

Defects in autophagy are frequently associated with cancer, thereby suggesting a potential tumor-suppressive role. The tumor-suppressing role of autophagy would involve: (1) maintenance of genetic/genomic stability; (2) degradation of oncogenic/damaged proteins, lipids, organelles and toxic cellular waste products; (3) limitation of cellular growth; (4) control and reduction of reactive oxygen species (ROS) production, which can cause DNA damage; (5) reduction of chronic inflammation; (6) regulation of immunosurveillance systems and (7) control over the induction of senescence and autophagic cell death [277,278] (Figure 14A). Strengthening this hypothesis, monoallelic loss of the autophagy gene *Beclin 1* has been found in 40-75% of human breast, prostate and ovarian cancers; and *Beclin 1*$^{+/-}$ mice have shown to develop lung cancers, liver cancers, and lymphomas [279]. In addition, mosaic loss of *ATG5* in mice produces chronic liver and pancreas inflammation and promotes the development of benign tumors [280,281]. It has been suggested that one link between defective autophagy and tumorigenesis may be the accumulation of the autophagy-aggregates p62, which have been found to inhibit tumor suppressor genes and promote oncogene activity [282]. However, whether autophagy-induced mechanisms are protective or carcinogenic is context-dependent. For example, while suppression of genome instability or chronic inflammation could be considered anti-tumorigenic actions on non-pathologic scenarios, they could help to create a favorable environment for cancer initiation. Therefore, although the previously mentioned reports confirm the role of autophagy in prevention of malignant transformation, genetic or pharmacological inhibition of autophagy has proven to restrict tumor viability and trigger apoptotic or necrotic cell death in other preclinical models [283–285].

Among the several evidence sustaining that autophagy is a highly plastic and dynamic process that can either repress the initial steps in carcinogenesis but also maintain tumor survival, there is the finding that autophagy constitutes a mean to cope with intracellular and environmental stress in the later stages of tumor progression [283,286,287]. In established tumors, stress is mostly caused by the conjunction of a high metabolic demand coupled to limited supplies of oxygen and nutrients on account of insufficient vascularization in regions distant to blood vessels. In this condition, autophagy promotes the degradation of intracellular components to provide enough substrates to support excessive cellular proliferation in the absence of extracellular nutrients (Figure 14B). Chemotherapy and/or radiation are other sources of stress in cancer cells. Treatment-related stress might activate autophagy and turn residual cells into a state of dormancy that may contribute to tumor resistance with eventual recurrence (Figure 14B) [288,289].

Evidence indicates that the elevated levels of autophagy lay the foundation of cancer cell's ability to tolerate the hostile tumor microenvironment and proliferate. Consistently, advanced tumors are often "addicted" to autophagy recycling pathways to maintain their metabolism [285,287,290,291]. As a proof of concept, the knockdown of essential autophagy genes has shown to confer or potentiate the induction of cell death in tumor

cells [250,292,293]. Moreover, it has been demonstrated that autophagy plays a crucial role in disabling anti-tumor immunosurveillance and facilitating the secretion of pro-tumorigenic factors, thus favoring tumor growth and dissemination (Figure 14B) [294,295].

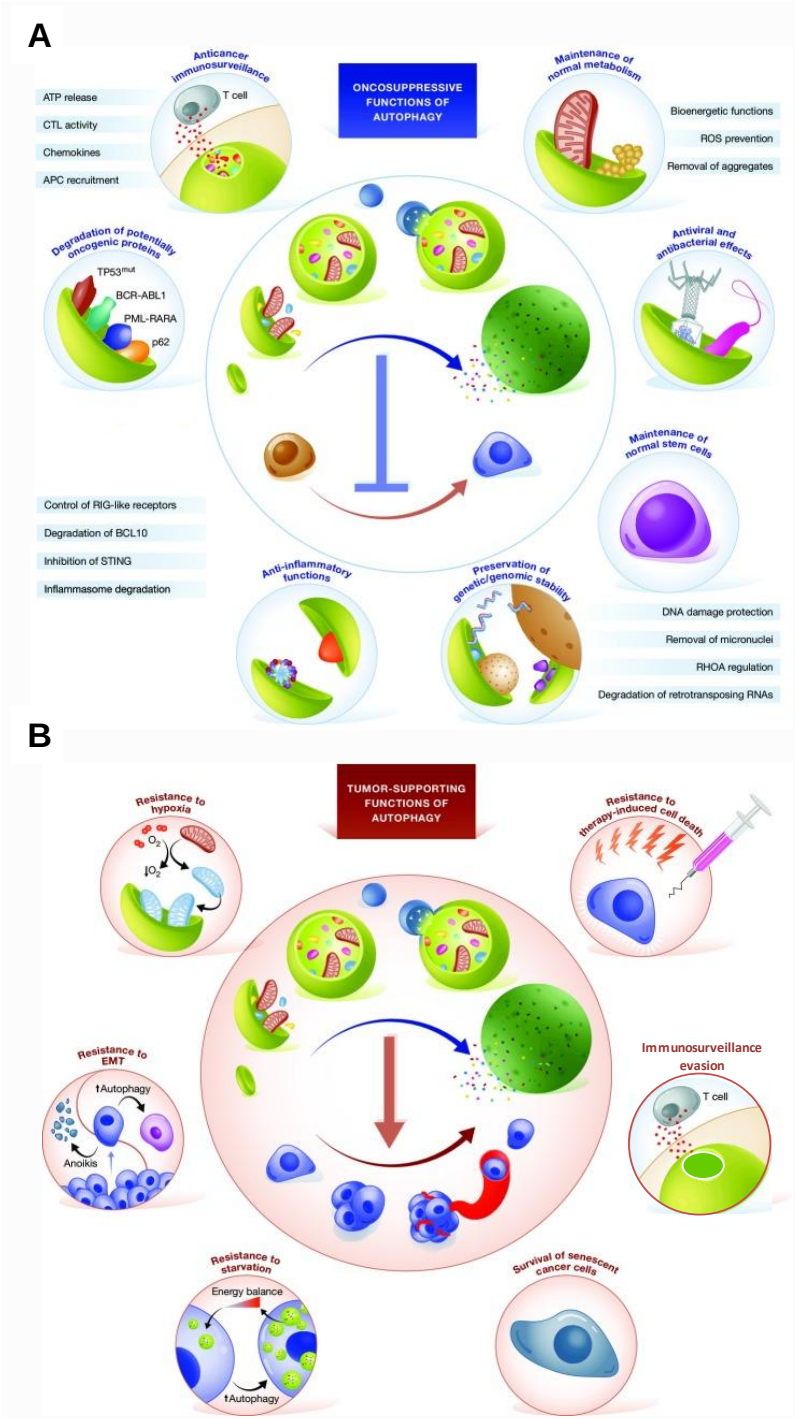

Figure 14. Oncosuppressive vs. tumor-supporting functions of autophagy. (A) Autophagy has been proposed to suppress malignant transformation by several mechanisms, including: control of cell growth, maintenance of normal bioenergetic functions and autophagic cell death; degradation of oncogenic/damaged proteins, lipids, organelles and toxic cellular, bacterial and viral products; control over optimal activation of senescence/stemness; preservation of genetic/genomic stability; control of inflammation; disposal of ROS; and execution of anticancer immunosurveillance. (B) In established tumors, autophagy is believed to promote tumor progression and resistance to therapy through conferring resistance to hypoxia and nutrient deprivation; inducing cancer cells to a state of dormancy/senescence in response to therapy; disabling anti-tumor immunosurveillance; and facilitating EMT transition and dissemination. CTL, cytotoxic T lymphocyte; APC, antigen-presenting cell; $TP53^{mut}$, mutant tumor protein p53; BCR, breakpoint cluster region; ABL1, ABL proto-oncogene 1; PML, pro-myelocytic leukemia; RARA, retinoic acid receptor alpha; RIG; retinoic acid inducible gene; BCL10, B-cell CLL/lymphoma 10; STING, stimulator of interferon genes; RHOA, Ras homolog family member; EMT, epithelial-to-mesenchymal transition. Figure adapted from [278].

Accordingly, autophagy inhibition has been proposed as an anti-cancer therapeutic alternative. Pharmacological inhibitors of autophagy include 3-methyadenine, wortmannin, LY294002, the anti-malarial drugs chloroquine (CQ) and its derivatives hydroxychloroquine (HCQ) and Lys05, bafilomycin A1, monensin, clomipramine, anti-schistome agent lucanthone and the newly developed ULK1/2 inhibitors SBI-0206965 MRT67307 and MRT68921 [250,296]. Among them, HCQ is the most clinically advanced molecule. HCQ has been shown to suppress tumor growth by disruption of autophagic flux and cargo degradation in multiple *in vivo* models, and is currently being tested in different phaseI/II clinical trials to study patients' responses to a HCQ based-therapy combined with a variety of anticancer regimens (reviewed in [297].

On the other hand, autophagy has been taken for a double-edge sword since it may play a role in mediating cell death in certain cellular contexts. The onset of this impression was the observation of morphological autophagy features in dying cancer cells, such as extensive cytoplasmic vacuolization and accumulation of large autophagosomes and autolysosomes coupled to an increased autophagic flux; what suggested that hyperactivation of autophagy may promote cell death [298–300]. Remarkably, many experts warned about the fact that autophagy frequently interacts or occurs concurrently with various types of cell death, making it difficult to distinguish between cell death really just orchestrated by autophagy and other forms of cell death activated by persistent autophagy [301,302]. To avoid misconception, the Nomenclature Committee of Cell Death defined autophagy-dependent cell death (ACD) as a form of regulated cell death that mechanistically exclusively depends on the autophagic machinery. Hence, genetic or chemical inhibition of autophagy would have to prevent cell death [263,303].

Nowadays, substantial evidences reinforce the theory that over-activation of autophagy can lead to cell death via autolysosomes self-digestion [298,302,304]. This type of cell death has been designated type-II cell death, as opposed to type-I, apoptosis, and type-III, necrosis. Apparently, the dichotomy between protective and detrimental autophagy is related to the cellular context and the stimulus length and strength. When the extent and duration of autophagy surpass a certain threshold that guarantees cell recovery, the pathway resolution may change from survival to death. This has been found to be

particularly relevant in apoptosis defective cells, like many HR-NB cell lines which harbor deleted or non-functional apoptotic genes and proteins (Table 9) [158,159,305,306]. Unlike to what happens in apoptosis, neither caspases activation, DNA degradation nor nuclear fragmentation are apparent in ACD. Instead, ACD is distinguished by degradation of intracellular membranes, mitochondria, polyribosomes, Golgi apparatus, endoplasmic reticulum and other cytoplasmic material before nuclear destruction. Therefore, an accepted presumption is that sustained autophagy might lead to excessive consumption and disintegration of essential cellular components until the "point of no-return" is crossed and the only possible outcome is death. However, it remains to be determined if the primary cause of ACD is unspecific bulk degradation of cytosolic organelles or selective removal of specific substrates or survival factors [298,304].

Given the fact that excessive autophagy can impair cell viability, induced over-activation of the pathway may offer an attractive strategy for cancer therapy, even though the consequence of promoting autophagy in tumor cells is still an incompletely understood process. Nevertheless, pro-autophagic drugs have emerged as a novel tool to sensitize cancer cells to conventional therapy or to directly kill them exploiting caspase-independent programmed cell death pathways, a particularly relevant feature when cancer cells display resistance to apoptosis. In the following, prototypic examples of ACD upon anticancer treatments will be discussed.

ACD was shown to be behind the cytotoxic activity of arsenic trioxide in T-lymphocytic leukemia and malignant glioma cells, which are resistant to many types of therapy including radiation, chemotherapy and a broad range of drugs. Thanks to these results, arsenic trioxide is now in clinical trials for the treatment of resistant malignant gliomas [307,308]. BH3-mimetics, which antagonize the anti-apoptotic BCL-2 family proteins, have been reported to engage ACD. For example, the BH3-mimetic gossypol has been reported to induce ACD in apoptosis-deficient malignant glioma and prostate cancer cells, while obatoclax has been shown to engage ACD in pediatric acute lymphoblastic leukemia, including glucocorticoid-resistant cases [309–312]. Tetrahydrocannabinol, the main active component of cannabinoids, and the cannabinoid agonist JWH-015 have been proven to respectively stimulate ACD in hepatocellular carcinoma and glioblastoma, both *in vitro* and *in vivo* [272,313]. The vitamin D3 analog EB1089 (Seocalcitol) has been shown to arrest tumor growth and sensitize breast cancer cells to radiation therapy through induction of ACD [314,315]. The results of Seocalcitol treatment in phase II clinical trials for advanced pancreatic and hepatocellular carcinoma patients suggests it may have a cytostatic activity with minimal side-effects and encourage the study of Seocalcitol as an adjuvant therapy in minimal disease states [316,317]. Moreover, several vitamin D3 analogs are now in clinical trials for the treatment of many tumors. The competitive BCR-ABL tyrosine-kinase inhibitor imatinib (widely used for the treatment of chronic myelogenous leukemia and other malignancies) is also supposed to work by induction of autophagy, even in multi-drug resistant tumor cells [318]. Although the anti-cancer properties of the natural mTORC1 inhibitor rapamycin were initially attributed to down-regulation of the AKT signaling, mTOR was found out to be a negative regulator of

autophagy. Since then, a growing collection of evidence suggests that rapamycin (and analogues) exert their tumor-suppressor activity by the stimulation of apoptosis-independent ACD. Among them, the dual mTOR inhibitors have demonstrated to be the most potent inducers of autophagy and significantly suppress tumor growth. mTOR inhibitors are in clinical trials for the treatment of different advanced solid tumors and hematologic malignancies [319–323]. Furthermore, mTOR inhibitors sensitize various tumor cells to radiation therapy [324–326].

Histone deacetylase inhibitors (HDACi) represent another class of anticancer agents shown to engage ACD in chondrosarcoma, glioma, cervical and hepatocellular carcinoma. The HDACi suberoylanilide hydroxamic acid (SAHA) is currently in clinical trials as it demonstrated to be effective in the treatment of hematologic and solid tumors, most likely through stimulation of autophagy via AKT/mTOR pathway inhibition [327–331]. Other autophagy-stimulating agents with tumor-suppressor activity include fluoxetine (a serotonin re-uptake inhibitor) and maprotiline (a norepinephrine re-uptake inhibitor) [332]. The tricyclic antidepressant imipramine and the anticoagulant ticlopidine have also been shown to synergistically trigger cell-lethal autophagy in an *in vivo* model of glioblastoma [333]. Finally, several conventional chemotherapeutic drugs have been reported to engage autophagy. Nonetheless, the common believe is that autophagy is induced after chemotherapy treatments as a cytoprotective response to the cellular stress imposed by the drugs.

The extensive evidence strengthening the notion that ACD could be exploited for cancer therapy makes critical to achieve a greater understanding of the pathways regulating autophagy, as well as the consequences of their activation in different tumoral contexts and the improvement in the identification of molecules which selectively regulate the pro-death branch of autophagy. The multifaceted nature of autophagy, its multilayered cross-talk with other forms of cell death and the outcome dependency on the genetic landscape and environmental factors of every cell are major challenges to determine when to administrate autophagy-inducer drugs. Thus, determination of a set of biomarkers to select when to apply which treatment to which patient would be essential to expand the use of autophagy in fighting cancer.

HYPOTHESIS AND OBJECTIVES

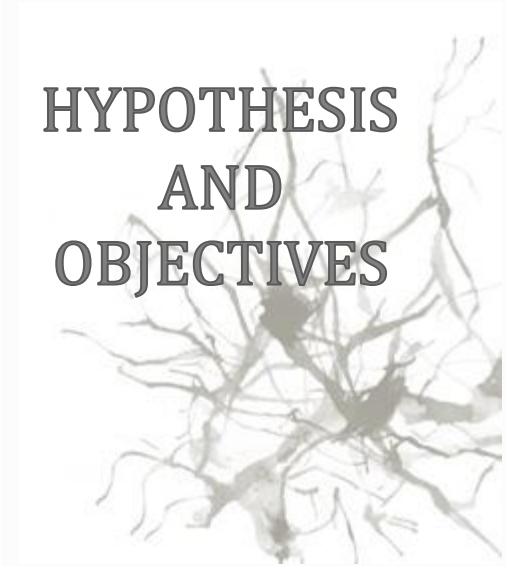

2. Hypothesis and objectives

Although the outcome for patients with NB has improved over the last decades, survival for high-risk patients remains poor, with less than 50% of children likely to achieve 5-year overall survival. The main factors of treatment failure and disease progression are the resistance mechanisms present in NB cells towards conventional chemo- and radiotherapy regimens. These chemotherapy-resistant NB still have not any curative options, what positions research on advances in treatment as a high-priority. Owing to the multiple alterations present in HR-NB cells that cause dysfunctional cell cycle arrest and apoptosis, newly developed targeted agents able to trigger alternative cell death pathways should be considered for this disease. In addition, the implementation of targeted therapies is encouraged to refine treatments to exclusively act in cancer cells, thus minimizing the side effects of non-selective chemotherapeutic drugs.

ABTL0812 is a first-in-class synthetic chemically modified polyunsaturated fatty acid which has been found to be cytotoxic in several cancer cell lines through the activation of autophagic cell death, what would provide an alternative pathway to overcome anti-apoptotic alterations present in HR-NB cells. Moreover, ABTL0812 mechanism of action is based on disrupting the AKT/mTOR signaling pathway, which is crucial for NB tumor growth, survival and chemoresistance. In addition, the PI3K/AKT/mTOR axis integrates all the New Drug Development Strategy (NDDS) prioritized targets for HR-NB. In light of this situation, we hypothesized whether ABTL0812 could be clinically effective for the treatment of HR-NB patients. The high tolerability and favorable results of ABTL0812 in adult clinical trials reinforced us to study ABTL0812 effects on HR-NB.

Our hypothesis will be evaluated through the following objectives:

Objective 1: Study the impact of ABTL0812 treatment in HR-NB models both *in vitro* and *in vivo*.

Objective 2: Characterize the mechanism of action of ABTL0812 in HR-NB.

Objective 3: Study ABTL0812 combination efficacy with current neuroblastoma therapies.

MATERIALS AND METHODS

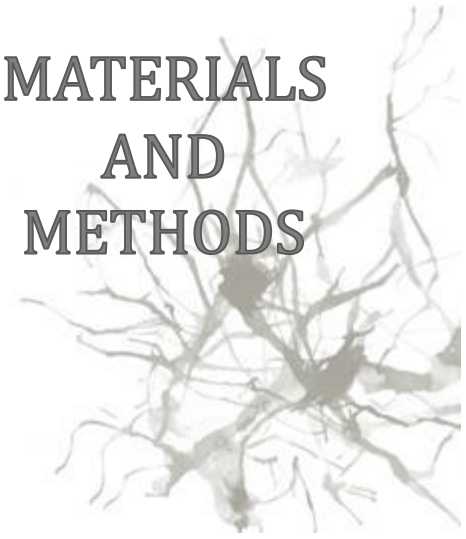

3. Materials and methods

3.1 Reagents

Reagents, working concentrations and suppliers used in this study are listed on Table 7:

Table 7. Reagents

Reagent	Description	Working concentration	Supplier
Cytotoxic or differentiating drugs			
ABTL0812	Polyunsaturated fatty acid derivative	20-50µM-120mg/kg (mice)	Ability Pharma.
cis-Diammineplatinum(II) dichloride	DNA crosslinking agent	25µM-2mg/kg (mice)	Sigma-Aldrich
Doxorrubicin hydrochloride (Adriamycin)	Topoisomerase II inhibitor	0,15-0,35µM	Selleckchem
SN-38 (Irinotecan)	Topoisomerase I inhibitor	4-16µM	Selleckchem
Topotecan hydrochloride	Topoisomerase I inhibitor	0,5-2µM	Selleckchem
Cyclophosphamide monohydrate	DNA crosslinking agent	1-2mM	Selleckchem
13-*cis* -retinoic acid (Isotretinoin)	Dopamin β-hydroxylase activator	5-20µM	Selleckchem
Inhibitors			
E64d	Cysteine-catepsines inhibitor	10µM	Sigma-Aldrich
Pepstatin A	Aspartic-proteases inhibitor	10µg/ml	Sigma-Aldrich
QVD-OPh	Pan-caspase inhibitor	20µM	Sigma-Aldrich
MG132	Proteasome inhibitor	0,5µM	Sigma-Aldrich
Stains			
Crystal violet	Cell proteins and DNA dye	5mg/ml	Sigma-Aldrich
Hoechst 33342	Nucleic acid dye	0,05µg/ml	Sigma-Aldrich
Propidium iodide	DNA intercalating dye	2,5µM	Thermo-Fisher
Solvents			
DMSO	Polar and non-polar solvent		Sigma-Aldrich
Ethanol absolut	Polar and non-polar solvent		PanReac
Glycerol	Polar and non-polar solvent		Sigma-Aldrich
PBS	Polar solvent		Thermo-Fisher
DEPC-treated water	Polar solvent		Thermo-Fisher
Supplier	**Headquarters**		
Ability Pharmaceuticals	Cerdanyola, BCN, Spain		
PanReac AppliChem	Castellar del Vallès, BCN, Spain		
Sigma-Aldrich	St. Louis, MO, USA		
Selleckchem	Houston, TX, USA		
Thermo-Fisher Scientific	Waltham, MA, USA		

3.2 Methods

3.2.1 Cell culture and cryopreservation of cell lines

The following cell lines and their corresponding medium were used for this study (Table 8 and 9). Cell cultures were maintained at 37ºC in a humidified atmosphere with 95% air and 5% CO_2. NB cells were tested for mycoplasma contamination periodically.

Table 8. Cell lines and medium

Cell line	Medium	Supplier	Headquarters
Neuroblastoma			
CHLA-90	IMDM + 10% FBSi (v/v) + 1% insulin-transferrin-selenium supplement (v/v) + 100U/ml penicillin-100µg/ml streptomycin + 5µg/ml plasmocin	COG	Lubboc, TX, USA
SK-N-BE(2)		PHECC	Salisbury, UK
LA1-5s		PHECC	Salisbury, UK
SK-N-AS		ATCC	Manassas, VA, USA
SH-SY5Y		ATCC	Manassas, VA, USA
IMR-32		ATCC	Manassas, VA, USA
Alveolar rhabdomyosarcoma			
RH30	MEM + 10% FBSi (v/v) + 2mM glutamine + 100U/ml penicillin-100µg/ml streptomycin + 5µg/ml plasmocin	ATCC	Manassas, VA, USA
CW		ATCC	Manassas, VA, USA
Embrional rhabdomyosarcoma			
HTB-82	MEM + 10% FBSi (v/v) + 2mM glutamine + 100U/ml penicillin-100µg/ml streptomycin + 5µg/ml plasmocin	ATCC	Manassas, VA, USA
RD		Dr. Beat Schäfer	University of Zürich, Switzerland
Ewing sarcoma			
TC-71	IMDM + 10% FBSi (v/v) + 1% insulin-transferrin-selenium supplement (v/v) + 100U/ml penicillin-100µg/ml streptomycin + 5µg/ml plasmocin	DSMZ	Braunschweig, Germany
SK-ES-1	MEM + 10% FBSi (v/v) + 2mM glutamine + 100U/ml penicillin-100µg/ml streptomycin + 5µg/ml plasmocin	ATCC	Manassas, VA, USA
Hepatoblastoma			
HEPG2	MEM + 10% FBSi (v/v) + 2mM glutamine + 100U/ml penicillin-100µg/ml streptomycin + 5µg/ml plasmocin	ATCC	Manassas, VA, USA
Medulloblastoma			
RES196	DMEM, high glucose, pyruvate + 10% FBSi (v/v) + 100U/ml penicillin-100µg/ml streptomycin + 5µg/ml plasmocin		Seattle Children's Hospital Research Insititute, WA, USA

Medium components	Supplier	Headquarters
IMDM	Thermo-Fisher Scientific	Waltham, MA, USA
MEM	Thermo-Fisher Scientific	
DMEM	Thermo-Fisher Scientific	
FBS	Thermo-Fisher Scientific	
ITS	Thermo-Fisher Scientific	
Penicillin-streptomycin	Thermo-Fisher Scientific	
Glutamine	Thermo-Fisher Scientific	
Plasmocin	InvivoGen	San Diego, CA, USA

IMDM, Iscove's Modified Dulbecco's Medium; MEM, Minimum Essential Medium; FBSi, heat-inactivated fetal bovine serum; ITS, insulin-transferrin-selenium supplement; COG, Children's Oncology Group Cell Culture and Xenograft Repository; PHECC, Public Health England Culture Collections; ATTC, American Type Culture Collection.

Table 9. Patient and derived NB cell lines characterization

Cell line	Age	Stage	Metastasis	Origin	Treatment	*MYCN* status	*ALK* status	Caspase-8	11q	p53
CHLA-90	8 years	4	Bone marrow	Unknown	+	Non amplified	F1245V Mut	+	+	E286K Mut, NF
SK-N-BE(2)	2 years	4	Bone marrow	Unknown	+	Amplified	WT	+	+	C135F Mut, NF
SK-N-AS	8 years	4	Bone marrow	Adrenal medulla	+	Non amplified	WT	-	-	Exon 9b AS, NF
LA1-5s	2 years	4	Bone marrow	Unknown	+	Amplified	F1174L Mut	+	+	C182X Mut, NF
SH-SY5Y	4 year	4	Bone marrow	Thorax	+	Amplified	PA, WT	-	-	WT, functional
IMR-32	1 year	4	Unknown	Abdomen	-	Non amplified	F1174L Mut	-	+	WT, functional

PA, partial amplification; WT, wild type; Mut, Mutated; -, lack of expression/loss of heterozigozity; +, expression; AS, alternative splicing; NF, non functional.

To maintain a continuous stock of cells, all cell lines used in the frame of this thesis were amplified, cryopreserved and stored. For long-term storage, early passages of cells were cryopreserved in liquid nitrogen to abrogate cellular processes. To ensure the cell integrity during the cryopreservation process, cells were frozen in cellular media supplemented with 10% of dimethyl sulfoxide (DMSO) and cryovials were placed into propanol-filled cooler before storage in a liquid nitrogen tank. Upon resuscitation, cells had to be thawed quickly with cellular media and re-suspended in 10 times media volume to dilute the DMSO. Then, cells were centrifuged and the supernatant was replaced for fresh media to seed them in appropriate culture dishes.

3.2.2 Cell death and viability assays

3.2.2.1 Cell proliferation assay (crystal violet)

Cells were seeded in 96-well plates at low density (n=6/condition) and left in standard culture conditions. Twenty-four hours later, the medium was aspirated and cells were treated with the indicated drugs diluted in the corresponding culture medium supplemented with 0.5% FBS. At the indicated times, cells were fixed with 1% glutaraldehyde (Sigma-Aldrich) and washed with PBS to remove the excess of glutaraldehyde. Then, wells were stained with 0.5% of crystal violet for twenty minutes. After that, an extensive washing with distilled water was performed to remove the excessive dye and plates were let dry. When violet crystals were dried, they were dissolved in 15% of acetic acid (Thermo-Fisher Scientific) and optical density was measured at 590nm using Epoch Microplate spectrophotometer (Biotek). The viability assays were repeated in three independent experiments.

3.2.2.2 Cell death: Hoechst and propidium iodide staining

Hoechst staining method consists of DNA staining with a fluorescent dye that becomes highly fluorescent when binds to adenosine-thymidine rich regions of genomic DNA. Hoechst 33342 is a cell-permeant nuclear stain excited by UV light (350nm) and emits blue fluorescent light (461nm) without affecting cell viability. Thus, Hoechst staining allows the characterization of apoptosis through the observation of nuclear chromatin condensation (pyknosis) and/or fragmentation using a fluorescent microscope.

On its behalf, propidium iodide (PI) is a dye that enters the cell when the membrane integrity is lost, as is the case for late-apoptotic and necrotic cells. PI is a fluorescent molecule excited by green fluorescent light (535nm) that intercalates between nucleic acids of double stranded DNA. When it bounds to DNA, it enhances its fluorescent emission in red light (617nm). Thereby, the determination of PI positive cells in a sample by fluorescence microscopy allows for necrosis and late apoptosis quantification.

To discriminate dead and apoptotic cells to assess cell death, cells were seeded in 24-well plates in standard culture conditions. Twenty-four hours later, the medium was aspirated, wells were rinsed with PBS and cells were treated with the indicated drugs diluted in culture medium supplemented with 0.5% FBS. At the indicated time post-treatment, a staining buffer consisting of 0.05µg/ml Hoechst 33342 and 2.5µM PI was added to the medium. The plates were let incubating with the staining buffer during fifteen minutes protected from light. Then, cells were observed using a fluorescent microscopy (Nikon Eclipse 90i, Nikon) exciting cells with UV light (for Hoechst staining) and green fluorescent light (for PI staining) under a 20X magnification. Dead cells as well as condensed or fragmented nuclei were counted from four representative images of each well. The count was repeated three times per condition in three independent experiments.

3.2.2.3 Apoptosis and autophagy rescue

Caspases are a family of intracellular cysteine proteases which activation is essential in the execution of apoptosis. QVD-OPh (QVD) is a cell-permeable, irreversible, specific broad-spectrum caspase inhibitor. Thereby, treatment with QVD prevents caspase activation abrogating apoptotic cell death.

E64d is a pro-drug ethyl ester of its biologically active acid form, E64c. E64d can permeate an intact cell and permanently block the activity of cysteine proteases cathepsins B, H, L and calpains by covalently binding to the sulfhydryl groups located in the proteases active site. By inhibiting the lysosomal proteases, E64d interferes with autolysosomal digestion. For optimal results, though, it should be used in combination with pepstatin A. Pepstatin A forms a highly selective reversible inhibitory complex with aspartic acid proteases such as pepsin, renin, cathepsin D, E, bovine chymosin, and protease B. Thus, it complements E64d protease inhibitory properties to prevent the degradation of the autolysosome cargo.

In order to distinguish whether HR-NB cells were dying by apoptosis or autophagy, cells were seeded in 24-well plates (5×10^4 or 2.3×10^4 cells/well for SK-N-BE(2) and LA1-5s, respectively) previously coated with poly-D-Lysine (40µg/ml; Sigma-Aldrich) and collagen (Corning). After twenty-four hours incubation in standard culture conditions, cells were pre-treated for two hours with either 20µM QVD or the mixture of lysosome proteases inhibitors E64d (10µM) and PA (10µg/ml). Afterwards, cells were washed with PBS and treated with the combination of ABTL0812 (20µM SK-N-BE(2), 30µM LA1-5s) and QVD or E64d+PA diluted in culture medium supplemented with 0.5% FBS. Cells were left in the

incubator forty-eight hours longer, but QVD was replaced every twenty-four hours in the corresponding wells. Forty-eight hours after treatment, cell death was scored using the Hoechst/PI staining method. The count of dead and apoptotic cells was repeated two times per condition in three independent experiments.

3.2.3 Chemical bacterial reverse mutation assay (Ames test)

The Ames test is based on the mutation incorporation test using the mutant Salmonella typhimurium strains TA98, TA100, TA102, TA1535 and TA1537 (Trinova Biochem). These strains are auxotrophic mutants unable to synthesize histidine from the ingredients of culture media, which, on the contrary, is an essential amino-acid for their survival. Thus, if the bacteria are able to grow in a histidine-free culture medium when they are incubated with the tested substance, it would indicate the capacity of the compound to induce mutations that return *Salmonella* strains to a prototrophic state (revertant strains). The strains used in the Ames test are particularly sensitive to mutations as they bear a mutation that generates partial loss of the lipopolysaccharide barrier that protects the surface of the bacteria, causing increased cell wall permeability. Moreover, these strains also carry disabling mutations in the DNA repair mechanisms. The rat liver enzyme S9 (Harlan) is often added to the Ames test to simulate the metabolic processes that would suffer the tested substance if it was ingested by a larger organism (like mammals).

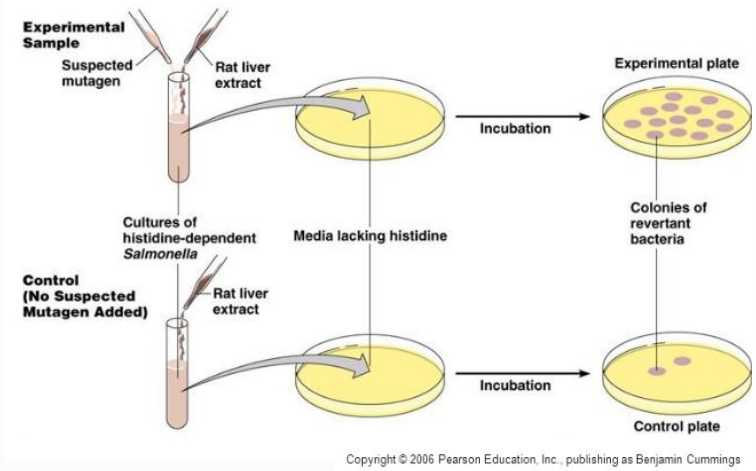

Figure 15. Ames test workflow. The auxotrophic *Salmonella* strains are suspended in growth medium containing the possible mutagen, a small amount of histidine and rat liver extract (optional). Then, *Salmonella* and media are spread on test plates or control plates (no mutagen added to the initial suspension). After 48h incubation, many revertant *Salmonella* colonies should appear in the experimental plates compared to control plates.

Briefly, the auxotrophic bacteria were spread on an agar plates suspended in growth medium complemented with different ABTL0812 concentrations (3-5000µg/plate), with or without the microsomal fraction S9 (concentration 38mg/ml) and with small amounts of histidine. The small amounts of histidine are required for initial growth of the bacteria to give them the opportunity to mutate. Once histidine is depleted, only bacteria that have

mutated and gained the ability to synthesize histidine would survive and form colonies. The spread plates were incubated forty-eight hours at 37ºC before proceeding to count the number of colonies in each plate (Figure 15). Determination of the number of revertant colonies induced by ABTL0812 with or without S9 metabolic activation is considered proportional to its mutagenicity.

3.2.4 Distribution of LC3-II by immunocytochemistry

Cells were seeded in 24-well plates (8×10^4 cells/well for SK-N-BE(2); 6×10^4 cells/well for LA1-5s), where slide covers coated with poli-L-lysine (40µg/ml; Sigma-Aldrich) had been previously included to favor cell adhesion. Cells were left twenty-four hours in standard culture conditions and then treated with the indicated treatments for twelve hours with culture medium supplemented with 0.5% FBS. Cells were rinsed with PBS and fixed with 4% paraformaldehyd (Sigma-Aldrich). Next, cells were washed three times with PBS and permeabilized with 0.02% saponin (Sigma-Aldrich) for seven minutes. After a wash with PBS, cells were incubated fifteen minutes with 0.01% saponin and 10mM glycine (Sigma-Aldrich), and 0.01% saponin,10mM glycine and 5% BSA (bovine serum albumin; Sigma-Aldrich) during one hour to block unspecific antibody binding. Afterwards, cells were incubated with the corresponding primary antibody (LC3-II, see Table 11) diluted in 0.01% saponin and 1% BSA in a wet chamber at 4ºC. From this point, the following steps must be done in a dark environment to protect the antibody fluorophores from light. Cells were washed five times with PBS and incubated in a wet chamber at room temperature with fluorophore-conjugated secondary antibody Alexa Fluor® 594 goat anti-rabbit IgG (Table 12) diluted in 0.01% saponin and 1% BSA. After five additional PBS washes, the slide covers were incubated five minutes with Hoechst to stain the nucleus, rinsed four more times, and mounted on a slide with a drop of Fluorsave mounting medium (Calbiochem). Finally, slides were observed using a fluorescent microscopy (Nikon Eclipse 90i, Nikon). Immunostaining was repeated three times per condition in three independent experiments.

3.2.5 Autophagic flux assessment

Cells were seeded in p60 plates (9×10^5/p60 for SK-N-BE(2); 4×10^5c/p60 for LA1-5s) and incubated in standard culture conditions for twenty-four hours. Following, the medium was removed and cells were pre-treated for two hours with lysosome proteases inhibitors E64d (10µM) and PA (10µg/ml) diluted in culture medium supplemented with 0.5% FBS. After pre-treatment, ABTL0812 30µM (SK-N-BE(2)) or 40µM (LA1-5s) was added to the medium for six hours. When the treatment was finished, cells were pelleted for further protein expression analysis (see below in section 3.2.8).

As the mix of E64d+PA inhibits the degradation of the autolysosomes, the autophagic circuit would not be completed and the vesicles would accumulate in the cytosol, thereby indicating that ABTL0812 triggers dynamic autophagy in HR-NB cells. The lysosomal suppression was repeated in three independent experiments.

3.2.6 Mouse xenografts

Mouse xenografts consist of injecting human tumoral cells in the flank of the mice. This method resembles better the human diseases because tumor cells are able to grow in contact with other cell types and tissues. For this study, all mice procedures were performed according to the guidelines of the Spaninsh Council for Animal Care and all protocols were approved by the Ethics Committee for Animal Experimentation of Vall d'Hebron Research Institute (protocol number-12/14 CEEA).

In order to assess the therapeutic potential of ABTL0812 in HR-NB, we performed a xenograft approach in NMRI-Foxn1$^{nu/nu}$ immunodeficient mice (NMRI-nude) using the human NB cell line SH-SY5Y. NMRI-Foxn1$^{nu/nu}$ mice bear a mutation in the *Foxn1* (forkhead box N1) gene that cause thymic aplasia, which results in a lack of T cells. This immunodeficient model has been widely used as a host for transplanted tumors and xenografts [334–336]. Hence, 5×10^6 SH-SY5Y cells were injected in the flank of 6 week-old NMRI-nude female *mice* (n=15/group; Janvier) in 300µl of PBS and Matrigel™ (Corning) in proportion 1:1. Animals were maintained in the specific-pathogen-free area of the Vall d'Hebron animal house.

Tumor formation was monitored by palpation every two or three days for two weeks. Once all mice had developed detectable tumors (~70mm^3), mice were randomly assigned in three groups to be treated with (1) vehicle (5% glycerol in water; Sigma-Aldrich), (2) 120mg/kg ABTL0812 or (3) 2mg/kg of cisplatin (CDDP). ABTL0812, diluted in 5% glycerol, and vehicle were orally administered with the help of an oral gavage needle seven times per week. CDDP, diluted in PBS, was administered by intraperitoneal injection two times per week. Tumor growth was measured using a digital caliper two or three times per week. Tumor volume was calculated using the formula (width^2×length/2). When primary tumors reached the 1600mm^3 growth limit, mice were euthanized and tumors excised and weighted. Then, tumors were divided into two portions: one portion was frozen and stored at -80ºC while the other one was fixed in 10% neutral buffered formalin (Sigma-Aldrich) and paraffin-embedded. From these samples, 5µm sections were stained with hematoxylin-eosin for histological analysis.

3.2.7 Proteasomal inhibition

The membrane-permeable proteasome inhibitor MG132 is a titerpene peptide aldehyde derived from a Chinese medicinal plant that inhibits the proteasome complex. It covalently binds to the β-subunit active site of the catalytic 20S core particles, effectively blocking the proteolytic activity of the 26S proteasome. Therefore, treatment with MG132 is used to study the effects of the ubiquitin-proteasomal system de-regulation.

With the aim to analyze whether ABTL0812 had an impact on the cells protein levels through proteasome-degradation pathway impairment, SK-N-BE(2) cells were seeded in p100 plates (2×10^6c/p100) and incubated in standard culture conditions. Twenty-four

hours later, the medium was removed and cells were pre-treated two hours with the proteasome inhibitor MG132 at concentration 0.5µM diluted in culture medium supplemented with 0.5% FBS. After the pre-treatment, ABTL0812 30µM was added to the medium during three hours. When the treatment was finished, cells were pelleted for further protein expression analysis (see below in section 3.2.8).

3.2.8 Analysis of mRNA expression levels (qRT-PCR)

3.2.8.1 RNA extraction and quantification

Before extraction, cells were collected, washed with PBS, and pelleted at 800g in a tabletop centrifuge. At this point, samples can be kept at -80ºC until further use.
Since mRNA samples are vulnerable to degradation induced by ribonucleases (RNases) and temperature-related effects, mRNA extraction and handling should be performed in a clean and quiet environment and samples should always be kept on ice, short-time storage at -20ºC, and long-time storage at -80ºC.

Total RNA was extracted using the RNeasy Mini Kit (Qiagen) following the manufacturer's protocol. It consists on a guanidine-isothiocyanate-based lysis buffer followed by the addition of ethanol to create the ideal binding conditions of RNA to the silica-membrane containing columns used for purification, which allows washing contaminants out. Finally, RNA is eluted with DEPC-treated RNase-free water (Thermo Fisher Scientific). Then, it was quantified by Nanodrop spectrophotometer (Thermo Fisher Scientific) and stored at -80ºC.

3.2.8.2 RNA reverse transcription

For mRNA expression analyses, RNA samples must be converted to complementary DNA (cDNA) through reverse transcription (RT). To this end, 500ng of total RNA were subjected to DNase I treatment (Qiagen) and RT using the High-Capacity cDNA Reverse Transcription Kit (Applied Biosystems) following the manufacturer's protocol. The RNA eluted with the protocol was loaded into a thermal cycler to continue with the RT procedure. Thermal cycler conditions were: 25ºC for ten minutes, 42ºC for sixty minutes to retro-transcribe RNA into cDNA, 95ºC during five minutes to stop the reaction, and 4ºC as long as needed to maintain samples at optimal conditions. For long-time storage, cDNA was kept at -20ºC.

3.2.8.3 Quantitative PCR

To analyze mRNA expression levels, cDNA samples were submitted to quantitative PCR (qPCR) using a SYBR-based protocol. Briefly, primers against the corresponding genes were designed using the NCBI primer designing tool (https://www.ncbi.nlm.nih.gov/tools/primer-blast/) pre-establishing an optimal melting temperature of 60ºC, a PCR product ranging from 80-200 nucleotides and adding exon-

exon span conditions. Exon-exon span restriction allows annealing of both primers in sequential exons or in an exon junction, impeding genomic DNA amplification. Primers were synthesized by Sigma-Aldrich. Before performing the qPCR, primers were tested in a conventional PCR. The primer sequences used in this project are listed in Table 10.

To perform the qPCR, 12.5ng/µl of cDNA, Power SYBR Green Master Mix (Thermo Fisher Scientific) and 0.4µM of primers were mixed. The qPCR reaction was run in 96-well plates per triplicate in an ABI700SDS equipment. The settings for mRNA detection were: initial denaturing of 95ºC for ten minutes, denaturing for fifteen seconds at 95ºC and one minute annealing process at 60ºC. These last two steps were repeated during forty cycles. The data from the qPCR reaction was analyzed with the 7900HT Sequence Detection System 2.3 software (Thermo Fisher Scientific) using the relative quantification method. According to this, the mRNA levels were quantified depending on the Ct values, which represent the number of cycles at which the fluorescence signal reached a predetermined threshold. This means that larger amounts of cDNA copies correlate with higher mRNA expression levels, indicated by lower Ct values that correlate with more intense fluorescent signal detected at earlier PCR cycles. To eliminate loading errors and normalize values, gene expression was normalized against *GADPH* housekeeping gene. The housekeeping Ct readings were subtracted from the Ct values of the gene of interest. The resulting fold-change relative quantification of gene expression was performed using the comparative $2^{(-\Delta\Delta Ct)}$ method [337].

Table 10. Primer sequences of genes used for RT-qPCR

Gene	Sequence (5' to 3')	Amplicon
MYCN	Fw: AGAGGAGACCCGCCCTAATC	100bp
	Rv: TCCAACACGGCTCTCCGA	
TRIB3	Fw: TACCTGCAAGGTGTACCCC	100bp
	Rv: GGTCCGAGTGAAAAAGGCGTA	
E2F1	Fw: CCTGGCCTACGTGACGTGTC	100bp
	Rv: CGGCTTGGAGCTGGGTCT	
E2F2	Fw: AGGGGAAGTGCATCAGAGTG	100bp
	Rv: GCGAAGTGTCATACCGAGTCT	
E2F3	Fw: AGGGCTCTCTTACACCGCACT	100bp
	Rv: AAATGCCACTCACACAATCCC	
GADPH	Fw: CGCTCTCTGCTCCTCCTGTT	100bp
	Rv: CCATGGTGTCTGAGCGATGT	

3.2.9 Analysis of protein expression levels (Western Blot)

3.2.9.1 Protein extraction

Protein extraction must preserve de integrity of the extracted proteins during the process; therefore, the extraction must be efficient and avoid degradation in order to get an accurate reflection of the proteins physiological state in the living cell.

Protein samples were extracted using RIPA buffer 1X (Thermo Fisher Scientific) supplemented with 1X EDTA-free complete protease inhibitor cocktail (Roche) and the phosphatase inhibitors sodium fluoride and sodium orthovanadate (Sigma-Aldrich). Cell lysis was performed on ice for twenty minutes prior centrifugation at 14000g and 4ºC during fifteen minutes. This process precipitates DNA and membranes while nuclear and cytosolic proteins remain in the supernatant. Protein samples were stored at -20ºC until further use.

3.2.9.2 Protein quantification

Protein concentration was determined using Lowry DC protein assay (Bio-Rad) following manufacturer's instructions. This method is based on the Biuret reaction, in which protein quantification is obtained by measuring the reaction of peptide bonds and radical groups with copper ions under alkaline conditions. Divalent cooper ions form complexes with the peptide bonds, reducing them to monovalent copper ions. The monovalent copper ions and the radical groups induce the reduction of the Folin-Ciocalteu reagent present in the Lowry kit, which changes from yellow to blue color.

Proteins were quantified by loading 1µl of cell lysates per well with a mix from the Lowry kit reagents in a transparent 96-well plate in triplicates. First, Lowry's reagents A and S were added in a ratio 100/2 in a volume of 25µl/well. Reagent B (Folin reagent) was added after loading the protein samples in a volume of 200µl/well. Then, plates were protected from light and incubated ten minutes at room temperature. Samples absorbance was read at 650-700nm using a spectrophotometer. Lastly, protein concentrations were quantified comparing the samples absorbance to a standard calibration curve done with reference BSA concentrations.

3.2.9.3 Western Blot

Western Blot samples were prepared to contain between 25-30µg of protein in RIPA buffer 1X mixed with loading buffer 1X (NuPAGE LSD Sample Buffer 4X; Invitrogen). The loading buffer gives density and negative charge to the samples, facilitating gel loading and protein migration during electrophoresis, respectively. Samples were always prepared in equal volume and quantity, and heated for ten minutes at 70ºC to ascertain complete protein denaturation. Before loading the samples in the gel, the proteins were reduced with ditiotreitol adding the NuPAGE™ Sample Reducing agent 1X (NuPAGE™ Sample

Reducing agent 10X; Thermo Fisher Scientific). Samples were run for forty five minutes at 200V at room temperature in pre-cast NuPAGE™ 4-12% Bis-Tris gels (Thermo Fisher Scientific) in MES- or MOPS- running buffer 1X (Thermo Fisher Scientific), depending on the size of the proteins of interest, supplemented with NuPAGE™ Antioxidant (Thermo Fisher Scientific). Precision Plus Protein™ Dual Color Standards (Bio-Rad) was used as protein ladder.

Once protein samples have been subjected to gel electrophoresis, proteins are transferred to membranes to allow further handling. In this thesis, polyvinylidine diflouride membranes (PVDF; GE Healthcare) were chosen to immobilize the proteins. PVDF membranes have a protein binding capacity of 170-200µg/cm^2, offering a high sensitivity and detection of poorly expressed proteins. Furthermore, as proteins bind to PVDF membranes through hydrophobic and dipole interactions they resist better membrane stripping, making them ideal for reprobing. As a counterpart, they display more background noise. For work performed in this thesis, proteins were transferred to PVDF membranes using the wet transfer method. Wet method consists of preparing a membrane sandwich and submerging it on transfer buffer inside a transfer tank. This method is the most traditional method and is useful for all types of proteins. First, PVDF membranes must be soaked in methanol (Acros Organics) one minute for activation. Then, membranes were hydrated and equilibrated with distilled water and transfer buffer, respectively. Once the membranes were activated, the transfer sandwich was mounted in the following order (Figure 16):

1. Pad wet in transfer buffer.
2. Whatman filter paper (Thermo Fisher Scientific) wet in transfer buffer (x2).
3. NuPAGE™ resolving gel.
4. PVDF membrane.
5. Whatman filter paper wet in transfer buffer (x2).
6. Pad wet in transfer buffer.

The membrane sandwich was submerged in a transfer tank filled with ice-cold transfer buffer. The sandwich should be completely covered and wet. Finally, transference was run at high voltage (110V) for one and a half hours at 4ºC. The composition of transfer buffer was: tris 25mM (Thermo Fisher Scientific), glycine 192mM (Alfa Aesar), methanol 20% (v/v); pH 8.3.

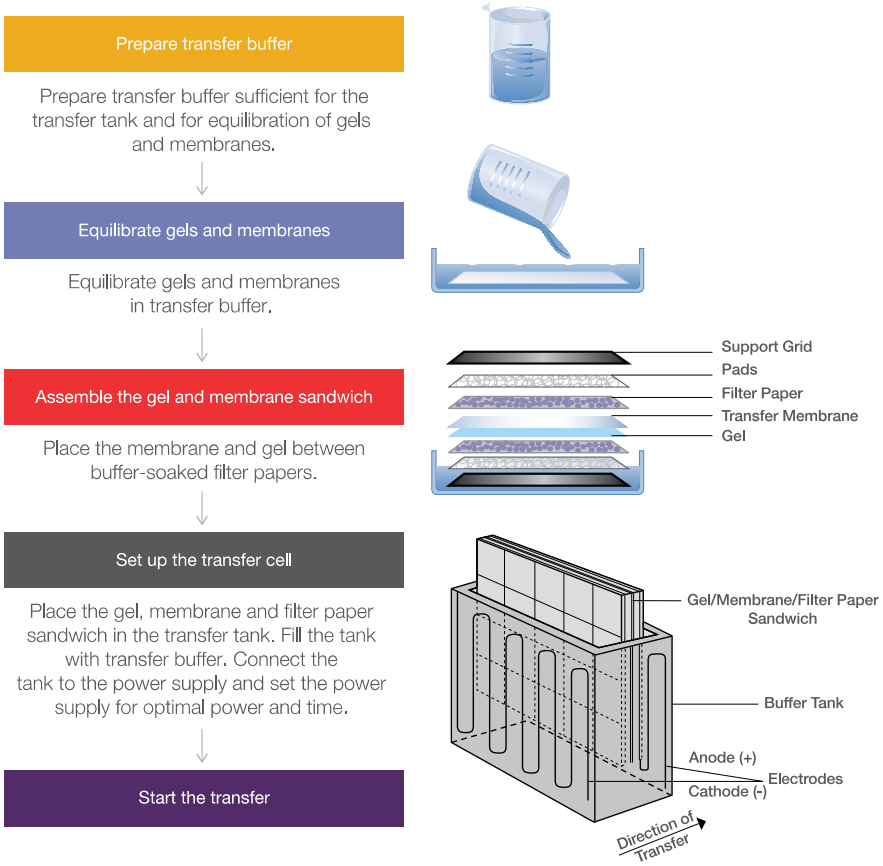

Figure 16. Western Blot protein wet transfer set-up. Before assembling the sandwich, its components are equilibrated in transfer buffer. Then, the sandwich is submerged inside a transfer tank filled with transfer buffer. Last, a current is applied to the tank to let proteins migrate from the gel to the membrane. Figure adapted from [338].

After protein transfer, membranes were quickly washed with tris-buffered saline with Tween-20 (TBS-T). The composition of TBS-T buffer was: tris 20mM, NaCl 150mM (PanReac), Tween-20 0.1% (v/v) (Sigma-Aldrich); pH 7.5. Afterwards, membranes were incubated with blocking solution TBS-T supplemented with 5% BSA or non-fat milk (PanReac) for one hour at room temperature, depending on the antibody conditions. Next, membranes were incubated overnight at 4ºC with the indicated primary antibodies (Table 11). The following day, primary antibodies were recycled and membranes were washed for five minutes three times with TBS-T. Then, membranes were incubated with host-corresponding secondary antibodies against the primary antibodies during one hour at room temperature. The secondary antibodies conditions used in this thesis are listed on Table 12. Secondary antibodies are usually conjugated to the horseradish peroxidase (HRP) enzyme, which transforms HRP substrates into chemiluminescence. Incubation of membranes with EZ-ECL Chemiluminescence Detection Kit (GE Healthcare) allows for antigen detection by exposing the membranes to X-ray films (Fujifilm) and further film revealing in a dark room.

Table 11. Primary antibodies

Antibody	MW (kDa)	Specie	Working dilution	Dilution media (w/v)	Supplier	Reference
Actin-HRP	45	Rabbit	1:40,000	5% BSA in TBS-T	SCBT	sc-1616*
AKT	60	Rabbit	1:5,000	5% BSA in TBS-T	CST	#9272
ATG5	55	Mouse	1:1,000	5% milk in TBS-T	Nanotools	ATG5-7C6
ATF4	49	Rabbit	1:2,000	5% milk in TBS-T	CST	#11815
Caspase-3	35	Rabbit	1:3,000	5% BSA in TBS-T	CST	#9662
Caspase-3 cleaved	19-17	Rabbit	1:750	5% BSA in TBS-T	CST	#9664
CHOP	27	Mouse	1:1,000	5% milk in TBS-T	CST	#2895
E2F1	60	Mouse	1:1,000	5% BSA in TBS-T	BD	#554213
E2F2	55	Rabbit	1:1,000	5% BSA in TBS-T	SCBT	sc-632
eIF2α	38	Rabbit	1:1,000	5% BSA in TBS-T	CST	#5324
GADPH	37	Mouse	1:10,000	5% milk in TBS-T	SCBT	sc-32233
LC3-II	19-17	Rabbit	1:10,000	5% BSA in TBS-T	Abcam	ab48394
MYCN	60	Mouse	1:2,000	5% BSA in TBS-T	SCBT	sc-53993
NOXA	8	Mouse	1:300	5% BSA in TBS-T	Merck	#114C307
p-AKT^{ser473}	60	Rabbit	1:500	5% BSA in TBS-T	CST	#9271
p-eIF2α	38	Rabbit	1:2,000	5% BSA in TBS-T	CST	#3398
p-H2AX	17	Mouse	1:1,000	5% BSA in TBS-T	Millipore	#05-636
p-PRAS40	40	Rabbit	1:2,000	5% BSA in TBS-T	CST	#2997
p-S6	32	Rabbit	1:10,000	5% BSA in TBS-T	CST	#4858
PARP	116	Rabbit	1:5,000	5% BSA in TBS-T	CST	#9542
PRAS40	40	Sheep	1:1,000	5% milk in TBS-T	MRC PPU	S115B
TRB-3	43	Rabbit	1:3,000	5% milk in TBS-T	Abcam	ab50516
Tubulin	50	Mouse	1:20,000	5% milk in TBS-T	Sigma-Aldrich	T5168
S6	32	Rabbit	1:5,000	5% BSA in TBS-T	CST	#2217

Supplier	Headquarters
Abcam	Cambride Biomedical Campus, Cambridge, UK
Becton Dickinson Biosciences	Franklin Lakes, NJ, USA
Cell Signaling Technologies	Beverly, MA, USA
Merck Millipore	Billerica, MA, USA
MRC PPU Reagents and Services	University of Dundee, Dundee, UK
Nanotools	Teningen, Germany
Sigma-Aldrich	St. Louis, MO, USA
Santa Cruz Biotechnology	Santa Cruz, CA, USA

MW, molecular weight; w/v, weight/volume; SCBT, Santa Cruz Biotechnology; CST, Cell Signaling Technologies; BD, Becton Dickinson Biosciences; MRC PPU, MRC Protein Phosphorylation and Ubiquitylation Unit; *discontinued and replaced by sc-47778.

Table 12. Secondary antibodies

Antibody	Specie	Working dilution	Dilution media (w/v)	Supplier	Reference
Anti-Rabbit IgG Alexa Fluor® 594	Goat	1:10,000	5% BSA in TBS-T	Thermo-Fisher	#A11037
Anti-Rabbit IgG-Peroxidase	Goat	1:10,000	5% BSA in TBS-T	Sigma-Aldrich	#A0545
Anti-Mouse IgG-Peroxidase	Rabbit	1:10,000	5% milk in TBS-T	Sigma-Aldrich	#A9044
Anti-Sheep IgG-Peroxidase	Donkey	1:10,000	5% milk in TBS-T	Sigma-Aldrich	#A3415
Supplier		**Headquarters**			
Thermo-Fisher Scientific		Waltham, MA, USA			
Sigma-Aldrich		St. Louis, MO, USA			

To detect proteins with different molecular weight and different host species, inactivation of the HRP previously bound to the membrane would be enough to eliminate the first antibody signal. To this aim, membranes were soaked during 30 minutes in 0.02% (w/v) sodium azide (PanReac), which inactivates the HRP enzyme of the secondary antibodies. After incubation with sodium azide, membranes were washed thoroughly in TBS-T before incubation with the next primary antibody. When the use of secondary antibodies from different species was not possible, membranes were stripped. Stripping releases the primary and secondary membrane-bound antibodies thanks to the action of denaturing buffers. For this thesis, fifteen minutes incubation with Re-Blot Mild Stripping Solution (Merck) diluted 1X in DEPC-treated water was used for membrane-reprobing. After incubation with Re-Blot solution, membranes were washed thoroughly in TBS-T before re-blocking.

3.2.10 Cell transfection

HR-NB cells were transfected with the soluble cationic lipid agent Lipofectamine 2000® (Thermo Fisher Scientific). In an aqueous media, the components of this reagent are self-assembled to form positively-charged liposomes that entrap nucleic acids inside the vesicle's membrane, thereby shielding their negative charge. After liposome-nucleic acid complex formation, the transfection complex interacts with the cell membrane and delivers the RNA into the cells through endocytosis. There, the RNA is expressed or induces expression silencing.

In this thesis, Lipofectamine 2000® was used for the lipoplexes formation with ATG5 siRNA (sequence: CAUCUGAGCUACCCGGAUA; Sigma-Aldrich) and their subsequent transfection. The protocol used was adapted from manufacturer's recommendations. Briefly, Lipofectamine 2000® diluted in OptiMEM (Thermo Fisher Scientific) and selected siRNA diluted individually in Opti-MEM at 25nM were mixed and incubated together for twenty minutes at room temperature to enhance the lipoplexes-siRNA formation. Afterwards, the lipoplexes were added into cellular media without antibiotics, which may interfere in cellular transfection. Following overnight transfection, the media was replaced with fully supplemented media in order to remove the lipoplexes to avoid toxicity that may be caused by the transfection reagents. To transfect in a p100, 1.2×10^6 or 1×10^6 cells/plate (SK-N-BE(2) or LA1-5s, respectively) were seeded in a volume of 6ml of

medium without antibiotics on a mix containing 24µl or 15µl of Lipofectamine per siRNA (SK-N-BE(2) or LA1-5s, respectively) diluted in 3ml of OptiMEM. Transfection efficiency was determined by the orange staining observed in cells transfected with BLOCK-iT^{TM} Fluorescent Oligo (Thermo Fisher Scientific) transfection control, a fluorescein-labeled dsRNA oligomer designed for use in transfection efficiency in RNAi experiments.

3.2.11 Statistical analysis

Unless otherwise stated, graphs represent the average of three independent experiments ± SEM. Statistical significance was determined by unpaired two-tailed Student's *t*-test or ANOVA Tukey's test (GraphPad Prism Software, USA). * means $p \leq 0.05$, ** means $p \leq 0.01$ and *** means $p \leq 0.001$.

RESULTS

4. Results

4.1 ABTL0812 impairs neuroblastoma cell growth regardless of their genetic profile

The large number of patient-derived neuroblastoma (NB) cell lines with diverse biologic characteristics generated in the past decade provides good model systems for the development of therapeutic strategies [339]. Thus, with the aim of evaluating the potential of ABTL0812 (ABTL) as a new therapeutic agent for high-risk NB tumors, a panel of NB cell lines with clinically-relevant molecular alterations was selected to analyze their sensitivity to ABTL0812. Given the heterogeneity, aggressiveness and multi-drug resistance (MDR) phenotype of high-risk NB, we carefully completed the panel with representatives of the major NB subclasses, including cell lines that reliably reflect sustained drug resistance to various classes of cytotoxic agents [165]. Mechanisms of NB MDR include elevated *MYCN* oncogene [340,341] and TrkB expression [90], drug inactivation [342], apoptosis deregulation [158], presence of cancer stem cells [343], alterations or mutations of drug targets [70], increased DNA repair capacity [344,345], and increased drug efflux [346,347]. Some key genetic alterations involved in these processes are *MYCN* amplification, *CASP8* methylation and mutations in *ALK* oncogene or in the *TP53* tumor suppressor among others [344,348–350]. Table 13 shows the status of these genes in chemosensitive and chemoresistant NB cell lines chosen to evaluate ABTL0812 therapeutic effects.

Table 13. Characteristics of NB cell lines

Cell line	Stage	*MYCN* status	*ALK* status	Caspase-8	11q	p53
CHLA-90	4	Non amplified	F1245V Mut	+	+	E286K Mut, NF
SK-N-BE(2)	4	Amplified	WT	+	+	C135F Mut, NF
SK-N-AS	4	Non amplified	WT	-	-	Exon 9b AS, NF
LA1-5s	4	Amplified	F1174L Mut	+	+	C182X Mut, NF
IMR-32	4	Amplified	PA, WT	-	-	WT, functional
SH-SY5Y	4	Non amplified	F1174L Mut	-	+	WT, functional

PA, partial amplification; WT, wild type; Mut, mutated; -, lack of expression; +, expression; AS, alternative splicing; NF, non-functional.

NB cells listed in Table 13 were treated with ABTL0812 at the indicated concentrations for three days. Crystal violet assay was performed to assess the effect of ABTL0812 on cell growth (Figure 17A). ABTL0812 impaired the growth of all tested NB cell lines with similar IC_{50} between 30-60μM (Table 14). In parallel, the same set of cell lines was treated with cisplatin (CDDP), a standard-of-care DNA-damaging agent used in the induction phase of high-risk NB treatment (Figure 17B). As expected, NB cells showed different susceptibility to CDDP depending mainly on their p53 status, but also on other prognostic markers specified in Table 13. On average, CHLA-90, SK-N-BE(2), SK-N-AS and LA-15s had a 31-fold higher CDDP IC_{50} compared to the IMR-32 and SH-SY5Y cell lines, which have functional p53. This allows us to differentiate between these two groups of cell lines as

chemoresistant or chemosensitive.

However, such resistance to classic chemotherapeutic drugs did not influence the cytotoxic effects of ABTL0812. ABTL0812 strongly impaired the viability of all six cell lines even though they have proved to be resistant to cisplatin, vincristine, doxorubicin or etoposide [164,165,351,352]. These results suggest that ABTL0812 is likely to be an effective therapeutic agent regardless of *MYCN* status, *TP53* mutations and presumably to other malignant prognostic markers.

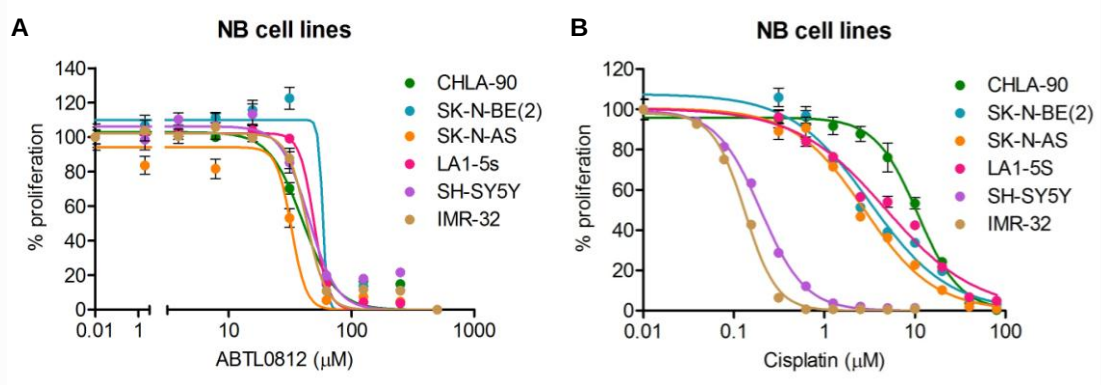

Figure 17. Dose-response curves for ABTL0812 and cisplatin in six NB cell lines. Cells were treated with (A) ABTL0812 and (B) cisplatin for 72h at the indicated concentrations. Cells were fixed with 1% glutaraldehyde at 72h post-treatment and the percentage of viable cells for each treatment was assessed by crystal violet staining. Data is presented as mean ± SEM of three independent experiments.

Table 14. IC_{50} values for ABTL0812 and CDDP in NB cell lines

Cell line	IC_{50} ABTL0812 [µM]	IC_{50} CDDP [µM]
CHLA-90	57.87 ± 0.78	10.80 ± 1.07
SK-N-BE(2)	58.70 ± 1.08	3.18 ± 1.10
SK-N-AS	32.49 ± 0.03	2.75 ± 1.09
LA1-5s	50.68 ± 1.34	4.79 ± 1.09
IMR-32	43.33 ± 0.22	0.13 ± 1.02
SH-SY5Y	43.35 ± 1.40	0.20 ± 1.02

4.2 ABTL0812 is not mutagenic and does not cause DNA damage

Since genotoxic potential is one of the most important criteria for predicting adverse side effects, ABTL0812 was tested for carcinogenicity. Carcinogenesis, also called oncogenesis or tumorigenesis**,** is the process whereby normal cells turn into cancer cells. This process is characterized by changes at cellular, genetic and epigenetic levels. The Ames test is a biological assay to assess the mutagenic potential of chemical compounds in bacteria. Several histidine-requiring bacterial strains of *Salmonella typhimurium*, each with a different type of mutation, are incubated with a single concentration of a test substance. Because of the original histidine mutation, the tester strain is not able to form colonies on histidine-free agar. However, if the test substance induces a mutation that generates a histidine-independent strain (reverse mutation), the latter will gain the ability to form colonies on minimal agar. The different strain mutations combined in the histidine gene are able to detect most genotoxic carcinogens. Furthermore, since most carcinogens are not directly carcinogenic but are active only after being metabolized, the compounds are tested both directly and in the presence of a mammalian metabolizing system. The 9000 supernatant fraction (S9) of a rat liver homogenate is used as a strong inductor of many xenobiotic metabolizing enzymes in combination with an NADPH-generating system [353].

In order to test the genotoxic potential of ABTL0812, *Salmonella typhimurium* strains TA98, TA100, TA102, TA1535 and TA1537 were incubated with increasing concentrations of ABTL0812 with or without metabolic activation by microsomal fraction S9. The result was that ABTL0812 did not raise in any case the number of revertant colonies, not even after metabolic activation (Figure 18).

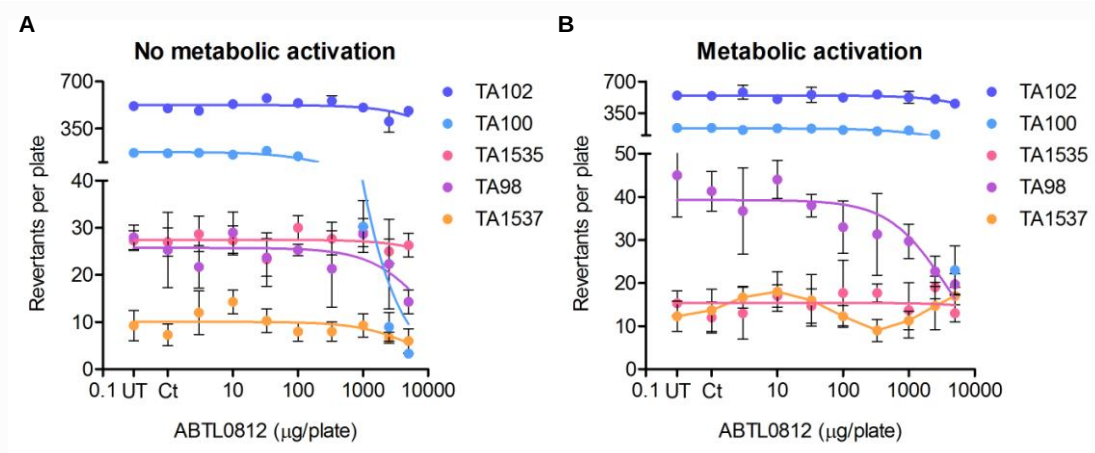

Figure 18. ABTL0812 is not mutagenic. Five *Salmonella typhimurium* strains were incubated with indicated ABTL0812 concentrations (3-5000µg/plate) without (A) or with (B) S9 microsomal fraction. Data is presented as mean ± SD of three independent experiments. UT, untreated; Ct, water control.

Furthermore, we tested whether ABTL0812 antitumoral effect causes a harmful effect in the DNA of dividing cells, as chemotherapeutic drugs usually do. To this aim, we assessed the levels of phosphorylated histone H2AX (p-H2AX) by immunoblot (Figure 19). H2AX is a member of the histone H2A family, one of the five histone families that package and organize eukaryotic DNA into chromatin. Histone H2AX phosphorylation in serine 139 specifically marks DNA double strand breaks and coordinates the recruitment of a number of proteins involved in DNA damage response and repair [354–356]. The results were that ABTL0812 did not trigger, or slightly did, histone H2AX phosphorylation; in contrast to the induction observed with CDDP, an alkylating chemotherapeutic drug used in NB therapy.

In conclusion, ABTL0812 is not mutagenic and does not damage DNA, which ensures a better safety profile than current chemotherapeutic drugs and fewer long-term side effects.

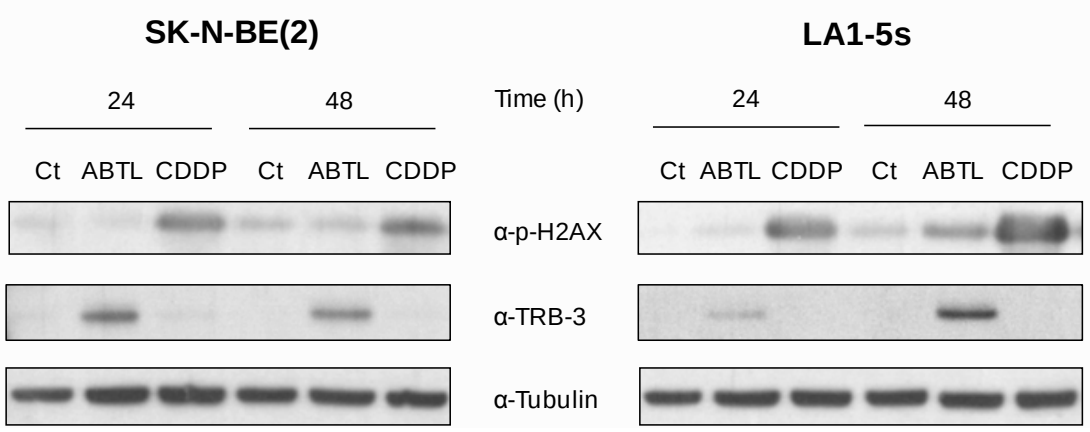

Figure 19. ABTL0812 does not induce DNA damage. NB cells were treated for 24h and 48h with vehicle (Ct), ABTL0812 20μM and CDDP 25μM. Protein expression levels were analyzed by WB. Anti-TRB-3 was used as a control for ABTL0812 response.

4.3 ABTL0812 induces cell death in neuroblastoma cell lines

4.3.1 ABTL0812 induces autophagy in neuroblastoma cell lines

ABTL0812 is known to impair tumor growth by activation of autophagic cell death [224]. Therefore, to ascertain whether ABTL0812 sets the autophagy program off in NB cells, we analyzed the distribution of the autophagosome membrane-bound lipidated protein light chain 3 (LC3) by immunhistochemistry using an anti-LC3 antibody. During autophagy the cytosolic soluble protein LC3-I is converted to LC3-II, which is bound to autophagosomal membranes. This process changes the diffuse ubiquitous LC3-I pattern to a punctuate/dot LC3-II pattern. This puncta pattern was observed in NB cells LA1-5s and SK-N-BE(2) treated with ABTL0812 (Figure 20) indicating that ABTL0812 activates autophagy in NB cells.

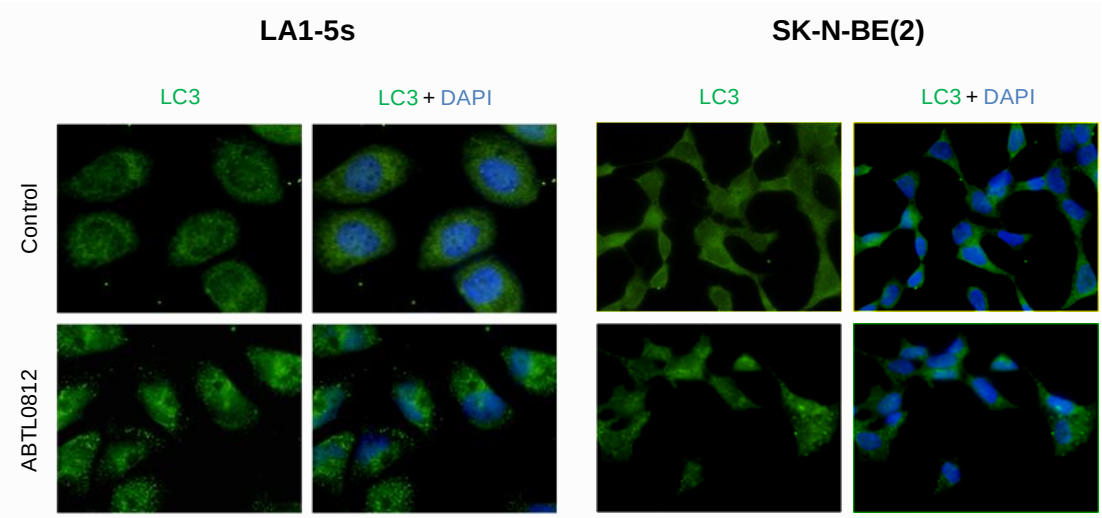

Figure 20. ABTL0812 induces autophagosome formation. NB cells were treated for 12h with ABTL0812 40µM (LA1-5s), 20µM (SK-N-BE(2)) or vehicle (ethanol) before immunostaining for endogenous LC3 (green) and nuclei with DAPI staining (blue). Dots represent LC3-II recruited by autophagosomes.

To detect if autophagic process was dynamic we measured the LC3-II turnover in cells treated with ABTL0812 in the presence and absence of lysosomal protease inhibitors Pepstatin A (PA) and E64d (Figure 21). LC3-II protein levels were increased in the presence of lysosomal inhibitors because autophagolysosome degradation was blocked, indicating ABTL0812 induces autophagic flux.

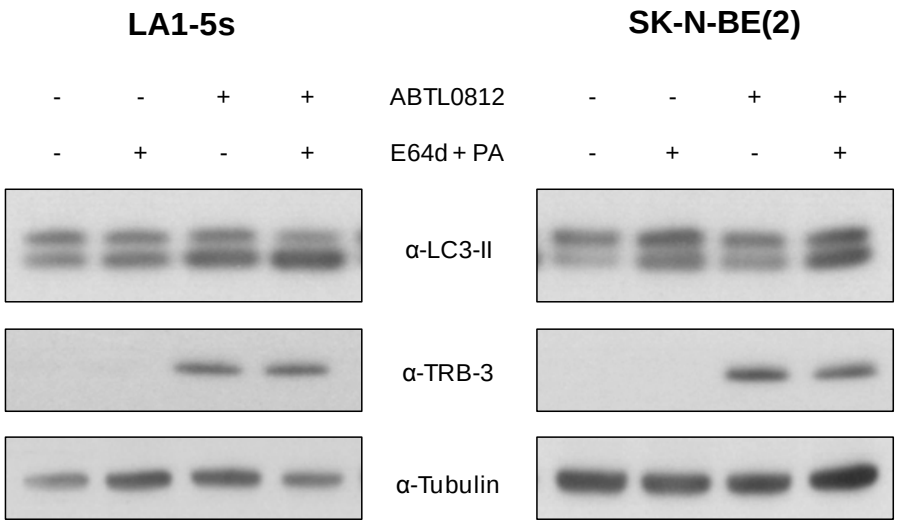

Figure 21. ABTL0812 induces autophagic flux. Cells were pre-treated 2h with vehicle (ethanol) or E64d (10μM) and PA (10μg/ml). ABTL0812 40μM (LA1-5s), 30μM (SK-N-BE(2)) or vehicle were added for 6h in the presence or absence of lysosomal inhibitors. Protein expression levels were analyzed by WB. Anti-TRB-3 was used as a control for ABTL0812 response.

4.3.2 ABTL0812 induces apoptosis in neuroblastoma cell lines

Despite we had already proved that ABTL0812 induces dynamic autophagy, we observed that cells treated with ABTL0812 and stained with Hoechst also showed the typical morphological features of apoptosis: chromatin condensation, nuclear fragmentation and formation of apoptotic bodies (Figure 22A).

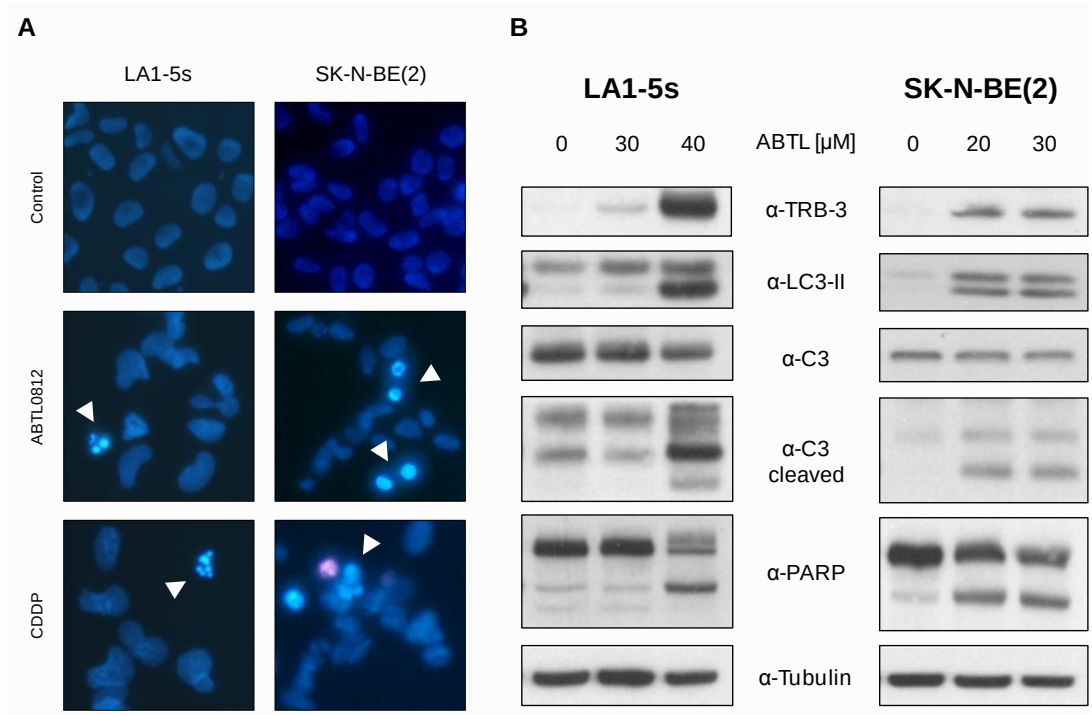

Figure 22. ABTL0812 induces apoptosis in NB cells. (A) Representative images of nuclear morphology assessment at 48h post-treatment with ABTL0812 (30μM LA1-5s, 20μM SK-N-BE(2)) or vehicle (ethanol). Arrowheads point towards condensed or fragmented nuclei. CDDP (25 μM) was used as a positive control of apoptosis. (B) NB cells were incubated 72h with indicated doses of ABTL0812. Protein expression levels were analyzed by WB. Anti-TRB-3 was used as a control for ABTL0812 response.

To confirm that apoptosis is involved in ABTL0812 induced cell death, we analyzed by WB the presence of apoptosis hallmarks upon ABTL0812 treatment. One of the most common signaling cascades involved in apoptosis is the cleaving and activation of effectors caspases and proteolysis of substrates, like PARP-1 [357]. The presence of active caspase forms (cleaved Caspase-3) and processing of PARP-1 in ABTL0812 treated cells proved that ABTL0812 also induces apoptotic cell death in NB cell lines (Figure 22B), unlike what has been reported in other non-pediatric tumors, such as lung an pancreatic [224], but in accordance to endometrial cancer models [225].

The role of autophagy and apoptosis in ABTL0812 anti-tumoral effect was further studied combining ABTL0812 with pharmacological inhibitors of both types of programmed cell death. To this aim, cells were pre-treated with (1) lysosomal protease inhibitors E64d/PA, which prevent the culmination of autophagy, or (2) QVD-OPh (QVD) a pan-caspase inhibitor that prevents activation of the major initiator caspase and effectors caspases. Cells with compromised autophagy and apoptosis were treated with ABTL0812 or vehicle during 48h and cell death was assessed using propidium iodide/Hoechst staining (Figure 23). Inhibition of either autophagy or apoptosis reduced ABTL0812 induced cell death.

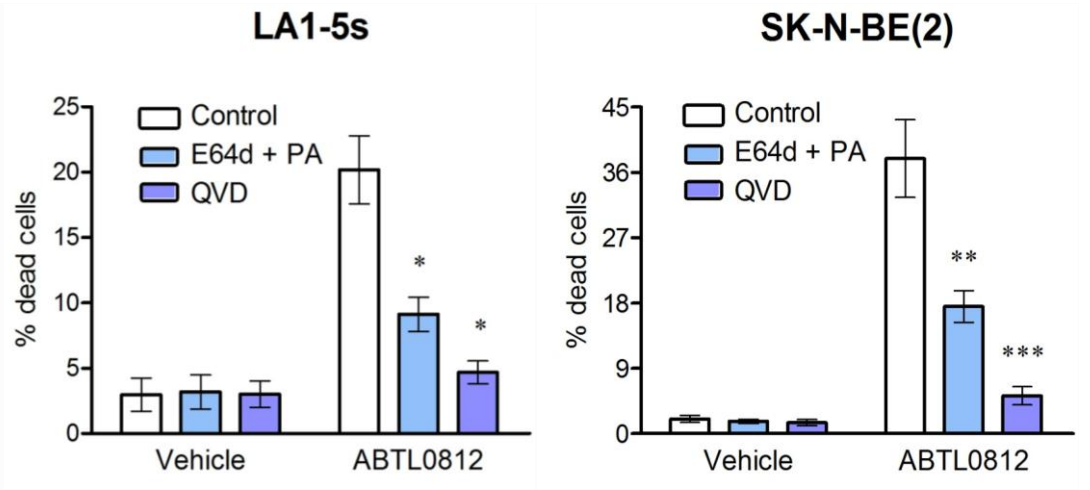

Figure 23. Inhibition of autophagy and apoptosis lessens ABTL0812-induced cell death. LA1-5s and SK-N-BE(2) NB cells were pre-treated 2h with vehicle (ethanol) or E64d (10µM) and PA (10µg/ml) or QVD (20µM). ABTL0812 30µM (LA1-5s), 20µM (SK-N-BE(2)) or vehicle (control) were added in the presence or absence of autophagy and apoptosis inhibitors. 48h post-treatment quantification of cell death was performed from four representative images of three replicates per condition. Data is presented as mean ± SEM of three independent experiments. *p≤0.05, **p≤0.01, ***p≤0.001 compared to ABTL0812 control.

4.4 ABTL0812 reduces tumor formation *in vivo* and has low toxicity profile

The impact of ABTL0812 treatment on NB cells was further evaluated *in vivo* using NB xenografts. 5×10^6 of viable SH-SY5Y cells were injected into the flank of 6 week-old female immunodeficient NMRI-nude mice (n=15/group). Tumor formation was followed by palpation two to three times a week. Two weeks post-injection, all mice had already developed tumors of an average volume of ~70mm^3. Then, mice were randomly assigned to be treated either with vehicle, 120mg/kg of ABTL0812 orally 7 times a week, or 2mg/kg of cisplatin by intraperitoneal injection (ip) two times a week (Figure 24A). Tumors detected in the ABTL0812 or CDDP group developed at a significant slower pace than vehicle-treated group (Figure 24B). All mice were euthanized at day 23 post-injection. The excised tumors of vehicle group were larger in size and heavier compared to ABTL0812 or CDDP treated tumors (Figure 24C). Histological analysis confirmed the presence of tumor cells in the extracted tissue fragments of the three groups (Figure 24D).

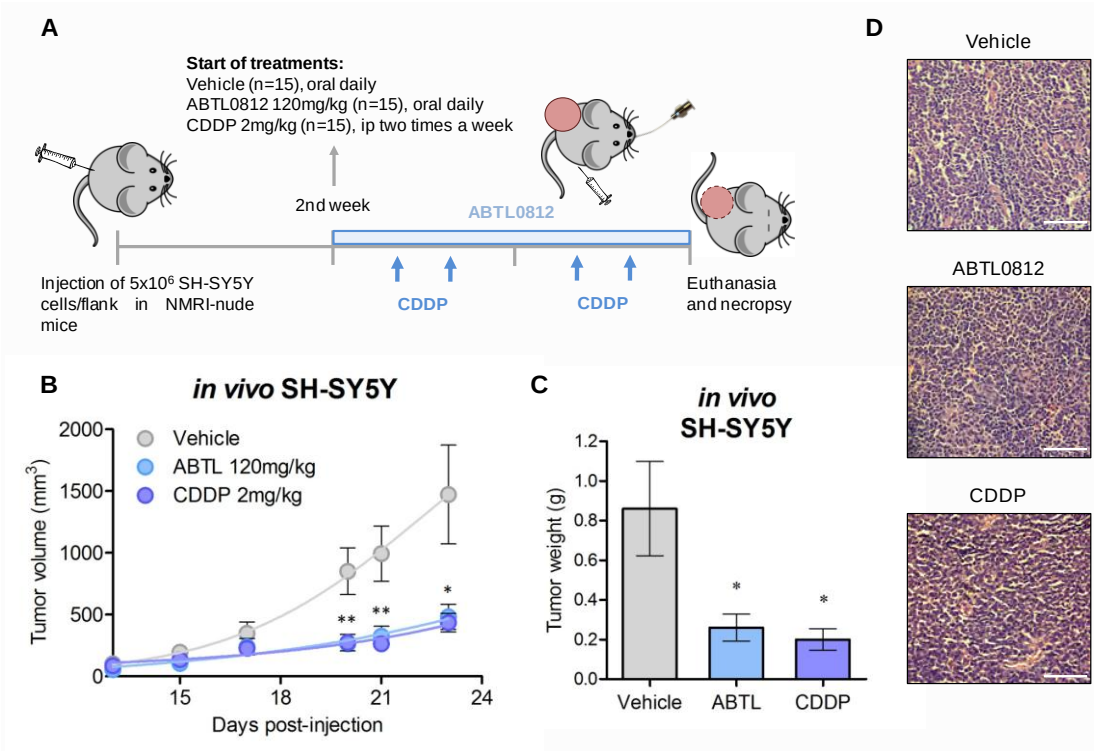

Figure 24. ABTL0812 reduces tumor growth in SH-SY5Y xenograft models. (A) Schematic representation of the experiment schedule. (B) Tumor volume of mice treated with vehicle, ABTL0812 or CDDP (n=15/group) measured for 23 days. Tumor growth was monitored using a digital caliper and tumor volume was calculated using the formula (width^2*length/2). Data is presented as mean ± SEM (C) Average weight of resected tumors. Graph shows mean ± SEM. (D) Representative hematoxilin-eosin stained images of NB xenografts. Scale bar 100µm. *p≤0.05, **p≤0.01 compared to vehicle.

Of note, ABTL0812 efficacy was comparable to CDDP. CDDP is a cytotoxic platinum compound proved to be effective in the *in vivo* treatment of NB and a well established standard of care of NB treatment [358,359]. Therefore, these results not only validate the *in vitro* results, but also indicate that ABTL0812 could be considered a potential therapy agent for high-risk NB.

In order to compare potential side effects after ABTL0812 and CDDP treatment, we did a complete blood cell count test (CBC) from five to twelve mice from each treatment group. The hematological analysis resumed in Table 15 showed that ABTL0812 had no impact on hematocrit, hemoglobin and red blood cell counts, neither in liver and kidney damage indicators AST, ALT and urea concentration. On the contrary, in agreement with previously published data [360,361], CDDP showed a slight reduction on the hematocrit concentration and the red blood cell counts, indicators of anemia due to bone marrow suppression as a result of direct myelotoxicity or cytokine-mediated inhibition of erythropoiesis. Other parameters were affected in both treatments, such as white blood cell counts, platelets, creatin kinase and LDH, often altered during cancer and cancer therapy.

Table 15. CBC test *in vivo* SH-SY5Y xenograft models treated with ABTL or CDDP

Paremeter	Vehicle	ABTL 120mg/kg	CDDP 2mg/kg	Ref. val.	Units
Hematocrit	41.53 ± 1.23	40.22 ± 0.63	* 37.33 ± 1.36	39 - 49	%
Hemoglobin	13.35 ± 0.41	13 ± 0.28	12.267 ± 0.49	10.2 - 16.6	g/dL
Red blood cell count	7.92 ± 0.29	7.92 ± 0.18	* 6.81 ± 0.39	7 - 12	mill/µL
White blood cell count	* 3.82 ± 0.4	* 3.94 ± 0.58	* 3.02 ± 0.29	6 - 15	10^3 /µL
Platelet count	* 1164.92 ± 63.8	* 1122.2 ± 109.12	* 916.67 ± 89.27	160 - 760	10^3 /µL
CK-NAC	501.83 ± 113.13	* 1020.4 ± 350.67	701.33 ± 276.18	39 - 729	UI/L
AST (GOT)	72.5 ± 7.66	109.6 ± 21.25	106.167 ± 15.30	55 - 266	UI/L
ALT (GPT)	32.75 ± 2.29	28 ± 2.86	35.33 ± 2.69	18 - 72	UI/L
Urea	43.5 ± 2.04	54.8 ± 4.91	59.3 ± 1.91	17 - 71	mg/dL
LDH	* 518.67 ± 54.27	* 799.2 ± 72.99	* 1154.33 ± 653.12	78 - 273	UI/L

4.5 ABTL0812 induces endoplasmatic reticulum stress and the unfolded protein response

Previous reports described that the ABTL0812 mechanism of action relies on the up-regulation of the pseudokinase TRB-3, which binds to AKT and prevents AKT phosphorylation and activation. Suppression of AKT/mTORC1 axis caused tumor growth inhibition and autophagy-mediated cancer cell death *in vitro* and *in vivo* [224,225]. Hence, we aimed to investigate whether this mechanism was reproducible in our model. To this aim, we monitored the AKT/mTORC1 pathway activity by WB in NB cells treated with ABTL0812 (Figure 25).

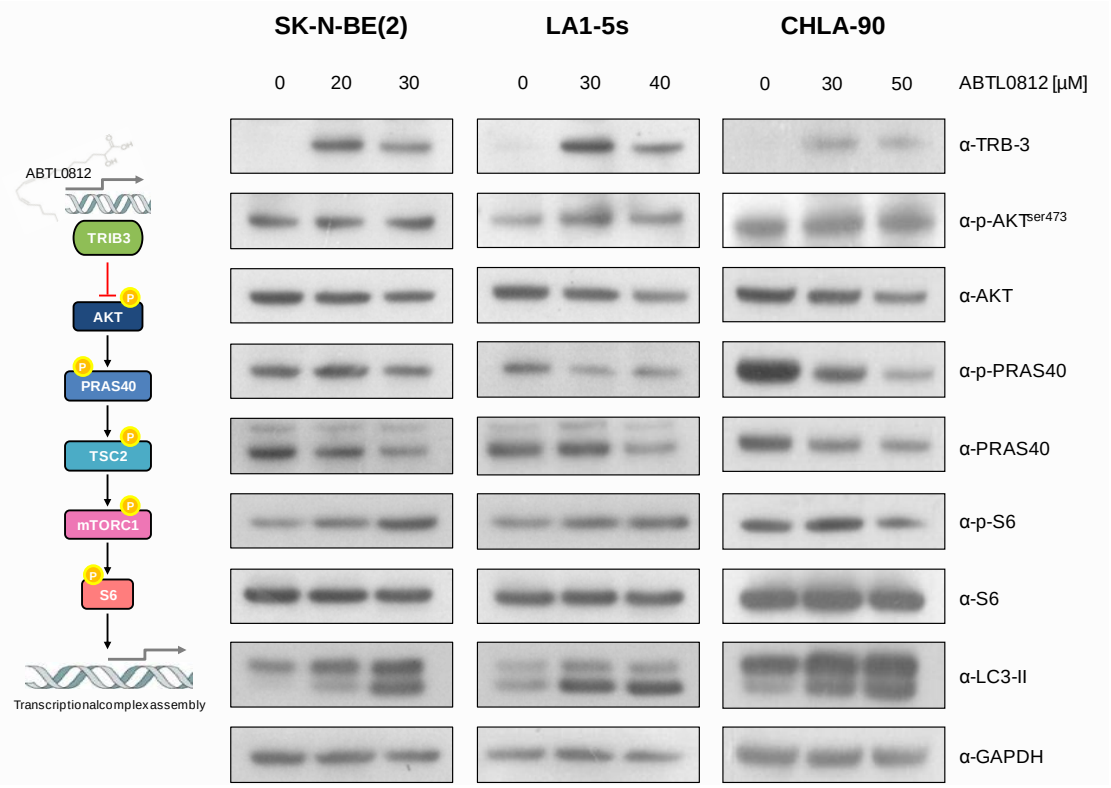

Figure 25. ABTL0812 does not modulate the AKT/mTORC1 pathway in NB. Cells were treated twenty-four hours with ABTL0812 at the indicated concentrations. Protein expression levels were analyzed by WB.

Three NB cell lines with different genetic background were treated with increasing doses of ABTL0812 and phosphorylation levels of AKT/mTORC1 axis proteins were measured. Unlike what had been formerly reported, ABTL0812 did not reduce phosphorylation of AKT/mTORC1 substrates, although TRB-3 and LC3-II levels were up-regulated.

The most prevalent mTOR-independent autophagy induction mechanism is the endoplasmatic reticulum (ER) stress. In order to validate the induction of ER stress-mediated cell death, we monitored the effects of ABTL0812 on the PERK signaling pathway, the UPR branch most closely related to ER stress-induced apoptosis (Figure 26). Protein analysis showed that ABTL0812 treatment induced phosphorylation of PERK's substrate p-eIF2α and selective translation of the downstream effectors ATF4/CHOP. Evidence suggests that CHOP inhibits pro-survival Bcl-2 protein thus de-repressing pro-apoptotic BH3 domain-only protein genes such as *PMAIP1* (NOXA). Up-regulation of BH3-only proteins is necessary for BAX-BAK-mediated smooth ER membrane permeabilization, calcium release and apoptosis onset [362,363].

Besides, our WB analysis demonstrated that elicitation of ER stress by ABTL0812 precedes the up-regulation of TRB-3 and the bi-lipidation of LC3.

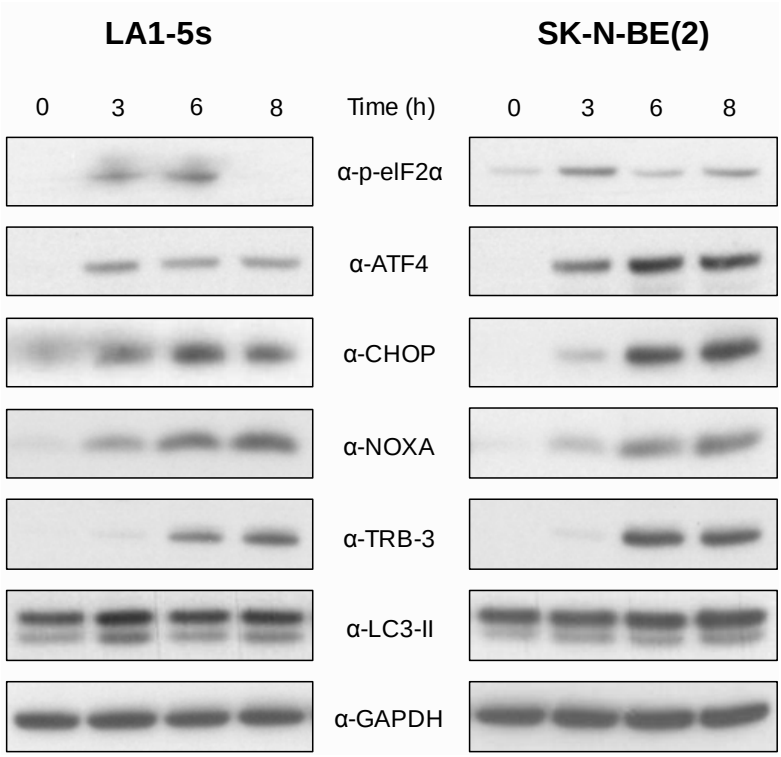

Figure 26. ABTL0812 triggers the UPR-PERK signaling pathway. Cells were treated during 0, 3, 6 and 8 hours with ABTL0812 40μM (LA1-5s) or ABTL0812 30μM (SK-N-BE(2)). Protein expression levels were analyzed by WB.

Overall, these data support the hypothesis that ABTL0812 may induce NB cell death through the induction of ER stress and associated UPR pathway.

4.6 ABTL0812 down-regulates MYCN expression

4.6.1 ABTL0812 decreases MYCN protein levels via ubiquitin-proteasome system

Amplification of the *MYCN* oncogene is present in about 20% of all NB and 40% of high-risk cases. The MYC family proteins (c-MYC, MYCN) are nuclear phosphoproteins that act as transcription factors, both activating and/or repressing the expression of their target genes. Gene expression profiles of *MYCN*-amplified tumors distinguish a subset of aggressive tumors with poor prognosis since MYCN regulates tumorigenesis-relevant processes such as cellular proliferation, growth factor dependence, response to anti-mitogenic signals, angiogenesis, metastasis, genomic instability, cell differentiation and cell adhesion. Clinical observations reciprocally show that *MYCN*-amplification is associated with NB tumorigenesis, rapid disease progression and poor patient outcome. Of note, NB patients' progression-free survival is *MYCN* dose-dependent, as higher copy number results in lower progression-free survival independently of patient age and disease stage. Based on these evidences, *MYCN*-amplification is one of the most powerful adverse prognostic markers for NB patient outcome [39,40].

The *MYCN* oncogene is located on the distal short arm of chromosome 2 (2p24). Although the exact mechanism by which amplification occurs is unknown, it usually results in 50 to 400 gene copies per cell, leading to the production of abnormally high levels of *MYCN* mRNA and protein. Despite the general consent that blocking *MYCN* expression may be beneficial for NB patients, the therapeutic implementation of this hypothesis is hampered by the lack of understanding of *MYCN* transcriptional regulation in NB. Although few transcription factors have been identified for basal MYCN expression, the available data suggests that MYCN regulation is not only mediated through transcription factors binding, but through cooperation with multiple non-adjacent regulatory regions. Such cooperative DNA-protein interactions could explain the inability of the available approaches to unveil the *MYCN* regulatory mechanism [364,365]

Another cell mechanism that unbalances MYCN protein levels is the disruption of proteasomal degradation. MYCN is an unstable protein with a rapid turnover commanded by the ubiquitin-ligase proteasome degradation pathway. However, MYC-family proteins can be aberrantly stabilized by an altered phosphorylation within the domain where ubiquitin-ligases bind to initiate proteasomal degradation. Particularly in NB, enhanced PI3K signaling contributes to oncogenic stabilization of MYCN extending the half-life of MYC and envisaging an alternative approach for targeting MYCN [40,366].

One of the most immediate outcomes of UPR activation is the up-regulation of chaperones and components of the endoplasmatic reticulum-associated degradation (ERAD) machinery to reestablish ER function and remove misfolded proteins. Because of this link between ER-enhanced activation of the ubiquitin-proteasome pathway and intra-tumoral MYCN regulation, we aimed to ascertain whether ABTL0812 ER stress induction could have an effect on MYCN protein levels (Figure 27).

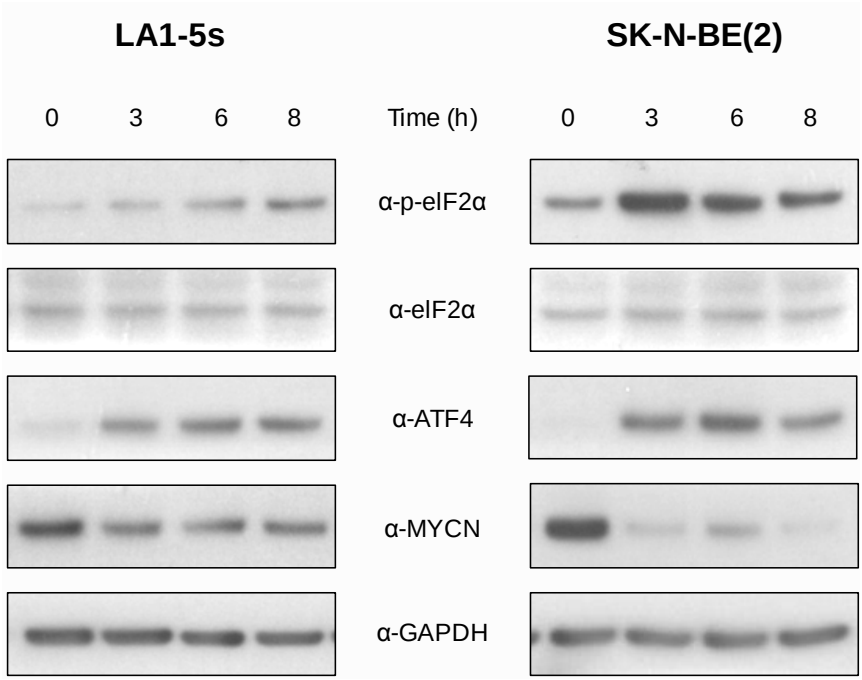

Figure 27. ABTL0812 reduces MYCN levels in NB cells. The indicated cell lines were treated during 0, 3, 6 and 8 hours with ABTL0812 30µM. Protein expression levels were analyzed by WB.

In order to determine whether the remarkable reduction of MYCN levels after ABTL0812 treatment were attributable to increased protein degradation, NB cells were co-incubated with the proteasome inhibitor MG132 and ABTL0812. While ABTL0812 efficiently decreased MYCN protein levels, the co-treatment with MG132 abolished ABTL0812 effects on MYCN, thereby indicating that ABTL0812-induced lessening of MYCN levels was, at least in part, due to disturbances of MYCN stability (Figure 28).

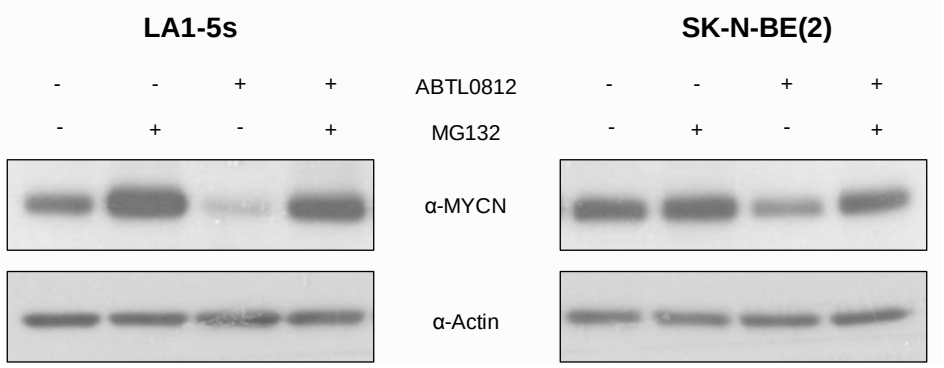

Figure 28. Proteasome inhibition blocks ABTL0812-induced degradation of MYCN. The indicated cell lines were pre-treated 2h with vehicle (ethanol) or MG132 0.5µM. ABTL0812 30µM or vehicle were added for 3h in the presence or absence of proteasomal inhibitor. Protein expression levels were analyzed by WB.

4.6.2 ABTL0812 represses *MYCN* transcription

In addition to MYNC protein stability impairment, we analyzed whether ABTL0812 also altered *MYCN* transcription. To this aim, *MYCN* expression levels were quantified by qRT-PCR after ABTL0812 treatment. Results show ABTL0812 sharply down-regulates *MYCN* expression (Figure 29A). Of note, in parallel to *MYCN*, *TRIB3* up-regulation was assessed as a control for ABTL0812 response (Figure 29B).

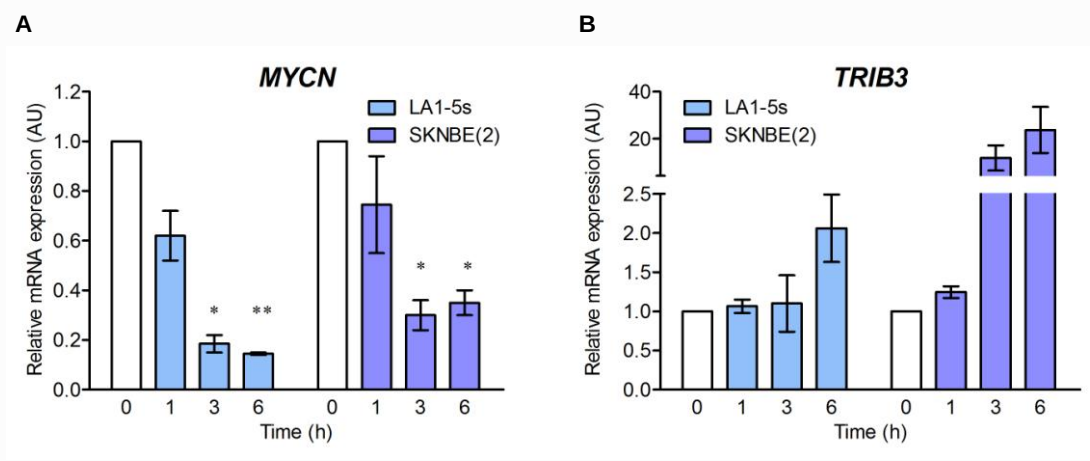

Figure 29. ABTL0812 significantly reduces *MYCN* transcription. The indicated NB cell lines were treated for 1, 3 and 6h with 30μM ABTL0812 or left untreated (0h). (A) MYCN and (B) TRB-3 mRNA levels were characterized by qRT-PCR. mRNA levels were normalized using GADPH mRNA. Data is presented as mean ± SEM of three independent experiments. *p≤0.05, **p≤0.01 compared to vehicle (white bars).

To date, little is known about which transcription factors regulate MYCN expression in NB. Thus far, only the zing finger transcription factors Sp1 and Sp3, and the E2F transcription factors family have been found to have binding sites in the *MYCN* promoter and to contribute to their expression [364,365,367].

Recent reports have uncovered a link between one of the UPR branches and the E2F and Sp1/3 transcription factors. On one hand, proteins processed and released during the UPR are able to enter the nucleus and bind the ER stress response element (ERSE) present on the E2F promoters, thereby repressing its expression [368,369]. On the other hand, the Sp family of proteins can also directly bind to the ERSE during a stress response and cooperate with the mentioned UPR proteins to induce transcriptional activation or repression of its target genes [370,371].
This prompted us to examine whether MYCN silencing depends on E2Fs down-regulation. NB cells were treated for 1, 3 and 6h with ABTL0812 or vehicle. mRNA and protein levels of MYCN, E2F transcription factors and other proteins related to the PERK/eIF2α/ATF4 pathway were analyzed by RT-qPCR and WB.

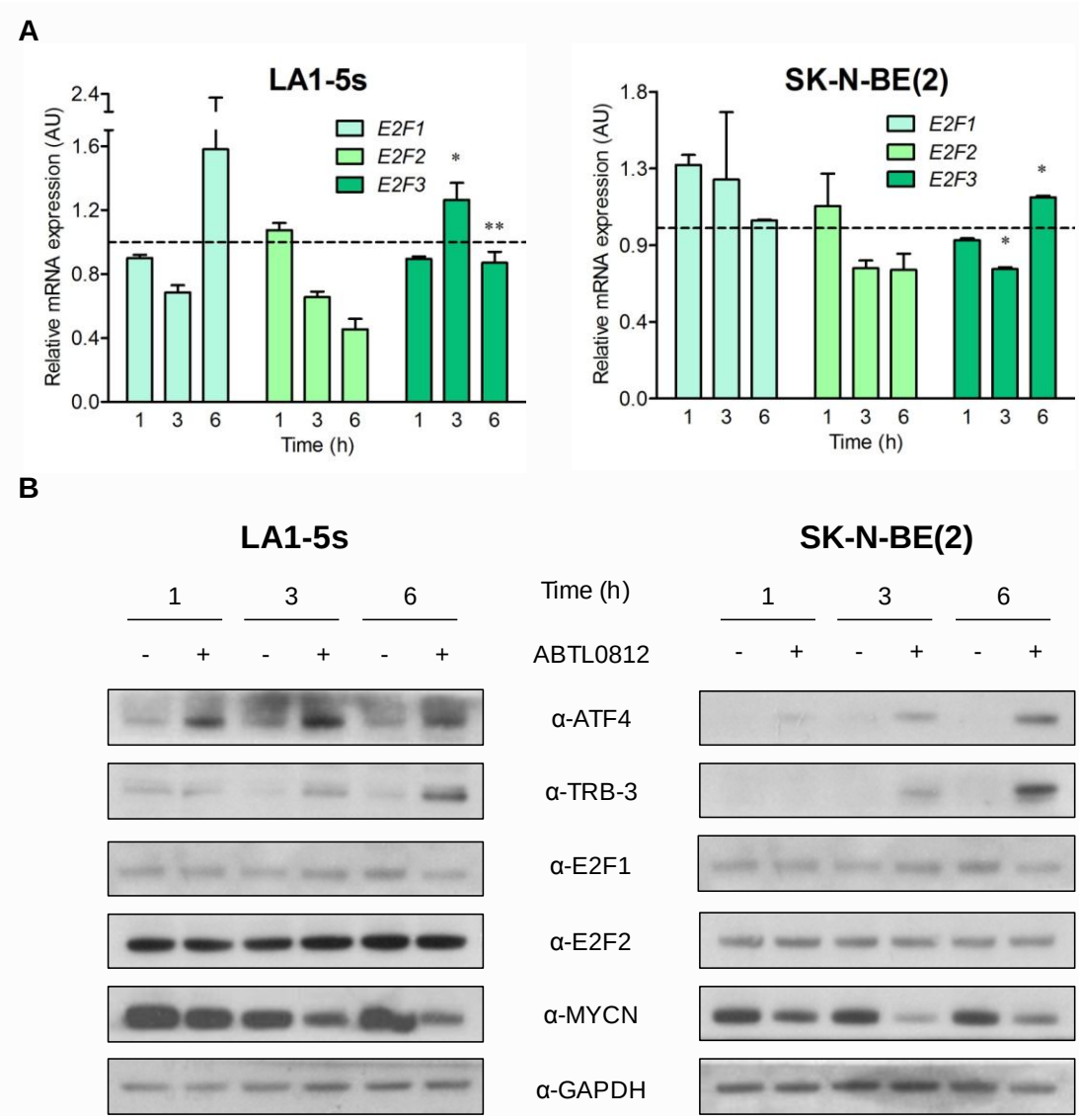

Figure 30. E2F factors regulation do not account for ABTL0812-induced reduction of MYCN levels. NB cells were treated for 1, 3 and 6h with vehicle (ethanol) or ABTL0812 30µM. (A) mRNA expression levels were measured by RT-qPCR. Expression levels were normalized using GAPDH. Graphs represent the mean ± SEM of three independent experiments. (B) Protein expression levels were analyzed by WB. *p≤0.05, **p≤0.01 compared to vehicle (dotted line).

The mRNA and protein analysis suggest that E2F factors are not implicated in MYCN down-regulation by ABTL0812. RT-qPCR results did not show any correlation between ABTL0812 treatment and E2F factors expression (Figure 30A). Moreover, while the WB exhibits a temporal correlation between treatment, activation of the PERK/eIF2α/ATF4 axis and MYCN down-regulation, no changes in E2F proteins levels were observed at these times (Figure 30B). In summary, these data do not support the hypothesis that E2F

factors down-regulation may be linked to MYCN inhibition in early stages of ER stress. Further experiments would be needed in order to find alternative transcriptional regulators of MYCN and their modulation in the context of ER stress.

4.7 ABTL0812 has a good combination profile with chemotherapeutic drugs used for high risk-neuroblastoma treatment

Although ABTL0812 has demonstrated to be effective as a single agent in *in vivo* NB models, the clinical treatment of the disease is highly complex, thus ABTL0812 may need to be used in combination with other chemotherapies.

Treatment regimens for relapsed or refractory disease in HR-NB encompass different combinations of doxorubicin, irinotecan, topotecan and cyclophsophamide chemotherapeutic drugs. Therefore, following the currently proposed treatment schemes, we analyzed the antitumoral effects of ABTL0812 in combination with the mentioned drugs. Clinically representative HR-NB cells were simultaneously treated with ABTL0812 and increasing doses of doxorubicin, irinotecan, topotecan and cyclophsophamide for 72 hours. Crystal violet assay was performed to assess cells growth inhibition (Figure 31).

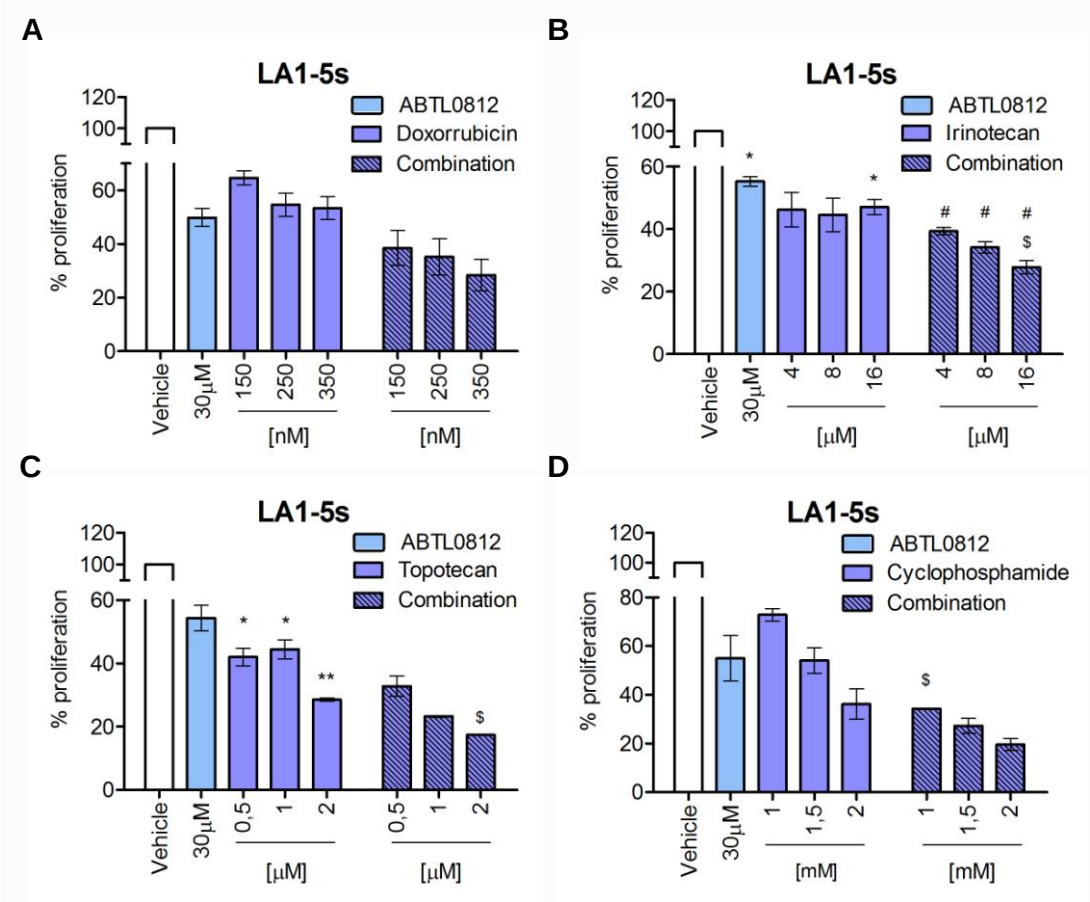

Figure 31. ABTL0812 has additive effects in combination with second line treatments. LA1-5s cells were treated with vehicle (ethanol), ABTL0812 30µM and the indicated doses of (A) doxorubicin, (B) irinotecan, (C) topotecan, and (D) cyclophosphamide as a single agent; alone (plain bars) or in combination with ABTL0812 30 µM (striped bars). Cells were fixed with 1%

glutaraldehyde 72h post-treatment and the percentage of viable cells for each treatment was assessed by crystal violet staining. Data is presented as mean ± SEM of three independent experiments. *p≤0.05, **p≤0.01 compared to vehicle; $^{\#}$p≤0.05 compared to ABTL0812 as a single agent; $^{\$}$p≤0.05 compared to the matching concentration of each drug as a single agent.

ABTL0812 demonstrated to be efficient in combination with chemotherapeutic agents used to treat refractory or relapsed NB even at sub-therapeutic doses.

4.8 ABTL0812 synergizes with biologic agents used for the treatment of neuroblastoma minimal residual disease

The latest phase of high-risk NB therapeutic regimen is the treatment of minimal residual disease (MRD). Strategies incorporated to MRD management are differentiation therapy, immunotherapy and metronomic chemotherapy [372,373]. Therapeutic administration of differentiating agent 13-*cis*-retinoic acid (13-cRA) has become part of standard HR-NB treatment regiments since the nineties. Hence, we treated LA1-5s and SK-N-BE(2) NB cell lines simultaneously with ABTL0812 and increasing doses of 13-cRA during twenty-four hours. Crystal violet staining was performed to assess cell growth (Figure 32A).

Administration of low 13-cRA doses had none or little effect in both cell lines while ABTL0812 reached a maximum of 40% of growth inhibition in SK-N-BE(2) cells. Nevertheless, ABTL0812 plus 13-cRA combination treatment significantly inhibited cell growth compared to individual agents, reaching approximately 70% of inhibition in SK-N-BE(2) and 80% in LA1-5s using 20µM ABTL0812 and 20µM 13-cRA concentrations (Figure 32A). Furthermore, ABTL0812 or 13-cRA treatment alone did not show any sign of caspase-3 or PARP-1 cleavage. However, the combination treatment showed prominent apoptosis induction (Figure 32B).

Moreover, not only apoptosis markers were raised in the combination treatment, but also ER stress proteins from the PERK axis, such as ATF4, TRB-3 and LC3-II. Interestingly, both, ABTL0812 and 13-cRA stimulated PERK's signaling pathway, but the combination strongly up-regulated the axis, probably tipping the scale enough to result in apoptotic cell death.

In conclusion, these results together with the fact that ABTL0812 has a potent anti-cancer effect in a broad range of genetically different cell lines, is not mutagenic and less toxic than conventional therapies, positions ABTL0812 as a potential therapeutic agent in the treatment of NB and supports the study of ABTL0812 in combination with current second line therapies and 13-cRA in *in vivo* experiments.

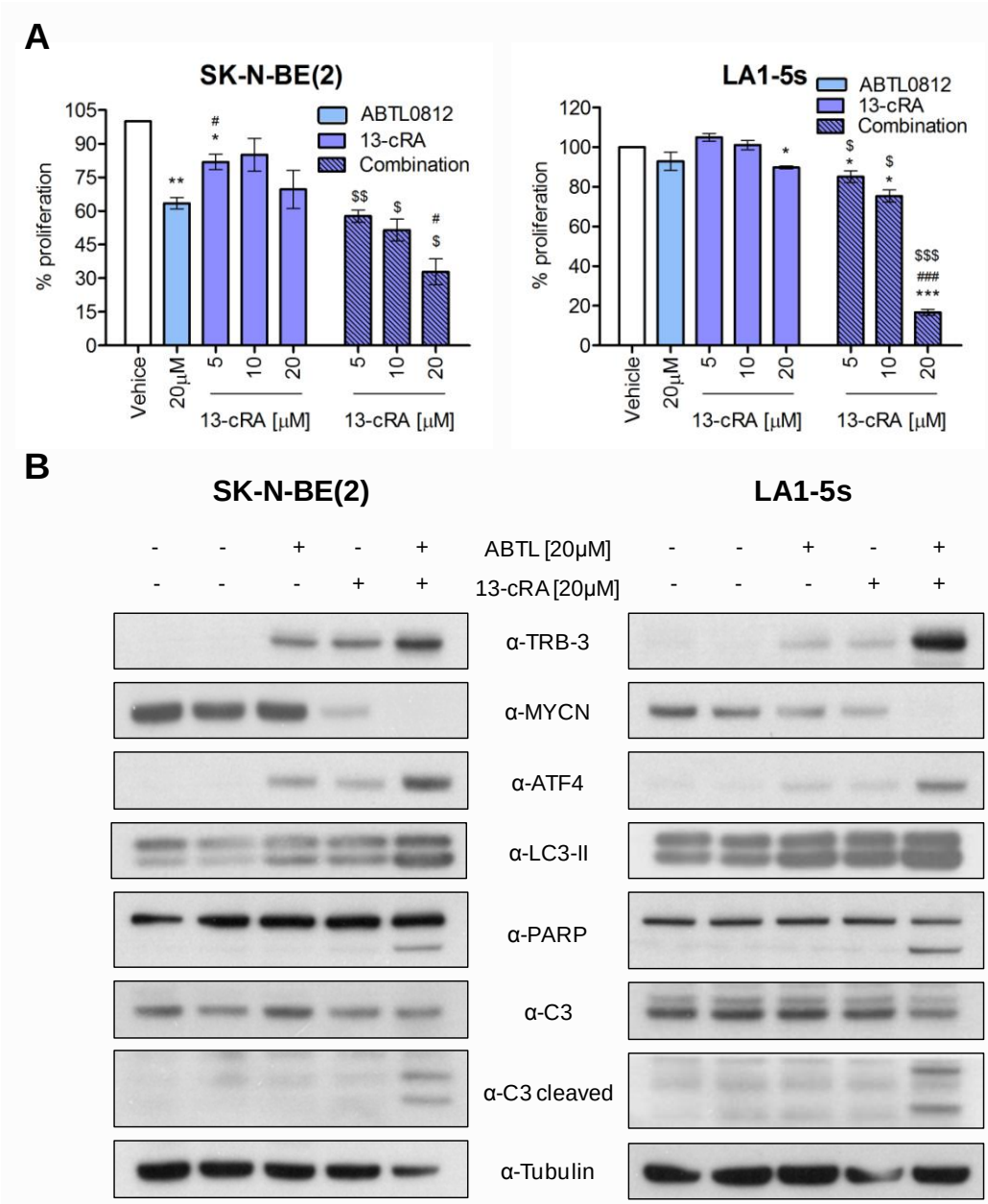

Figure 32. ABTL0812 synergizes with 13-*cis*-retinoic acid. SK-N-BE(2) and LA1-5s were treated with vehicle (ethanol), ABTL0812 20μM and the indicated doses of 13-cRA, alone or in combination with ABTL0812. (A) Cells were fixed with 1% glutaraldehyde 24h post-treatment and the percentage of viable cells for each treatment was assessed by crystal violet staining. Data is presented as mean ± SEM of three independent experiments. Plain bars represent single agent treatments, striped bars represent combined treatments. *p≤0.05, **p≤0.01, ***p≤0.001 compared to vehicle; $^{\#}$p≤0.05, $^{\#\#\#}$p≤0.001 compared to ABTL0812 as a single agent; $^{\$}$p≤0.05, $^{\$\$}$p≤0.01, $^{\$\$\$}$p≤0.001 compared to the matching concentration of RA as single agent. (B) Protein expression levels were analyzed by WB 24h post-treatment.

4.9 ABTL0812 is a therapeutic candidate for multiple pediatric solid tumors

Deregulated MYCN expression is not limited to NB pathogenesis and aggressiveness but is associated with the development of a large list of tumors that express MYCN during normal development.

Since several pediatric solid tumors are known to be dependent on MYCN expression [39,47] and we have proven that ABTL0812 targets MYCN, we wondered if ABTL0812 could be a therapeutic option for those unmanageable tumors. To this aim, a clinically representative panel of pediatric cancer cell lines harboring MYCN amplification or over-expression was treated with increasing concentrations of ABTL0812 during 72 hours. Then, crystal violet staining was performed to assess cells growth inhibition and/or cell death. All cell lines responded with similar IC_{50} between 30-60µM, showing that ABTL0812 is an effective agent for childhood cancers (Figure 33).

A

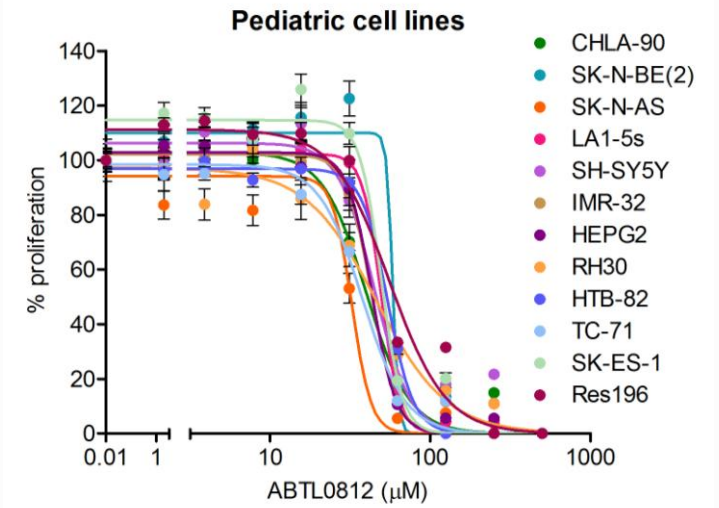

B

Tumor cell line	IC_{50} [µM]
Neuroblastoma	
CHLA-90	57.87 ± 0.78
SK-N-BE(2)	58.70 ± 1.08
SK-N-AS	32.49 ± 0.03
LA1-5s	50.68 ± 1.34
SH-SY5Y	43.35 ± 1.40
IMR-32	43.33 ± 0.22
Hepatoblastoma	
Hep2G	43.20 ± 2.41
Alveolar rhabdomyosarcoma	
RH30	39.82 ± 8.60
CW	53.02 ± 6.00
Embrional rhabdomyosarcoma	
HTB-82	55.17 ± 3.61
RD	36.22 ± 18.4
Ewing sarcoma	
TC-71	37.55 ± 0.42
SK-ES-1	49.64 ± 0.40
Medulloblastoma	
Res196	53.70 ± 0.15

Figure 33. Dose-response curves and IC_{50} for ABTL0812 in a panel of pediatric cancer cell lines. (A) Cells were treated with ABTL0812 for 72h at the indicated concentrations. Cells were fixed with 1% glutaraldehyde at 72h post-treatment and the percentage of viable cells for each treatment was assessed by crystal violet staining. (B) IC_{50} summary calculated from the dose-response curves. Data is presented as mean ± SEM of three independent experiments.

Now that over-ER stress stimulation is emerging as a novel strategy to cope with cancer, further experiments would be required to characterize the most potent or chemosensitizing drug combinations for each type of tumor to ideally proceed to verify their therapeutic efficacy in clinical trials.

DISCUSSION

5. Discussion

5.1 ABTL0812 as a therapeutic candidate for high-risk neuroblastoma

The clinical course of NB is very heterogeneous, ranging from spontaneous regression without the need for treatment or complete remission following conventional treatment, to resistance to intensive multimodal therapies. Survival probabilities for patients classified as high-risk (HR-NB) approach 40% despite the aggressive treatment. Therefore, although the outcome for certain subsets of NB has improved over the past few decades, survival of high-risk NB patients remains one of the most defiant challenges in pediatric oncology [7,25].

The urgent need to find therapeutic alternatives for multi-drug-resistant HR-NB or relapsed NB prompted us to ascertain whether the singular mechanism of action of ABTL0812 to inhibit the AKT/mTOR axis (Figure 34A) could make a change in this devastating scenario. In NB, constitutively enhanced PI3K/AKT/mTOR signaling has been shown to correlate with poor prognosis, increased tumor cell growth, proliferation, survival, angiogenesis, glucose metabolism and resistance to chemotherapy [158,230–233]. Moreover, the PI3K/AKT/mTOR axis integrates all the New Drug Development Strategy (NDDS) prioritized targets for HR-NB and directly regulates active stabilization of MYCN through GSK3β and mTORC1 phosphorylation [234,235] (Figure 34B). Previous pharmacological inhibition of the pathway in genetically engineered murine models of NB and medulloblastoma showed outstanding anti-tumor effects mediated by MYCN degradation, demonstrating the significant dependency of these tumors on this oncoprotein [374–376].

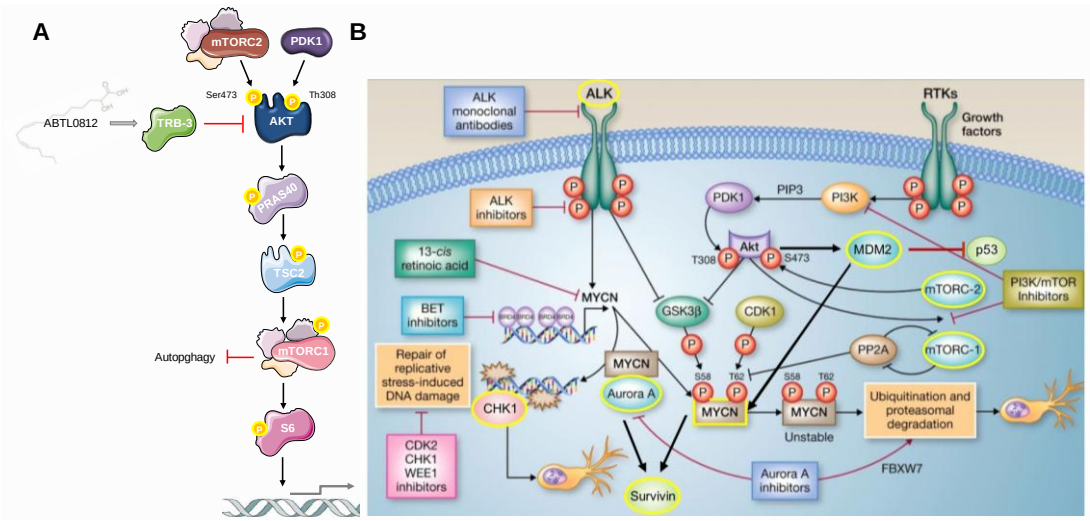

Figure 34. ABTL0812 mechanism of action and regulation of prioritized NB therapeutic targets. (A) Schematic representation of ABTL0812 mechanism of action described by Tatiana Erazo *et al*. [224]. (B) Integration of the NDDS targets (circled in yellow) within the PI3K/AKT/mTOR pathway. Figure adapted from [210].

Therefore, on the basis of extensive pre-clinical evidence, we assumed that ABTL0812 blockade of mTORC1 and mTORC2 signaling could be clinically efficacious in HR-NB and possibly other MYCN-driven tumors that have aberrant amplification, expression or stabilization of MYCN. However, it should be pointed out that despite the robust rationale for their development in pediatric malignancies, clinical trials of PI3K or combined mTORC1/2 inhibitors in children have been extremely limited due to the lack of interest from pharmaceutical companies. For now, early phase studies have been restricted to rapalogs (mTORC1-only inhibitors) and AKT inhibitors [199,377,378]. To make things worse, selective targeting of mTORC1 by rapalogs has demonstrated to be inefficient against the negative feedback loops resulting from mTORC1 inhibition which can re-activate AKT and lead to rebounded activation of uninhibited isoforms or signaling through compensatory pathways [194,195]. Nevertheless, ABTL0812 is a first-in-class drug that inhibits the PI3K-AKT-mTOR pathway by inducing TRB-3, a pseudokinase that binds to AKT impeding its phosphorylation and thus inhibiting AKT activation. Therefore, by activation of an endogenous inhibitor of AKT, ABTL0812 completely differentiates from classical ATP-competitive, allosteric or irreversible PI3K-AKT-mTOR inhibitors. In addition, ABTL0812 avoids the negative feed-back loop mediated by upstream kinases (PI3K, AKT and ERK) observed with rapamycin and conventional rapalogs, allowing long-term inhibition of the PI3K-AKT-mTOR pathway. Actually, ABTL0812 adult clinical trials have been coursing without signs of acquired resistances, while signs of efficacy are being observed, possibly due to PI3K-AKT-mTOR inhibition through the activation of an endogenous mechanism, in contrast to specific mTORC1 inhibitors. Therefore, we still had a strong rationale to study ABTL0812 effects on NB cell lines.

The cytotoxic activity of ABTL0812 was tested in a panel of NB cell lines derived from NB patients who were going through distinct points of the disease course (Table 9). The panel included a representative majority of cell lines that reflected the drug-resistant phenotype acquired after intense chemotherapy. Furthermore, the cell lines comprised in the panel also featured a wide-range combination of genetic and biologic risk factors involved in the definition of high-risk NB and predisposition, or not, to develop towards a resistant phenotype. ABTL0812 demonstrated to overcome drug resistances in multiple NB cells. Our results show that ABTL0812 inhibits growth of both chemosensitive and chemoresistant NB cells regardless of any malignant prognostic marker used in clinics. This suggests that even a genetically altered cell population that had emerged under chemotherapy pressure (e.g. non-functional p53 cells) would not escape to ABTL0812 cytotoxicity. This feature is highly significant, as when standard therapeutic regimens (based on intensive chemotherapy) are exhausted, no reliable options are left for refractory or relapsed patients. Current efforts at outlining alternative treatment strategies for refractory and relapsed patients are focusing on the development of small biologic molecules active towards tumors with alterations acquired under conventional chemotherapy that provides drug resistance [7,164]. Our results position ABTL0812 in a good place as a therapeutic candidate for those disadvantaged cases.

Nevertheless, despite all the newly generated agents and targeted therapies under study,

the most conventional strategies and effective current salvage treatments for HR-NB are still based on conservative chemotherapeutic agents and radiation. Unfortunately, while the establishment and refinement of these regimens has resulted in significant improvements in event-free survival and relapse rates, the same regimens put NB patients in a risk situation of substantial disease-related and treatment-induced toxicity. Nearly all patients treated for high-risk NB experience substantial treatment-associated acute toxicity, including severe transient myelosuppression, chemotherapy-induced renal dysfunction and poor weight gain. On top of that, given the intensive chemotherapeutic and radiation regimens that NB patients undergo at a young age, almost all survivors are expected to have long-term health issues related to their treatment. Common late effects of chemotherapy and radiation encompass learning difficulties, vision problems, hearing loss, growth and developmental delays, muscle and bone growth complications, seizures, infertility, loss of function of certain organs and increased risk of developing a second cancer. The risk of developing late effects depends on various factors such as the specific drugs used during treatment, the dosage of those drugs and the child's age during treatment [4,8,379] (Table 16).

Table 16. Acute and late side-effects of neuroblastoma therapy

Acute effects	Late effects
Pain	Impaired growth and developmental delays
Neurological symptoms	Delayed/impaired puberty or infertility
Nausea and vomiting	Hypothyroidism
Severe myelosuppression	Vision problems
Risk of infection	Hearing loss
Mucositis	Chronic diarrhoea
Veno-occlusive disease	Pulmonary fibrosis
Renal dysfunction	Neurological impairment
Electrolyte imbalance	Learning difficulties
Impaired growth and poor weight gain	Scoliosis
	Dental abnormalities
	Chronic kidney disease
	Benign neoplasms
	Malign neoplasm

Most of these severe, life-threatening side-effects of NB treatment can be explained by the mechanism of action of chemotherapy and radiation. Radiation and the majority of chemotherapeutic drugs work by disruption of DNA strings. For example, cisplatin is an alkylating agent that crosslinks DNA in several ways, doxorubicin intercalates between DNA base pairs, etoposide forms a complex with DNA and toposomeirase II to prevent religation of DNA strands, and cyclophosphamide crosslinks between DNA strands at guanine bases. The initial reaction of a cell to DNA damage is to activate DNA repair

processes; yet with increasing levels of DNA damage, the cell switches to cell cycle arrest or to apoptosis [380]. However, sometimes the DNA-damaging agents cause genotoxicity (mutations, chromosome aberrations, etc.); still cells do not undergo apoptosis. In fact, these damaged cells continue to grow and multiply, which may affect normal growth and development of body organs and tissues or make them become neoplasic. Moreover, chemotherapeutic agents and radiation therapies are not specific and do not differentiate between normal healthy cells and tumor cells.

As a sign, various publications directly relate some of the long-term disorders and injuries suffered by NB survivors to agents used in modern NB therapy. For example, the high prevalence of hypothyroidism in NB survivors comes from ^{131}I-mIBG and external beam radiotherapy thyroid damage. Growth failure, short stature, vertebral damage, scoliosis, poor weight gain and chronic diarrhea are as well consequences of exposure to total body irradiation [381–384]. Total body irradiation, or focused radiation in affected areas, has also been associated to development of diabetes mellitus and metabolic syndrome, premature ovarian failure, azoospermia and oligospermia. The use of alkylating agents is also related to metabolic and reproductive disorders, while exposure to carboplatins originates hearing loss problems [381–383,385,386]. Finally, multivariate analyses have identified exposure to topoisomerase inhibitors, alkylating agents and radiotherapy as risk factors for the development of secondary cancers, like leukemia and renal cell carcinoma [382,387,388].

These observations underscore the need for less toxic therapies. Thus, one of the required characteristics when it comes to the design of new therapeutic strategies should be to not directly interact or damage DNA. Our analyses have shown that ABTL0812 is a safe therapeutic agent in the sense that it does not cause DNA breaks, therefore preventing any of the treatment-related morbidities discussed before.
Further confirmations regarding the safety and efficacy of ABTL0812 have also been demonstrated in adult phase I/II study (NCT02201823). In the first-in-human phase I/Ib clinical trial (twenty-nine patients with advanced solid tumors), ABTL0812 showed great safety, tolerability and signs of efficacy. Remarkably, one patient with endometrial cancer had long-term disease stabilization for over fourteen months and one patient with cholangiocarcinoma was stable for eighteen months. Given the extremely low toxicity profile of ABTL0812, the recommended phase II dose had to be determined based on pharmacokinetic and pharmacodynamics analysis as the maximum tolerated dose was not achieved in phase I/Ib because no dose-limiting toxicities were identified. The few adverse events reported were mild (mostly grade 1-2) and mainly associated with drug administration. The most common were asthenia (34%), nausea and vomiting (31%) and throat burning (24%).

The results of our HR-NB *in vivo* model kept in line with the safety and efficacy of ABTL0812 observed in the adult clinical trials. The *in vivo* was designed to compare anti-tumor activity and potential acute toxicities of ABTL0812 vs. cisplatin (CDDP). ABTL0812 not only proved to be as efficient as the standard therapeutic agent in a chemosensitive

model but also matched good tolerability, as reflected by the low weight fluctuation. ABTL0812 even improved the outcome of several blood-test parameters used to measure toxicity, suggesting a trend to have a better tolerability profile than CDDP. Specifically, mice treated with CDDP showed a slight reduction on the hematocrit concentration and red blood cell counts, whereas mice treated with ABTL0812 had normal values. It is generally accepted that treatments with chemotherapeutic drugs have undesirable side effects because they affect healthy tissues or organs that divide quickly, such as the bone marrow. Therefore, the most common and severe acute side effects of chemotherapy are (1) decrease of red blood cells, (2) decrease of platelets, and (3) decrease of white blood cells, among many others. Bone marrow damage and consequent red blood cells production impairment implies a decreased flow of oxygenated blood to tissues, hence, fatigue. Fatigue is the most common symptom of anemia and one of the most reported chemotherapy adverse side effects. ABTL0812 seems to not have any impact in red blood cells production, what would safe patients from suffering anemia.

In conclusion, (1) the potential of ABTL0812 to be effective even in the most discouraging scenarios, (2) the fact that it has equalized the efficacy of standard-treatments *in vivo* and (3) the expected good tolerability outstand ABTL0812 as a promising drug to treat HR-NB patients.

5.2 Integrating endoplasmatic reticulum stress signaling in cancer therapy

The first publication depicting ABTL0812 signaling pathway made apparent that ABTL0812 induced macroautophagy-mediated cancer cell death by inhibition of the AKT/mTORC1 axis (macroautophagy will be herein referred to as autophagy). Erazo and colleagues [224] showed in lung (A549 cells) and pancreatic (MiaPaCa-2 cells) adult cancer models that ABTL0812 would primary target PPARα/ɣ receptors causing up-regulation of TRB-3, a pseudokinase that can interact with AKT and prevent its phosphorylation [224,389,390]. This mechanism of action was also demonstrated in endometrial cancer models [225]. TRB-3 overexpression would result in the inhibition of the AKT/mTORC1 pathway and autophagy induction, since mTORC1 plays a central role in its regulation. The mTORC1 complex belongs to a network that serves as a sensor of the cell's nutrient supplies and accordingly balances anabolic and catabolic metabolism through autophagy in order to maintain homeostasis [248,250,391,392].

Autophagy is considered to be a dynamic process that comprises three sequential steps: (1) formation of double membrane vesicles known as autophagosomes, (2) the fusion of autophagosomes with lysosomes and (3) degradation of autolysosomes [237]. So far, autophagy is a homeostatic and evolution-conserved process that breaks down cellular organelles and proteins and maintains cell biosynthesis during nutrient deprivation or metabolic stress. Autophagy is primarily considered a cytoprotective mechanism used to promote cell survival under basal and stressful conditions. However, it has also been referred to as a double-edged sword since, in certain cellular contexts, excessive or sustained autophagy may induce a caspase-independent type of programmed cell death, the autophagic cell death. During autophagic cell death, the autophagic vesicles accumulate in the cytosol of dying cells and engulf bulk cytoplasm and cytoplasmic organelles. Thus, it is important to distinguish between cytoprotective autophagy and the cellular settings in which autophagy can cause cell death [248–250,393]. Shen and Codogno [394] proposed three criteria to define cell death by autophagy: (1) cell death occurrence has to be independent of apoptosis, (2) there has to be an increase in autophagic flux (degradation), and not just an increase in autophagic markers in dying cells and (3) genetic or pharmacologic suppression of autophagy has to prevent cell death. However, the same authors stress the complexity of excluding apoptosis from autophagy due to the intricate relationship between these two processes and the difficulty of suppressing autophagy key proteins by siRNA silencing. Therefore, the principal methods used to monitor autophagic activation are the detection of autophagosome formation by fluorescence and electron microscopy and the quantification of autophagic flux by WB analysis [237]. The term autophagic flux refers to the whole dynamic process of autophagy: formation of autophagosomes, fusion of autophagosomes with lysosomes and cargo and vesicle degradation. Formation and expansion of autophagosomes require recruitment and conversion of cytosolic-associated LC3-I into the autophagosome membrane-bound lipidated form LC3-II. LC3-II remains on mature autophagosomes until after their fusion with lysosomes. Thus, autophagic flux can be monitored by detection of LC3-II accumulation in the presence of lysosomal degradation inhibitors since the transit

of LC3-II through the autophagic pathway will be blocked [248–250].

Our results did indeed confirm that ABTL0812 induced autophagy in NB cells. Following the mentioned guidelines, we detected recruitment and transition of LC3-I to LC3-II by immunochemistry in NB cells treated with ABTL0812. Moreover, incubation of treated cells with lysosomal protease inhibitors resulted in LC3-II accretion, what suggests that the generated vesicles take part in an autophagic flux. However, in spite of autophagy induction, we could not translate the reported ABTL0812 mechanism of action to NB cell lines. Unlike what had been described for lung, pancreatic and endometrial cancer cells, ABTL0812 did not reduce phosphorylation of AKT nor mTORC1 substrates, although TRB-3 and LC3-II levels were upregulated. Thus, initiation of autophagy-mediated cell death in NB could not be explained by inhibition of the AKT/mTOR axis.
Far from being a troublesome setback, the finding that ABTL0812 works differently depending on the cellular context was somehow expected. Additionally, we also found that besides autophagy, NB cells were dying by apoptosis, in accordance with what was observed for endometrial cancer models [225]. NB cells treated with ABTL0812 presented the typical morphological features of apoptosis: loss of adhesion, rounding of adherent cells, cell shrinkage, chromatin condensation, nuclear fragmentation and formation of apoptotic bodies. Cleavage of effector caspase-3 and proteolysis of executor substrates were also detected. None of these apoptotic hallmarks could be noticed in neither in A549 nor MiaPaCa-2 cells, even if the same authors proved that those cells are apoptosis-competent [224]. The disparity between cell fate outcomes and the observation that the AKT/mTOR axis was not affected by ABTL0812 activity in NB urged us to search for other mechanisms that could explain the appearance of both apoptosis and autophagy in NB cells treated with ABTL0812.

The multiple direct and indirect interactions between autophagy and apoptosis machinery has long been discussed in the literature. Under certain conditions, autophagy may promote cell survival and prevent apoptosis by clearing misfolded/unfolded proteins and damaged organelles and inhibiting caspases activation. However, under other conditions, autophagy may conclude in cell death in concert with apoptosis or independently in the event of apoptotic failure [395–397]. In order to elucidate whether the purpose autophagy was to minimize death by apoptosis or to promote programmed cell death, the anti-tumoral effect of ABTL0812 was studied in cells with compromised apoptosis or autophagy. The read-out of this experiment made evident that inhibition of autophagy rescued from cell death. This discarded the hypothesis that autophagy is triggered as a protective mechanism in front of ABTL0812 treatment and reinforced the idea that in this scenario autophagy is a pro-death process in coordination with apoptosis. Then, we aimed to ascertain whether autophagy was a previous step required for the activation of apoptosis, as it was the case for endometrial cancer cells [225], or both pathways had the same influence on promoting ABTL0812 cell death. Discouragingly, the monitoring of autophagy and apoptotic markers in ATG5 knocked-down NB cells treated with ABTL0812 did not lead to any solid conclusions (Annex 1). Even though ATG5 (a key protein for autophagosome elongation) was silenced, an increase in LC3-II could still be detected.

That meant both pathways were active. Therefore, despite the cleavage of apoptosis substrates, the experiment did not give any clue about the sequence/time-regulated dependency of these processes. The motives behind the failure of this strategy may fall on two possibilities. First, ATG5 only needs to be present in a small fraction to maintain its functionality. Thus, the conventional knockdown may not be sensitive enough to suppress autophagy effectively. Second, the intricate relationship between the autophagy and apoptotic machinery makes difficult to exclude apoptosis from the pro-death phase of autophagy. The crosstalk between autophagy and apoptosis is highly complex as both signaling networks intersect at several levels. Some of the proteins that regulate autophagosome formation and elongation have been shown to be involved in the induction of intrinsic apoptosis. Cleavage of ATG5 generates a truncated ATG5 product that translocates to the mitochondria. There, it binds to anti-apoptotic Bcl-xL, allowing Bax/Bak pore formation, cytochrom C release and consequent caspase activation [398]. Similar to ATG5, the resulting products of cleaved Beclin 1 (protein from the nucleation complex) translocate to the mitochondria and trigger apoptosis by mitochondrial outer membrane permeabilization [312,399–401].
However, integration between these two processes is bidirectional and several apoptotic proteins are in turn involved in autophagy induction. It has been described that the anti-apoptotic Bcl-2 proteins localized in the ER interact with and sequester Beclin 1, preventing autophagosomes formation [402–405]. Only in response to stress/death stimuli, JNK1 phosphorylates Bcl-2/Bcl-xL resulting in Beclin 1 release and autophagy promotion, probably as an attempt to recover cellular homeostasis from damage [268,406,407]. Other apoptotic proteins known to induce autophagy are BAD, BAK, BNIP3, NIX, HBMG1 and NOXA, which work by disruption of the bound between Beclin 1 and Bcl-2 [404,408–411] or Mcl-1 [412]. Additionally, nuclear p53 was discovered to stimulate autophagy through transcriptional activation of the lysosomal protein DRAM [312,413,414]. In short, the crosstalk between autophagy and apoptosis is quite complex as both pathways may be triggered by common upstream signals. This intricate relationship obstructed our attempts to decipher if autophagy was absolutely necessary to complete ABTL012 mechanism of action. Further efforts are needed to fully comprehend whether there is an ordering behind activation of these processes or they act concomitantly, eventually tipping the balance to survival or death.

Recent work (Muñoz *et al.* 2019, submitted) suggests that ABTL0812 cytotoxic outcomes in adult cancer cells are mediated by endoplasmatic reticulum stress (ER stress) induction. The ER stress is a harmful condition caused by an imbalance between the accumulation of unfolded or misfolded proteins in the ER lumen and correctly folded proteins transported out the ER. Protein folding in the ER is a highly sensitive process that can be disturbed due to changes in the Ca^{2+} levels, redox state, nutrient status, chaperone mutations, and presence of pathogens, pharmacological agents, inflammation, and even normal differentiation and function of secretory cells. To overcome ER stress, cells have an evolutionary conserved ER-specific signal transduction pathway called the unfolded protein response (UPR), whose primary aim is to re-establish ER homeostasis.
The UPR is divided in three branches initiated by different upstream signaling

transmembrane proteins that sense ER stress and begin a cascade of protective actions, like increased synthesis of ER chaperones, retrograde transport/elimination of misfolded proteins and transient attenuation of protein translation. However, when adaptation fails, chronically prolonged ER stress triggers cell suicide by apoptosis. Under physiological conditions, the luminal domains of the stress receptors form a complex with the chaperone GRP78 (also termed BiP), which keeps them inactive. When misfolded/unfolded proteins accumulate in the reticulum, they sequester the chaperones GRP78 and the three UPR arms become active and transmit signals to the cytosol and nucleus. The specific transmembrane proteins that trigger the UPR are: the inositol-requiring enzyme-1α (IRE1α), the activating transcription factor 6 (ATF6), and the protein kinase RNA-like endoplasmatic reticulum kinase (PERK) [264,362,363,368,415,416].

IRE1α is a transmembrane protein with a cytosolic serine/threonine kinase domain and an endoribonuclease domain. Under an ER stress situation, the IRE1α pathway is immediately activated. Active IRE1α cleaves XBP1 mRNA creating the spliced mature form XBP1s, a transcriptional regulator that binds to the promoters of genes involved in the restoration of ER homeostasis. The IRE1α pathway signaling usually gets weaker as time goes by. However, if stress is prolonged and severe, chronic IRE1α signaling favors regulated IRE1-dependent decay (RIDD), turns on apoptosis-signaling kinases and stabilizes C/EBP homologous protein (CHOP), a transcription factor that modulates gene expression to favor apoptosis (Figure 35).

ATF6 is a transmembrane protein that contains a cytosolic basic leucine zipper domain. When unfolded/misfolded proteins accumulate in the ER lumen ATF6 translocates to the Golgi apparatus where is cleaved into two fragments. The cytosolic fragment ATF6f, mediates the adaptative response to protein misfolding by playing an important role in lipid biogenesis, ER expansion; and promoting the transcription of genes involved in ER homeostasis restoration (Figure 35).

PERK is a transmembrane protein with a cytosolic serine/threonine kinase domain. Under ER stress conditions, PERK gets activated and phosphorylates the eukaryotic initiation factor eIF2α, causing attenuation of general protein translation but selectively increasing cap-independent translation of mRNAs such as ATF4 mRNA. ATF4 is a transcription factor that regulates ER stress response genes that play a crucial role in adaptation to stress conditions. One of the most important ATF4 targets is *CHOP*, which encodes for a transcription factor that paradoxically participates either in ER stress-corrective actions as well as initiation of ER stress-mediated apoptosis cascade. In relation to its protective functions, CHOP (also termed GADD135) suppresses ATF4 translation and drives eIF2α dephosphorylation in order to restore global mRNA translation. On the other hand, under severe and prolonged stress conditions CHOP promotes apoptotic cell death by repression of *BCL2* and *MCL1*; up-regulation of *BIM*, *PUMA*, *PMAIP1* (NOXA), *TRIB3*, *DR5* and *ERO1α*; BAX translocation to the mitochondria and cleavage of ER specific caspases. Finally, as mentioned, CHOP also targets *GADD34*, a protein that mediates eIF2α dephosphorylation (Figure 35). In a scenario of acute and chronic stress this would

contribute to accumulation of unfolded proteins in the ER and allow translation of other pro-apoptotic mRNAs. Therefore, PERK activation promotes both adaptative or apoptotic responses depending on the severity of the stress. A chronic activation of PERK is necessary to reach CHOP steady levels needed to promote cell death, as both ATF4 and CHOP mRNAs and proteins have short half-lives [264,362,417].

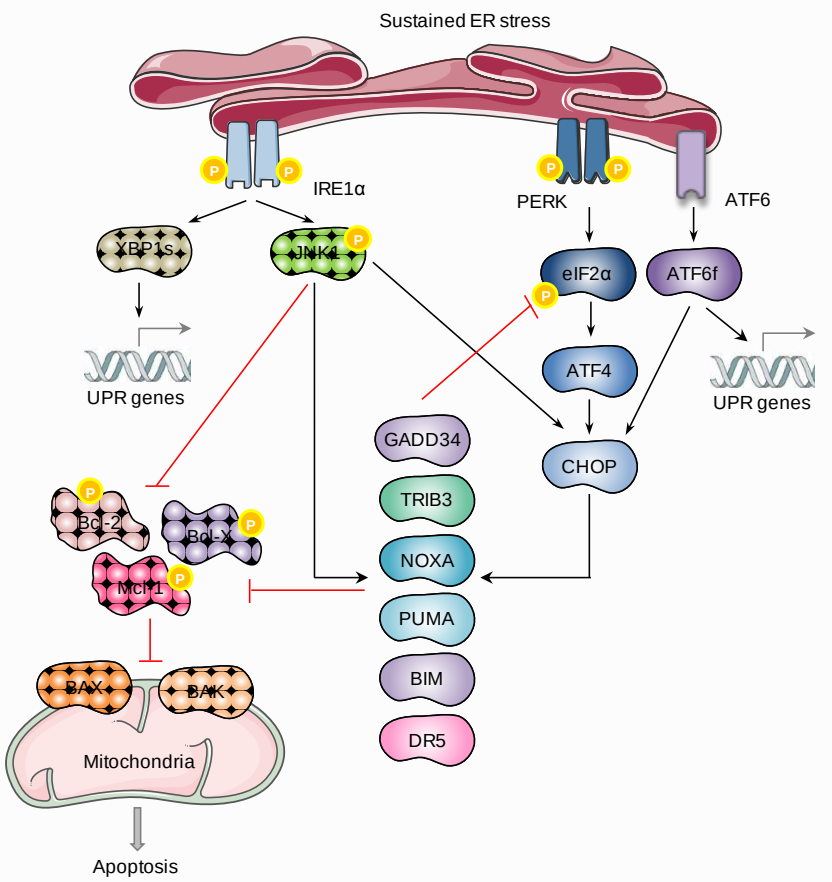

Figure 35. ER stress response/UPR induced apoptosis pathways. In case of severe and chronic ER stress, PERK, IRE1α and ATF6 drive multiple signaling outputs that lead to apoptosis. IRE1α dimerization produces the splicing of the active transcription factor XBP1 (XBP1s), which controls the transcription of genes involved in protein folding, protein quality, ER-associated degradation (ERAD), phospholipids synthesis and redox homeostasis. IRE1α also activates c-Jun N-terminal kinase (JNK1). JNK1 phosphorylation of the members of the Bcl-2 family strongly influences induction of apoptosis. On the other hand, PERK phosphorylates eIF2α to allow *ATF4* translation, a transcription factor that controls the transcription of genes involved in autophagy, apoptosis, amino acid metabolism and antioxidant responses. ATF4 stimulates CHOP expression, which induces eIF2α dephosphorylation through GADD34, inhibits Bcl-2 anti-apoptotic proteins and up-regulates the pro-apoptotic proteins PUMA, NOXA and BIM. These last ones regulate the heterodimerization and activation of pro-apoptotic BAX and BAK in the mitochondria, leading to apoptosis. CHOP also stimulates expression of the cell surface death receptor DR5 and TRB-3. The cytosolic domain fragment (ATF6f) of ATF6 is processed and released under ER stress conditions. ATF6f controls the up-regulation of genes encoding ERAD components, ER homeostasis and XBP1.

A diversity of studies have shown that autophagy can be potentially activated by the UPR and collaborate in cell apoptosis under ER stress conditions. Autophagy participation can be due to apoptosis stimulation or excessive stimulation of self-digestion, committing cells to autophagic cell death [418]. Among the different hypothesis by which these two pathways crosstalk there is the PERK/eIF2α/ATF4 driven transcriptional regulation of *ATG* and *TRIB3* genes [264,272,368], the XBP1 transcriptional activation of *BECN1* [419], and the Beclin 1/Bcl-2/Bcl-X disruption mediated by JNK phosphorylation and Ca^{2+} activation of death-associated protein kinase (DAPK) [420].

The integrated response elicited by the three ER stress sensors contributes to either adaptation or death, but it remains unknown how each branch contributes to the final biological effect. A generalized hypothesis is that upon ER stress, the UPR up-regulates the expression of both pro-survival and pro-death proteins, which some of them can exchange roles depending on the cellular context. However, intensity and duration of ER stress will be critical factors to definitely resolve whether cells can recover from the insult or it is something insuperable. Most of the attempts made to address how cells sense excessive ER stress agree on that low and moderate ER stress signals lead to reinforcement of corrective pathways through IRE1α, ATF6 and weak PERK activation; whereas PERK pathway is the most active during apoptotic phase of chronic ER stress. For instance, during persistent ER stress IRE1α and ATF6 signaling are attenuated so that PERK apoptotic signals dominate and inhibit the activity of pro-survival factors, shifting cell fate to death [362,421–423]. Recently, Pagliarini *et al.* [369] determined that the transcription factor E2F1 was responsible for the survival/death switch under advanced stages of the UPR. E2F1 belongs to the E2F family of transcription factors, which regulate the expression of genes required in cell cycle control. Individual E2F proteins activate distinct target genes necessary in its totality to progress from G1 to S phase. Nevertheless, E2F1 has the unique capacity to mediate the induction of apoptosis up-regulating pro-apoptotic genes and inhibiting anti-apoptotic signals [424]. E2F1 has a bifunctional role and its activity as a cell growth promoter or tumor suppressor is dependent on the cell context and presence of other family or interacting proteins. In the context of ER stress, E2F1 basal levels have a pro-survival role and inhibit PUMA and NOXA expression. Then, coordinated down-regulation in time of E2F1 protein levels during prolonged ER stress by ATF6-E2F7 complex sustains the expression of BH3-only and TRB-3 proteins up-regulated by ATF4 at early UPR stages. Consequently, finely regulation of E2F1 expression levels during prolonged ER stress coincides with the point of no return for determining the execution phase of the apoptotic pathway [368,369].

Our experiments validating (1) the generation of autophagic flux in cells treated with ABTL0812, (2) the observation of apoptotic morphological features and presence of apoptosis hallmarks upon ABTL0812 treatment, and (3) partial abrogation of ABTL0812 anti-tumor activity in the presence of autophagy and apoptosis inhibitors fit in with the theory that ABTL0812 could cause NB cell death through disruption of ER homeostasis and long-term activation of UPR response. Other authors have linked the antitumoral activity of certain compounds with their capacity to induce ER stress-associated cell

death, primarily by activation of PERK [425–429]. The analyses performed to track ABTL0812 molecular mechanism of action pointed towards the same conclusion, indicating that ABTL0812 triggered PERK activation, eIF2α phosphorylation, downstream ATF4/CHOP sustained up-regulation and eventual E2F1 down-regulation, inducing autophagy and apoptosis (Annex 2).

It has been thoroughly discuss in previous sections that the main drawbacks of chemotherapeutic DNA damage-based drugs currently used in HR-NB treatments are chemoresistance and toxic side-effects. Remarkably, HR-NB chemoresistance mechanisms as inaccurate p53 signaling, increased levels of Bcl-2 and Mcl-1, and caspase 8 silencing converge in the mitochondrial apoptotic pathway and are the reason why activation of pro-apoptotic BH3-only proteins fails in this tumor subtype. BAD, BID, BIM, NOXA and PUMA are examples of pro-apototic BH3-domain-only proteins whose activation depends on caspase 8-mediated signaling and/or p53-mediated transcription. Their physiological role is to interact with pro-survival Bcl-2 members (Bcl-2, Bcl-x_L, Mcl-1) to enable the release of Bak and Bax to form pores in the outer mitochondrial membrane, permitting cytochrom *c* diffusion and formation of the apoptosome [148,157,430]. It can be hypothesized that one mechanism to restore apoptosis sensitivity in HR-NB tumors may be to find new agents that get to stimulate the last phases of apoptosis independently of the presence upstream alterations that truncate the pathway. ABTL0812 provides an alternative approach to skip the inherent subversion of apoptosis pathways by triggering the apoptotic branches of the UPR response and impeded BH3-only proteins, as NOXA. Activation of JNK (via IRE1α) and CHOP (via PERK) during severe ER stress allows activation of executioner caspases independently of the status of p53, caspase 8 and/or anti-apoptotic Bcl-2 family members. Moreover, Ca^{2+} release from the ER upon PERK activation also leads to mitochondrial permeabilization ad cytochrome *c* leakage. This way, ABTL0812 may overcome some of the protective alterations observed in HR-NB cells (mutations in p53, *BCL2*, *MCL1*, *CASP8*, etc.) and offer an opportunity to patients who do not respond to conventional therapy.

The other major flaw of chemotherapy regimens are toxic side-effects. Improvement in tolerability and avoidance of late toxicities can be achieved by the identification of alternative therapies that selectively protect normal cells in order to achieve long-term cure while improving survivor's quality of life. One of the most prominent differences between non-transformed cells and tumor cells are the particular metabolic functions required by tumor cells to sustain uncontrolled proliferation. As a result of unconstrained growth and fast expansion, tumor cells suffer from insufficient vascularization, low oxygen supply, glucose shortage, amino acids deprivation and acidic pH. Remarkably, all of these are ER stress stimuli [431]. Furthermore, overexpression of oncogenes (like *MYCN* in HR-NB) or loss-of-function mutations in tumor suppressor genes entail an increased protein synthesis that demands the UPR activation to ameliorate ER protein folding capacity [264,368,429]. Consequently, numerous studies suggest that, unlike normal cells, cancer cells display chronic low/mild-levels of protective UPR pathways to adapt and progress under stressful environmental conditions [432–440]. As much as it may be an advantage

to adapt to a hostile microenvironment, chronic UPR activation sets tumor cells apart from normal cells and provides a tumor-specific target for potential therapeutic interventions. Because cancer cells have the protective components of the UPR chronically engaged their margin to accommodate additional stress is smaller. Treatment of tumor cells with drugs able to specifically induce further ER stress, such ABTL0812, would aggravate the pre-existing bearable ER stress conditions, tipping the scale towards domination of pro-apoptotic UPR outcomes. Conversely, under the same stress stimulus normal cells would initiate their ER stress response from an inactive state so they would have more leeway to withstand stress. Presumably, this strategy would stand ABTL0812 as a selective anti-tumor agent safer than conventional chemotherapy because it would target for attack specific molecular features of the tumor itself that differentiate it from normal tissue; contrary to chemotherapeutic drugs which have a broad effect on organs and tissues [8,145,441].

Overall, drugs able to trigger excessive or prolonged PERK/ATF4/CHOP activation, like ABTL0812, constitute a potential therapeutic strategy for selective inhibition of tumor growth in HR-NB patients. Accordingly, some new drugs designed to augment the ER stress on cancer cells and induce UPR-derived apoptosis are being studied in clinical trials for pediatric cancer patients (Table 17). Here below, these promising UPR-inducer anticancer agents are discussed. Bortezomib (Velcade®) is an example of a proteasome inhibitor that has reached successful clinical trials. Proteasome blocking impairs the ER-assisted degradation (ERAD), a process triggered by the UPR to get rid of the unfolded/damaged proteins accumulated in the ER. The consequent excessive increase in the ER protein burden is supposed to tilt the balance towards the UPR pro-apoptosis facet. Ritonavir is a HIV protease inhibitor that interferes with the ERAD machinery, causing a decrease in protein degradation and accumulation of polyubiquitinated proteins, similar to bortezomib. Together with an increase in *GRP78* and *CHOP* expression, ritonavir would cause irresolvable ER stress and cell death. Tanespimycin and Alvespimycin are first-generation inhibitors of the molecular chaperone heat shock protein 90 (HSP90). Disruption of the interaction between client proteins and chaperones results in an inability to proceed with normal protein folding, hence stimulation of all three branches of the UPR. Once the ER stress is sustained beyond the “point-of-no-return” ER stress-mediated apoptosis ensues. Isoflavones such as genistein, have shown to fulfill its anticancer potential via UPR activation thanks to a strong induction of several ER stress-relevant regulators, including *CHOP*. Prolonged elevated expression of *CHOP* would lead to mitochondrial permeability and activation of executer caspases. Nonsteroidal anti-inflammatory drugs that inhibit the enzyme cyclooxigenase-2 (COX-2), like Celecoxib, also induce Ca^{2+} leakage from the ER into the cytosol, potentially triggering the pro-apoptotic branches of the ER stress response independently of its activity as a COX-2 inhibitor. Last, photodynamic therapy (PDT) consists in the selective irradiation of a photosensitive drug that is preferentially accumulated in the ER membrane of tumor cells. Radiation generates ROS that will end up causing severe irreparable ER stress and cell death via persistent PERK signaling [429,442–444]. The tumor-specific exploitation of the UPR is expected to result in antitumor effects of the drug itself or, at least, sensitization of tumor

cells towards chemotherapeutic agents, offering a target for combination therapy [445], what will be discussed in the following sections.

Table 17. Clinical trials targeting the UPR components in pediatric cancer

Drug	Disease	Intervention	Phase	Sponsor	NCT id.
Proteosome inhibitors: induce UPR overwhelming the ERAD pathway					
Bortezomib	Neuroblastoma	Molecularly guided therapy	II	SHH	NCT02559778
	Lymphoma, NB and other pediatric solid tumors	Combinatory treatment with vorinostat	I	NCI	NCT01132911
	Neuroblastoma	Combinatory treatment with DFMO	II	SHH	NCT02139397
	Neuroblastoma	Combinatory treatment with irinotecan	I	University of Michigan Rogel Cancer Center	NCT00644696
HIV protease inhibitors: interfere with ERAD and activates the UPR					
Ritonavir	Disseminated NB and other solid tumors with brain metastases	Combinatory treatment with external-beam radiation	II	Oncology Institute of Southern Switzerland	NCT00637637
HSP90 inhibitors: trigger all UPR branches					
Tanespimycin	Leukemia, NB and other pediatric solid tumors	Targeted therapy	I	NCI	NCT00093821
Alvespimycin	NB and other solid tumors	Targeted therapy	I	NCI	NCT00089362
Isoflavones: block adaptative induction of GRP78 in response to hypoglycemia					
Genistein	Lymphoma, NB and other pediatric solid tumors	Targeted therapy	II	University of Virginia	NCT02624388
COX-2 selective nonsteroid inhibitors: inhibit ER Ca^{2+} pump and aggravate ER stress					
Celecoxib	NB and other pediatric solid tumors	Combinatory treatment with chemotherapy	II	Emory University	NCT02574728
	Leukemia, lymphoma, NB and other pediatric solid tumors	Combinatory treatment with chemotherapy	II	Dana-Farber Cancer Institute	NCT00357500
	Neuroblastoma	Metronomic therapy with chemotherapy	II	University of Cologne	NCT02641314
	Neuroblastoma	Combinatory treatment with chemotherapy	I	NANT	NCT02030964
ER photosensitizers: generate ROS and induce the UPR					
PDT	NB and head and neck cancers	Conventional surgery	I	Roswell Park Cancer Institute	NCT00470496

ERAD, ER-associated degradation; ROS, reactive oxygen species; COX-2, cyclooxygenase-2; PDT, photodynamic therapy; SHH, Spectrum Health Hospitals; NCI, National Cancer Institute; NANT, New Approaches to Neuroblastoma Therapy; NCT id., National Clinical Trial identifier number.

.

5.3 ABTL0812 decreases protein levels of the “undruggable” MYCN

Amplification of the proto-oncogene *MYCN* occurs in approximately 20% of NBs and is present in about nearly 50% of HR-NB cases. *MYCN* amplification is one of the most powerful clinically relevant adverse prognostic biomarkers for NB outcome, as it is strongly associated with high-risk chemotherapy-refractory disease independently of other clinical variables [13,37,38]. The mechanism by which *MYCN* amplification occurs is unknown but usually results in an increase of fifty to four-hundred copies per cell. Consequently, patients with *MYCN* amplification have abnormally high levels of *MYCN* mRNA and protein. Those who harbor higher *MYCN* copy number will face poorer progression-free survival expectations.

Aberrant MYCN overexpression plays a critical role in NB tumorigenesis-relevant processes such as uncontrolled growth, vasculogenesis and higher invasion capacities [39,44,46]. The ability of MYCN to reprogram cellular development falls under its function as a broad transcription factor, activating or repressing the expression of its target genes. Genes targeted by MYCN are involved in cell cycle, cell proliferation, apoptosis, DNA repair, ribosomal assembly, nucleotide biosynthesis, cell adhesion and migration, angiogenesis and neuronal differentiation [27,57–60].

Due to the overwhelming transforming potential of MYCN, its expression is tightly regulated at both transcriptional and translational level in normal cells. MYCN protein levels are regulated in two ways: (1) protein turnover and degradation and (2) protein stability. During the prophase, MYCN is phosphorylated at serine 62 (Ser62) by cyclin B and Cdk1. Ser62 phosphorylation serves as a substrate for GSK3β phosphorylation at threonine 58 (Thr58), what stabilizes the protein. Once stable, though, MYCN has a very short half-life (approx. twenty to thirty minutes) with its turnover occurring during mitosis. Signaling for MYCN degradation starts with Thr58 phosphorylation, which renders MYCN proteins exposed to be recognized by FBW7, a component of the E3 ubiquitin-protein ligase complex. FBW7 binding directs MYCN to proteasomal degradation via the ubiquitin-proteasome system (UPS).
Besides FBW7 and other undefined additional proteins, MYCN proteosomal degradation also depends on Aurora A kinase (AURKA) activity. AURKA is a mitotic kinase that has been found to contribute to MYCN stabilization through inhibition of FBW7 ubiquitination. Of note, *AURKA* oncogene is frequently over-expressed in *MYCN*–amplified and many other tumors, and cooperation between *AURKA* and *MYCN* is assumed to promote NB tumorigenesis and tumor growth [47,48,446,447].

Because of evidence demonstrating MYCN role in the pathogenesis of HR-NB, and potential activity as a driver oncogene of other tumor types, blockade of MYCN signaling represents a compelling therapeutic approach in cancer research. In addition, physiologic MYCN expression is restricted to the early stages of embryonic development, making it a tumor specific target in post-natal ages, further strengthening its election as a promising target. However, selective down-regulation of MYCN has been considered unattainable

due to the “undruggable” nature of this protein [40,47,448].

In light of the importance of the UPS pathway to mediate MYCN degradation, numerous efforts have been made to target oncogenic stabilization of MYCN, like promoting AURKA dissociation or interfering with abnormally enhanced PI3K/AKT/GSK3β signaling, a predominant feature in aggressive NBs [229,366,446] (Figure 36). The MLN8237 AURKA inhibitor is currently under clinical trials for HR-NB (NCT01154816, NCT02444884 and NCT01601535) but early phase II results revealed a weak antitumor activity [449]. Regarding the PI3K/AKT/GSK3β part, specific RTK inhibitors (upstream of PI3K) are being developed. For the moment the RTK inhibitor Lestaurtinib (CEP-701) has shown good tolerability and positive results in NCT00084422 phase I trial [86,450]. Moreover, several clinical trials testing rapalogs efficacy are ongoing (Table 18). However, as MYCN stability depends on multiple independent factors (AURKA, RTK/PI3K/AKT/GSK3β and others), one-way MYCN inhibition often induces feedback activation in the other signaling pathways. Therefore, one by one, these inhibitors are unlikely to affect MYCN protein, supporting the need to test these agents in combination [210,448].

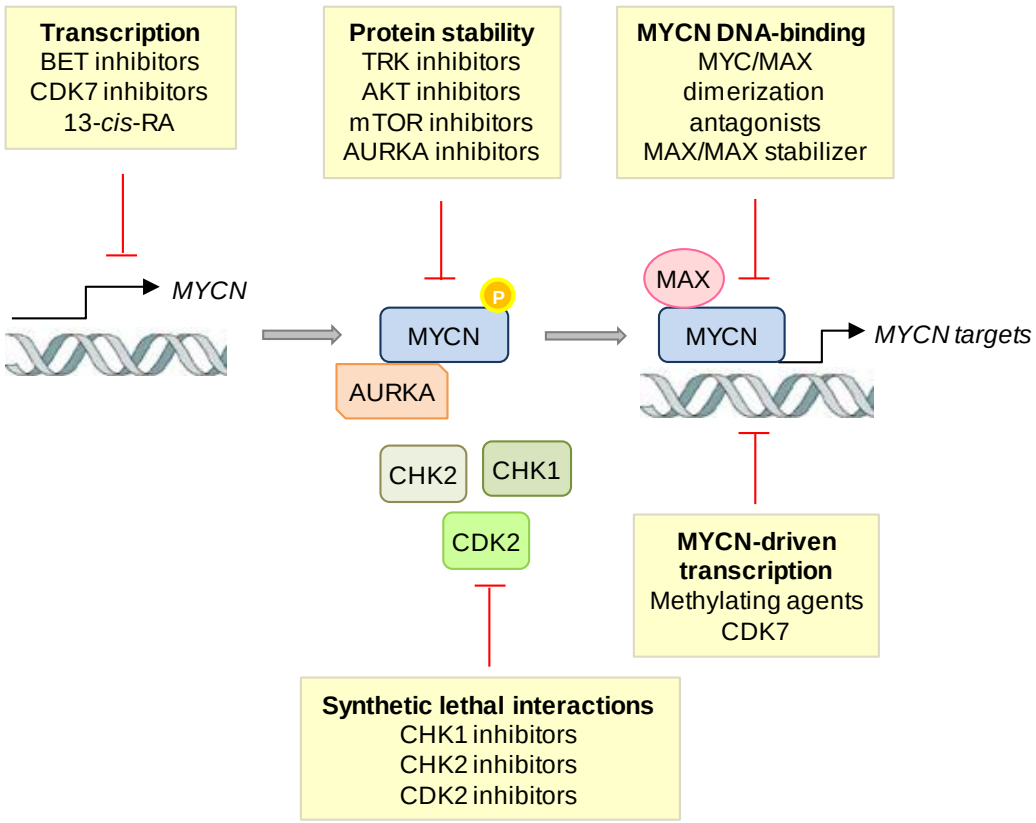

Figure 36. Therapeutic strategies targeting MYCN. Diverse pharmacologic strategies have been developed to target MYCN indirectly, via limiting *MYCN* transcription, MYCN protein stability and MYCN functions as a transcription factor. Moreover, strategies based on synthetic lethality interactions have also been developed. Figure adapted from [39].

Our results exhibiting that ABTL0812 promotes MYCN proteasomal degradation offer an alternative approach to target MYCN. One of the many adaptative mechanisms activated over the course of the UPR is a cascade of signal transduction reactions destined to alleviate the accumulation of unfolded/misfolded proteins in the ER. The re-adjustment of proper ER protein folding is conceived in three offensives: (1) an increase in the expression of ER chaperones, (2) the inhibition of protein entry into the ER by arresting mRNA translation, and (3) the destruction of unfolded/damaged proteins by a process named ER-assisted degradation (ERAD). The ERAD system is setup through XBP1s signaling in the context of ER stress. ERAD is recognized as the predominant cellular mechanism for removal of unfolded proteins that exceed ER chaperones folding capacity through activation of the UPS. This way, soluble proteins are linearized, retro-translocated to the cytosol, conjugated with ubiquitin and delivered to the proteasome, where they are deubiquitinated, and broken in oligopeptides [264,415,421,451]. It seems that triggering of the UPR by ABTL0812 includes the stimulation of the ERAD, facilitating proteasome translocation of proteins that accumulate in the ER. Our hypothesis is that due to the large MYCN production and high turnover rate, newly synthesized MYCN proteins may accumulate in the ER waiting to be folded, creating a situation that would worsen chaperone’s saturation under ER stress conditions. Hence, the excessive unfolded MYCN proteins would be processed through the ERAD pathway and directed to proteasome for degradation, relieving cell’s protein burden. This mechanism to enhance MYCN degradation would not be dependent on post-translational modifications mediated by the excessive PI3K/AKT/GSK3β signaling that has been shown to abnormally extend MYCN half-life in NB cells, suggesting that it may be a more solid way to achieve a reduction of MYCN levels. However, further experiments would be required to verify this hypothesis.
Although the experiments carried out using proteasome inhibitors indicated that ABTL0812 effects on MYCN are due to increased protein degradation, it still remains unknown whether it is meant to be a non-specific UPR consequence or maybe ABTL0812 could be targeting other proteins required for MYCN proteasomal degradation, like the ubiquitin ligase FBW7 or the ubiquitin-specific protease USP7 (also known as HAUSP). Relative to this issue, the majority of *MYCN*-amplified neuroblastoma cells have been found to bear *AURKA* overexpression [446,452,453], which disrupts the association between FBW7 and MYCN preventing its degradation. Conversely, pathologic increased levels of USP7 have been correlated with an increase of MYCN functions in HR-NB tumor samples, suggesting that an enlargement of the de-ubiquitination process may be involved in MYCN aberrant stability [454,455]. Therefore, the possible contribution of these proteins on ABTL0812-mediated lessening of MYCN levels should be explored by double-checking FBW7/USP7 expression coupled to the ubiquitination status of MYCN after ABTL0812 treatment.

Another proposed mechanism to lower *MYCN*-amplification impact is to directly disrupt *MCYN* transcription (Figure 36). With the help of *MYCN* transcriptional studies, the regulators and response elements within the *MYCN* transcript have been identified. In neuronal cells, *MYCN* is regulated in its promoter region by the activating members of the E2F family of transcription factors (E2F1, E2F2, and E2F3). The E2F transcription factors

are known for their involvement in timely regulation of gene expression required for cell-cycle progression, apoptosis, differentiation, and DNA repair [456]. In response to different mitogenic signals, the E2F factors bind to a highly conserved region of 200bp in the *MYCN* gene that controls the promoter activity and stimulates *MYCN* expression. Because E2Fs initiate MYCN mRNA transcription at the G1-S boundary and protein degradation ends in M phase, MYCN has a tooth-like pattern expression throughout the cell cycle, with low levels in early G1.However, as many authors have argued, other elements present on the *MYCN* basal promoter contribute to its regulation. For instance, the promoter region also contains a GC-rich motif, a CT-box and an E-box binding site. CT-box and CG-motifs are nearly identical and may functionally overlap. The GC-box sequence can be found in the promoters of many eukaryotic genes and is thought to be the recognition site for positive regulatory transcription factors such as Sp1, Sp3 and related zinc finger transcription factors. Sp1 is a ubiquitous general transcription factor that regulates the transcription of a large number of genes involved in cell proliferation, response to DNA damage and apoptosis [457]. Occupation of the GC-box/CT-box by Sp1 correlates with *MYCN* transcription, justifying why along with the E2F factors the Sp1 or Sp1-like proteins are presented as important drivers of *MYCN* expression [365,367,458–460].

Interestingly, a correlation between the ER stress-mediated genetic regulation and the E2F and Sp1 family proteins has been recently described. Cleaved ATF6 and XBP1s have been shown to form part of a protein complex that transcriptionally represses multiple E2F proteins during the UPR. Therefore, ER perturbations and UPR activation result in E2Fs down-regulation [369,461]. With respect to Sp1 modulation, it is known that Sp family proteins form a critical part of the ER stress-inducible binding factor (ERSF), a complex responsible for the induction of ER stress-dependent responses [371]. Therefore, it is plausible to argue that *MCYN* transcription could be altered in an ER stress situation because of the inhibition of E2F proteins or the interaction of Sp proteins within the transcriptional complex responsible for activation or repression of stress-target genes. In agreement with this hypothesis, our results show that *MYCN* is transcriptionally repressed upon ABTL0812 treatment and UPR induction. However, we were not able to elucidate exactly the process by which the UPR was inhibiting *MYCN*. Specific analyses discarded that down-regulation of MYCN was mediated by changes in the E2F factors expression, neither at mRNA nor protein levels. However, these results do not completely rule out this hypothesis, since other mechanism could be involved. First, post-translational modifications of Sp1, Sp3 and E2F proteins alter their transcriptional activities. Therefore, it may not be necessary to change the expression levels of these proteins to readjust their positive or negative effects over target genes [364,462]. Second, many authors have demonstrated that E2F and Sp proteins interact with each other to activate the transcription of genes that contain binding sites for either one or both factors [458,463,464]. This suggests that *MYCN* UPR-mediated regulation may not be explained only through variations in one of these factors but through changes in the relation between E2F and Sp1 proteins in the *MYCN* promoter. Furthermore, we cannot discard that E2Fs or Sp factors may exert its effects via multiple non-adjacent regulatory regions

or co-regulators recruitment [364,367]. In conclusion, in order to understand MYCN regulation in NB, further experiments would be needed to (1) identify all the control elements within the *MYCN* promoter and characterize the proteins that bind to these elements, (2) determine the post-translational modifications of E2F and Sp proteins under an ER stress-context, and (3) unveil the consequences of the interaction between E2F and Sp1 family members and/or other transcription factors that bind ERSE motifs.

Finally, apart from regulating MYCN transcription factors, the ER stress could be down-regulating MYCN mRNA levels by direct mRNA degradation. At high levels of stress signaling, the UPR branch triggered by the activation of IRE1α contributes to rather promiscuous degradation of mRNAs localized in the ER through a process referred to as regulated IRE1α-dependent decay (RIDD). The purpose of RIDD is to relieve acute ER stress by degrading the mRNAs load of the ER. Activation of RIDD depends on cell’s proteome activity and tendency to fail to carry out proper ER protein-folding. The proposed RIDD working model is that once the accumulation of unfolded/misfolded proteins triggers IRE1α activation, IRE1α may act directly on the target mRNAs through its RNase domain, through recruitment/activation of a second ribonuclease, or through mediation of ribosomal stalling and mRNA fragmentation by no-go decay [264,265,362,465]. Keeping in mind this UPR outcome, additional experiments should be directed to ascertain whether there is a link between IRE1α activation and the decrease of MYCN mRNA levels.

Be that as it may, ABTL0812 targeting of *MYCN* transcription represents an improved approach to treat HR-NB, since the majority of efforts to directly target MYCN with small molecules have ended up with discouraging results. This failure is most likely because MYCN does not stably fold and is inherently unstructured, with no surfaces for ligand binding [39,47]. However, to date, direct genetic blockage of *MYCN* as an alternative for protein targeting, has remained elusive. Even though siRNAs against MYCN have successfully demonstrated to decrease proliferation and induce neuronal differentiation *in vitro*, such tools have had limited success *in vivo* due to delivery problems. Therefore, instant action of an oral drug as ABTL0812 on *MYCN* mRNA levels sets a new precedent in regard to the possibilities of targeting MYCN in the clinics.

Overall, ABTL0812 reduces MYCN at mRNA and protein levels, what represents a significant step-forward because nearly all indirect MYCN inhibitors being developed are still emerging as clinically available therapeutics (Table 18). This dual action of ABTL0812 on MYCN indicates that ABTL0812 treatment might be beneficial not only in *MYCN*-driven tumors with genetic amplification, but also in tumors where protein over-expression does not correlate with genetic amplification [466].

Table 18. Targeted therapies against MYCN

Mechanism of action	Drug	Developmental phase	Pediatric NCT id.
Drugs targeting MYCN transcription			
BET inhibitors	OTX015	Phase I - Adult cancers	
	GSK525762	Phase I/II - Adult cancers	
	JQ1	Preclinical	
	Pfi1	Preclinical	
	CPI203	Preclinical	
Differentiating agent	13-*cis*-RA (Isotretinoin)	Current therapy	
Drugs targeting MYCN DNA-binding functions			
MYC/MAX dimerization antagonists	Omomyc	Preclinical	
	10058-F4	Preclinical	
	Mycro3	Preclinical	
MAX/MAX stabilizer	NSC13728	Preclinical	
Drugs exploiting synthetic–lethal interactions of MYCN			
CHK1 inhibitors	LY2606368 (Prexasertib)	Phase I	NCT02808650
	GDC-0575	Phase I - Adult cancers	
	GDC-0425	Phase I - Adult cancers	
CDK2 inhibitor	SCH727965	Phase I/II - Adult cancers	
CHK1, CHK2 and CDK2 inhibitors	SCH900776 (MK-8776)	Phase I/II - Adult cancers	
Drugs targeting MYCN functions			
CDK7 inhibitor	SY-1365	Phase I - Adult cancers	
Methylating agents	Valproic acid	Phase I	NCT02446431, NCT01204450, NCT01861989
	BL1521	Preclinical	
Drugs targeting MYCN oncogenic stabilization			
AURKA inhibitor	AT9283	Phase I	NCT00985868
	MLN8237 (Alisertib)	Phase I/II	NCT01154816, NCT02444884, NCT01601535
TRK inhibitors	CEP-701 (Lestaurtinib)	Phase I/II/III	NCT00084422, NCT00557193
AKT inhibitors	Perifosine	Phase I	NCT01049841, NCT00776867
	MK2206	Phase I	NCT01231919
mTOR inhibitors	Ridaforulimus (MK-8669)	Phase I	NCT00704054, NCT01431534, NCT01431547
	Rapamycin	Phase I/II	NCT01467986, NCT01282697, NCT02975882, NCT02574728, NCT03155620, NCT03213678
	Temsirolimus	Phase I/II	NCT01049841, NCT01614197, NCT00106353, NCT01182883, NCT00880282, NCT02446431, NCT01614795, NCT01767194, NCT01204450, NCT00808899, NCT02343718
	Everolimus	Phase I/II	NCT01734512, NCT03632317, NCT02638428, NCT01523977, NCT00187174, NCT03245151
	OSI027	Phase I - Adult cancers	
	AZD2014	Phase I/II - Adult cancers	
	MLN0128	Phase I/II - Adult cancers	
	BKM120	Phase I/II - Adult cancers	
	GDC-0980	Phase I/II - Adult cancers	
	NVP-BEZ235	Phase I/II - Adult cancers	

BET, bromodomain extra-terminal; RA, retinoic acid; AURKA, Aurora kinase A; NCT id., National Clinical Trial identifier number.

5.4 Outlines for an ABTL0812 phase I/II study in children and adolescents with relapsed or refractory neuroblastoma

ABTL0812 is currently in a phase Ib/IIa clinical trials in adult patients with advanced solid tumors in combination with standard chemotherapy (NCT03366480). A phase I/Ib clinical trial (NCT02201823) was successfully completed in 2015 demonstrating the safety and tolerability of ABTL0812 and allowing the determination of the adult recommended phase II dose. Additionally, some signs of efficacy were detected, as shown by several long disease stabilizations, including two patients that were stable for more than one year [226,227]. , and showed a good safety profile with tolerable side effects, a safe pharmacokinetic profile for the scheduled formulation (continuous oral administration) and the capacity to up-regulate TRB-3 and CHOP mRNA in blood samples from patients [459, Muñoz *et al.* submitted]. The 17% of patients with cholangiocarcinoma, endometrial and colon cancers displayed disease stabilization as best response. The excellent safety profile and its potential efficacy led to ABTL0812 being tested as first line therapy in an ongoing phase Ib/IIa trial that is evaluating the safety and activity of the drug in combination with standard chemotherapy (carboplatin and paclitaxel in endometrial and squamous non-small cell lung carcinoma. The phase Ib has been successfully completed, demonstrating that ABTL0812 does not increase the toxicities associated to chemotherapy [228]. The phase IIa started in May 2018 and is currently ongoing. Additionally, this trial has a biomarkers discovery and development program associated. To date, TRB-3 and CHOP mRNAs are being evaluated in blood (a surrogate tissue) from patient. It has been detected that both are induced by ABTL0812 monotherapy and in combination with chemotherapy [225, Muñoz *et al.* 2019, submitted, López-Plana *et al.* 2019, submitted]. This further confirms the ABTL0812 mechanism of action in humans. Moreover, a phase I/II study will start in in September 2019, where ABTL0812 will be combined with gemcitabine and nab-paclitaxel (Abraxane) as first line therapy in patients with advanced metastatic pancreatic cancer.

The therapeutic potential of ABTL0812 in pediatric tumors such as NB is supported by the preclinical data presented in this thesis. First, ABTL0812 has been shown to be effective in all pediatric cell lines tested, regardless of their genetic profile. On the contrary, NB cell lines respond differently to current chemotherapies (i.e. CDDP) depending on MYCN and p53 status and other malignant prognostic markers. It is important to emphasize this finding because it makes a distinction between ABTL0812 therapeutic possibilities and current chemotherapies, and adds a new therapeutic value to ABTL0812. Second, ABTL0812 proved to have similar antitumor effects to CDDP in a HR-NB mouse model, but fewer toxic side effects were reported. Third, ABTL0812 produces cell death through a novel alternative strategy, irreversible ER stress induction. This mechanism allows cells to surpass the apoptosis-resistant features often present in NB and other pediatric cancers. Moreover, it preferentially targets tumor cells making it a safe and tumor-specific therapy. Finally, ABTL0812 has shown the unique feature of targeting MYCN, an oncogenic driver for several pediatric malignancies known for more than 30 years but considered an unattainable target until recently [47].

In relation to NB therapeutic targets, the ITCC, ENCCA and SIOPEN resolved in the NDDS joint action to highlight 7 targets for developing drugs that provide more effective treatments: ALK, MEK, CDK4/6, MDM2, MYCN, BIRC5 and CHK1 [207]. The selection of therapeutic targets was subjected to tumor biology, tumor-specificity and evidences of their necessity for tumor progression. Among them, MYCN was classified as a high priority target as its correlates with poor outcome in several pediatric solid tumors [38,39,208,209]. However, pharmacologic inhibition of MYCN has not yet delivered viable therapeutics to the clinic.

As a whole, according to the NDDS guidelines ABTL0812 represents an important achievement for the developmental therapeutics as it has demonstrated to act on one high-priority target (MYCN) and to trigger molecular pathways specifically relevant for tumor viability (UPR). The potential clinical benefits of ABTL0812 together with the favorable results in phase I/II clinical trial for adult malignancies prompted us to provide patients with HR-NB with what seems to be safe and effective alternative. To this aim, we proceeded to plan how a plausible clinical trial for the use of ABTL0812 in NB patients would be delineated.

The development of drugs for rare diseases like childhood cancers is particularly challenging. Pediatric drugs are classified in a segment of the drug market known as “therapeutic orphans”. Pediatric clinical trials face a great number of additional challenges compared to adult trials. For example, recruitment of pediatric population is harder because of fewer patient registries and lack of the infrastructure needed to identify potential participants. Also, as it addresses a vulnerable population, obtaining consent can be difficult and extra protection to minimize risk is demanded. In addition to such ethical and legal concerns, the difficulties regarding evaluation of drug tolerability and efficacy and low profitability of the trial have lead to low investment in pediatric drugs development [467]. Sadly, the development of drugs for NB is still driven by the adult condition and not the mechanism of action of the drug. The only way to get newer, better drugs for children with NB is to wisely prioritize drug development and accelerate clinical trials, making the process smoother and less risky for industry and academic partners. Remarkably, in 2015 ABTL0812 obtained the Orphan Drug Designation (ODD) from the FDA and the EMA for the treatment of NB. In addition, Ability Pharmaceuticals contacted the EMA to seek advice on the development of ABTL0812 for the treatment of NB. Scientific advice was obtained from the Committee for Medicinal Products for Human Use (CHMP) (procedure nº: EMEA/H/SA/3021/1/2015/PED/SME/III). Among other issues, the CHMP suggested (1) the selection of the most appropriate chemotherapy regimen to combine with ABTL0812 for the treatment of recurrent or refractory NB, and (2) the need to devise a protocol for a phase I/II clinical trial to study the safety, tolerability and efficacy of ABTL0812 alone and in combination with chemotherapy. Although ABTL0812 has demonstrated efficacy as a single agent in *in vivo* HR-NB models, the clinical treatment of the disease is highly complex, so ABTL0812 may need to be used in combination with other chemotherapeutic agents. In regard to this point, ABTL0812 had previously exhibited a potentiation effect in animal models in combination with several cytotoxic drugs without increasing

chemotherapy-caused toxicity in any case. ABTL0812 has been tested in combination with docetaxel, paclitaxel/carboplatin and permetrexed for lung cancer; with paclitaxel/carboplatin in endometrial cancer; with paclitaxel and nab-paclitaxel/gemcitabine in pancreatic cancer; and with paclitaxel in breast cancer [225, López-Plana *et al*. 2019 submited, unpublished data].

In order to fulfill EMA's scientific advice, we searched in the literature the results of phase II studies dedicated to evaluate therapies currently used to treat HR-NB patients with refractory or relapsed disease (i.e. second-line and minimal residual disease treatments). This way we would anticipate the combination with the best therapeutic potential and avoid unnecessary treatments to patients. Our search was particularly focused in this subset of patients because the NDDS considers that the appropriate population of children for entry into early phase I/II studies should include (1) HR-NB patients showing early progressive disease during frontline treatment, (2) HR-NB patients with refractory disease after second-line chemotherapy, (3) NB patients with early relapse (during therapy or before one year after diagnosis) and (4) patients with late relapses (more than one year after diagnosis) [207]. We found that the SIOPEN frontline phase II/III trials TVD (topotecan-vincristine-doxorubicin) [168,468], TOTEM (topotecan-temozolomide) [173] and COG's irinotecan-temozolomide [177,178] and topotecan-cyclophosphamide combination [170,171] have become the most common second-line regimens in Europe for patients who do not achieve complete response with induction chemotherapy or patients with relapsed NB. Another phase II clinical trial with promising results is COG's topotecan-cyclophosphamide-etoposide combinations [172]. Furthermore, revision of the database www.clinicaltrials.gov and different publications showed that targeted therapies currently under phase I and II trials for the treatment of recurrent or refractory NB are often combined with one or several drugs of these backbone chemotherapy regimens. Such is the case of the BEACON study (NCT02308527) where the anti-VEGF monoclonal antibody Bevacizumab is being investigated in combination with temozolomide, irinotecan-temozolomide or topotecan-temozolomide. Therefore, we considered that pre-clinical in vitro combination of ABTL0812 with any of the previously exposed chemotherapy drugs would be essential to provide evidence of additive effects or synergy and no-antagonism to the chosen chemotherapy regimen prior to entry into clinical trials.

Our results showed that ABTL0812 had a good combination profile with each drug tested in selected HR-NB cell lines with diverse genetic profiles, including amplification of MYCN and mutations in p53. The combination of low doses of ABTL0812 with irinotecan, topotecan, cyclophosphamide and doxorubicin, separately, resulted in additive cell death effect. The importance of combinations is to enhance the apoptotic response of chemotherapy and overcome resistances in a context where deregulation of more than one biological pathway takes part in disease progression. Hence, the primary goal for composite treatments is to offer rational drug combinations that target independent pathways such that the existing resistance mechanisms within the tumor cells for one therapy would be unlikely to suppress the activity of the other agent/s. Thus, the development of adaptation mechanisms like oncogenic bypass or pathway redundancy by

tumor cells is more complex and limited. This treatment strategy is termed “orthogonal therapy” [148] and could be the case of ABTL0812 plus any chemotherapeutic drug since ABTL0812 mechanism of action integrates multiple pathways completely different from topoisomerase I inhibitors, DNA crosslinking or intercalating agents among others.

Besides treatment-resistances, toxicity is another significant problem of conventional chemotherapeutic agents. Especially in the case of NB, the natural heterogeneity of the tumor makes necessary to treat patients with multi-agent therapies. Unfortunately, this chemotherapeutic “cocktails” may cause severe toxicity in normal tissues and long-term side effects [145]. For this reason, cumulative toxicities of additional agents must be carefully taken into account and lots of efforts have been made to reformulate chemotherapy regimens to maintain benefits while reducing side effects.
Our results suggest that administration of ABTL0812 together with chemotherapy could allow lowering the dose of chemo drugs as, overall, the combination lessens the threshold for apoptosis induction. This way, ABTL0812 would widen the drugs therapeutic index by diminishing their harmful effects.

In conclusion, the translational relevance of these experiments is that ABTL0812, a well-tolerated, not mutagenic neither a DNA-damaging drug that has shown activity against most of NB cell lines *in vitro*, could enhance activity of second-line chemotherapeutic drugs with proved clinical efficacy against recurrent and refractory HR-NB [168,171,173,178]. We propose that these combinations deserve further evaluation since we have demonstrated positive *in vitro* effects between ABTL0812 and irinotecan, topotecan, cyclophosphamide and doxorubicin in multidrug-resistant HR-NB cell lines. Nevertheless, the favorable outcome of the anticipated regimens should be demonstrated in *in vivo* models, ideally well-characterized PDX models, before the best combinations were to be proposed for a clinical trial for children with recurrent and/or refractory NB.

Besides second-line treatments, we also considered the combination of ABTL0812 with biologic agents used for the treatment of NB minimal residual disease (MRD). This was based on the new strategy to identify the best therapies distinguishing between subsets of patients, based on the discovery of different molecular and biological characteristics. For example, some agents will only show efficacy in patients with minimal tumor burden, thus, they must have to be analyzed separately from those presenting larger tumor bulks. Therefore, to cover all areas, we aimed to ascertain whether the combination of ABTL0812 with drugs used for the treatment of MRD would be as well appropriate to improve survival of HR-NB patients. Maintenance therapy is based on immunotherapy and differentiating agents, such as 13-*cis*-retinoic acid (13-cRA, also named isotretinoin). Differentiation therapy has become part of standard therapy since a COG’s clinical trial proved that administration of 13-cRA improved the 3 year event-free survival in patients with MRD with minimal toxicity [134]. 13-cRA is a synthetic derivative of vitamin A that has been shown to induce differentiation and slow the growth of NB cells through interaction with nuclear retinoid receptors. Retinoid receptors divide into retinoic acid receptors (RARα, RARβ, RARγ) and retinoic X receptors (RXRα, RXRβ, RXRγ). All of them are

ligand-inducible transcription factors which interact with specific DNA sequences called retinoic acid response elements (RAREs), found in many promoters. Hence, retinoids regulate expression of multiple genes that play important roles in proliferation, differentiation and apoptosis [163,469,470].

The exact mechanisms through which 13-cRA induces growth arrest and cell differentiation or apoptosis in NB remain unclear. However, in 1985, Thiele et al. reported that RA treatment decreased *MYCN* expression and that this down-regulation preceded cell-cycle arrest and morphological changes [471]. Nowadays, it is evident that early *MYCN* modulation is a critical step in differentiation, growth arrest and other processes triggered by 13-cRA, in both MYCN-amplified and non-amplified NB cell lines [364,472,473]. Intriguingly, no homology areas with canonic RARE are found within the *MYCN* gene. It was not until 1997 that Wada *et al.* figured out that the essential sequence for the transcriptional response to RA was located in the positions -186 to -160 within the *MYCN* promoter. This sequence was thereinafter called “retinoic acid responsive region” (RARR) [474]. Two regulatory sequences were identified in this region: a GC-rich motif and a CT-box. Both are known to be capable of binding the transcription factors Sp1 and Sp3, which are known *MYCN* regulators [459,460,470]. Therefore, Sp proteins were thought to mediate *MYCN* down-regulation after RA treatment. However, it has not been possible to demonstrate that RA causes neither any post-translational modification nor any changes in the steady levels or the nuclear/cytoplasmatic distribution of Sp proteins. The last considered option is that RA may be exerting its effects through cooperation of multiple non-adjacent regulatory regions. For example, down-regulation of *MYCN* by RA might involve functional and/or physical interactions of Sp1/Sp3 with the E2F transcription factors, which have a close binding site within the *MYCN* promoter [364,458,463,464]. In any case, the ability of 13-cRA to down-regulate MYCN caught our attention given that it represents an important therapeutic target for HR-NB, as it has been largely discussed in this thesis. Therefore, we decided to test the combination of two drugs that decrease MYCN levels, like 13-cRA and ABTL0812. Our *in vitro* results showed that the combination of 13-cRA with ABTL0812 significantly impaired cells viability, even though the dose of ABTL0812 used was much lower than its IC_{50} and the 13-cRA concentrations were lower than what literature recommends to reach cytotoxic effects [475–477]. In addition, our molecular assays demonstrated that both ABTL0812 and 13-cRA induced the PERK/ATF4/CHOP axis, triggering autophagy, apoptosis and finally leading to NB cell death. The PERK signaling activity of each individual drug was added up in the combination treatment, driving to an enhanced pathway activation.

Although the link between ABTL0812 and the triggering of the PERK branch of the UPR has been already unveiled in this thesis, the link between 13-cRA and ER stress is not so clear. Several authors suggest that differentiation by RA and derivatives involves ER stress induction mainly via PERK pathway [478–481]. In this sense, it is reasonable that the combination treatment strongly upregulates ATF4, TRB-3 and LC3-II, all of them PERK effector proteins. Importantly, we found that 13-cRA may sensitize NB cells to ER stress-derived death induced by ABTL0812 and to growth arrest/apoptosis possibly

derived from MYCN targeting, which is clearly depleted in the combination treatment. 13-cRA could be working in parallel to ABTL0812 to achieve aggravation of ER stress, facilitating that lower drug concentrations sufficiently exacerbate ER stress to shift the balance from pro-survival UPR to pro-apoptotic in tumor cells. Therefore, optimal antitumor efficacy of ABTL0812 and 13-cRA might be achieved assuring minimal systemic side effects. Altogether, this result strengthens the notion that the ER stress response offers a mechanism to be exploited to develop rational drug design programs to provide new, safer and more effective anti-cancer therapeutic strategies.
In line with the subject of easing effective drug levels, another remarkable point of this combination is that although 13-cRA is a well-established agent in clinics, full benefits of this agent depend on achieving adequate drug concentrations and planning a correct treatment schedule, as exemplified by the opposite results extracted from the European Neuroblastoma Study Group clinical trial [482] and the U.S. Children Cancer Group trial [483]. These studies reflect that insufficient 13-cRA dosage can prevent treatment's successful outcome. Therefore, the finding that combined administration of ABTL0812 and 13-cRA improves the efficiency of 13-cRA makes easier to achieve optimal results even if the 13-cRA dispensed dose does not reach therapeutic concentrations.
Thanks to the good tolerability profile of 13-cRA as a single-agent, it is being used as a potential backbone on which to build combination therapies. For instance, the COG has already completed a phase I trial for children with refractory solid tumors that consisted in combining 13-cRA with the histone deacetylase inhibitor vorinostat [484]. The COG has also completed a phase III trial combining 13-cRA plus the chimeric anti-GD_2 antibody ch14.18 with a significantly improved outcome compared to standard therapy in patients with HR-NB [146]. Another phase I clinical trial for relapsed and refractory NB sponsored by M.D. Anderson Cancer Center and AstraZeneca is the combination of 13-cRA and Zactima (ZD6474), a dual small molecule inhibitor of the vascular endothelial and epidermal growth factor receptors and RET tyrosine kinases [485]. All these examples reinforce the idea that a proposal for a clinical trial based on the combined administration of 13-cRA and ABTL0812 could be considered for patients with relapsed or refractory NB.

The success of some therapies that included new targeted-agents lead the way to test if these treatment schedules may be effective as front-line therapies [163]. In order to meet this demand, the neuroblastoma NDDS supports compliance with the following four steps for clinical evaluation of new drugs: (1) check for safety and tolerability in early phase clinical trials, (2) execution of parallel randomized later-phase clinical trials, (3) verification by molecular profiling and (4) introduction into randomized front-line trials. The assessment of drugs that show promise in early phase trials in randomized multi-arm/multi-stage trials facilitates the transition from phase II trials in combination with second-line therapies to evaluation in studies for improvement of front-line therapies [207]. Thus, there is the prospect that good results in ABTL0812 early phase I trials get to fast implementation in front-line studies, given the urgent need to improve drug development in pediatric malignancies.

The difficulty to conduct pediatric clinical trials and obtain high-quality clinical data

coupled to poor marketability and profitability of new commercialized agents largely influence the decision not to invest in pediatric drugs or rare diseases, like HR-NB, of many pharmaceutical companies. This negative attitude towards pediatric drug development has serious consequences. Because of it, the EMA and FDA launched an improved regulatory framework to boost investment in orphan diseases. At the base of this program is the Orphan Drug Designation (ODD). The ODD provides a guaranteed status to a drug or biological product to use for the treatment of a rare disease and allows the sponsor to benefit from a wide range of incentives to develop clinical studies. In Europe, according to EMA's regulatory policies, these incentives should include: protocol assistance, access to a centralized authorization procedure, ten years of market exclusivity, additional incentives for micro/small/medium-size enterprises, fee reductions for regulatory activities and exclusive grant programs [486,487]. The ultimate objective of this project is to improve pediatric pharmacotherapy through collaboration among industry, government and academia. The sponsor of ABTL0812 obtained the ODD from the European Commission for the treatment of NB in 2015. The application was submitted in December 2014 (reference number EMA/OD/326/14) to the Committee for Orphan Medicinal Products (COMP) based on the low prevalence of the condition in the European Union (1.1/10,000), the fact that NB is a life-threatening and chronically debilitating condition, and the significant benefit obtained with ABTL0812 in preclinical models. In March 2015, the COMP viewed the submission favorably (EMA/COMP/65737/2015) and the product was included in the Community registry of orphan drugs with number EU/3/15/1485. In addition, ABTL0812 granted and ODD from the FDA in August 2015. Hopefully, the ABTL0812's ODD status and its associated incentives would help the clinical development of ABTL0812 in NB and other pediatric solid tumors.

5.5 Expanding the therapeutic possibilities of ABTL0812

Aberrant MYCN expression is not only seen in NBs. For instance, most of the solid tumors derived from the nervous system lineage present MYCN genetic amplification and/or overexpression, like medulloblastoma, retinoblastoma, astrocytoma, meningioma, glioblastoma multiforme and, obviously, neuroblastoma. Other non-neuronal tumors that feature high MYCN expression are castration-resistant neuroendocrine prostate cancers, breast cancers, hematologic malignancies, Wilm's tumors, small cell lung cancer, pancreatic tumors and the majority of all rhabdomyosarcoma cases yet is predominantly found in the alveolar subset (Table 19). Although *MYCN* amplification has not been reported as a prognostic marker for all those tumor types, MYCN altered expression has been associated with tumor onset and malignancy [39,40,47]. Among the mentioned tumor types there are some of the most common pediatric solid tumors: medulloblastoma, astrocytoma, glioblastoma multiforme, Wilm's tumor, retinoblastoma and rhabdomyosarcoma (other than NB). Even though pediatric cancer death rates have descended over 50% since 1970, cancer still is the second leading cause of death for children in the developed countries, placed only after accidental deaths [488,489]. Unfortunately, this indicates that despite the improvements made in therapeutic regimens design and supportive care, there is a subset of pediatric patients for whose new alternative treatments are needed. Future treatment decisions to cover these unmet patients should be arranged regarding the molecular features of the tumor and feasibility of treatments of being tumor-specific. Thus, thanks to the promising results obtained in HR-NB cells, where ABTL0812 treatment demonstrated a clear down-regulation of MYCN, we decided to test whether ABTL0812 could represent an alternative for other types of MYCN-driven pediatric tumors. Our results showed that representative cell lines of pediatric hepatoblastoma, medullobastoma, alveolar rhabdomyosarcoma, embrional rhabdomyosarcoma and Ewing sarcoma responded to ABTL0812 treatment to a similar extend than HR-NB cell lines, providing a rationale to further investigate the therapeutic potential of ABTL0812 in a wider range of tumors in which MYCN-dependence could be exploited.

Table 19. MYCN-expressing tumors

Cancer	Clinical implications	Reference
Tumors harboring either *MYCN*-amplification and overexpression or overexpression only		
Neuroblastoma	Driver oncogene, poor prognosis factor	Brodeur *et al*. 1984
Medullobastoma	Driver oncogene, poor prognosis factor, pro-metastatic factor	Swartling *et al.* 2010
Retinoblastoma	Associated to tumor initiation, poor prognosis factor	Rushlow *et al.* 2013
Astrocytoma, meningioma	Poor prognosis factor	Estiar *et al.* 2017
Glioblastoma multiforme	Associated to tumor initiation, poor prognosis factor	Hui *et al.* 2001, Bjerke *et al.* 2013, Testa *et al.* 2018
NEPC	Associated to transformation from PCA, poor prognosis factor	Beltran *et al.* 2011
Lymphoma, AML, CLL, ALL	Associated to tumor initiation, poor prognosis factor	Hirvonen *et al.* 1993, Ma *et al.* 2011, Astolfi *et al.* 2014
Small celll lung cancer	Associated to tumor initiation, poor prognosis factor	Wong *et al.* 1986
Wilm's tumor	Poor prognosis factor	Williams *et al.* 2015
Rhabdomyosarcoma	Poor prognosis factor	Williamson *et al.* 2005
Tumors harboring MYCN overexpression only		
Breast cancer	Poor prognosis factor	Mizukami *et al.* 1995
Pancreatic tumors	Associated to glucagon-producing tumors subtype	Fielitz *et al.* 2016

NEPC, neuroendocrine prostate cancer; PCA, prostate adenocarcinoma; AML, acute myeloid leukemia; CLL, chronic lymphocytic leukemia; ALL, acute lymphoblastic leukemia.

CONCLUSIONS

6. Conclusions

First: ABTL0812 inhibits growth of neuroblastoma cells *in vitro* regardless of their drug-resistant phenotype and their genetic alterations.

Second: ABTL0812 is not mutagenic and does not induce DNA damage, thereby providing a high safety profile.

Third: ABTL0812 has good tolerability *in vivo* and has a similar therapeutic efficacy as cisplatin, one of the chemotherapies used in the treatment of high-risk neuroblastoma patients.

Fourth: ABTL0812 induces autophagy and apoptosis in neuroblastoma cell lines through disruption of endoplasmatic reticulum homeostasis and long-term activation of the unfolded protein response.

Fifth: ABTL0812 promotes MYCN proteasomal-mediated degradation and transcriptional repression.

Sixth: ABTL0812 could be used in combination with other chemotherapeutic drugs such as doxorubicin, irinotecan, topotecan and cyclophosphamide.

Seventh: The combination of ABTL0812 with the differentiating agent 13-*cis*-retinoic acid has a synergistic effect.

Eighth: ABTL0812 inhibits the growth of several pediatric cancer cell lines derived from tumors such as hepatoblastoma, medulloblastoma, rhabdomyosarcoma and Ewing sarcoma, thereby providing a rationale to design a more inclusive ABTL0812 phase I clinical trial for pediatric cancers.

REFERENCES

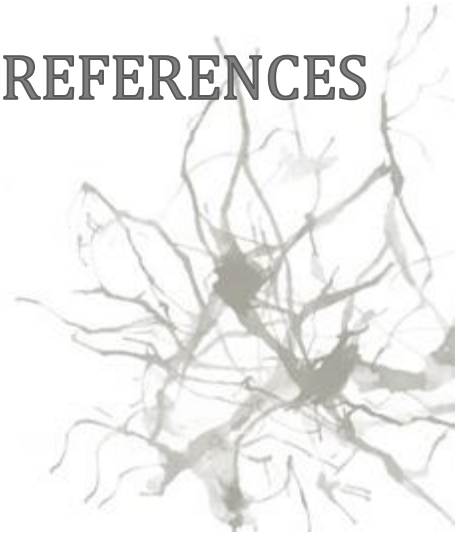

7. References

1. Ward E, DeSantis C, Robbins A, Kohler B, Jemal A (2014) Childhood and adolescent cancer statistics, 2014. *CA Cancer J Clin* **64**: 83–103.
2. Cancer Statistics Review, 1975-2015 - SEER Statistics.
3. Brodeur GM, Bagatell R (2014) Mechanisms of neuroblastoma regression. *Nat Rev Clin Oncol* **11**: 704–713.
4. Irwin MS, Park JR (2015) Neuroblastoma. *Pediatr Clin North Am* **62**: 225–256.
5. Colon NC, Chung DH (2011) Neuroblastoma. *Adv Pediatr* **58**: 297–311.
6. Maris JM, Hogarty MD, Bagatell R, Cohn SL (2007) Neuroblastoma. *Lancet* **369**: 2106–2120.
7. Newman EA, Nuchtern JG (2016) Recent biologic and genetic advances in neuroblastoma: Implications for diagnostic, risk stratification, and treatment strategies. *Semin Pediatr Surg* **25**: 257–264.
8. Matthay KK, Maris JM, Schleiermacher G, Nakagawara A, Mackall CL, Diller L, Weiss WA (2016) Neuroblastoma. *Nat Rev Dis Prim* **2**: 16078.
9. Gamazon ER, Pinto N, Konkashbaev A, Im HK, Diskin SJ, London WB, Maris JM, Dolan ME, Cox NJ, Cohn SL (2012) Trans-population Analysis of Genetic Mechanisms of Ethnic Disparities in Neuroblastoma Survival. *JNCI J Natl Cancer Inst* **105**: 302–309.
10. Tomolonis JA, Agarwal S, Shohet JM (2018) Neuroblastoma pathogenesis: deregulation of embryonic neural crest development. *Cell Tissue Res* **372**: 245–262.
11. Maris JM (2010) Recent advances in neuroblastoma. *N Engl J Med* **362**: 2202–2211.
12. Fort P, Théveneau E (2014) PleiotRHOpic: Rho pathways are essential for all stages of Neural Crest development. *Small GTPases* **5**: e27975.
13. Seeger RC, Brodeur GM, Sather H, Dalton A, Siegel SE, Wong KY, Hammond D (1985) Association of Multiple Copies of the N- *myc* Oncogene with Rapid Progression of Neuroblastomas. *N Engl J Med* **313**: 1111–1116.
14. Marshall GM, Carter DR, Cheung BB, Liu T, Mateos MK, Meyerowitz JG, Weiss WA (2014) The prenatal origins of cancer. *Nat Rev Cancer* **14**: 277–289.
15. Krona C, Carén H, Sjöberg R-M, Sandstedt B, Laureys G, Kogner P, Martinsson T (2008) Analysis of neuroblastoma tumour progression; loss of PHOX2B on 4p13 and 17q gain are early events in neuroblastoma tumourigenesis. *Int J Oncol* **32**: 575–583.
16. Reiff T, Tsarovina K, Majdazari A, Schmidt M, del Pino I, Rohrer H (2010) Neuroblastoma phox2b variants stimulate proliferation and dedifferentiation of immature sympathetic neurons. *J Neurosci* **30**: 905–915.
17. Bourdeaut F, Trochet D, Janoueix-Lerosey I, Ribeiro A, Deville A, Coz C, Michiels J-F, Lyonnet S, Amiel J, Delattre O (2005) Germline mutations of the paired-like homeobox 2B (PHOX2B) gene in neuroblastoma. *Cancer Lett* **228**: 51–58.
18. Molenaar JJ, Domingo-Fernández R, Ebus ME, Lindner S, Koster J, Drabek K, Mestdagh P, van Sluis P, Valentijn LJ, van Nes J, et al. (2012) LIN28B induces neuroblastoma and enhances MYCN levels via let-7 suppression. *Nat Genet* **44**: 1199–1206.
19. Diskin SJ, Capasso M, Schnepp RW, Cole KA, Attiyeh EF, Hou C, Diamond M, Carpenter EL, Winter C, Lee H, et al. (2012) Common variation at 6q16 within HACE1 and LIN28B influences susceptibility to neuroblastoma. *Nat Genet* **44**: 1126–1130.
20. He J, Yang T, Zhang R, Zhu J, Wang F, Zou Y, Xia H (2016) Potentially functional polymorphisms in the LIN28B gene contribute to neuroblastoma susceptibility in Chinese children. *J Cell Mol Med* **20**: 1534–1541.
21. Bosse KR, Maris JM (2016) Advances in the translational genomics of neuroblastoma: From improving risk stratification and revealing novel biology to identifying actionable genomic alterations. *Cancer* **122**: 20–33.
22. Satgé D, Moore SW, Stiller CA, Niggli FK, Pritchard-Jones K, Bown N, Bénard J, Plantaz D (2003) Abnormal constitutional karyotypes in patients with neuroblastoma: a report of four new cases and review of 47 others in the literature. *Cancer Genet Cytogenet* **147**: 89–98.
23. Brodeur GM (2003) Neuroblastoma: biological insights into a clinical enigma. *Nat Rev Cancer* **3**: 203–216.
24. Janoueix-Lerosey I, Schleiermacher G, Michels E, Mosseri V, Ribeiro A, Lequin D, Vermeulen

J, Couturier J, Peuchmaur M, Valent A, et al. (2009) Overall genomic pattern is a predictor of outcome in neuroblastoma. *J Clin Oncol* **27**: 1026–1033.
25. Ahmed AA, Zhang L, Reddivalla N, Hetherington M (2017) Neuroblastoma in children: Update on clinicopathologic and genetic prognostic factors. *Pediatr Hematol Oncol* **34**: 165–185.
26. Theissen J, Oberthuer A, Hombach A, Volland R, Hertwig F, Fischer M, Spitz R, Zapatka M, Brors B, Ortmann M, et al. (2014) Chromosome 17/17q gain and unaltered profiles in high resolution array-CGH are prognostically informative in neuroblastoma. *Genes Chromosomes Cancer* **53**: 639–649.
27. Bown N, Lastowska M, Cotterill S, O'Neill S, Ellershaw C, Roberts P, Lewis I, Pearson AD, U.K. Cancer Cytogenetics Group and the U.K. Children's Cancer Study Group (2001) 17q gain in neuroblastoma predicts adverse clinical outcome. U.K. Cancer Cytogenetics Group and the U.K. Children's Cancer Study Group. *Med Pediatr Oncol* **36**: 14–19.
28. Caron H, van Sluis P, de Kraker J, Bökkerink J, Egeler M, Laureys G, Slater R, Westerveld A, Voûte PA, Versteeg R (1996) Allelic loss of chromosome 1p as a predictor of unfavorable outcome in patients with neuroblastoma. *N Engl J Med* **334**: 225–230.
29. Carén H, Kryh H, Nethander M, Sjöberg R-M, Träger C, Nilsson S, Abrahamsson J, Kogner P, Martinsson T (2010) High-risk neuroblastoma tumors with 11q-deletion display a poor prognostic, chromosome instability phenotype with later onset. *Proc Natl Acad Sci U S A* **107**: 4323–4328.
30. Attiyeh EF, London WB, Mossé YP, Wang Q, Winter C, Khazi D, McGrady PW, Seeger RC, Look AT, Shimada H, et al. (2005) Chromosome 1p and 11q Deletions and Outcome in Neuroblastoma. *N Engl J Med* **353**: 2243–2253.
31. Schleiermacher G, Michon J, Ribeiro A, Pierron G, Mosseri V, Rubie H, Munzer C, Bénard J, Auger N, Combaret V, et al. (2011) Segmental chromosomal alterations lead to a higher risk of relapse in infants with MYCN-non-amplified localised unresectable/disseminated neuroblastoma (a SIOPEN collaborative study). *Br J Cancer* **105**: 1940–1948.
32. George RE, London WB, Cohn SL, Maris JM, Kretschmar C, Diller L, Brodeur GM, Castleberry RP, Look AT (2005) Hyperdiploidy plus nonamplified MYCN confers a favorable prognosis in children 12 to 18 months old with disseminated neuroblastoma: a Pediatric Oncology Group study. *J Clin Oncol* **23**: 6466–6473.
33. Bowman LC, Castleberry RP, Cantor A, Joshi V, Cohn SL, Smith EI, Yu A, Brodeur GM, Hayes FA, Look AT (1997) Genetic staging of unresectable or metastatic neuroblastoma in infants: a Pediatric Oncology Group study. *J Natl Cancer Inst* **89**: 373–380.
34. Look AT, Hayes FA, Shuster JJ, Douglass EC, Castleberry RP, Bowman LC, Smith EI, Brodeur GM (1991) Clinical relevance of tumor cell ploidy and N-myc gene amplification in childhood neuroblastoma: a Pediatric Oncology Group study. *J Clin Oncol* **9**: 581–591.
35. Schwab M, Alitalo K, Klempnauer KH, Varmus HE, Bishop JM, Gilbert F, Brodeur G, Goldstein M, Trent J (1983) Amplified DNA with limited homology to myc cellular oncogene is shared by human neuroblastoma cell lines and a neuroblastoma tumour. *Nature* **305**: 245–248.
36. Ambros PF, Ambros IM, Brodeur GM, Haber M, Khan J, Nakagawara A, Schleiermacher G, Speleman F, Spitz R, London WB, et al. (2009) International consensus for neuroblastoma molecular diagnostics: report from the International Neuroblastoma Risk Group (INRG) Biology Committee. *Br J Cancer* **100**: 1471–1482.
37. Riley RD, Heney D, Jones DR, Sutton AJ, Lambert PC, Abrams KR, Young B, Wailoo AJ, Burchill SA (2004) A systematic review of molecular and biological tumor markers in neuroblastoma. *Clin Cancer Res* **10**: 4–12.
38. Brodeur GM, Seeger RC, Schwab M, Varmus HE, Bishop JM (1984) Amplification of N-myc in untreated human neuroblastomas correlates with advanced disease stage. *Science* **224**: 1121–1124.
39. Rickman DS, Schulte JH, Eilers M (2018) The Expanding World of N-MYC–Driven Tumors. *Cancer Discov* **8**: 150–163.
40. Cheung L, E. J, Haber M, D. M (2013) The MYCN Oncogene. In, *Oncogene and Cancer - From Bench to Clinic*. InTech.
41. Cole MD, Cowling VH (2008) Transcription-independent functions of MYC: regulation of translation and DNA replication. *Nat Rev Mol Cell Biol* **9**: 810–815.
42. Adhikary S, Eilers M (2005) Transcriptional regulation and transformation by Myc proteins. *Nat*

Rev Mol Cell Biol **6**: 635–645.
43. Grimmer MR, Weiss WA (2006) Childhood tumors of the nervous system as disorders of normal development. *Curr Opin Pediatr* **18**: 634–638.
44. Weiss WA, Aldape K, Mohapatra G, Feuerstein BG, Bishop JM (1997) Targeted expression of MYCN causes neuroblastoma in transgenic mice. *EMBO J* **16**: 2985–2995.
45. Huang M, Weiss WA (2013) Neuroblastoma and MYCN. *Cold Spring Harb Perspect Med* **3**: a014415.
46. Goodman LA, Liu BC, Thiele CJ, Schmidt ML, Cohn SL, Yamashiro JM, Pai DS, Ikegaki N, Wada RK (1997) Modulation of N-myc expression alters the invasiveness of neuroblastoma. *Clin Exp Metastasis* **15**: 130–139.
47. Beltran H (2014) The N-myc Oncogene: Maximizing its Targets, Regulation, and Therapeutic Potential. *Mol Cancer Res* **12**: 815–822.
48. Lutterbach B, Hann SR (1994) Hierarchical phosphorylation at N-terminal transformation-sensitive sites in c-Myc protein is regulated by mitogens and in mitosis. *Mol Cell Biol* **14**: 5510–5522.
49. Fernandez PC, Frank SR, Wang L, Schroeder M, Liu S, Greene J, Cocito A, Amati B (2003) Genomic targets of the human c-Myc protein. *Genes Dev* **17**: 1115–1129.
50. Blackwood EM, Eisenman RN (1991) Max: a helix-loop-helix zipper protein that forms a sequence-specific DNA-binding complex with Myc. *Science* **251**: 1211–1217.
51. Corvetta D, Chayka O, Gherardi S, D'Acunto CW, Cantilena S, Valli E, Piotrowska I, Perini G, Sala A (2013) Physical interaction between MYCN oncogene and polycomb repressive complex 2 (PRC2) in neuroblastoma: functional and therapeutic implications. *J Biol Chem* **288**: 8332–8341.
52. Iraci N, Diolaiti D, Papa A, Porro A, Valli E, Gherardi S, Herold S, Eilers M, Bernardoni R, Valle G Della, et al. (2011) A SP1/MIZ1/MYCN Repression Complex Recruits HDAC1 at the *TRKA* and *p75NTR* Promoters and Affects Neuroblastoma Malignancy by Inhibiting the Cell Response to NGF. *Cancer Res* **71**: 404–412.
53. Lorenzin F, Benary U, Baluapuri A, Walz S, Jung LA, von Eyss B, Kisker C, Wolf J, Eilers M, Wolf E (2016) Different promoter affinities account for specificity in MYC-dependent gene regulation. *Elife* **5**:.
54. Guo J, Li T, Schipper J, Nilson KA, Fordjour FK, Cooper JJ, Gordân R, Price DH (2014) Sequence specificity incompletely defines the genome-wide occupancy of Myc. *Genome Biol* **15**: 482.
55. Cheung N-K V, Cheung IY, Kushner BH, Ostrovnaya I, Chamberlain E, Kramer K, Modak S (2012) Murine anti-GD2 monoclonal antibody 3F8 combined with granulocyte-macrophage colony-stimulating factor and 13-cis-retinoic acid in high-risk patients with stage 4 neuroblastoma in first remission. *J Clin Oncol* **30**: 3264–3270.
56. Łastowska M, Viprey V, Santibanez-Koref M, Wappler I, Peters H, Cullinane C, Roberts P, Hall AG, Tweddle DA, Pearson ADJ, et al. (2007) Identification of candidate genes involved in neuroblastoma progression by combining genomic and expression microarrays with survival data. *Oncogene* **26**: 7432–7444.
57. McMahon SB (2008) Control of nucleotide biosynthesis by the MYC oncoprotein. *Cell Cycle* **7**: 2275–2276.
58. Bell E, Lunec J, Tweddle DA (2007) Cell cycle regulation targets of MYCN identified by gene expression microarrays. *Cell Cycle* **6**: 1249–1256.
59. Dang C V, O'Donnell KA, Zeller KI, Nguyen T, Osthus RC, Li F (2006) The c-Myc target gene network. *Semin Cancer Biol* **16**: 253–264.
60. Slack A, Lozano G, Shohet JM (2005) MDM2 as MYCN transcriptional target: implications for neuroblastoma pathogenesis. *Cancer Lett* **228**: 21–27.
61. Schulte JH, Bachmann HS, Brockmeyer B, Depreter K, Oberthür A, Ackermann S, Kahlert Y, Pajtler K, Theissen J, Westermann F, et al. (2011) High ALK receptor tyrosine kinase expression supersedes ALK mutation as a determining factor of an unfavorable phenotype in primary neuroblastoma. *Clin Cancer Res* **17**: 5082–5092.
62. Janoueix-Lerosey I, Lequin D, Brugières L, Ribeiro A, de Pontual L, Combaret V, Raynal V, Puisieux A, Schleiermacher G, Pierron G, et al. (2008) Somatic and germline activating mutations of the ALK kinase receptor in neuroblastoma. *Nature* **455**: 967–970.

63. Mossé YP, Laudenslager M, Longo L, Cole KA, Wood A, Attiyeh EF, Laquaglia MJ, Sennett R, Lynch JE, Perri P, et al. (2008) Identification of ALK as a major familial neuroblastoma predisposition gene. *Nature* **455**: 930–935.
64. Chen Y, Takita J, Choi YL, Kato M, Ohira M, Sanada M, Wang L, Soda M, Kikuchi A, Igarashi T, et al. (2008) Oncogenic mutations of ALK kinase in neuroblastoma. *Nature* **455**: 971–974.
65. Schulte JH, Lindner S, Bohrer A, Maurer J, De Preter K, Lefever S, Heukamp L, Schulte S, Molenaar J, Versteeg R, et al. (2013) MYCN and ALKF1174L are sufficient to drive neuroblastoma development from neural crest progenitor cells. *Oncogene* **32**: 1059–1065.
66. Heukamp LC, Thor T, Schramm A, De Preter K, Kumps C, De Wilde B, Odersky A, Peifer M, Lindner S, Spruessel A, et al. (2012) Targeted expression of mutated ALK induces neuroblastoma in transgenic mice. *Sci Transl Med* **4**: 141ra91.
67. Berry T, Luther W, Bhatnagar N, Jamin Y, Poon E, Sanda T, Pei D, Sharma B, Vetharoy WR, Hallsworth A, et al. (2012) The ALK(F1174L) mutation potentiates the oncogenic activity of MYCN in neuroblastoma. *Cancer Cell* **22**: 117–130.
68. Schönherr C, Ruuth K, Kamaraj S, Wang C-L, Yang H-L, Combaret V, Djos A, Martinsson T, Christensen JG, Palmer RH, et al. (2012) Anaplastic Lymphoma Kinase (ALK) regulates initiation of transcription of MYCN in neuroblastoma cells. *Oncogene* **31**: 5193–5200.
69. De Brouwer S, De Preter K, Kumps C, Zabrocki P, Porcu M, Westerhout EM, Lakeman A, Vandesompele J, Hoebeeck J, Van Maerken T, et al. (2010) Meta-analysis of neuroblastomas reveals a skewed ALK mutation spectrum in tumors with MYCN amplification. *Clin Cancer Res* **16**: 4353–4362.
70. Bresler SC, Weiser DA, Huwe PJ, Park JH, Krytska K, Ryles H, Laudenslager M, Rappaport EF, Wood AC, McGrady PW, et al. (2014) ALK mutations confer differential oncogenic activation and sensitivity to ALK inhibition therapy in neuroblastoma. *Cancer Cell* **26**: 682–694.
71. Carpenter EL, Mossé YP (2012) Targeting ALK in neuroblastoma—preclinical and clinical advancements. *Nat Rev Clin Oncol* **9**: 391–399.
72. Palmer RH, Vernersson E, Grabbe C, Hallberg B (2009) Anaplastic lymphoma kinase: signalling in development and disease. *Biochem J* **420**: 345–361.
73. Li X-Q, Hisaoka M, Shi D-R, Zhu X-Z, Hashimoto H (2004) Expression of anaplastic lymphoma kinase in soft tissue tumors: an immunohistochemical and molecular study of 249 cases. *Hum Pathol* **35**: 711–721.
74. Dirks WG, Fähnrich S, Lis Y, Becker E, MacLeod RAF, Drexler HG (2002) Expression and functional analysis of the anaplastic lymphoma kinase (*ALK*) gene in tumor cell lines. *Int J Cancer* **100**: 49–56.
75. Valentijn LJ, Koster J, Zwijnenburg DA, Hasselt NE, van Sluis P, Volckmann R, van Noesel MM, George RE, Tytgat GAM, Molenaar JJ, et al. (2015) TERT rearrangements are frequent in neuroblastoma and identify aggressive tumors. *Nat Genet* **47**: 1411–1414.
76. Pugh TJ, Morozova O, Attiyeh EF, Asgharzadeh S, Wei JS, Auclair D, Carter SL, Cibulskis K, Hanna M, Kiezun A, et al. (2013) The genetic landscape of high-risk neuroblastoma. *Nat Genet* **45**: 279–284.
77. Molenaar JJ, Koster J, Zwijnenburg DA, van Sluis P, Valentijn LJ, van der Ploeg I, Hamdi M, van Nes J, Westerman BA, van Arkel J, et al. (2012) Sequencing of neuroblastoma identifies chromothripsis and defects in neuritogenesis genes. *Nature* **483**: 589–593.
78. Sausen M, Leary RJ, Jones S, Wu J, Reynolds CP, Liu X, Blackford A, Parmigiani G, Diaz LA, Papadopoulos N, et al. (2013) Integrated genomic analyses identify ARID1A and ARID1B alterations in the childhood cancer neuroblastoma. *Nat Genet* **45**: 12–17.
79. Scaruffi P, Cusano R, Dagnino M, Tonini GP (1999) Detection of DNA polymorphisms and point mutations of high-affinity nerve growth factor receptor (TrkA) in human neuroblastoma. *Int J Oncol* **14**: 935–938.
80. Ireland CM (1989) Activated N-ras oncogenes in human neuroblastoma. *Cancer Res* **49**: 5530–5533.
81. De La Fuente R, Baumann C, Viveiros MM (2011) Role of ATRX in chromatin structure and function: implications for chromosome instability and human disease. *Reproduction* **142**: 221–234.
82. Cheung N-K V, Zhang J, Lu C, Parker M, Bahrami A, Tickoo SK, Heguy A, Pappo AS, Federico S, Dalton J, et al. (2012) Association of age at diagnosis and genetic mutations in

patients with neuroblastoma. *JAMA* **307**: 1062–1071.
83. Peifer M, Hertwig F, Roels F, Dreidax D, Gartlgruber M, Menon R, Krämer A, Roncaioli JL, Sand F, Heuckmann JM, et al. (2015) Telomerase activation by genomic rearrangements in high-risk neuroblastoma. *Nature* **526**: 700–704.
84. Kogner P, Barbany G, Dominici C, Castello MA, Raschella G, Persson H (1993) *Coexpression of Messenger RNA for TRK Protooncogene and Low Affinity Nerve Growth Factor Receptor in Neuroblastoma with Favorable Prognosis1*.
85. Light JE, Koyama H, Minturn JE, Ho R, Simpson AM, Iyer R, Mangino JL, Kolla V, London WB, Brodeur GM (2012) Clinical significance of NTRK family gene expression in neuroblastomas. *Pediatr Blood Cancer* **59**: 226–232.
86. Brodeur GM, Minturn JE, Ho R, Simpson AM, Iyer R, Varela CR, Light JE, Kolla V, Evans AE (2009) Trk receptor expression and inhibition in neuroblastomas. *Clin Cancer Res* **15**: 3244–3250.
87. Lucarelli E, Kaplan D, Thiele CJ (1997) Activation of trk-A but not trk-B signal transduction pathway inhibits growth of neuroblastoma cells. *Eur J Cancer* **33**: 2068–2070.
88. Lau DT, Hesson LB, Norris MD, Marshall GM, Haber M, Ashton LJ (2012) Prognostic Significance of Promoter DNA Methylation in Patients with Childhood Neuroblastoma. *Clin Cancer Res* **18**: 5690–5700.
89. Nakagawara A, Arima M, Azar CG, Scavarda NJ, Brodeur GM (1992) Inverse relationship between trk expression and N-myc amplification in human neuroblastomas. *Cancer Res* **52**: 1364–1368.
90. Ho R, Eggert A, Hishiki T, Minturn JE, Ikegaki N, Foster P, Camoratto AM, Evans AE, Brodeur GM (2002) Resistance to Chemotherapy Mediated by TrkB in Neuroblastomas. *Cancer Res* **62**:.
91. Vo KT, Matthay KK, Neuhaus J, London WB, Hero B, Ambros PF, Nakagawara A, Miniati D, Wheeler K, Pearson ADJ, et al. (2014) Clinical, biologic, and prognostic differences on the basis of primary tumor site in neuroblastoma: a report from the international neuroblastoma risk group project. *J Clin Oncol* **32**: 3169–3176.
92. Morgenstern DA, London WB, Stephens D, Volchenboum SL, Simon T, Nakagawara A, Shimada H, Schleiermacher G, Matthay KK, Cohn SL, et al. (2016) Prognostic significance of pattern and burden of metastatic disease in patients with stage 4 neuroblastoma: A study from the International Neuroblastoma Risk Group database. *Eur J Cancer* **65**: 1–10.
93. Taggart DR, London WB, Schmidt M Lou, DuBois SG, Monclair TF, Nakagawara A, De Bernardi B, Ambros PF, Pearson ADJ, Cohn SL, et al. (2011) Prognostic value of the stage 4S metastatic pattern and tumor biology in patients with metastatic neuroblastoma diagnosed between birth and 18 months of age. *J Clin Oncol* **29**: 4358–4364.
94. DuBois SG, Kalika Y, Lukens JN, Brodeur GM, Seeger RC, Atkinson JB, Haase GM, Black CT, Perez C, Shimada H, et al. (1999) Metastatic sites in stage IV and IVS neuroblastoma correlate with age, tumor biology, and survival. *J Pediatr Hematol Oncol* **21**: 181–189.
95. Han W, Wang H-M (2015) Refractory diarrhea: A paraneoplastic syndrome of neuroblastoma. *World J Gastroenterol* **21**: 7929.
96. Hero B, Schleiermacher G (2013) Update on pediatric opsoclonus myoclonus syndrome. *Neuropediatrics* **44**: 324–329.
97. London WB, Castleberry RP, Matthay KK, Look AT, Seeger RC, Shimada H, Thorner P, Brodeur G, Maris JM, Reynolds CP, et al. (2005) Evidence for an Age Cutoff Greater Than 365 Days for Neuroblastoma Risk Group Stratification in the Children's Oncology Group. *J Clin Oncol* **23**: 6459–6465.
98. Strenger V, Kerbl R, Dornbusch HJ, Ladenstein R, Ambros PF, Ambros IM, Urban C (2007) Diagnostic and prognostic impact of urinary catecholamines in neuroblastoma patients. *Pediatr Blood Cancer* **48**: 504–509.
99. Isgrò MA, Bottoni P, Scatena R (2015) Neuron-Specific Enolase as a Biomarker: Biochemical and Clinical Aspects. In, *Advances in experimental medicine and biology* pp 125–143.
100. Di Cataldo A, Dau D, Conte M, Parodi S, De Bernardi B, Giuliano M, Pession A, Viscardi E, Luksch R, Castellano A, et al. (2009) Diagnostic and prognostic markers in infants with disseminated neuroblastoma: a retrospective analysis from the Italian Cooperative Group for Neuroblastoma. *Med Sci Monit* **15**: MT11-8.

101. Hann HW, Evans AE, Siegel SE, Wong KY, Sather H, Dalton A, Hammond D, Seeger RC (1985) Prognostic importance of serum ferritin in patients with Stages III and IV neuroblastoma: the Childrens Cancer Study Group experience. *Cancer Res* **45**: 2843–2848.
102. Simon T, Hero B, Benz-Bohm G, von Schweinitz D, Berthold F (2008) Review of image defined risk factors in localized neuroblastoma patients: Results of the GPOH NB97 trial. *Pediatr Blood Cancer* **50**: 965–969.
103. Decarolis B, Schneider C, Hero B, Simon T, Volland R, Roels F, Dietlein M, Berthold F, Schmidt M (2013) Iodine-123 Metaiodobenzylguanidine Scintigraphy Scoring Allows Prediction of Outcome in Patients With Stage 4 Neuroblastoma: Results of the Cologne Interscore Comparison Study. *J Clin Oncol* **31**: 944–951.
104. Sharp SE, Parisi MT, Gelfand MJ, Yanik GA, Shulkin BL (2013) Functional-metabolic imaging of neuroblastoma. *Q J Nucl Med Mol Imaging* **57**: 6–20.
105. Matthay KK, Shulkin B, Ladenstein R, Michon J, Giammarile F, Lewington V, Pearson ADJ, Cohn SL (2010) Criteria for evaluation of disease extent by 123I-metaiodobenzylguanidine scans in neuroblastoma: a report for the International Neuroblastoma Risk Group (INRG) Task Force. *Br J Cancer* **102**: 1319–1326.
106. Sharp SE, Shulkin BL, Gelfand MJ, Salisbury S, Furman WL (2009) 123I-MIBG scintigraphy and 18F-FDG PET in neuroblastoma. *J Nucl Med* **50**: 1237–1243.
107. Shimada H, Umehara S, Monobe Y, Hachitanda Y, Nakagawa A, Goto S, Gerbing RB, Stram DO, Lukens JN, Matthay KK (2001) International neuroblastoma pathology classification for prognostic evaluation of patients with peripheral neuroblastic tumors: a report from the Children's Cancer Group. *Cancer* **92**: 2451–2461.
108. Brodeur GM, Pritchard J, Berthold F, Carlsen NL, Castel V, Castelberry RP, De Bernardi B, Evans AE, Favrot M, Hedborg F (1993) Revisions of the international criteria for neuroblastoma diagnosis, staging, and response to treatment. *J Clin Oncol* **11**: 1466–1477.
109. Tolbert VP, Matthay KK (2018) Neuroblastoma: clinical and biological approach to risk stratification and treatment. *Cell Tissue Res* **372**: 195–209.
110. Monclair T, Brodeur GM, Ambros PF, Brisse HJ, Cecchetto G, Holmes K, Kaneko M, London WB, Matthay KK, Nuchtern JG, et al. (2009) The International Neuroblastoma Risk Group (INRG) staging system: an INRG Task Force report. *J Clin Oncol* **27**: 298–303.
111. Cohn SL, Pearson ADJ, London WB, Monclair T, Ambros PF, Brodeur GM, Faldum A, Hero B, Iehara T, Machin D, et al. (2009) The International Neuroblastoma Risk Group (INRG) classification system: an INRG Task Force report. *J Clin Oncol* **27**: 289–297.
112. Strother DR, London WB, Schmidt M Lou, Brodeur GM, Shimada H, Thorner P, Collins MH, Tagge E, Adkins S, Reynolds CP, et al. (2012) Outcome After Surgery Alone or With Restricted Use of Chemotherapy for Patients With Low-Risk Neuroblastoma: Results of Children's Oncology Group Study P9641. *J Clin Oncol* **30**: 1842–1848.
113. Rubie H, De Bernardi B, Gerrard M, Canete A, Ladenstein R, Couturier J, Ambros P, Munzer C, Pearson ADJ, Garaventa A, et al. (2011) Excellent Outcome With Reduced Treatment in Infants With Nonmetastatic and Unresectable Neuroblastoma Without *MYCN* Amplification: Results of the Prospective INES 99.1. *J Clin Oncol* **29**: 449–455.
114. Baker DL, Schmidt ML, Cohn SL, Maris JM, London WB, Buxton A, Stram D, Castleberry RP, Shimada H, Sandler A, et al. (2010) Outcome after Reduced Chemotherapy for Intermediate-Risk Neuroblastoma. *N Engl J Med* **363**: 1313–1323.
115. Hero B, Simon T, Spitz R, Ernestus K, Gnekow AK, Scheel-Walter H-G, Schwabe D, Schilling FH, Benz-Bohm G, Berthold F (2008) Localized infant neuroblastomas often show spontaneous regression: results of the prospective trials NB95-S and NB97. *J Clin Oncol* **26**: 1504–1510.
116. De Bernardi B, Mosseri V, Rubie H, Castel V, Foot A, Ladenstein R, Laureys G, Beck-Popovic M, de Lacerda AF, Pearson ADJ, et al. (2008) Treatment of localised resectable neuroblastoma. Results of the LNESG1 study by the SIOP Europe Neuroblastoma Group. *Br J Cancer* **99**: 1027–1033.
117. De Bernardi B, Gerrard M, Boni L, Rubie H, Cañete A, Di Cataldo A, Castel V, Forjaz de Lacerda A, Ladenstein R, Ruud E, et al. (2009) Excellent Outcome With Reduced Treatment for Infants With Disseminated Neuroblastoma Without *MYCN* Gene Amplification. *J Clin Oncol* **27**: 1034–1040.

118. Perez CA, Matthay KK, Atkinson JB, Seeger RC, Shimada H, Haase GM, Stram DO, Gerbing RB, Lukens JN (2000) Biologic variables in the outcome of stages I and II neuroblastoma treated with surgery as primary therapy: a children's cancer group study. *J Clin Oncol* **18**: 18–26.
119. Nuchtern JG, London WB, Barnewolt CE, Naranjo A, McGrady PW, Geiger JD, Diller L, Schmidt M Lou, Maris JM, Cohn SL, et al. (2012) A prospective study of expectant observation as primary therapy for neuroblastoma in young infants: a Children's Oncology Group study. *Ann Surg* **256**: 573–580.
120. Marachelian A, Shimada H, Sano H, Jackson H, Stein J, Sposto R, Matthay KK, Baker D, Villablanca JG (2012) The significance of serial histopathology in a residual mass for outcome of intermediate risk stage 3 neuroblastoma. *Pediatr Blood Cancer* **58**: 675–681.
121. Matthay KK, Perez C, Seeger RC, Brodeur GM, Shimada H, Atkinson JB, Black CT, Gerbing R, Haase GM, Stram DO, et al. (1998) Successful treatment of stage III neuroblastoma based on prospective biologic staging: a Children's Cancer Group study. *J Clin Oncol* **16**: 1256–1264.
122. Defferrari R, Mazzocco K, Ambros IM, Ambros PF, Bedwell C, Beiske K, Bénard J, Berbegall AP, Bown N, Combaret V, et al. (2015) Influence of segmental chromosome abnormalities on survival in children over the age of 12 months with unresectable localised peripheral neuroblastic tumours without MYCN amplification. *Br J Cancer* **112**: 290–295.
123. Kohler JA, Rubie H, Castel V, Beiske K, Holmes K, Gambini C, Casale F, Munzer C, Erminio G, Parodi S, et al. (2013) Treatment of children over the age of one year with unresectable localised neuroblastoma without MYCN amplification: results of the SIOPEN study. *Eur J Cancer* **49**: 3671–3679.
124. Pinto NR, Applebaum MA, Volchenboum SL, Matthay KK, London WB, Ambros PF, Nakagawara A, Berthold F, Schleiermacher G, Park JR, et al. (2015) Advances in Risk Classification and Treatment Strategies for Neuroblastoma. *J Clin Oncol* **33**: 3008–3017.
125. Kreissman SG, Seeger RC, Matthay KK, London WB, Sposto R, Grupp SA, Haas-Kogan DA, Laquaglia MP, Yu A, Diller L, et al. (2013) Purged versus non-purged peripheral blood stem-cell transplantation for high-risk neuroblastoma (COG A3973): a randomised phase 3 trial. *Lancet Oncol*.
126. Park JR, Scott JR, Stewart CF, London WB, Naranjo A, Santana VM, Shaw PJ, Cohn SL, Matthay KK (2011) Pilot induction regimen incorporating pharmacokinetically guided topotecan for treatment of newly diagnosed high-risk neuroblastoma: a Children's Oncology Group study. *J Clin Oncol* **29**: 4351–4357.
127. Ladenstein R, Valteau-Couanet D, Brock P, Yaniv I, Castel V, Laureys G, Malis J, Papadakis V, Lacerda A, Ruud E, et al. (2010) Randomized Trial of prophylactic granulocyte colony-stimulating factor during rapid COJEC induction in pediatric patients with high-risk neuroblastoma: the European HR-NBL1/SIOPEN study. *J Clin Oncol* **28**: 3516–3524.
128. Pearson AD, Pinkerton CR, Lewis IJ, Imeson J, Ellershaw C, Machin D (2008) High-dose rapid and standard induction chemotherapy for patients aged over 1 year with stage 4 neuroblastoma: a randomised trial. *Lancet Oncol* **9**: 247–256.
129. Castel V, Tovar JA, Costa E, Cuadros J, Ruiz A, Rollan V, Ruiz-Jimenez JI, Perez-Hernández R, Cañete A (2002) The role of surgery in stage IV neuroblastoma. *J Pediatr Surg* **37**: 1574–1578.
130. Adkins ES, Sawin R, Gerbing RB, London WB, Matthay KK, Haase GM (2004) Efficacy of complete resection for high-risk neuroblastoma: a Children's Cancer Group study. *J Pediatr Surg* **39**: 931–936.
131. Yanik GA, Parisi MT, Naranjo A, Nadel H, Gelfand MJ, Park JR, Ladenstein RL, Poetschger U, Boubaker A, Valteau-Couanet D, et al. (2018) Validation of Postinduction Curie Scores in High-Risk Neuroblastoma: A Children's Oncology Group and SIOPEN Group Report on SIOPEN/HR-NBL1. *J Nucl Med* **59**: 502–508.
132. Yang X, Chen J, Wang N, Liu Z, Li F, Zhou J, Tao B (2018) Impact of extent of resection on survival in high-risk neuroblastoma: A systematic review and meta-analysis. *J Pediatr Surg*.
133. von Allmen D, Davidoff AM, London WB, Van Ryn C, Haas-Kogan DA, Kreissman SG, Khanna G, Rosen N, Park JR, La Quaglia MP (2017) Impact of Extent of Resection on Local Control and Survival in Patients From the COG A3973 Study With High-Risk Neuroblastoma. *J*

Clin Oncol **35**: 208–216.
134. Matthay KK, Villablanca JG, Seeger RC, Stram DO, Harris RE, Ramsay NK, Swift P, Shimada H, Black CT, Brodeur GM, et al. (1999) Treatment of High-Risk Neuroblastoma with Intensive Chemotherapy, Radiotherapy, Autologous Bone Marrow Transplantation, and 13- *cis* -Retinoic Acid. *N Engl J Med* **341**: 1165–1173.
135. Ladenstein R, Philip T, Lasset C, Hartmann O, Garaventa A, Pinkerton R, Michon J, Pritchard J, Klingebiel T, Kremens B, et al. (1998) Multivariate analysis of risk factors in stage 4 neuroblastoma patients over the age of one year treated with megatherapy and stem-cell transplantation: a report from the European Bone Marrow Transplantation Solid Tumor Registry. *J Clin Oncol* **16**: 953–965.
136. Seif AE, Naranjo A, Baker DL, Bunin NJ, Kletzel M, Kretschmar CS, Maris JM, McGrady PW, von Allmen D, Cohn SL, et al. (2013) A pilot study of tandem high-dose chemotherapy with stem cell rescue as consolidation for high-risk neuroblastoma: Children's Oncology Group study ANBL00P1. *Bone Marrow Transplant* **48**: 947–952.
137. Granger M, Grupp SA, Kletzel M, Kretschmar C, Naranjo A, London WB, Diller L (2012) Feasibility of a tandem autologous peripheral blood stem cell transplant regimen for high risk neuroblastoma in a cooperative group setting: a Pediatric Oncology Group study: a report from the Children's Oncology Group. *Pediatr Blood Cancer* **59**: 902–907.
138. Berthold F, Boos J, Burdach S, Erttmann R, Henze G, Hermann J, Klingebiel T, Kremens B, Schilling FH, Schrappe M, et al. (2005) Myeloablative megatherapy with autologous stem-cell rescue versus oral maintenance chemotherapy as consolidation treatment in patients with high-risk neuroblastoma: a randomised controlled trial. *Lancet Oncol* **6**: 649–658.
139. Ladenstein R, Pötschger U, Pearson ADJ, Brock P, Luksch R, Castel V, Yaniv I, Papadakis V, Laureys G, Malis J, et al. (2017) Busulfan and melphalan versus carboplatin, etoposide, and melphalan as high-dose chemotherapy for high-risk neuroblastoma (HR-NBL1/SIOPEN): an international, randomised, multi-arm, open-label, phase 3 trial. *Lancet Oncol* **18**: 500–514.
140. Yalçin B, Kremer LC, Caron HN, van Dalen EC (2013) High-dose chemotherapy and autologous haematopoietic stem cell rescue for children with high-risk neuroblastoma. *Cochrane database Syst Rev* **8**: CD006301.
141. Matthay KK, Reynolds CP, Seeger RC, Shimada H, Adkins ES, Haas-Kogan D, Gerbing RB, London WB, Villablanca JG (2009) Long-term results for children with high-risk neuroblastoma treated on a randomized trial of myeloablative therapy followed by 13-cis-retinoic acid: a children's oncology group study. *J Clin Oncol* **27**: 1007–1013.
142. Mueller I, Ehlert K, Endres S, Pill L, Siebert N, Kietz S, Brock P, Garaventa A, Valteau-Couanet D, Janzek E, et al. (2018) Tolerability, response and outcome of high-risk neuroblastoma patients treated with long-term infusion of anti-GD $_2$ antibody ch14.18/CHO. *MAbs* **10**: 55–61.
143. Dhillon S (2015) Dinutuximab: First Global Approval. *Drugs* **75**: 923–927.
144. Ladenstein R, Weixler S, Baykan B, Bleeke M, Kunert R, Katinger D, Pribill I, Glander P, Bauer S, Pistoia V, et al. (2013) Ch14.18 antibody produced in CHO cells in relapsed or refractory Stage 4 neuroblastoma patients. *MAbs* **5**: 801–809.
145. Ganeshan VR, Schor NF (2011) Pharmacologic Management of High-Risk Neuroblastoma in Children. *Pediatr Drugs* **13**: 245–255.
146. Yu AL, Gilman AL, Ozkaynak MF, London WB, Kreissman SG, Chen HX, Smith M, Anderson B, Villablanca JG, Matthay KK, et al. (2010) Anti-GD2 antibody with GM-CSF, interleukin-2, and isotretinoin for neuroblastoma. *N Engl J Med* **363**: 1324–1334.
147. Matthay KK, Reynolds CP, Seeger RC, Shimada H, Adkins ES, Haas-Kogan D, Gerbing RB, London WB, Villablanca JG (2009) Long-term results for children with high-risk neuroblastoma treated on a randomized trial of myeloablative therapy followed by 13-cis-retinoic acid: a children's oncology group study. *J Clin Oncol* **27**: 1007–1013.
148. Holohan C, Van Schaeybroeck S, Longley DB, Johnston PG (2013) Cancer drug resistance: an evolving paradigm. *Nat Rev Cancer* **13**: 714–726.
149. Longley D, Johnston P (2005) Molecular mechanisms of drug resistance. *J Pathol* **205**: 275–292.
150. Eleveld TF, Oldridge DA, Bernard V, Koster J, Colmet Daage L, Diskin SJ, Schild L, Bentahar NB, Bellini A, Chicard M, et al. (2015) Relapsed neuroblastomas show frequent RAS-MAPK

pathway mutations. *Nat Genet* **47**: 864–871.
151. Reynolds CP (2004) Detection and treatment of minimal residual disease in high-risk neuroblastoma. *Pediatr Transplant* **8 Suppl 5**: 56–66.
152. Taylor ST, Hickman JA, Dive C (2000) Epigenetic determinants of resistance to etoposide regulation of Bcl-X(L) and Bax by tumor microenvironmental factors. *J Natl Cancer Inst* **92**: 18–23.
153. Tweddle DA, Pearson ADJ, Haber M, Norris MD, Xue C, Flemming C, Lunec J (2003) The p53 pathway and its inactivation in neuroblastoma. *Cancer Lett* **197**: 93–98.
154. Dole M, Nuñez G, Merchant AK, Maybaum J, Rode CK, Bloch CA, Castle VP (1994) Bcl-2 inhibits chemotherapy-induced apoptosis in neuroblastoma. *Cancer Res* **54**: 3253–3259.
155. Fulda S, Meyer E, Debatin K-M (2002) Inhibition of TRAIL-induced apoptosis by Bcl-2 overexpression. *Oncogene* **21**: 2283–2294.
156. Abel F, Sjöberg R-M, Nilsson S, Kogner P, Martinsson T (2005) Imbalance of the mitochondrial pro- and anti-apoptotic mediators in neuroblastoma tumours with unfavourable biology. *Eur J Cancer* **41**: 635–646.
157. Goldsmith KC, Hogarty MD (2005) Targeting programmed cell death pathways with experimental therapeutics: opportunities in high-risk neuroblastoma. *Cancer Lett* **228**: 133–141.
158. Fulda S (2009) Tumor resistance to apoptosis. *Int J Cancer* **124**: 511–515.
159. Teitz T, Wei T, Valentine MB, Vanin EF, Grenet J, Valentine VA, Behm FG, Look AT, Lahti JM, Kidd VJ (2000) Caspase 8 is deleted or silenced preferentially in childhood neuroblastomaswith amplification of MYCN. *Nat Med* **6**: 529–535.
160. Tajiri T, Liu X, Thompson PM, Tanaka S, Suita S, Zhao H, Maris JM, Prendergast GC, Hogarty MD (2003) Expression of a MYCN-interacting isoform of the tumor suppressor BIN1 is reduced in neuroblastomas with unfavorable biological features. *Clin Cancer Res* **9**: 3345–3355.
161. Gogolin S, Dreidax D, Becker G, Ehemann V, Schwab M, Westermann F (2010) MYCN/MYC-mediated drug resistance mechanisms in neuroblastoma. *Int J Clin Pharmacol Ther* **48**: 489–491.
162. Bader P, Schilling F, Schlaud M, Girgert R, Handgretinger R, Klingebiel T, Treuner J, Liu C, Niethammer D, Beck JF Expression analysis of multidrug resistance associated genes in neuroblastomas. *Oncol Rep* **6**: 1143–1146.
163. Wagner LM, Danks MK (2009) New therapeutic targets for the treatment of high-risk neuroblastoma. *J Cell Biochem* **107**: 46–57.
164. Michaelis M, Klassert D, Barth S, Suhan T, Breitling R, Mayer B, Hinsch N, Doerr HW, Cinatl J, Cinatl J, et al. (2009) Chemoresistance acquisition induces a global shift of expression of aniogenesis-associated genes and increased pro-angogenic activity in neuroblastoma cells. *Mol Cancer* **8**: 80.
165. Keshelava N, Seeger RC, Groshen S, Reynolds CP (1998) Drug resistance patterns of human neuroblastoma cell lines derived from patients at different phases of therapy. *Cancer Res* **58**: 5396–5405.
166. Bomgaars LR, Bernstein M, Krailo M, Kadota R, Das S, Chen Z, Adamson PC, Blaney SM (2007) Phase II Trial of Irinotecan in Children With Refractory Solid Tumors: A Children's Oncology Group Study. *J Clin Oncol* **25**: 4622–4627.
167. Hawkins DS, Bradfield S, Whitlock JA, Krailo M, Franklin J, Blaney SM, Adamson PC, Reaman G (2006) Topotecan by 21-day continuous infusion in children with relapsed or refractory solid tumors: A Children's Oncology Group study. *Pediatr Blood Cancer* **47**: 790–794.
168. Amoroso L, Erminio G, Makin G, Pearson ADJ, Brock P, Valteau-Couanet D, Castel V, Pasquet M, Laureys G, Thomas C, et al. (2018) Topotecan-Vincristine-Doxorubicin in Stage 4 High-Risk Neuroblastoma Patients Failing to Achieve a Complete Metastatic Response to Rapid COJEC: A SIOPEN Study. *Cancer Res Treat* **50**: 148–155.
169. Garaventa A, Luksch R, Biasotti S, Severi G, Pizzitola MR, Viscardi E, Prete A, Mastrangelo S, Podda M, Haupt R, et al. (2003) A phase II study of topotecan with vincristine and doxorubicin in children with recurrent/refractory neuroblastoma. *Cancer* **98**: 2488–2494.
170. London WB, Frantz CN, Campbell LA, Seeger RC, Brumback BA, Cohn SL, Matthay KK,

Castleberry RP, Diller L (2010) Phase II randomized comparison of topotecan plus cyclophosphamide versus topotecan alone in children with recurrent or refractory neuroblastoma: a Children's Oncology Group study. *J Clin Oncol* **28**: 3808–3815.

171. Saylors RL, Stine KC, Sullivan J, Kepner JL, Wall DA, Bernstein ML, Harris MB, Hayashi R, Vietti for the Pediatric Oncology G TJ, Pediatric Oncology Group (2001) Cyclophosphamide Plus Topotecan in Children With Recurrent or Refractory Solid Tumors: A Pediatric Oncology Group Phase II Study. *J Clin Oncol* **19**: 3463–3469.
172. Simon T, Längler A, Harnischmacher U, Frühwald MC, Jorch N, Claviez A, Berthold F, Hero B (2007) Topotecan, cyclophosphamide, and etoposide (TCE) in the treatment of high-risk neuroblastoma. Results of a phase-II trial. *J Cancer Res Clin Oncol* **133**: 653–661.
173. Di Giannatale A, Dias-Gastellier N, Devos A, Mc Hugh K, Boubaker A, Courbon F, Verschuur A, Ducassoul S, Malekzadeh K, Casanova M, et al. (2014) Phase II study of temozolomide in combination with topotecan (TOTEM) in relapsed or refractory neuroblastoma: A European Innovative Therapies for Children with Cancer-SIOP-European Neuroblastoma study. *Eur J Cancer* **50**: 170–177.
174. Rubie H, Chisholm J, Defachelles AS, Morland B, Munzer C, Valteau-Couanet D, Mosseri V, Bergeron C, Weston C, Coze C, et al. (2006) Phase II study of temozolomide in relapsed or refractory high-risk neuroblastoma: a joint Société Française des Cancers de l'Enfant and United Kingdom Children Cancer Study Group-New Agents Group Study. *J Clin Oncol* **24**: 5259–5264.
175. Pourquier P, Waltman JL, Urasaki Y, Loktionova NA, Pegg AE, Nitiss JL, Pommier Y (2001) *Topoisomerase I-mediated Cytotoxicity of N-Methyl-N-nitro-N-nitrosoguanidine: Trapping of Topoisomerase I by the O 6-Methylguanine 1*.
176. Pourquier P, Pilon AA, Kohlhagen G, Mazumder A, Sharma A, Pommier Y (1997) Trapping of mammalian topoisomerase I and recombinations induced by damaged DNA containing nicks or gaps. Importance of DNA end phosphorylation and camptothecin effects. *J Biol Chem* **272**: 26441–26447.
177. Bagatell R, London WB, Wagner LM, Voss SD, Stewart CF, Maris JM, Kretschmar C, Cohn SL (2011) Phase II Study of Irinotecan and Temozolomide in Children With Relapsed or Refractory Neuroblastoma: A Children's Oncology Group Study. *J Clin Oncol* **29**: 208–213.
178. Kushner BH, Kramer K, Modak S, Cheung N-K V. (2006) Irinotecan Plus Temozolomide for Relapsed or Refractory Neuroblastoma. *J Clin Oncol* **24**: 5271–5276.
179. Zhou G, Bao ZQ, Dixon JE (1995) Components of a new human protein kinase signal transduction pathway. *J Biol Chem* **270**: 12665–12669.
180. Wilson JS, Gains JE, Moroz V, Wheatley K, Gaze MN (2014) A systematic review of 131I-meta iodobenzylguanidine molecular radiotherapy for neuroblastoma. *Eur J Cancer* **50**: 801–815.
181. Taggart D, Dubois S, Matthay KK (2008) Radiolabeled metaiodobenzylguanidine for imaging and therapy of neuroblastoma. *Q J Nucl Med Mol Imaging* **52**: 403–418.
182. Matthay KK, Yanik G, Messina J, Quach A, Huberty J, Cheng S-C, Veatch J, Goldsby R, Brophy P, Kersun LS, et al. (2007) Phase II study on the effect of disease sites, age, and prior therapy on response to iodine-131-metaiodobenzylguanidine therapy in refractory neuroblastoma. *J Clin Oncol* **25**: 1054–1060.
183. DuBois SG, Groshen S, Park JR, Haas-Kogan DA, Yang X, Geier E, Chen E, Giacomini K, Weiss B, Cohn SL, et al. (2015) Phase I Study of Vorinostat as a Radiation Sensitizer with 131I-Metaiodobenzylguanidine (131I-MIBG) for Patients with Relapsed or Refractory Neuroblastoma. *Clin Cancer Res* **21**: 2715–2721.
184. Lee JW, Lee S, Cho HW, Ma Y, Yoo KH, Sung KW, Koo HH, Cho EJ, Lee S-K, Lim DH (2017) Incorporation of high-dose 131I-metaiodobenzylguanidine treatment into tandem high-dose chemotherapy and autologous stem cell transplantation for high-risk neuroblastoma: results of the SMC NB-2009 study. *J Hematol Oncol* **10**: 108.
185. Mossé YP, Lim MS, Voss SD, Wilner K, Ruffner K, Laliberte J, Rolland D, Balis FM, Maris JM, Weigel BJ, et al. (2013) Safety and activity of crizotinib for paediatric patients with refractory solid tumours or anaplastic large-cell lymphoma: a Children's Oncology Group phase 1 consortium study. *Lancet Oncol* **14**: 472–480.
186. Minturn JE, Evans AE, Villablanca JG, Yanik GA, Park JR, Shusterman S, Groshen S,

Hellriegel ET, Bensen-Kennedy D, Matthay KK, et al. (2011) Phase I trial of lestaurtinib for children with refractory neuroblastoma: a new approaches to neuroblastoma therapy consortium study. *Cancer Chemother Pharmacol* **68**: 1057–1065.

187. George RE, Lahti JM, Adamson PC, Zhu K, Finkelstein D, Ingle AM, Reid JM, Krailo M, Neuberg D, Blaney SM, et al. (2010) Phase I study of decitabine with doxorubicin and cyclophosphamide in children with neuroblastoma and other solid tumors: a Children's Oncology Group study. *Pediatr Blood Cancer* **55**: 629–638.
188. Pinto N, DuBois SG, Marachelian A, Diede SJ, Taraseviciute A, Glade Bender JL, Tsao-Wei D, Groshen SG, Reid JM, Haas-Kogan DA, et al. (2018) Phase I study of vorinostat in combination with isotretinoin in patients with refractory/recurrent neuroblastoma: A new approaches to Neuroblastoma Therapy (NANT) trial. *Pediatr Blood Cancer* **65**: e27023.
189. Children's Oncology Group M, Fouladi M, Furman WL, Chin T, Freeman BB, Dudkin L, Stewart CF, Krailo MD, Speights R, Ingle AM, et al. (2006) Phase I study of depsipeptide in pediatric patients with refractory solid tumors: a Children's Oncology Group report. *J Clin Oncol* **24**: 3678–3685.
190. Maurer BJ, Kang MH, Villablanca JG, Janeba J, Groshen S, Matthay KK, Sondel PM, Maris JM, Jackson HA, Goodarzian F, et al. (2013) Phase I trial of fenretinide delivered orally in a novel organized lipid complex in patients with relapsed/refractory neuroblastoma: a report from the New Approaches to Neuroblastoma Therapy (NANT) consortium. *Pediatr Blood Cancer* **60**: 1801–1808.
191. Amoroso L, Haupt R, Garaventa A, Ponzoni M (2017) Investigational drugs in phase II clinical trials for the treatment of neuroblastoma. *Expert Opin Investig Drugs* **26**: 1281–1293.
192. Johnsen JI, Segerström L, Orrego A, Elfman L, Henriksson M, Kågedal B, Eksborg S, Sveinbjörnsson B, Kogner P (2008) Inhibitors of mammalian target of rapamycin downregulate MYCN protein expression and inhibit neuroblastoma growth in vitro and in vivo. *Oncogene* **27**: 2910–2922.
193. Kushner BH, Cheung N-K V, Modak S, Becher OJ, Basu EM, Roberts SS, Kramer K, Dunkel IJ (2017) A phase I/Ib trial targeting the Pi3k/Akt pathway using perifosine: Long-term progression-free survival of patients with resistant neuroblastoma. *Int J cancer* **140**: 480–484.
194. LoRusso PM (2016) Inhibition of the PI3K/AKT/mTOR Pathway in Solid Tumors. *J Clin Oncol* **34**: 3803–3815.
195. O'Reilly KE, Rojo F, She Q-B, Solit D, Mills GB, Smith D, Lane H, Hofmann F, Hicklin DJ, Ludwig DL, et al. (2006) mTOR Inhibition Induces Upstream Receptor Tyrosine Kinase Signaling and Activates Akt. *Cancer Res* **66**: 1500–1508.
196. Cloughesy TF, Yoshimoto K, Nghiemphu P, Brown K, Dang J, Zhu S, Hsueh T, Chen Y, Wang W, Youngkin D, et al. (2008) Antitumor activity of rapamycin in a Phase I trial for patients with recurrent PTEN-deficient glioblastoma. *PLoS Med* **5**: e8.
197. Bagatell R, Norris R, Ingle AM, Ahern C, Voss S, Fox E, Little AR, Weigel BJ, Adamson PC, Blaney S (2014) Phase 1 trial of temsirolimus in combination with irinotecan and temozolomide in children, adolescents and young adults with relapsed or refractory solid tumors: A children's oncology group study. *Pediatr Blood Cancer* **61**: 833–839.
198. Mody R, Naranjo A, Van Ryn C, Yu AL, London WB, Shulkin BL, Parisi MT, Servaes S-E-N, Diccianni MB, Sondel PM, et al. (2017) Irinotecan–temozolomide with temsirolimus or dinutuximab in children with refractory or relapsed neuroblastoma (COG ANBL1221): an open-label, randomised, phase 2 trial. *Lancet Oncol* **18**: 946–957.
199. Geoerger B, Kieran MW, Grupp S, Perek D, Clancy J, Krygowski M, Ananthakrishnan R, Boni JP, Berkenblit A, Spunt SL (2012) Phase II trial of temsirolimus in children with high-grade glioma, neuroblastoma and rhabdomyosarcoma. *Eur J Cancer* **48**: 253–262.
200. DuBois SG, Marachelian A, Fox E, Kudgus RA, Reid JM, Groshen S, Malvar J, Bagatell R, Wagner L, Maris JM, et al. (2016) Phase I Study of the Aurora A Kinase Inhibitor Alisertib in Combination With Irinotecan and Temozolomide for Patients With Relapsed or Refractory Neuroblastoma: A NANT (New Approaches to Neuroblastoma Therapy) Trial. *J Clin Oncol* **34**: 1368–1375.
201. Saulnier Sholler GL, Gerner EW, Bergendahl G, MacArthur RB, VanderWerff A, Ashikaga T, Bond JP, Ferguson W, Roberts W, Wada RK, et al. (2015) A Phase I Trial of DFMO Targeting Polyamine Addiction in Patients with Relapsed/Refractory Neuroblastoma. *PLoS One* **10**:

e0127246.
202. Russell H V., Groshen SG, Ara T, DeClerck YA, Hawkins R, Jackson HA, Daldrup-Link HE, Marachelian A, Skerjanec A, Park JR, et al. (2011) A phase I study of zoledronic acid and low-dose cyclophosphamide in recurrent/refractory neuroblastoma: A new approaches to neuroblastoma therapy (NANT) study. *Pediatr Blood Cancer* **57**: 275–282.
203. Kushner BH, Ostrovnaya I, Cheung IY, Kuk D, Kramer K, Modak S, Yataghene K, Cheung NK (2015) Prolonged progression-free survival after consolidating second or later remissions of neuroblastoma with Anti-GD2 immunotherapy and isotretinoin: a prospective Phase II study. *Oncoimmunology* **4**: e1016704.
204. Wagner LM, Adams VR (2017) Targeting the PD-1 pathway in pediatric solid tumors and brain tumors. *Onco Targets Ther* **10**: 2097–2106.
205. Louis CU, Savoldo B, Dotti G, Pule M, Yvon E, Myers GD, Rossig C, Russell H V, Diouf O, Liu E, et al. (2011) Antitumor activity and long-term fate of chimeric antigen receptor-positive T cells in patients with neuroblastoma. *Blood* **118**: 6050–6056.
206. Federico SM, McCarville MB, Shulkin BL, Sondel PM, Hank JA, Hutson P, Meagher M, Shafer A, Ng CY, Leung W, et al. (2017) A Pilot Trial of Humanized Anti-GD2 Monoclonal Antibody (hu14.18K322A) with Chemotherapy and Natural Killer Cells in Children with Recurrent/Refractory Neuroblastoma. *Clin Cancer Res* **23**: 6441–6449.
207. Moreno L, Caron H, Geoerger B, Eggert A, Schleiermacher G, Brock P, Valteau-Couanet D, Chesler L, Schulte JH, De Preter K, et al. (2017) Accelerating drug development for neuroblastoma - New Drug Development Strategy: an Innovative Therapies for Children with Cancer, European Network for Cancer Research in Children and Adolescents and International Society of Paediatric Oncology Europe Neuroblastoma project. *Expert Opin Drug Discov* **12**: 801–811.
208. Pfister S, Remke M, Benner A, Mendrzyk F, Toedt G, Felsberg J, Wittmann A, Devens F, Gerber NU, Joos S, et al. (2009) Outcome Prediction in Pediatric Medulloblastoma Based on DNA Copy-Number Aberrations of Chromosomes 6q and 17q and the *MYC* and *MYCN* Loci. *J Clin Oncol* **27**: 1627–1636.
209. Williamson D, Lu Y-J, Gordon T, Sciot R, Kelsey A, Fisher C, Poremba C, Anderson J, Pritchard-Jones K, Shipley J (2005) Relationship between MYCN copy number and expression in rhabdomyosarcomas and correlation with adverse prognosis in the alveolar subtype. *J Clin Oncol* **23**: 880–888.
210. Barone G, Anderson J, Pearson ADJ, Petrie K, Chesler L (2013) New strategies in neuroblastoma: Therapeutic targeting of MYCN and ALK. *Clin Cancer Res* **19**: 5814–5821.
211. Escribá P V., Busquets X, Inokuchi J, Balogh G, Török Z, Horváth I, Harwood JL, Vígh L (2015) Membrane lipid therapy: Modulation of the cell membrane composition and structure as a molecular base for drug discovery and new disease treatment. *Prog Lipid Res* **59**: 38–53.
212. Nagatsuka I, Yamada N, Shimizu S, Ohira M, Nishino H, Seki S, Hirakawa K (2002) Inhibitory effect of a selective cyclooxygenase-2 inhibitor on liver metastasis of colon cancer. *Int J Cancer* **100**: 515–519.
213. Oshima M, Dinchuk JE, Kargman SL, Oshima H, Hancock B, Kwong E, Trzaskos JM, Evans JF, Taketo MM (1996) Suppression of intestinal polyposis in Apc delta716 knockout mice by inhibition of cyclooxygenase 2 (COX-2). *Cell* **87**: 803–809.
214. McCormick DL, Moon RC (1983) Inhibition of mammary carcinogenesis by flurbiprofen, a non-steroidal antiinflammatory agent. *Br J Cancer* **48**: 859–861.
215. Papadimitrakopoulou VA, William WN, Dannenberg AJ, Lippman SM, Lee JJ, Ondrey FG, Peterson DE, Feng L, Atwell A, El-Naggar AK, et al. (2008) Pilot randomized phase II study of celecoxib in oral premalignant lesions. *Clin Cancer Res* **14**: 2095–2101.
216. Bertagnolli MM (2007) Chemoprevention of colorectal cancer with cyclooxygenase-2 inhibitors: two steps forward, one step back. *Lancet Oncol* **8**: 439–443.
217. Bresalier RS, Sandler RS, Quan H, Bolognese JA, Oxenius B, Horgan K, Lines C, Riddell R, Morton D, Lanas A, et al. (2005) Cardiovascular events associated with rofecoxib in a colorectal adenoma chemoprevention trial. *N Engl J Med* **352**: 1092–1102.
218. Ríos-Marco P, Marco C, Gálvez X, Jiménez-López JM, Carrasco MP (2017) Alkylphospholipids: An update on molecular mechanisms and clinical relevance. *Biochim Biophys Acta - Biomembr* **1859**: 1657–1667.

219. Kostadinova A, Topouzova-Hristova T, Momchilova A, Tzoneva R, Berger MR (2015) Antitumor Lipids—Structure, Functions, and Medical Applications. *Adv Protein Chem Struct Biol* **101**: 27–66.
220. van Blitterswijk WJ, Verheij M (2013) Anticancer mechanisms and clinical application of alkylphospholipids. *Biochim Biophys Acta - Mol Cell Biol Lipids* **1831**: 663–674.
221. Pachioni J de A, Magalhães JG, Lima EJC, Bueno L de M, Barbosa JF, de Sá MM, Rangel-Yagui CO (2013) Alkylphospholipids - a promising class of chemotherapeutic agents with a broad pharmacological spectrum. *J Pharm Pharm Sci* **16**: 742–759.
222. Sun W, Modak S (2012) Emerging treatment options for the treatment of neuroblastoma: potential role of perifosine. *Onco Targets Ther* **5**: 21–29.
223. Cerezo J, Zúñiga J, Bastida A, Requena A, Cerón-Carrasco JP (2011) Atomistic molecular dynamics simulations of the interactions of oleic and 2-hydroxyoleic acids with phosphatidylcholine bilayers. *J Phys Chem B* **115**: 11727–11738.
224. Erazo T, Lorente M, Lopez-Plana A, Munoz-Guardiola P, Fernandez-Nogueira P, Garcia-Martinez JA, Bragado P, Fuster G, Salazar M, Espadaler J, et al. (2016) The New Antitumor Drug ABTL0812 Inhibits the Akt/mTORC1 Axis by Upregulating Tribbles-3 Pseudokinase. *Clin Cancer Res* **22**: 2508–2519.
225. Felip I, Moiola CP, Megino-Luque C, Lopez-Gil C, Cabrera S, Solé-Sánchez S, Muñoz-Guardiola P, Megias-Roda E, Pérez-Montoyo H, Alfon J, et al. (2019) Therapeutic potential of the new TRIB3-mediated cell autophagy anticancer drug ABTL0812 in endometrial cancer. *Gynecol Oncol*.
226. Alfon J, Vidal L, Gaba L, Victoria I, Gil M, Laquente B, Brunet M, Colom H, Ramis J, Perez-Montoyo H, et al. (2016) Determination of recommended phase II dose of ABTL0812, a novel regulator of Akt/mTOR axis, by pharmacokinetic-pharmacodynamic modelling. *Ann Oncol* **27**:.
227. Vidal L, Gaba L, Victoria I, Gil-Martin M, Laquente B, Cortal M, Brunet M, Paredes P, Gomez-Ferreria M, Alfon J, et al. (2015) Abstract LB-C18: First-in-Human Clinical Trial of ABTL0812, a Compound that Inhibits PI3K/Akt/mTOR Pathway by Upregulating TRIB3, in Patients with Advanced Solid Tumors. In, *Clinical Trials* p LB-C18-LB-C18. American Association for Cancer Research.
228. Farinas-Madrid L, Estévez-García P, Perez-Fidalgo JA, Bosch-Barrera J, Moran T, Nadal E, Rodriguez Freixinos V, Calvo E, Falcon A, Martín-Martorell P, et al. (2019) Phase 1 of ABTL0812, a proautophagic drug, in combination with paclitaxel and carboplatin at first-line in advanced endometrial cancer and squamous cell lung carcinoma. *J Clin Oncol* **37**: 3089–3089.
229. Fulda S (2009) The PI3K/Akt/mTOR pathway as therapeutic target in neuroblastoma. *Curr Cancer Drug Targets* **9**: 729–737.
230. Boller D, Schramm A, Doepfner KT, Shalaby T, von Bueren AO, Eggert A, Grotzer MA, Arcaro A (2008) Targeting the phosphoinositide 3-kinase isoform p110delta impairs growth and survival in neuroblastoma cells. *Clin Cancer Res* **14**: 1172–1181.
231. Li Z, Thiele CJ (2007) Targeting Akt to increase the sensitivity of neuroblastoma to chemotherapy: lessons learned from the brain-derived neurotrophic factor/TrkB signal transduction pathway. *Expert Opin Ther Targets* **11**: 1611–1621.
232. Manning BD, Cantley LC (2007) AKT/PKB Signaling: Navigating Downstream. *Cell* **129**: 1261–1274.
233. Opel D, Poremba C, Simon T, Debatin K-M, Fulda S (2007) Activation of Akt predicts poor outcome in neuroblastoma. *Cancer Res* **67**: 735–745.
234. Sjostrom SK, Finn G, Hahn WC, Rowitch DH, Kenney AM (2005) The Cdk1 complex plays a prime role in regulating N-myc phosphorylation and turnover in neural precursors. *Dev Cell* **9**: 327–338.
235. Kenney AM, Widlund HR, Rowitch DH (2004) Hedgehog and PI-3 kinase signaling converge on Nmyc1 to promote cell cycle progression in cerebellar neuronal precursors. *Development* **131**: 217–228.
236. Mehrpour M, Botti J, Codogno P (2012) Mechanisms and regulation of autophagy in mammalian cells. *Atlas Genet Cytogenet Oncol Haematol*.
237. Zhang X, Chen S, Huang K, Le W (2013) Why should autophagic flux be assessed? *Acta Pharmacol Sin* **34**: 595–599.

238. Meijer AJ, Codogno P (2009) Autophagy: Regulation and role in disease. *Crit Rev Clin Lab Sci* **46**: 210–240.
239. Sarkar S (2013) Regulation of autophagy by mTOR-dependent and mTOR-independent pathways: autophagy dysfunction in neurodegenerative diseases and therapeutic application of autophagy enhancers. *Biochem Soc Trans* **41**: 1103–1130.
240. Dennis MD, Baum JI, Kimball SR, Jefferson LS (2011) Mechanisms Involved in the Coordinate Regulation of mTORC1 by Insulin and Amino Acids. *J Biol Chem* **286**: 8287–8296.
241. Sancak Y, Peterson TR, Shaul YD, Lindquist RA, Thoreen CC, Bar-Peled L, Sabatini DM (2008) The Rag GTPases bind raptor and mediate amino acid signaling to mTORC1. *Science* **320**: 1496–1501.
242. Haar E Vander, Lee S, Bandhakavi S, Griffin TJ, Kim D-H (2007) Insulin signalling to mTOR mediated by the Akt/PKB substrate PRAS40. *Nat Cell Biol* **9**: 316–323.
243. Inoki K, Li Y, Zhu T, Wu J, Guan K-L (2002) TSC2 is phosphorylated and inhibited by Akt and suppresses mTOR signalling. *Nat Cell Biol* **4**: 648–657.
244. Inoki K, Zhu T, Guan K-L (2003) TSC2 mediates cellular energy response to control cell growth and survival. *Cell* **115**: 577–590.
245. Egan DF, Shackelford DB, Mihaylova MM, Gelino S, Kohnz RA, Mair W, Vasquez DS, Joshi A, Gwinn DM, Taylor R, et al. (2011) Phosphorylation of ULK1 (hATG1) by AMP-activated protein kinase connects energy sensing to mitophagy. *Science* **331**: 456–461.
246. Kim J, Kundu M, Viollet B, Guan K-L (2011) AMPK and mTOR regulate autophagy through direct phosphorylation of Ulk1. *Nat Cell Biol* **13**: 132–141.
247. Gwinn DM, Shackelford DB, Egan DF, Mihaylova MM, Mery A, Vasquez DS, Turk BE, Shaw RJ (2008) AMPK phosphorylation of raptor mediates a metabolic checkpoint. *Mol Cell* **30**: 214–226.
248. Eberhart K, Oral O, Gozuacik D (2014) Induction of Autophagic Cell Death by Anticancer Agents. *Autophagy Cancer, Other Pathol Inflammation, Immunity, Infect Aging* 179–202.
249. Mizushima N (2007) Autophagy: process and function. *Genes Dev* **21**: 2861–2873.
250. Yang ZJ, Chee CE, Huang S, Sinicrope FA (2011) The role of autophagy in cancer: therapeutic implications. *Mol Cancer Ther* **10**: 1533–1541.
251. Glancy B, Balaban RS (2012) Role of Mitochondrial Ca $^{2+}$ in the Regulation of Cellular Energetics. *Biochemistry* **51**: 2959–2973.
252. Denton RM (2009) Regulation of mitochondrial dehydrogenases by calcium ions. *Biochim Biophys Acta - Bioenerg* **1787**: 1309–1316.
253. Kaur J, Debnath J (2015) Autophagy at the crossroads of catabolism and anabolism. *Nat Rev Mol Cell Biol* **16**: 461–472.
254. Cárdenas C, Miller RA, Smith I, Bui T, Molgó J, Müller M, Vais H, Cheung K-H, Yang J, Parker I, et al. (2010) Essential regulation of cell bioenergetics by constitutive InsP3 receptor Ca2+ transfer to mitochondria. *Cell* **142**: 270–283.
255. Hardie DG, Ross FA, Hawley SA (2012) AMPK: a nutrient and energy sensor that maintains energy homeostasis. *Nat Rev Mol Cell Biol* **13**: 251–262.
256. Shaw RJ (2009) LKB1 and AMP-activated protein kinase control of mTOR signalling and growth. *Acta Physiol* **196**: 65–80.
257. Meley D, Bauvy C, Houben-Weerts JHPM, Dubbelhuis PF, Helmond MTJ, Codogno P, Meijer AJ (2006) AMP-activated Protein Kinase and the Regulation of Autophagic Proteolysis. *J Biol Chem* **281**: 34870–34879.
258. Zhang D, Wang W, Sun X, Xu D, Wang C, Zhang Q, Wang H, Luo W, Chen Y, Chen H, et al. (2016) AMPK regulates autophagy by phosphorylating BECN1 at threonine 388. *Autophagy* **12**: 1447–1459.
259. Rashid H-O, Yadav RK, Kim H-R, Chae H-J (2015) ER stress: Autophagy induction, inhibition and selection. *Autophagy* **11**: 1956–1977.
260. Kania E, Pająk B, Orzechowski A (2015) Calcium Homeostasis and ER Stress in Control of Autophagy in Cancer Cells. *Biomed Res Int* **2015**: 1–12.
261. Krebs J, Agellon LB, Michalak M (2015) Ca(2+) homeostasis and endoplasmic reticulum (ER) stress: An integrated view of calcium signaling. *Biochem Biophys Res Commun* **460**: 114–121.
262. Verfaillie T, Salazar M, Velasco G, Agostinis P (2010) Linking ER Stress to Autophagy: Potential Implications for Cancer Therapy. *Int J Cell Biol* **2010**: 1–19.

263. Klionsky DJ, Abdelmohsen K, Abe A, Abedin MJ, Abeliovich H, Acevedo Arozena A, Adachi H, Adams CM, Adams PD, Adeli K, et al. (2016) Guidelines for the use and interpretation of assays for monitoring autophagy (3rd edition). *Autophagy* **12**: 1–222.
264. Sano R, Reed JC (2013) ER stress-induced cell death mechanisms. *Biochim Biophys Acta - Mol Cell Res* **1833**: 3460–3470.
265. Hetz C (2012) The unfolded protein response: controlling cell fate decisions under ER stress and beyond. *Nat Rev Mol Cell Biol* **13**: 89–102.
266. Qin L, Wang Z, Tao L, Wang Y (2010) ER stress negatively regulates AKT/TSC/mTOR pathway to enhance autophagy. *Autophagy* **6**: 239–247.
267. Cheng X, Liu H, Jiang C-C, Fang L, Chen C, Zhang X-D, Jiang Z-W (2014) Connecting endoplasmic reticulum stress to autophagy through IRE1/JNK/beclin-1 in breast cancer cells. *Int J Mol Med* **34**: 772–781.
268. Wei Y, Pattingre S, Sinha S, Bassik M, Levine B (2008) JNK1-mediated phosphorylation of Bcl-2 regulates starvation-induced autophagy. *Mol Cell* **30**: 678–688.
269. Margariti A, Li H, Chen T, Martin D, Vizcay-Barrena G, Alam S, Karamariti E, Xiao Q, Zampetaki A, Zhang Z, et al. (2013) *XBP1* mRNA Splicing Triggers an Autophagic Response in Endothelial Cells through *BECLIN-1* Transcriptional Activation. *J Biol Chem* **288**: 859–872.
270. Kim KW, Moretti L, Mitchell LR, Jung DK, Lu B (2010) Endoplasmic reticulum stress mediates radiation-induced autophagy by perk-eIF2alpha in caspase-3/7-deficient cells. *Oncogene* **29**: 3241–3251.
271. Rzymski T, Milani M, Singleton DC, Harris AL (2009) Role of ATF4 in regulation of autophagy and resistance to drugs and hypoxia. *Cell Cycle* **8**: 3838–3847.
272. Salazar M, Carracedo A, Salanueva IJ, Hernández-Tiedra S, Lorente M, Egia A, Vázquez P, Blázquez C, Torres S, García S, et al. (2009) Cannabinoid action induces autophagy-mediated cell death through stimulation of ER stress in human glioma cells. *J Clin Invest* **119**: 1359–1372.
273. Pike LRG, Singleton DC, Buffa F, Abramczyk O, Phadwal K, Li J-L, Simon AK, Murray JT, Harris AL (2013) Transcriptional up-regulation of ULK1 by ATF4 contributes to cancer cell survival. *Biochem J* **449**: 389–400.
274. Kouroku Y, Fujita E, Tanida I, Ueno T, Isoai A, Kumagai H, Ogawa S, Kaufman RJ, Kominami E, Momoi T (2007) ER stress (PERK/eIF2alpha phosphorylation) mediates the polyglutamine-induced LC3 conversion, an essential step for autophagy formation. *Cell Death Differ* **14**: 230–239.
275. Kalvakolanu D V., Gade P (2012) IFNG and autophagy. *Autophagy* **8**: 1673–1674.
276. Zalckvar E, Berissi H, Eisenstein M, Kimchi A (2009) Phosphorylation of Beclin 1 by DAP-kinase promotes autophagy by weakening its interactions with Bcl-2 and Bcl-XL. *Autophagy* **5**: 720–722.
277. Rybstein MD, Bravo-San Pedro JM, Kroemer G, Galluzzi L (2018) The autophagic network and cancer. *Nat Cell Biol* **20**: 243–251.
278. Galluzzi L, Pietrocola F, Bravo-San Pedro JM, Amaravadi RK, Baehrecke EH, Cecconi F, Codogno P, Debnath J, Gewirtz DA, Karantza V, et al. (2015) Autophagy in malignant transformation and cancer progression. *EMBO J* **34**: 856–880.
279. Qu X, Yu J, Bhagat G, Furuya N, Hibshoosh H, Troxel A, Rosen J, Eskelinen E-L, Mizushima N, Ohsumi Y, et al. (2003) Promotion of tumorigenesis by heterozygous disruption of the beclin 1 autophagy gene. *J Clin Invest* **112**: 1809–1820.
280. Rosenfeldt MT, O'Prey J, Morton JP, Nixon C, MacKay G, Mrowinska A, Au A, Rai TS, Zheng L, Ridgway R, et al. (2013) p53 status determines the role of autophagy in pancreatic tumour development. *Nature* **504**: 296–300.
281. Takamura A, Komatsu M, Hara T, Sakamoto A, Kishi C, Waguri S, Eishi Y, Hino O, Tanaka K, Mizushima N (2011) Autophagy-deficient mice develop multiple liver tumors. *Genes Dev* **25**: 795–800.
282. Mathew R, Karp CM, Beaudoin B, Vuong N, Chen G, Chen H-Y, Bray K, Reddy A, Bhanot G, Gelinas C, et al. (2009) Autophagy suppresses tumorigenesis through elimination of p62. *Cell* **137**: 1062–1075.
283. White E (2012) Deconvoluting the context-dependent role for autophagy in cancer. *Nat Rev Cancer* **12**: 401–410.

284. Amaravadi RK, Yu D, Lum JJ, Bui T, Christophorou MA, Evan GI, Thomas-Tikhonenko A, Thompson CB (2007) Autophagy inhibition enhances therapy-induced apoptosis in a Myc-induced model of lymphoma. *J Clin Invest* **117**: 326–336.
285. Degenhardt K, Mathew R, Beaudoin B, Bray K, Anderson D, Chen G, Mukherjee C, Shi Y, Gélinas C, Fan Y, et al. (2006) Autophagy promotes tumor cell survival and restricts necrosis, inflammation, and tumorigenesis. *Cancer Cell* **10**: 51–64.
286. Lane JD, Agostinis P (2017) Editorial: Self-Eating on Demand: Autophagy in Cancer and Cancer Therapy. *Front Oncol* **7**:.
287. Rabinowitz JD, White E (2010) Autophagy and Metabolism. *Science (80-)* **330**: 1344–1348.
288. Kang C, Elledge SJ (2016) How autophagy both activates and inhibits cellular senescence. *Autophagy* **12**: 898–899.
289. Morselli E, Galluzzi L, Kepp O, Vicencio J-M, Criollo A, Maiuri MC, Kroemer G (2009) Anti- and pro-tumor functions of autophagy. *Biochim Biophys Acta - Mol Cell Res* **1793**: 1524–1532.
290. Lock R, Roy S, Kenific CM, Su JS, Salas E, Ronen SM, Debnath J (2011) Autophagy facilitates glycolysis during Ras-mediated oncogenic transformation. *Mol Biol Cell* **22**: 165–178.
291. Ma X-H, Piao S, Wang D, Mcafee QW, Nathanson KL, Lum JJ, Li LZ, Amaravadi RK (2011) Measurements of Tumor Cell Autophagy Predict Invasiveness, Resistance to Chemotherapy, and Survival in Melanoma. *Clin Cancer Res* **17**: 3478–3489.
292. Wei H, Wei S, Gan B, Peng X, Zou W, Guan J-L (2011) Suppression of autophagy by FIP200 deletion inhibits mammary tumorigenesis. *Genes Dev* **25**: 1510–1527.
293. Guo JY, Chen H-Y, Mathew R, Fan J, Strohecker AM, Karsli-Uzunbas G, Kamphorst JJ, Chen G, Lemons JMS, Karantza V, et al. (2011) Activated Ras requires autophagy to maintain oxidative metabolism and tumorigenesis. *Genes Dev* **25**: 460–470.
294. Viry E, Noman MZ, Arakelian T, Lequeux A, Chouaib S, Berchem G, Moussay E, Paggetti J, Janji B (2016) Hijacker of the Antitumor Immune Response: Autophagy Is Showing Its Worst Facet. *Front Oncol* **6**: 246.
295. Keulers TG, Schaaf MBE, Rouschop KMA (2016) Autophagy-Dependent Secretion: Contribution to Tumor Progression. *Front Oncol* **6**: 251.
296. White E, Mehnert JM, Chan CS (2015) Autophagy, Metabolism, and Cancer. *Clin Cancer Res* **21**: 5037–5046.
297. Rebecca VW, Amaravadi RK (2016) Emerging strategies to effectively target autophagy in cancer. *Oncogene* **35**: 1–11.
298. Fulda S, Kögel D (2015) Cell death by autophagy: emerging molecular mechanisms and implications for cancer therapy. *Oncogene* **34**: 5105–5113.
299. Shao Y, Gao Z, Marks PA, Jiang X (2004) Apoptotic and autophagic cell death induced by histone deacetylase inhibitors. *Proc Natl Acad Sci U S A* **101**: 18030–18035.
300. Schweichel J-U, Merker H-J (1973) The morphology of various types of cell death in prenatal tissues. *Teratology* **7**: 253–266.
301. Napoletano F, Baron O, Vandenabeele P, Mollereau B, Fanto M (2019) Intersections between Regulated Cell Death and Autophagy. *Trends Cell Biol* **29**: 323–338.
302. Nikoletopoulou V, Markaki M, Palikaras K, Tavernarakis N (2013) Crosstalk between apoptosis, necrosis and autophagy. *Biochim Biophys Acta - Mol Cell Res* **1833**: 3448–3459.
303. Galluzzi L, Vitale I, Aaronson SA, Abrams JM, Adam D, Agostinis P, Alnemri ES, Altucci L, Amelio I, Andrews DW, et al. (2018) Molecular mechanisms of cell death: recommendations of the Nomenclature Committee on Cell Death 2018. *Cell Death Differ* **25**: 486–541.
304. Denton D, Kumar S (2019) Autophagy-dependent cell death. *Cell Death Differ* **26**: 605–616.
305. Law BYK, Chan WK, Xu SW, Wang JR, Bai LP, Liu L, Wong VKW (2015) Natural small-molecule enhancers of autophagy induce autophagic cell death in apoptosis-defective cells. *Sci Rep* **4**: 5510.
306. Yu L, Alva A, Su H, Dutt P, Freundt E, Welsh S, Baehrecke EH, Lenardo MJ (2004) Regulation of an ATG7-beclin 1 program of autophagic cell death by caspase-8. *Science* **304**: 1500–1502.
307. Qian W, Liu J, Jin J, Ni W, Xu W (2007) Arsenic trioxide induces not only apoptosis but also autophagic cell death in leukemia cell lines via up-regulation of Beclin-1. *Leuk Res* **31**: 329–339.

308. Kanzawa T, Zhang L, Xiao L, Germano IM, Kondo Y, Kondo S (2005) Arsenic trioxide induces autophagic cell death in malignant glioma cells by upregulation of mitochondrial cell death protein BNIP3. *Oncogene* **24**: 980–991.
309. Lian J, Wu X, He F, Karnak D, Tang W, Meng Y, Xiang D, Ji M, Lawrence TS, Xu L (2011) A natural BH3 mimetic induces autophagy in apoptosis-resistant prostate cancer via modulating Bcl-2–Beclin1 interaction at endoplasmic reticulum. *Cell Death Differ* **18**: 60–71.
310. Bonapace L, Bornhauser BC, Schmitz M, Cario G, Ziegler U, Niggli FK, Schäfer BW, Schrappe M, Stanulla M, Bourquin J-P (2010) Induction of autophagy-dependent necroptosis is required for childhood acute lymphoblastic leukemia cells to overcome glucocorticoid resistance. *J Clin Invest* **120**: 1310–1323.
311. Voss V, Senft C, Lang V, Ronellenfitsch MW, Steinbach JP, Seifert V, Kogel D (2010) The Pan-Bcl-2 Inhibitor (-)-Gossypol Triggers Autophagic Cell Death in Malignant Glioma. *Mol Cancer Res* **8**: 1002–1016.
312. Maiuri MC, Criollo A, Tasdemir E, Vicencio JM, Tajeddine N, Hickman JA, Geneste O, Kroemer G (2007) BH3-Only Proteins and BH3 Mimetics Induce Autophagy by Competitively Disrupting the Interaction between Beclin 1 and Bcl-2/Bcl-X_L. *Autophagy* **3**: 374–376.
313. Vara D, Salazar M, Olea-Herrero N, Guzmán M, Velasco G, Díaz-Laviada I (2011) Anti-tumoral action of cannabinoids on hepatocellular carcinoma: role of AMPK-dependent activation of autophagy. *Cell Death Differ* **18**: 1099–1111.
314. DeMasters G, Di X, Newsham I, Shiu R, Gewirtz DA (2006) Potentiation of radiation sensitivity in breast tumor cells by the vitamin D_3 analogue, EB 1089, through promotion of autophagy and interference with proliferative recovery. *Mol Cancer Ther* **5**: 2786–2797.
315. Høyer-Hansen M, Bastholm L, Mathiasen IS, Elling F, Jäättelä M (2005) Vitamin D analog EB1089 triggers dramatic lysosomal changes and Beclin 1-mediated autophagic cell death. *Cell Death Differ* **12**: 1297–1309.
316. Dalhoff K, Dancey J, Astrup L, Skovsgaard T, Hamberg KJ, Lofts FJ, Rosmorduc O, Erlinger S, Bach Hansen J, Steward WP, et al. (2003) A phase II study of the vitamin D analogue Seocalcitol in patients with inoperable hepatocellular carcinoma. *Br J Cancer* **89**: 252–257.
317. Evans TRJ, Colston KW, Lofts FJ, Cunningham D, Anthoney DA, Gogas H, de Bono JS, Hamberg KJ, Skov T, Mansi JL (2002) A phase II trial of the vitamin D analogue Seocalcitol (EB1089) in patients with inoperable pancreatic cancer. *Br J Cancer* **86**: 680–685.
318. Basciani S, Vona R, Matarrese P, Ascione B, Mariani S, Gnessi L, Malorni W, Straface E, Straface E, Lucia MB (2007) Imatinib interferes with survival of multi drug resistant Kaposi's sarcoma cells. *FEBS Lett* **581**: 5897–5903.
319. Janes MR, Limon JJ, So L, Chen J, Lim RJ, Chavez MA, Vu C, Lilly MB, Mallya S, Ong ST, et al. (2010) Effective and selective targeting of leukemia cells using a TORC1/2 kinase inhibitor. *Nat Med* **16**: 205–213.
320. Chresta CM, Davies BR, Hickson I, Harding T, Cosulich S, Critchlow SE, Vincent JP, Ellston R, Jones D, Sini P, et al. (2010) AZD8055 is a potent, selective, and orally bioavailable ATP-competitive mammalian target of rapamycin kinase inhibitor with in vitro and in vivo antitumor activity. *Cancer Res* **70**: 288–298.
321. Iwamaru A, Kondo Y, Iwado E, Aoki H, Fujiwara K, Yokoyama T, Mills GB, Kondo S (2007) Silencing mammalian target of rapamycin signaling by small interfering RNA enhances rapamycin-induced autophagy in malignant glioma cells. *Oncogene* **26**: 1840–1851.
322. Haritunians T, Mori A, O'Kelly J, Luong QT, Giles FJ, Koeffler HP (2007) Antiproliferative activity of RAD001 (everolimus) as a single agent and combined with other agents in mantle cell lymphoma. *Leukemia* **21**: 333–339.
323. Yee KWL, Zeng Z, Konopleva M, Verstovsek S, Ravandi F, Ferrajoli A, Thomas D, Wierda W, Apostolidou E, Albitar M, et al. (2006) Phase I/II Study of the Mammalian Target of Rapamycin Inhibitor Everolimus (RAD001) in Patients with Relapsed or Refractory Hematologic Malignancies. *Clin Cancer Res* **12**: 5165–5173.
324. Kim KW, Hwang M, Moretti L, Jaboin JJ, Cha YI, Lu B (2008) Autophagy upregulation by inhibitors of caspase-3 and mTOR enhances radiotherapy in a mouse model of lung cancer. *Autophagy* **4**: 659–668.
325. Cao C, Subhawong T, Albert JM, Kim KW, Geng L, Sekhar KR, Gi YJ, Lu B (2006) Inhibition of Mammalian Target of Rapamycin or Apoptotic Pathway Induces Autophagy and

Radiosensitizes PTEN Null Prostate Cancer Cells. *Cancer Res* **66**: 10040–10047.
326. Paglin S, Lee N-Y, Nakar C, Fitzgerald M, Plotkin J, Deuel B, Hackett N, McMahill M, Sphicas E, Lampen N, et al. (2005) Rapamycin-Sensitive Pathway Regulates Mitochondrial Membrane Potential, Autophagy, and Survival in Irradiated MCF-7 Cells. *Cancer Res* **65**: 11061–11070.
327. Liu Y-L, Yang P-M, Shun C-T, Wu M-S, Weng J-R, Chen C-C (2010) Autophagy potentiates the anti-cancer effects of the histone deacetylase inhibitors in hepatocellular carcinoma. *Autophagy* **6**: 1057–1065.
328. Fu J, Shao C-J, Chen F-R, Ng H-K, Chen Z-P (2010) Autophagy induced by valproic acid is associated with oxidative stress in glioma cell lines. *Neuro Oncol* **12**: 328–340.
329. Cao Q, Yu C, Xue R, Hsueh W, Pan P, Chen Z, Wang S, McNutt M, Gu J (2008) Autophagy induced by suberoylanilide hydroxamic acid in Hela S3 cells involves inhibition of protein kinase B and up-regulation of Beclin 1. *Int J Biochem Cell Biol* **40**: 272–283.
330. Marks PA (2007) Discovery and development of SAHA as an anticancer agent. *Oncogene* **26**: 1351–1356.
331. Yamamoto S, Tanaka K, Sakimura R, Okada T, Nakamura T, Li Y, Takasaki M, Nakabeppu Y, Iwamoto Y Suberoylanilide hydroxamic acid (SAHA) induces apoptosis or autophagy-associated cell death in chondrosarcoma cell lines. *Anticancer Res* **28**: 1585–1591.
332. Cloonan SM, Williams DC (2011) The antidepressants maprotiline and fluoxetine induce Type II autophagic cell death in drug-resistant Burkitt's lymphoma. *Int J cancer* **128**: 1712–1723.
333. Shchors K, Massaras A, Hanahan D (2015) Dual Targeting of the Autophagic Regulatory Circuitry in Gliomas with Repurposed Drugs Elicits Cell-Lethal Autophagy and Therapeutic Benefit. *Cancer Cell* **28**: 456–471.
334. Jubierre L, Soriano A, Planells-Ferrer L, París-Coderch L, Tenbaum SP, Romero OA, Moubarak RS, Almazán-Moga A, Molist C, Roma J, et al. (2016) BRG1/SMARCA4 is essential for neuroblastoma cell viability through modulation of cell death and survival pathways. *Oncogene* **35**: 5179–5190.
335. Soriano A, París-Coderch L, Jubierre L, Martínez A, Zhou X, Piskareva O, Bray I, Vidal I, Almazán-Moga A, Molist C, et al. (2016) MicroRNA-497 impairs the growth of chemoresistant neuroblastoma cells by targeting cell cycle, survival and vascular permeability genes. *Oncotarget* **7**:.
336. Planells-Ferrer L, Urresti J, Soriano A, Reix S, Murphy DM, Ferreres JC, Borràs F, Gallego S, Stallings RL, Moubarak RS, et al. (2014) MYCN repression of Lifeguard/FAIM2 enhances neuroblastoma aggressiveness. *Cell Death Dis* **5**: e1401–e1401.
337. Livak KJ, Schmittgen TD (2001) Analysis of relative gene expression data using real-time quantitative PCR and the 2(-Delta Delta C(T)) Method. *Methods* **25**: 402–408.
338. ThermoFisher scientific. Protein transfer technical handbook.
339. Cimmino F, Spano D, Capasso M, Zambrano N, Russo R, Zollo M, Iolascon A (2007) Comparative proteomic expression profile in all-trans retinoic acid differentiated neuroblastoma cell line. *J Proteome Res* **6**: 2550–2564.
340. Maris JM, Matthay KK (1999) Molecular Biology of Neuroblastoma. *J Clin Oncol* **17**: 2264–2264.
341. Planells-Ferrer L, Urresti J, Soriano A, Reix S, Murphy DM, Ferreres JC, Borràs F, Gallego S, Stallings RL, Moubarak RS, et al. (2014) MYCN repression of Lifeguard/FAIM2 enhances neuroblastoma aggressiveness. *Cell Death Dis* **5**: e1401.
342. Yu DMT, Huynh T, Truong AM, Haber M, Norris MD (2015) ABC transporters and neuroblastoma. *Adv Cancer Res* **125**: 139–170.
343. Khalil MA, Hrabeta J, Cipro S, Stiborova M, Vicha A, Eckschlager T (2012) Neuroblastoma stem cells-mechanisms of chemoresistance and histonedeacetylase inhibitors Minireview**. *Neoplasma* **59**:.
344. Keshelava N, Zuo JJ, Chen P, Waidyaratne SN, Luna MC, Gomer CJ, Triche TJ, Reynolds CP (2001) Loss of p53 function confers high-level multidrug resistance in neuroblastoma cell lines. *Cancer Res* **61**: 6185–6193.
345. Murakami-Tonami Y, Ikeda H, Yamagishi R, Inayoshi M, Inagaki S, Kishida S, Komata Y, Jan Koster, Takeuchi I, Kondo Y, et al. (2016) SGO1 is involved in the DNA damage response in MYCN-amplified neuroblastoma cells. *Sci Rep* **6**: 31615.
346. Gottesman MM, Fojo T, Bates SE (2002) Multidrug resistance in cancer: role of ATP–

dependent transporters. *Nat Rev Cancer* **2**: 48–58.
347. de Cremoux P, Jourdan-Da-Silva N, Couturier J, Tran-Perennou C, Schleiermacher G, Fehlbaum P, Doz F, Mosseri V, Delattre O, Klijanienko J, et al. (2007) Role of chemotherapy resistance genes in outcome of neuroblastoma. *Pediatr Blood Cancer* **48**: 311–317.
348. Goldschneider D, Horvilleur E, Plassa L-F, Guillaud-Bataille M, Million K, Wittmer-Dupret E, Danglot G, de Thé H, Bénard J, May E, et al. (2006) Expression of C-terminal deleted p53 isoforms in neuroblastoma. *Nucleic Acids Res* **34**: 5603–5612.
349. Bourdon J-C, Fernandes K, Murray-Zmijewski F, Liu G, Diot A, Xirodimas DP, Saville MK, Lane DP (2005) p53 isoforms can regulate p53 transcriptional activity. *Genes Dev* **19**: 2122–2137.
350. Tweddle DA, Pearson ADJ, Haber M, Norris MD, Xue C, Flemming C, Lunec J (2003) The p53 pathway and its inactivation in neuroblastoma. *Cancer Lett* **197**: 93–98.
351. Charlet J, Schnekenburger M, Brown KW, Diederich M (2012) DNA demethylation increases sensitivity of neuroblastoma cells to chemotherapeutic drugs. *Biochem Pharmacol* **83**: 858–865.
352. Lu J, Guan S, Zhao Y, Yu Y, Wang Y, Shi Y, Mao X, Yang KL, Sun W, Xu X, et al. (2016) Novel MDM2 inhibitor SAR405838 (MI-773) induces p53-mediated apoptosis in neuroblastoma. *Oncotarget* **7**: 82757–82769.
353. Hengstler JG, Oesch F (2001) Ames Test. In, *Encyclopedia of Genetics* pp 51–54. Elsevier.
354. Mei L, Hu Q, Peng J, Ruan J, Zou J, Huang Q, Liu S, Wang H (2015) Phospho-histone H2AX is a diagnostic and prognostic marker for epithelial ovarian cancer. *Int J Clin Exp Pathol* **8**: 5597–5602.
355. Sanders SL, Arida AR, Phan FP (2010) Requirement for the phospho-H2AX binding module of Crb2 in double-strand break targeting and checkpoint activation. *Mol Cell Biol* **30**: 4722–4731.
356. Wilson AJ, Holson E, Wagner F, Zhang Y-L, Fass DM, Haggarty SJ, Bhaskara S, Hiebert SW, Schreiber SL, Khabele D (2011) The DNA damage mark pH2AX differentiates the cytotoxic effects of small molecule HDAC inhibitors in ovarian cancer cells. *Cancer Biol Ther* **12**: 484–493.
357. Kaufmann SH, Desnoyers S, Ottaviano Y, Davidson NE, Poirier GG (1993) Specific proteolytic cleavage of poly(ADP-ribose) polymerase: an early marker of chemotherapy-induced apoptosis. *Cancer Res* **53**: 3976–3985.
358. Cece R, Barajon I, Tredici G Cisplatin induces apoptosis in SH-SY5Y human neuroblastoma cell line. *Anticancer Res* **15**: 777–782.
359. Sun Y-X, Yang J, Wang P-Y, Li Y-J, Xie S-Y, Sun R-P, Li Y-J, Li Y-J, Xie S-Y, Xie S-Y, et al. (2013) Cisplatin regulates SH-SY5Y cell growth through downregulation of BDNF via miR-16. *Oncol Rep* **30**: 2343–2349.
360. Nurgalieva Z, Liu C-C, Du XL (2011) Chemotherapy use and risk of bone marrow suppression in a large population-based cohort of older women with breast and ovarian cancer. *Med Oncol* **28**: 716–725.
361. Kuhn J (2002) Chemotherapy-associated hematopoietic toxicity. *Am J Heal Pharm* **59**:.
362. Tabas I, Ron D (2011) Integrating the mechanisms of apoptosis induced by endoplasmic reticulum stress. *Nat Cell Biol* **13**: 184–190.
363. Szegezdi E, Logue SE, Gorman AM, Samali A (2006) Mediators of endoplasmic reticulum stress-induced apoptosis. *EMBO Rep* **7**: 880–885.
364. Kanemaru KK, Tuthill MC, Takeuchi KK, Sidell N, Wada RK (2008) Retinoic acid induced downregulation of MYCN is not mediated through changes in Sp1/Sp3. *Pediatr Blood Cancer* **50**: 806–811.
365. Strieder V, Lutz W (2003) E2F Proteins Regulate *MYCN* Expression in Neuroblastomas. *J Biol Chem* **278**: 2983–2989.
366. Vaughan L, Clarke PA, Barker K, Chanthery Y, Gustafson CW, Tucker E, Renshaw J, Raynaud F, Li X, Burke R, et al. (2016) Inhibition of mTOR-kinase destabilizes MYCN and is a potential therapy for MYCN-dependent tumors. *Oncotarget* **7**: 57525–57544.
367. Kramps C, Strieder V, Sapetschnig A, Suske G, Lutz W (2004) E2F and Sp1/Sp3 Synergize but Are Not Sufficient to Activate the *MYCN* Gene in Neuroblastomas. *J Biol Chem* **279**: 5110–5117.
368. Corazzari M, Gagliardi M, Fimia GM, Piacentini M (2017) Endoplasmic Reticulum Stress,

Unfolded Protein Response, and Cancer Cell Fate. *Front Oncol* **7**: 78.
369. Pagliarini V, Giglio P, Bernardoni P, De Zio D, Fimia GM, Piacentini M, Corazzari M (2015) Downregulation of E2F1 during ER stress is required to induce apoptosis. *J Cell Sci* **128**: 1166–1179.
370. Dauer P, Gupta VK, McGinn O, Nomura A, Sharma NS, Arora N, Giri B, Dudeja V, Saluja AK, Banerjee S (2017) Inhibition of Sp1 prevents ER homeostasis and causes cell death by lysosomal membrane permeabilization in pancreatic cancer. *Sci Rep* **7**: 1564.
371. Abdelrahim M, Liu S, Safe S (2005) Induction of Endoplasmic Reticulum-induced Stress Genes in Panc-1 Pancreatic Cancer Cells Is Dependent on Sp Proteins. *J Biol Chem* **280**: 16508–16513.
372. Wagner LM, Danks MK (2009) New therapeutic targets for the treatment of high-risk neuroblastoma. *J Cell Biochem* **107**: 46–57.
373. Mullassery D, Dominici C, Jesudason EC, McDowell HP, Losty PD (2009) Neuroblastoma: contemporary management. *Arch Dis Child Educ Pract Ed* **94**: 177–185.
374. Chanthery YH, Gustafson WC, Itsara M, Persson A, Hackett CS, Grimmer M, Charron E, Yakovenko S, Kim G, Matthay KK, et al. (2012) Paracrine signaling through MYCN enhances tumor-vascular interactions in neuroblastoma. *Sci Transl Med* **4**: 115ra3.
375. Swartling FJ, Grimmer MR, Hackett CS, Northcott PA, Fan Q-W, Goldenberg DD, Lau J, Masic S, Nguyen K, Yakovenko S, et al. (2010) Pleiotropic role for MYCN in medulloblastoma. *Genes Dev* **24**: 1059–1072.
376. Chesler L, Schlieve C, Goldenberg DD, Kenney A, Kim G, McMillan A, Matthay KK, Rowitch D, Weiss WA (2006) Inhibition of phosphatidylinositol 3-kinase destabilizes Mycn protein and blocks malignant progression in neuroblastoma. *Cancer Res* **66**: 8139–8146.
377. Fouladi M, Perentesis JP, Phillips CL, Leary S, Reid JM, McGovern RM, Ingle AM, Ahern CH, Ames MM, Houghton P, et al. (2014) A phase I trial of MK-2206 in children with refractory malignancies: a Children's Oncology Group study. *Pediatr Blood Cancer* **61**: 1246–1251.
378. Gore L, Trippett TM, Katzenstein HM, Boklan J, Narendran A, Smith A, Macy ME, Rolla K, Pediatric Oncology Experimental Therapeutics Investigators' Consortium (POETIC) N, Narashimhan N, et al. (2013) A multicenter, first-in-pediatrics, phase 1, pharmacokinetic and pharmacodynamic study of ridaforolimus in patients with refractory solid tumors. *Clin Cancer Res* **19**: 3649–3658.
379. Late Effects of Neuroblastoma Treatment | CNCF.
380. Bernstein C, Bernstein H, Payne CM, Garewal H (2002) DNA repair/pro-apoptotic dual-role proteins in five major DNA repair pathways: fail-safe protection against carcinogenesis. *Mutat Res* **511**: 145–178.
381. Cohen LE, Gordon JH, Popovsky EY, Gunawardene S, Duffey-Lind E, Lehmann LE, Diller LR (2014) Late effects in children treated with intensive multimodal therapy for high-risk neuroblastoma: High incidence of endocrine and growth problems. *Bone Marrow Transplant* **49**: 502–508.
382. Laverdière C, Liu Q, Yasui Y, Nathan PC, Gurney JG, Stovall M, Diller LR, Cheung N-K, Wolden S, Robison LL, et al. (2009) Long-term outcomes in survivors of neuroblastoma: a report from the Childhood Cancer Survivor Study. *J Natl Cancer Inst* **101**: 1131–1140.
383. van Santen HM, de Kraker J, Vulsma T (2005) Endocrine late effects from multi-modality treatment of neuroblastoma. *Eur J Cancer* **41**: 1767–1774.
384. Willi SM, Cooke K, Goldwein J, August CS, Olshan JS, Moshang T (1992) Growth in children after bone marrow transplantation for advanced neuroblastoma compared with growth after transplantation for leukemia or aplastic anemia. *J Pediatr* **120**: 726–732.
385. Landier W, Knight K, Wong FL, Lee J, Thomas O, Kim H, Kreissman SG, Schmidt M Lou, Chen L, London WB, et al. (2014) Ototoxicity in children with high-risk neuroblastoma: prevalence, risk factors, and concordance of grading scales--a report from the Children's Oncology Group. *J Clin Oncol* **32**: 527–534.
386. Meacham LR, Sklar CA, Li S, Liu Q, Gimpel N, Yasui Y, Whitton JA, Stovall M, Robison LL, Oeffinger KC (2009) Diabetes Mellitus in Long-term Survivors of Childhood Cancer. *Arch Intern Med* **169**: 1381.
387. Applebaum MA, Vaksman Z, Lee SM, Hungate EA, Henderson TO, London WB, Pinto N, Volchenboum SL, Park JR, Naranjo A, et al. (2017) Neuroblastoma survivors are at increased

risk for second malignancies: A report from the International Neuroblastoma Risk Group Project. *Eur J Cancer* **72**: 177–185.
388. Wilson CL, Ness KK, Neglia JP, Hammond S, Shnorhavorian M, Leisenring WL, Stovall M, Robison LL, Armstrong GT (2013) Renal carcinoma after childhood cancer: a report from the childhood cancer survivor study. *J Natl Cancer Inst* **105**: 504–508.
389. Liu J, Zhang W, Chuang GC, Hill HS, Tian L, Fu Y, Moellering DR, Garvey WT (2012) Role of TRIB3 in regulation of insulin sensitivity and nutrient metabolism during short-term fasting and nutrient excess. *Am J Physiol Endocrinol Metab* **303**: E908-16.
390. Du K, Herzig S, Kulkarni RN, Montminy M (2003) TRB3: A tribbles Homolog That Inhibits Akt/PKB Activation by Insulin in Liver. *Science (80-)* **300**: 1574–1577.
391. Salazar M, Lorente M, García-Taboada E, Hernández-Tiedra S, Davila D, Francis SE, Guzmán M, Kiss-Toth E, Velasco G (2013) The pseudokinase tribbles homologue-3 plays a crucial role in cannabinoid anticancer action. *Biochim Biophys Acta* **1831**: 1573–1578.
392. Benbrook DM, Long A (2012) Integration of autophagy, proteasomal degradation, unfolded protein response and apoptosis. *Exp Oncol* **34**: 286–297.
393. Sharma K, Le N, Alotaibi M, Gewirtz DA (2014) Cytotoxic autophagy in cancer therapy. *Int J Mol Sci* **15**: 10034–10051.
394. Shen H-M, Codogno P (2011) Autophagic cell death: Loch Ness monster or endangered species? *Autophagy* **7**: 457–465.
395. Song S, Tan J, Miao Y, Li M, Zhang Q (2017) Crosstalk of autophagy and apoptosis: Involvement of the dual role of autophagy under ER stress. *J Cell Physiol* **232**: 2977–2984.
396. Mukhopadhyay S, Panda PK, Sinha N, Das DN, Bhutia SK (2014) Autophagy and apoptosis: where do they meet? *Apoptosis* **19**: 555–566.
397. Booth LA, Tavallai S, Hamed HA, Cruickshanks N, Dent P (2014) The role of cell signalling in the crosstalk between autophagy and apoptosis. *Cell Signal* **26**: 549–555.
398. Yousefi S, Perozzo R, Schmid I, Ziemiecki A, Schaffner T, Scapozza L, Brunner T, Simon H-U (2006) Calpain-mediated cleavage of Atg5 switches autophagy to apoptosis. *Nat Cell Biol* **8**: 1124–1132.
399. Djavaheri-Mergny M, Maiuri MC, Kroemer G (2010) Cross talk between apoptosis and autophagy by caspase-mediated cleavage of Beclin 1. *Oncogene* **29**: 1717–1719.
400. Wirawan E, Vande Walle L, Kersse K, Cornelis S, Claerhout S, Vanoverberghe I, Roelandt R, De Rycke R, Verspurten J, Declercq W, et al. (2010) Caspase-mediated cleavage of Beclin-1 inactivates Beclin-1-induced autophagy and enhances apoptosis by promoting the release of proapoptotic factors from mitochondria. *Cell Death Dis* **1**: e18.
401. Noble CG, Dong J-M, Manser E, Song H (2008) Bcl-xL and UVRAG cause a monomer-dimer switch in Beclin1. *J Biol Chem* **283**: 26274–26282.
402. Marquez RT, Xu L (2012) Bcl-2:Beclin 1 complex: multiple, mechanisms regulating autophagy/apoptosis toggle switch. *Am J Cancer Res* **2**: 214–221.
403. Chang NC, Nguyen M, Germain M, Shore GC (2010) Antagonism of Beclin 1-dependent autophagy by BCL-2 at the endoplasmic reticulum requires NAF-1. *EMBO J* **29**: 606–618.
404. Levine B, Sinha SC, Kroemer G (2008) Bcl-2 family members: Dual regulators of apoptosis and autophagy. *Autophagy* **4**: 600–606.
405. Pattingre S, Tassa A, Qu X, Garuti R, Liang XH, Mizushima N, Packer M, Schneider MD, Levine B (2005) Bcl-2 antiapoptotic proteins inhibit Beclin 1-dependent autophagy. *Cell* **122**: 927–939.
406. Wei Y, Sinha S, Levine B (2008) Dual role of JNK1-mediated phosphorylation of Bcl-2 in autophagy and apoptosis regulation. *Autophagy* **4**: 949–951.
407. Sui X, Kong N, Ye L, Han W, Zhou J, Zhang Q, He C, Pan H (2014) p38 and JNK MAPK pathways control the balance of apoptosis and autophagy in response to chemotherapeutic agents. *Cancer Lett* **344**: 174–179.
408. Kang R, Livesey KM, Zeh HJ, Loze MT, Tang D (2010) HMGB1: a novel Beclin 1-binding protein active in autophagy. *Autophagy* **6**: 1209–1211.
409. Tang D, Kang R, Livesey KM, Cheh C-W, Farkas A, Loughran P, Hoppe G, Bianchi ME, Tracey KJ, Zeh HJ, et al. (2010) Endogenous HMGB1 regulates autophagy. *J Cell Biol* **190**: 881–892.
410. Schwarten M, Mohrlüder J, Ma P, Stoldt M, Thielmann Y, Stangler T, Hersch N, Hoffmann B,

Merkel R, Willbold D (2009) Nix directly binds to GABARAP: a possible crosstalk between apoptosis and autophagy. *Autophagy* **5**: 690–698.

411. Bellot G, Garcia-Medina R, Gounon P, Chiche J, Roux D, Pouysségur J, Mazure NM (2009) Hypoxia-induced autophagy is mediated through hypoxia-inducible factor induction of BNIP3 and BNIP3L via their BH3 domains. *Mol Cell Biol* **29**: 2570–2581.
412. Elgendy M, Sheridan C, Brumatti G, Martin SJ (2011) Oncogenic Ras-induced expression of Noxa and Beclin-1 promotes autophagic cell death and limits clonogenic survival. *Mol Cell* **42**: 23–35.
413. Eisenberg-Lerner A, Bialik S, Simon H-U, Kimchi A (2009) Life and death partners: apoptosis, autophagy and the cross-talk between them. *Cell Death Differ* **16**: 966–975.
414. Crighton D, Wilkinson S, O'Prey J, Syed N, Smith P, Harrison PR, Gasco M, Garrone O, Crook T, Ryan KM (2006) DRAM, a p53-Induced Modulator of Autophagy, Is Critical for Apoptosis. *Cell* **126**: 121–134.
415. Rozpedek W, Pytel D, Mucha B, Leszczynska H, Diehl JA, Majsterek I (2016) The Role of the PERK/eIF2α/ATF4/CHOP Signaling Pathway in Tumor Progression During Endoplasmic Reticulum Stress. *Curr Mol Med* **16**: 533–544.
416. Xu C, Bailly-Maitre B, Reed JC (2005) Endoplasmic reticulum stress: cell life and death decisions. *J Clin Invest* **115**: 2656–2664.
417. Rutkowski DT, Arnold SM, Miller CN, Wu J, Li J, Gunnison KM, Mori K, Sadighi Akha AA, Raden D, Kaufman RJ (2006) Adaptation to ER Stress Is Mediated by Differential Stabilities of Pro-Survival and Pro-Apoptotic mRNAs and Proteins. *PLoS Biol* **4**: e374.
418. Buytaert E, Callewaert G, Vandenheede JR, Agostinis P Deficiency in apoptotic effectors Bax and Bak reveals an autophagic cell death pathway initiated by photodamage to the endoplasmic reticulum. *Autophagy* **2**: 238–240.
419. Margariti A, Li H, Chen T, Martin D, Vizcay-Barrena G, Alam S, Karamariti E, Xiao Q, Zampetaki A, Zhang Z, et al. (2013) XBP1 mRNA splicing triggers an autophagic response in endothelial cells through BECLIN-1 transcriptional activation. *J Biol Chem* **288**: 859–872.
420. Zalckvar E, Berissi H, Mizrachy L, Idelchuk Y, Koren I, Eisenstein M, Sabanay H, Pinkas-Kramarski R, Kimchi A (2009) DAP-kinase-mediated phosphorylation on the BH3 domain of beclin 1 promotes dissociation of beclin 1 from Bcl-XL and induction of autophagy. *EMBO Rep* **10**: 285–292.
421. Vandewynckel Y-P, Laukens D, Geerts A, Bogaerts E, Paridaens A, Verhelst X, Janssens S, Heindryckx F, Van Vlierberghe H (2013) The paradox of the unfolded protein response in cancer. *Anticancer Res* **33**: 4683–4694.
422. Lin JH, Li H, Zhang Y, Ron D, Walter P (2009) Divergent effects of PERK and IRE1 signaling on cell viability. *PLoS One* **4**: e4170.
423. Lin JH, Li H, Yasumura D, Cohen HR, Zhang C, Panning B, Shokat KM, LaVail MM, Walter P (2007) IRE1 Signaling Affects Cell Fate During the Unfolded Protein Response. *Science (80-)* **318**: 944–949.
424. DeGregori J, Leone G, Miron A, Jakoi L, Nevins JR (1997) Distinct roles for E2F proteins in cell growth control and apoptosis. *Proc Natl Acad Sci U S A* **94**: 7245–7250.
425. Li H, Chen H, Li R, Xin J, Wu S, Lan J, Xue K, Li X, Zuo C, Jiang W, et al. (2018) Cucurbitacin I induces cancer cell death through the endoplasmic reticulum stress pathway. *J Cell Biochem*.
426. Wang X, Xia H-Y, Qin H-Y, Kang X-P, Hu H-Y, Zheng J, Jiang J-Y, Yao L-A, Xu Y-W, Zhang T, et al. (2018) 20(S)-protopanaxadiol induces apoptosis in human umbilical vein endothelial cells by activating the PERK-eIF2alpha-ATF4 signaling pathway. *J Cell Biochem*.
427. Banerjee S, Zhang W (2018) Endoplasmic Reticulum: Target for Next Generation Cancer Therapy. *ChemBioChem*.
428. Cheng C, Dong W (2018) Aloe-Emodin Induces Endoplasmic Reticulum Stress-Dependent Apoptosis in Colorectal Cancer Cells. *Med Sci Monit* **24**: 6331–6339.
429. Verfaillie T, Garg AD, Agostinis P (2013) Targeting ER stress induced apoptosis and inflammation in cancer. *Cancer Lett* **332**: 249–264.
430. Fulda S (2013) Targeting apoptosis pathways in childhood malignancies. *Cancer Lett* **332**: 369–373.
431. Koritzinsky M, Levitin F, van den Beucken T, Rumantir RA, Harding NJ, Chu KC, Boutros PC,

Braakman I, Wouters BG (2013) Two phases of disulfide bond formation have differing requirements for oxygen. *J Cell Biol* **203**: 615–627.

432. Ghosh R, Lipson KL, Sargent KE, Mercurio AM, Hunt JS, Ron D, Urano F (2010) Transcriptional regulation of VEGF-A by the unfolded protein response pathway. *PLoS One* **5**: e9575.
433. Ye J, Koumenis C (2009) ATF4, an ER stress and hypoxia-inducible transcription factor and its potential role in hypoxia tolerance and tumorigenesis. *Curr Mol Med* **9**: 411–416.
434. Köditz J, Nesper J, Wottawa M, Stiehl DP, Camenisch G, Franke C, Myllyharju J, Wenger RH, Katschinski DM (2007) Oxygen-dependent ATF-4 stability is mediated by the PHD3 oxygen sensor. *Blood* **110**: 3610–3617.
435. Fels DR, Koumenis C (2006) The PERK/eIF2alpha/ATF4 module of the UPR in hypoxia resistance and tumor growth. *Cancer Biol Ther* **5**: 723–728.
436. Hu P, Han Z, Couvillon AD, Kaufman RJ, Exton JH (2006) Autocrine tumor necrosis factor alpha links endoplasmic reticulum stress to the membrane death receptor pathway through IRE1alpha-mediated NF-kappaB activation and down-regulation of TRAF2 expression. *Mol Cell Biol* **26**: 3071–3084.
437. Ma Y, Hendershot LM (2004) The role of the unfolded protein response in tumour development: friend or foe? *Nat Rev Cancer* **4**: 966–977.
438. Scortegagna M, Kim H, Li J-L, Yao H, Brill LM, Han J, Lau E, Bowtell D, Haddad G, Kaufman RJ, et al. (2014) Fine Tuning of the UPR by the Ubiquitin Ligases Siah1/2. *PLoS Genet* **10**: e1004348.
439. Romero-Ramirez L, Cao H, Nelson D, Hammond E, Lee A-H, Yoshida H, Mori K, Glimcher LH, Denko NC, Giaccia AJ, et al. (2004) XBP1 Is Essential for Survival under Hypoxic Conditions and Is Required for Tumor Growth. *Cancer Res* **64**: 5943–5947.
440. Shuda M, Kondoh N, Imazeki N, Tanaka K, Okada T, Mori K, Hada A, Arai M, Wakatsuki T, Matsubara O, et al. (2003) Activation of the ATF6, XBP1 and grp78 genes in human hepatocellular carcinoma: a possible involvement of the ER stress pathway in hepatocarcinogenesis. *J Hepatol* **38**: 605–614.
441. Zage P (2018) Novel Therapies for Relapsed and Refractory Neuroblastoma. *Children* **5**: 148.
442. Garg AD, Agostinis P (2014) ER stress, autophagy and immunogenic cell death in photodynamic therapy-induced anti-cancer immune responses. *Photochem Photobiol Sci* **13**: 474–487.
443. Healy SJM, Gorman AM, Mousavi-Shafaei P, Gupta S, Samali A (2009) Targeting the endoplasmic reticulum-stress response as an anticancer strategy. *Eur J Pharmacol* **625**: 234–246.
444. Yeh T-C, Chiang P-C, Li T-K, Hsu J-L, Lin C-J, Wang S-W, Peng C-Y, Guh J-H (2007) Genistein induces apoptosis in human hepatocellular carcinomas via interaction of endoplasmic reticulum stress and mitochondrial insult. *Biochem Pharmacol* **73**: 782–792.
445. Schönthal AH (2009) Endoplasmic reticulum stress and autophagy as targets for cancer therapy. *Cancer Lett* **275**: 163–169.
446. Otto T, Horn S, Brockmann M, Eilers U, Schüttrumpf L, Popov N, Kenney AM, Schulte JH, Beijersbergen R, Christiansen H, et al. (2009) Stabilization of N-Myc is a critical function of Aurora A in human neuroblastoma. *Cancer Cell* **15**: 67–78.
447. Gregory MA, Hann SR (2000) c-Myc proteolysis by the ubiquitin-proteasome pathway: stabilization of c-Myc in Burkitt's lymphoma cells. *Mol Cell Biol* **20**: 2423–2435.
448. Gustafson WC, Weiss WA (2010) Myc proteins as therapeutic targets. *Oncogene* **29**: 1249–1259.
449. Mosse YP, Fox E, Teachey DT, Reid JM, Sagfren SL, Carol H, Lock RB, Houghton PJ, Smith MA, Hall DC, et al. (2019) A Phase 2 Study of Alisertib in Children with Recurrent/Refractory Solid Tumors or Leukemia: Children's Oncology Group Phase 1 and Pilot Consortium ADVL0921). *Clin Cancer Res* clincanres.2675.2018.
450. Minturn JE, Evans AE, Villablanca JG, Yanik GA, Park JR, Shusterman S, Groshen S, Hellriegel ET, Bensen-Kennedy D, Matthay KK, et al. (2011) Phase I trial of lestaurtinib for children with refractory neuroblastoma: a new approaches to neuroblastoma therapy consortium study. *Cancer Chemother Pharmacol* **68**: 1057–1065.
451. Digaleh H, Kiaei M, Khodagholi F (2013) Nrf2 and Nrf1 signaling and ER stress crosstalk:

implication for proteasomal degradation and autophagy. *Cell Mol Life Sci* **70**: 4681–4694.
452. Sato M, Rodriguez-Barrueco R, Yu J, Do C, Silva JM, Gautier J (2015) MYC is a critical target of FBXW7. *Oncotarget* **6**: 3292–3305.
453. Brockmann M, Poon E, Berry T, Carstensen A, Deubzer HE, Rycak L, Jamin Y, Thway K, Robinson SP, Roels F, et al. (2013) Small molecule inhibitors of aurora-a induce proteasomal degradation of N-myc in childhood neuroblastoma. *Cancer Cell* **24**: 75–89.
454. Tavana O, Li D, Dai C, Lopez G, Banerjee D, Kon N, Chen C, Califano A, Yamashiro DJ, Sun H, et al. (2016) HAUSP deubiquitinates and stabilizes N-Myc in neuroblastoma. *Nat Med* **22**: 1180–1186.
455. Fan Y-H, Cheng J, Vasudevan SA, Dou J, Zhang H, Patel RH, Ma IT, Rojas Y, Zhao Y, Yu Y, et al. (2013) USP7 inhibitor P22077 inhibits neuroblastoma growth via inducing p53-mediated apoptosis. *Cell Death Dis* **4**: e867.
456. Polager S, Ofir M, Ginsberg D (2008) E2F1 regulates autophagy and the transcription of autophagy genes. *Oncogene* **27**: 4860–4864.
457. Torabi B, Flashner S, Beishline K, Sowash A, Donovan K, Bassett G, Azizkhan-Clifford J (2018) Caspase cleavage of transcription factor Sp1 enhances apoptosis. *Apoptosis* **23**: 65–78.
458. Tuthill MC, Wada RK, Arimoto JM, Sugino CN, Kanemaru KK, Takeuchi KK, Sidell N N-myc oncogene expression in neuroblastoma is driven by Sp1 and Sp3. *Mol Genet Metab* **80**: 272–280.
459. Inge TH, Casson LK, Priebe W, Trent JO, Georgeson KE, Miller DM, Bates PJ (2002) Importance of Sp1 consensus motifs in the MYCN promoter. *Surgery* **132**: 232–238.
460. Lutz W, Schwab M (1997) *In vivo regulation of single copy and ampli®ed N-myc in human neuroblastoma cells*.
461. Obiedat A, Seidel E, Mahameed M, Berhani O, Tsukerman P, Voutetakis K, Chatziioannou A, McMahon M, Avril T, Chevet E, et al. (2019) Transcription of the NKG2D ligand MICA is suppressed by the IRE1/XBP1 pathway of the unfolded protein response through the regulation of E2F1. *FASEB J* **33**: 3481–3495.
462. Black AR, Azizkhan-Clifford J (1999) Regulation of E2F: a family of transcription factors involved in proliferation control. *Gene* **237**: 281–302.
463. Karlseder J, Rotheneder H, Wintersberger E (1996) Interaction of Sp1 with the growth- and cell cycle-regulated transcription factor E2F. *Mol Cell Biol* **16**: 1659–1667.
464. Lin SY, Black AR, Kostic D, Pajovic S, Hoover CN, Azizkhan JC (1996) Cell cycle-regulated association of E2F1 and Sp1 is related to their functional interaction. *Mol Cell Biol* **16**: 1668–1675.
465. Hollien J, Weissman JS (2006) Decay of endoplasmic reticulum-localized mRNAs during the unfolded protein response. *Science* **313**: 104–107.
466. Chan HS, Gallie BL, DeBoer G, Haddad G, Ikegaki N, Dimitroulakos J, Yeger H, Ling V (1997) MYCN protein expression as a predictor of neuroblastoma prognosis. *Clin Cancer Res* **3**: 1699–1706.
467. Tsukamoto K, Carroll KA, Onishi T, Matsumaru N, Brasseur D, Nakamura H (2016) Improvement of Pediatric Drug Development: Regulatory and Practical Frameworks. *Clin Ther* **38**: 574–581.
468. Garaventa A, Luksch R, Biasotti S, Severi G, Pizzitola MR, Viscardi E, Prete A, Mastrangelo S, Podda M, Haupt R, et al. (2003) A phase II study of topotecan with vincristine and doxorubicin in children with recurrent/refractory neuroblastoma. *Cancer* **98**: 2488–2494.
469. Szabó DR, Baghy K, Szabó PM, Zsippai A, Marczell I, Nagy Z, Varga V, Éder K, Tóth S, Buzás EI, et al. (2014) Antitumoral effects of 9-cis retinoic acid in adrenocortical cancer. *Cell Mol Life Sci* **71**: 917–932.
470. Balmer JE, Blomhoff R (2002) Gene expression regulation by retinoic acid. *J Lipid Res* **43**: 1773–1808.
471. Thiele CJ, Reynolds CP, Israel MA (1985) Decreased expression of N-myc precedes retinoic acid-induced morphological differentiation of human neuroblastoma. *Nature* **313**: 404–406.
472. Yuza Y, Agawa M, Matsuzaki M, Yamada H, Urashima M (2003) Gene and protein expression profiling during differentiation of neuroblastoma cells triggered by 13-cis retinoic acid. *J Pediatr Hematol Oncol* **25**: 715–720.

473. Reynolds CP, Wang Y, Melton LJ, Einhorn PA, Slamon DJ, Maurer BJ (2000) Retinoic-acid-resistant neuroblastoma cell lines show altered MYC regulation and high sensitivity to fenretinide. *Med Pediatr Oncol* **35**: 597–602.
474. Wada RK, Pai DS, Huang J, Yamashiro JM, Sidell N (1997) Interferon-gamma and retinoic acid down-regulate N-myc in neuroblastoma through complementary mechanisms of action. *Cancer Lett* **121**: 181–188.
475. Shelake S, Eslin D, Sutphin RM, Sankpal UT, Wadwani A, Kenyon LE, Tabor-Simecka L, Bowman WP, Vishwanatha JK, Basha R (2015) Combination of 13 cis -retinoic acid and tolfenamic acid induces apoptosis and effectively inhibits high-risk neuroblastoma cell proliferation. *Int J Dev Neurosci* **46**: 92–99.
476. Tosun M, Soysal Y, Mas NG, Karabekir HS (2015) Comparison of the Effects of 13- *cis* Retinoic Acid and Melatonin on the Viabilities of SH-SY5Y Neuroblastoma Cell Line. *J Korean Neurosurg Soc* **57**: 147.
477. Hadjidaniel MD, Reynolds CP (2010) Antagonism of Cytotoxic Chemotherapy in Neuroblastoma Cell Lines by 13-cis-Retinoic Acid Is Mediated by the Antiapoptotic Bcl-2 Family Proteins. *Mol Cancer Ther* **9**: 3164–3174.
478. Masciarelli S, Capuano E, Ottone T, Divona M, De Panfilis S, Banella C, Noguera NI, Picardi A, Fontemaggi G, Blandino G, et al. (2018) Retinoic acid and arsenic trioxide sensitize acute promyelocytic leukemia cells to ER stress. *Leukemia* **32**: 285–294.
479. Anding AL, Jones JD, Newton MA, Curley RW, Clagett-Dame M (2018) 4-HPR Is an Endoplasmic Reticulum Stress Aggravator and Sensitizes Breast Cancer Cells Resistant to TRAIL/Apo2L. *Anticancer Res* **38**: 4403–4416.
480. Liu L, Liu C, Zhong Y, Apostolou A, Fang S (2012) ER stress response during the differentiation of H9 cells induced by retinoic acid. *Biochem Biophys Res Commun* **417**: 738–743.
481. Armstrong JL, Flockhart R, Veal GJ, Lovat PE, Redfern CPF (2010) Regulation of Endoplasmic Reticulum Stress-induced Cell Death by ATF4 in Neuroectodermal Tumor Cells. *J Biol Chem* **285**: 6091–6100.
482. Kohler JA, Imeson J, Ellershaw C, Lie SO (2000) A randomized trial of 13-Cis retinoic acid in children with advanced neuroblastoma after high-dose therapy. *Br J Cancer* **83**: 1124–1127.
483. Matthay KK, Reynolds CP (2000) Is there a role for retinoids to treat minimal residual disease in neuroblastoma? *Br J Cancer* **83**: 1121–1123.
484. Fouladi M, Park JR, Stewart CF, Gilbertson RJ, Schaiquevich P, Sun J, Reid JM, Ames MM, Speights R, Ingle AM, et al. (2010) Pediatric phase I trial and pharmacokinetic study of vorinostat: a Children's Oncology Group phase I consortium report. *J Clin Oncol* **28**: 3623–3629.
485. Zage PE, Zeng L, Palla S, Fang W, Nilsson MB, Heymach J V., Zweidler-McKay PA (2010) A novel therapeutic combination for neuroblastoma. *Cancer* **116**: NA-NA.
486. Orphan incentives | European Medicines Agency.
487. Developing Products for Rare Diseases & Conditions | FDA.
488. Robin NH, Farmer MB, Whelan K, Alva E (2018) Epidemiology of Childhood Cancer. *Pediatr Cancer Genet* 1–20.
489. Tsui PC, Lee Y-F, Liu ZWY, Ip LRH, Piao W, Chiang AKS, Lui VWY (2017) An update on genomic-guided therapies for pediatric solid tumors. *Future Oncol* **13**: 1345–1358.

ANNEX

8. Annex

8.1 Characterization of ABTL0812-induced cell death

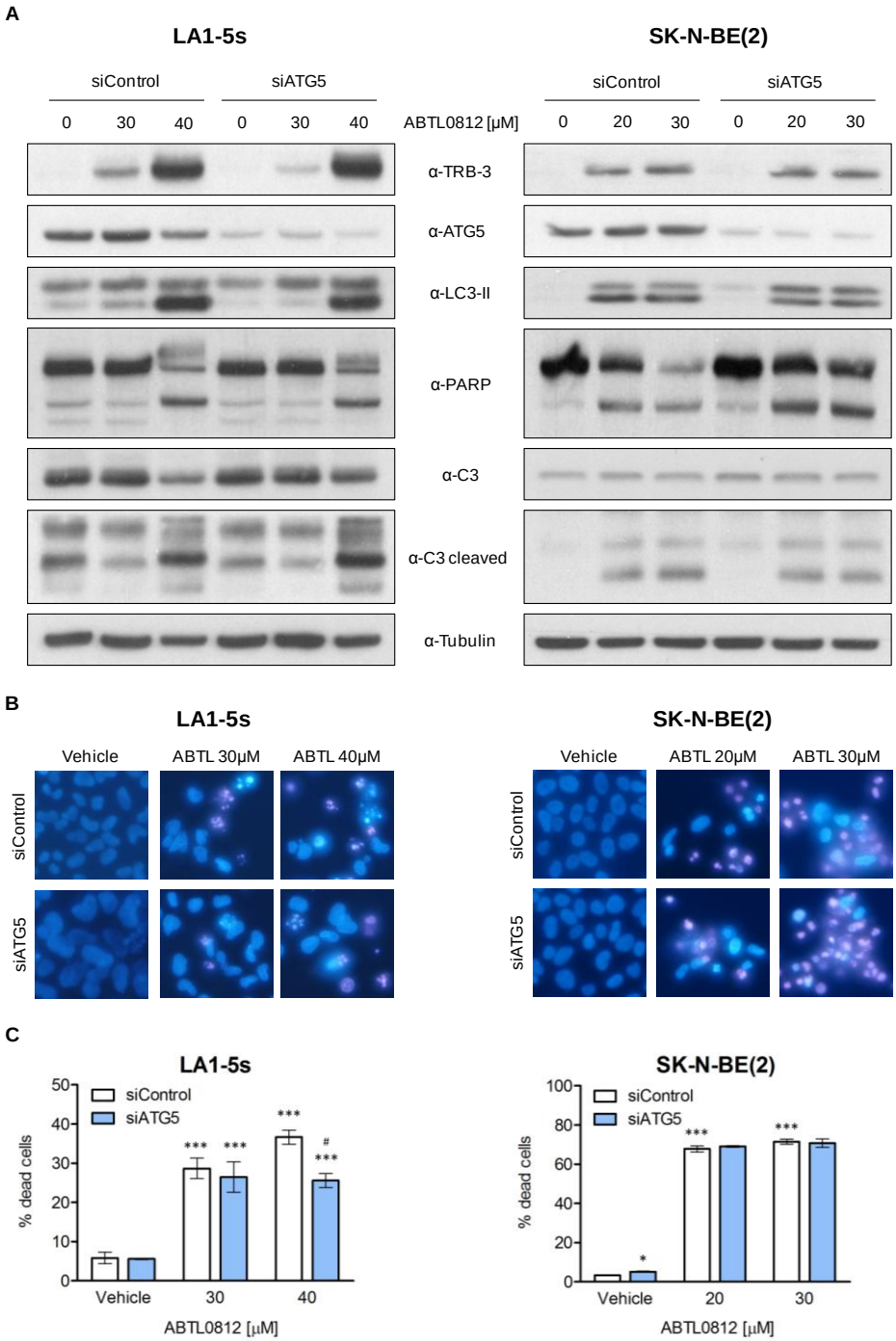

Annex 1. ATG5 inhibition is not sufficient to block autophagy. In order to ascertain whether autophagy was a necessary step previous to apoptosis, LA1-5s and SK-N-BE(2) NB cells were transfected with siRNA control or siRNA against ATG5. As ATG5 is an essential protein for autophagosome formation, its inhibition should impair the autophagic pathway. After 48h, cells were treated with the indicated ABTL0812 (ABTL) concentrations or vehicle (ethanol). (A) Protein expression levels were analyzed by WB 72h post-treatment. Anti-TRB-3 was used as a control for ABTL0812 response. (B) Representative images of nuclear morphology assessment at 72h post-treatment with ABTL0812. (C) Quantification of cell death was performed 72h post-treatment from 4 representative images of 3 replicates per condition. Data is presented as mean ± SEM of three independent experiments. *p≤0.05, **p≤0.01, ***p≤0.001 compared to vehicle; $^{\#}$p≤0.05 compared to the corresponding siControl. Results were that despite ATG5 silencing, autophagy was still occurring, as could be deduced by the increase in LC3-II. Therefore, this experiment did not allow us to figure out whether the activation of apoptosis (measured by the cleavage of apoptotic substrates and quantification of apoptotic nuclei) was independent or subsequent to autophagy. The main conclusion of this experiment is that individual ATG5 inhibition is not sufficient to prevent autophagosome formation.

8.2 Monitoring endoplasmatic reticulum stress induction by ABTL0812

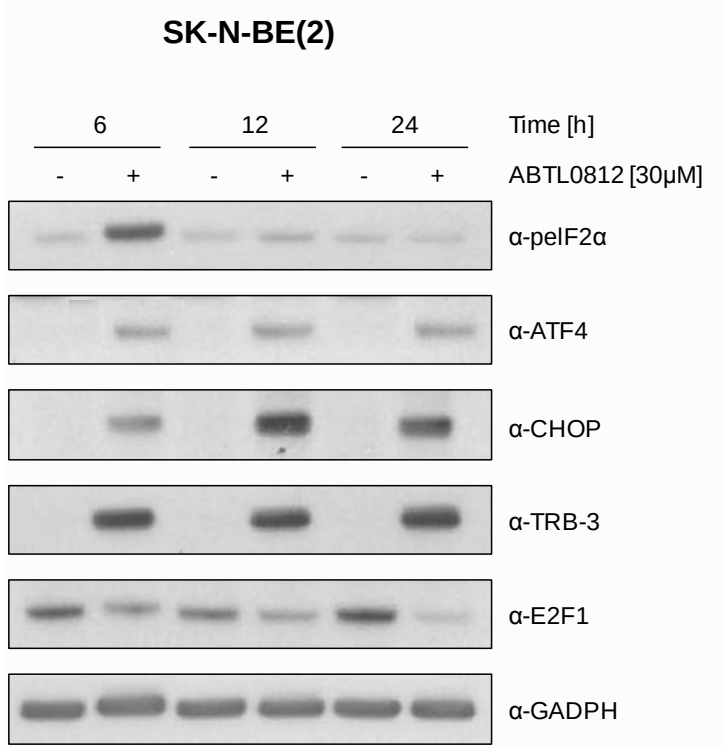

Annex 2. E2F1 down-regulation allows for UPR life-to-death switch. SK-N-BE(2) cells were treated with ABTL0812 30μM or vehicle (ethanol) for 6h, 12h and 24h. Protein expression levels were analyzed by WB. Recently, the role of E2F1 has been described as a potential mechanistic survival/death switch under ER stress conditions [369]. ER stress-mediated E2F1 down-regulation might contribute to the life/death cell decision under prolonged ER stress [368]. The results demonstrated a time-dependent down-regulation of E2F1. Therefore, E2F1 withdrawal could mark the point of no return of the execution phase of the UPR apoptotic pathway.

8.3 Publications

During the PhD thesis I have had the pleasure to collaborate on several research projects that produced as a result the following publications:

1. Soriano A, Masanas M, Boloix A, Masiá N, **París-Coderch L**, Piskareva O, Jiménez C, Henrich K-O, Roma J, Westermann F, et al. (2019) Functional high-throughput screening reveals miR-323a-5p and miR-342-5p as new tumor-suppressive microRNA for neuroblastoma. *Cell Mol Life Sci* **76**: 2231–2243.

2. Sánchez-Cid L, Pons M, Lozano JJ, Rubio N, Guerra-Rebollo M, Soriano A, **Paris-Coderch L**, Segura MF, Fueyo R, Arguimbau J, et al. (2017) MicroRNA-200, associated with metastatic breast cancer, promotes traits of mammary luminal progenitor cells. *Oncotarget* **8**: 83384–83406.

3. Jubierre L, Soriano A, Planells-Ferrer L, **París-Coderch L**, Tenbaum SP, Romero OA, Moubarak RS, Almazán-Moga A, Molist C, Roma J, et al. (2016) BRG1/SMARCA4 is essential for neuroblastoma cell viability through modulation of cell death and survival pathways. *Oncogene* **35**: 5179–5190.

4. Soriano A, **París-Coderch L**, Jubierre L, Martínez A, Zhou X, Piskareva O, Bray I, Vidal I, Almazán-Moga A, Molist C, et al. (2016) MicroRNA-497 impairs the growth of chemoresistant neuroblastoma cells by targeting cell cycle, survival and vascular permeability genes. *Oncotarget* **7**: 9271-9287

5. Boloix A, **París-Coderch L**, Soriano A, Roma J, Gallego S, Sánchez de Toledo J, Segura MF (2016) Novel micro RNA-based therapies for the treatment of neuroblastoma. *An Pediatr (Barc)* **85**: 109.e1-109.e6.